

ORIGINAL PAGE IS
OF POOR QUALITY



Rockwell International

Rocketdyme Division
6633 Canoga Avenue
Canoga Park, California 91304

RSS-8826-12

REAL-TIME FAILURE CONTROL (SAFD)

NAS8-40000

FINAL REPORT

JULY 1990

PREPARED BY

Hagop V. Panossian, Ph.D.
Principal Investigator
Principal Engineer
Control/Structure
System Dynamics

Victoria R. Kemp
Member of Tech. Staff
System Dynamics

Sherry J. Eckerling
Member of Tech. Staff
System Dynamics

APPROVED BY

Mike H. Taniguchi
Manager
System Dynamics

Wm. J. McFarlen
Program Manager
SSME Technology

D/0526f

(NASA-CR-184025) REAL-TIME FAILURE CONTROL
(SAFD) Final Report (Rockwell International
Corp.) 195 p CSCL 14D

N91-11233

Unclas
G3/38 0310577

1. SUMMARY

The Real-Time Failure Control program involves development of a failure detection algorithm, referred to as "System for Failure and Anomaly Detection (SAFD)," for the Space Shuttle Main Engine (SSME). This failure detection approach is signal-based and it entails monitoring SSME measurement signals based on predetermined and computed mean values and standard deviations. Twenty-four engine measurements are included in the algorithm and provisions are made to add more parameters if needed. Each of the (first) values of every measurement signal at the algorithm start is checked against safety limits determined by a precomputed mean value (MV)+/- and a given multiple of a precomputed standard deviation (SD). If several parameters exceed these limits a failure is signalled. During the first two seconds (after algorithm start) a moving average (MA) and a SD is computed on-line, by averaging the values of each parameter in a 200 ms duration, and is updated at every time interval. The moving average is checked against a similar safety band around the precomputed MV for each parameter and if several anomalies are registered a failure is signalled by the algorithm. At the end of the two-second interval the MA is fixed as the mean value for the rest of the algorithm operation and a safety band is placed above and below this value equal to a multiple of the computed SD. The MA is continuously updated and checked against this safety band. Once more if several parameters exceed the limits a failure is signalled. At the start of every scheduled power transient the algorithm is stopped. It is re-initiated after two seconds from the termination of the power transient and the process is repeated.

This final report is divided into six major sections. The most encompassing of all is the discussion section that has sub-sections on: 1) SAFD algorithm development, 2) SAFD simulations, 3) DTM failure simulations, 4) closed-loop simulation, 5) SAFD current limitations, and 6) enhancements planned for. The report will cover background information, new developments, and future plans for the algorithm implementation and enhancements.

2. TABLE OF CONTENTS

	Page
1. SUMMARY	1
2. TABLE OF CONTENTS	2
3. LIST OF FIGURES	3
4. LIST OF TABLES	4
5. INTRODUCTION	5
6. DISCUSSION	10
6.1 BACKGROUND	10
6.1.1 INCIDENTS	11
6.1.2 PARAMETER IDENTIFICATION (PID) NUMBER ASSOCIATION WITH TEST	17
6.1.3 UPDATING AND FINALIZATION OF SAFD MONITORED PARAMETERS	18
6.1.4 SSME CRITICAL OPERATING PARAMETERS	19
6.1.5 CHARACTERISTIC EFFECTS OF PRESSURIZATION AND VENTING ON SAFD PARAMETERS	20
6.2 SAFD ALGORITHM AND SIMULATIONS	22
6.2.1 SAFD OBJECTIVE AND SCOPE	23
6.2.2 THE CURRENT SAFD ALGORITHM	24
6.2.3 SAFD REFINEMENTS	25
6.2.4 SAFD ALGORITHM SIMULATIONS	29
6.2.5 HEURISTIC EVALUATIONS AND SENSITIVITY ANALYSIS	33
6.3 SSME DTM FAILURE SIMULATIONS.....	34
6.3.1 DTM SIMULATION OF TEST 901-284	34
6.3.2 TEST 901-284	35
6.3.3 TEST 902-428	37
6.3.4 TEST 750-285	38
6.4 SSME DTM HYPOTHETICAL FAILURE SIMULATIONS	39
6.5 CLOSED-LOOP (DTM-SAFD) SIMULATIONS	42
6.6 LESSONS LEARNED	45
7. CONCLUSIONS	47
8. RECOMMENDATIONS	49
9. BIBLIOGRAPHY/REFERENCES	52
10. APPENDIX	53

3. LIST OF FIGURES

FIGURE NO.	TITLE	PAGE
1	Pressurization/Venting Effects on Parameters	84
2.	Closure of GOX and Fluid Repressurization Valves' Effect on Parameters	85
3.	SAFD Algorithm Schematic	86
4A - 4C	Slope-Average Approach on Test 901-364	87
5A1 - 5H2	Test 750-285	90
6A1 - 6F2	Test 901-340	98
7A - 7I	Test 902-471	104
8A - 8I	Test 901-340	113
9A - 9L	Test 901-284	122
10A - 10G	Test 902-428	133
11A - 11F	Fuel Leakage Flow Simulation on Test 750-285	140
12	SSME Flow Schematic 100% RPL	143
12A - 12T	Fuel Leakage Simulation on Hypothetical Failure	144
13A	SSME Flow Schematic 100% RPL	154
13B - 13R	HPFT Discharge Flow Blockage	155
14A - 14I	Closed-Loop Simulation of Leakage: Approach 1	165
15A - 15I	Closed-Loop Simulation of Blockage: Approach 2	174
16	Effects of GOX and Fuel Repressurized Valve Closures	183
17	Effects of Venting/Repressurization	184
18A - 18E	Nonlinear Behavior	185
19	LOX/Venting Repressurization Profile	190
20	Advanced Fault Detection	191
21	SSME Flight 51F HPFT Discharge Temp. Sensor Failure	192
22	Sensor Failure Detection Simulations	193
23	Test 901-436	194

4. LIST OF TABLES

TABLE NO.	TITLE	PAGE
6.1.1	Detailed Comparison of SSME Failures	54
6.1.2	Mean Values and Standard Deviations	55
6.1.3	Preliminary Choice of Tests for SAFD Simulations	58
6.1.4	SSME Failure Modes from FMEA	59
6.1.5	Data Conversion Routine	60
6.1.6	Original SAFD Monitored Parameters	63
6.1.7	Current SAFD Monitored Parameters	64
6.1.8	SSME Critical Operating Parameters	65
6.1.9	LOX Venting Effects on Engine Parameters	66
6.2.1	Values for $N2 \cdot \sigma$	67
6.2.2A-F	Simulation Results for Test 901-284	68
6.2.3	Signal Limit Composition	74
6.2.4	Simulation Results for Test 901-340	75
6.2.5	Simulation Results for Test 902-491	76
6.2.6	Comparison of Results	77
6.2.7A-D	Simulation Runs	78
6.4.1	Parameter Descriptions	82
6.5.1	Parameter Descriptions	164

5. INTRODUCTION

Anomalous behavior during Space Shuttle Main Engine (SSME) hot-fire testing is presently detected via measurement redlines that are implemented on key measured parameters. In order to avoid the cost incurred and the impact on the SSME flight schedule due to failures, it is very desirable to have an advanced failure detection system that can minimize damage and that can detect as many failures as possible, quickly and efficiently, prior to catastrophes. The safe operation of any complex system, such as the SSME, rests on the reliability of the control and fault detection systems and the speed of detection and identification of component, sensor, or actuator failures. In the recent past, fault detection and isolation has raised the interest of many researchers [1-7]. Most major techniques to failure detection can be categorized as either model-based or signal-based approaches.

Model-based techniques rely on analytical redundancy [4-8]. Analytically generated "measurement" outputs are compared with hardware measurements by using present and/or previous values of some variables in conjunction with their mathematical relationships. The fault detection process herein encompasses three major tasks: 1) residual generation that entails taking the difference between the analytical and measured values, 2) statistical testing and signature generation, and 3) diagnostics and decision making.

On the other hand, signal-based techniques are hardware intensive and sensor/actuator driven. In this approach, the major undertakings include: 1) limit/trend checking by comparison of plant outputs with normal operational limits, 2) sensor/actuator/component redundancy, whereby a single value from measurements of several identical sensors is used according to some decision mechanism, 3) frequency spectrum analyses by using plant measurements, wherein frequency spectrums are compared with normal spectrums [9-12].

An algorithm is hereby developed, referred to as "System for Anomaly and Failure Detection (SAFD)," that permits fault detection during SSME hot-fire testing by a simple signal-based approach.

The method entails monitoring the signal averages for 24 SAFD parameters and comparing the signal averages to upper and lower signal safety limits. The reason for monitoring the averages of signals, rather than their actual values, is to smooth or filter out most of the undesirable effects of sensor noise. Moreover, the safety limits are placed above and below the fixed average value for each parameter with a bandwidth of $n*SD$, where n is a pre-determined constant that is large enough to avoid false alarms and small enough to make the algorithm sensitive to actual failures.

The SAFD algorithm, as it is currently configured, works during SSME steady-state operation, starting at five seconds after engine start or two seconds after the completion of each scheduled power transient. Moreover, an added safety feature is included that checks the value of each SAFD parameter at the first incoming measurement against pre-determined expected values. In case several parameters exceed or are below their expected values, by more than a pre-determined margin, then a failure is signalled. This feature will ensure the normal engine operation by identifying any failure that could have happened during start/power transients. Also, if any sensor indicates a negative output, it is automatically disqualified and eliminated from the algorithm. However, there is no means of sensor failure detection in the present SAFD set-up.

As described in the final reports of Phase I and II of the SAFD algorithm development contract [13], the original algorithm entailed failure detection based on three approaches. The first approach encompassed the first two-second interval after algorithm start and it used precomputed mean value (MV) and standard deviation (SD) for each of the 23 parameters monitored. The moving average (MA) was checked against safety limits, placed above and below the fixed MV, equal to n_1*SD . The MA was computed continuously from the start of the algorithm until the end of the two-second interval and updated at every sampling instant of 80 milliseconds (thus, at the end of the two-second interval the MA was the average of 2 sec. worth of 25 data points). If several parameters indicated exceedence of the safety limits (due to the MA exceedence (Approach 1)), then a failure was flagged out. At the end of the two-second interval, the MA value was fixed and used as the MV for the rest of the algorithm operation. In approach 2, the continuously updated MA was compared to the safety limits, placed around this MV, equal

to $n_2 * SD$. In Approach 3, the actual signal was compared to the safety limits placed around the continuously updated MA and equal to a bandwidth of $n_3 * SD$. Five SSME incident tests were simulated during Phase I and II [13] and the algorithm performed well as compared to the engine redlines.

During the course of the present contract, the SAFD algorithm was refined and modified in several areas. Namely, the safety feature for anomaly check at the start of the algorithm, that was mentioned in the summary section was added and the MA was reduced from a two-second average to a 200 millisecond moving average. The reason for this action was to make the MA more sensitive to sudden changes. The on-line check for anomaly that used the actual signal values for failure detection (Approach 2, utilized in the original SAFD algorithm) was eliminated, since the instrumentation noise level (excursions) could trigger false alarms. The use of a MA computed as the average of only the most recent five signal measurement values, as opposed to twenty-five, is more sensitive to sudden failures and the averaging process removes most of the undesirable signal noise, thus avoiding false alarms without having to artificially increase the safety bandwidth. Some of the originally monitored engine parameters are not currently in use (the sensors have been eliminated). Thus, the list of measurements monitored by SAFD were updated and a new set of 24 parameters were included. Most of the engine redlines are in this list. Moreover, the sampling interval was reduced to 40 msec. with an option of reducing it to 20 msec, if hardware capabilities permit.

Eight SAFD algorithm simulations on actual data from SSME incident tests were carried out during the current phase of the Real-Time Failure Control contract. Three real incident tests and two hypothetical failures were simulated by the SSME Digital Transient Model (DTM). Moreover, over 40 incident tests were carefully studied for useful information. Currently, the SAFD algorithm can handle only steady-state operating conditions. However, the start anomaly check is really a post transient failure detection approach that will detect any anomalous developments that happen during start or power transient. There are some other perturbations, due either to transients like fuel or liquid oxygen (LOX) venting and repressurization effects or to fuel or gaseous oxygen (GOX) valve closure effects, that makes the present SAFD approach a little sluggish, in that the safety bandwidth has to be large enough to cover such excursions. Moreover,

there are nonlinear effects that appear in the behavior of some parameters (such as the HPOT pump discharge temperature that takes over 60 seconds to reach steady-state and has an excursion of over 50°F) for which special provisions need to be made to avoid false alarms. In addition, the SAFD performance is a function of the multiplying factor n , and that of the number of required parameters that show anomalous behavior for an engine shutdown decision.

Nevertheless, SAFD, as it is presently configured, is very effective (much better than redlines) in detecting slow developing failures and it is slightly better than the redlines in fast failures, such as structural ruptures. Several of the SAFD advantages include: 1) the requirement of a multiple parameter anomaly for a failure decision (this avoids false alarms), 2) the option of choosing a different bandwidth for different parameters and even for different intervals, 3) the use of a moving average that removes noise effects and is sufficiently short-term to enhance its sensitivity and use of the SD and the average values, and 4) the flexibility of the algorithm for further expansions and enhancements, among others.

There are means of modifying the algorithm that will make it more encompassing and that will be discussed in what follows. An automated selection of the optimal safety bandwidth and the number of anomalous parameters required for a sure failure can be developed. Most of the shortcomings of the SAFD algorithm can thus be eliminated and plans for accomplishing this will be discussed later.

This report covers: 1) background information on past SSME failures and problems involving their detection, 2) detailed descriptions and simulation plots of the SAFD algorithm, 3) detailed descriptions of the DTM failure simulations, 4) the closed-loop simulation (DTM failure simulations with the SAFD in the loop), 5) limitations and advantages of the algorithm, and 6) plans for future work for the enhancement of SAFD.

The objective of the present contract is to develop a failure detection algorithm that will enhance and refine the "failure control techniques for the SSME" and demonstrate the operability of the SAFD algorithm in a closed-loop manner via engine simulations. The Rocketdyne Digital Transient

Model (DTM) was used to accomplish the goal. It will be shown that the SAFD algorithm is capable of detecting performance degradation and anomalous behavior of the SSME earlier and faster than the existing redline system.

6. DISCUSSION

Fault detection system design involves several complex issues, such as quick response prior to significant performance degradation or damage as well as consideration of system redundancy. Advanced fault detection algorithms, based on careful consideration of system dynamic characteristics, can often lead to significant reduction of hardware redundancy. There are three main concerns in any fault detection and identification process. The primary objective invariably is to establish that a failure has occurred with a high degree of certainty. The type and location of failure as well as the extent of degradation are two of the remaining concerns that should be addressed appropriately. The principal thrust of the present algorithm involves the fault detection problem.

6.1 BACKGROUND

There were four major tasks identified in the statement of work of the present contract. The first task involved algorithm refinement, the second task was on provisions for avoidance of premature cutoff, the third task entailed simulation with the SAFD algorithm using real incident test data, and the fourth task was related to the closed-loop simulation of DTM on-line with the SAFD algorithm. The initial phase of the contract was directed towards the study and evaluation of all SSME incident tests, identification of areas of refinement in the algorithm, analyses of the characteristic behavior of key engine parameters and the availability of sensors and measurements that can easily be utilized for the algorithm implementation.

6.1.1 INCIDENTS

The occurrence of an anomaly or a failure is classified as a "major" or a "minor" incident based on: a) the extent of damage, b) pressure, temperature, speed and vibration levels in excess of normal end item operating levels, and c) internal and/or external fires or explosions [13].

SAFD Parameter Selection Criteria [14].

The compilation in Table 6.1.1 is the list of all major failures or incidents of the SSME from 1977 to the present. The Table summarizes data on 40 failures that include: 1) test number, 2) the engine number on which failure occurred, 3) the date of anomaly, 4) duration from the start in seconds, 5) engine power level at the time of failure, 6) brief description of failure, 7) classification of failure as major or critical, 8) the location or unit that experienced the failure, 9) the redline parameter that caused engine cutoff initiation, and 10) parameters, other than the redline parameter, that showed significant change due to the failure.

Forty (40) past incident tests were reviewed, excluding tests where:

- anomaly occurred after engine cutoff or during transient
- where no striking changes were indicated.

A total of 40 tests were used to select the 24 parameters for the SAFD algorithm. Those measurement parameters were chosen that represented "key" aspects of SSME operation. Fifty-seven (57) measurements were examined for: a) anomaly induced percentage change from steady-state operation, b) rate of percentage change, c) interim from first indications of an anomaly to cut off. Each of the above factors were weighed and accordingly, the most appropriate parameters were selected for use in the algorithm.

A database was developed whereby all the generic and specific characteristics of various incident tests were listed. This data was used to evaluate the significant parameters for failure detection use.

Also included in the evaluations were failure mode qualitative characteristics where generic descriptions of the incident type and a sample of indicative parameters were studied. Shown are examples of indicative parameters where an anomaly induces change from the steady-state value. These are summarized in Section 6.1.1.1 as failure investigations including incident and damage descriptions.

A summary of data is also presented that includes: 1) sensor measurement standard deviations, 2) test-to-test envelope database definition, 3) data for time-sliced value deviations from the average steady-state sensor measurements, and 4) 31 database inputs for each test (see Table 6.1.2).

Generated was data on engine parameters, mean values and standard deviations from actual and simulated data. This is summarized in the form of predicted and actual values following one another; P for predicted and A for actual. These were all from engines with a previous record. As can be seen from Table 6.1.2A, the predicted and the actual standard deviations are often drastically different. Once again, looking at the HPOT discharge temperature channel B values, the engine-to-engine standard deviation for the predicted value at the 109% power level is 61.07373 while the actual value is 118.6592 (almost double).

Differences of the above mentioned nature raise the concern of using precomputed means and standard deviations for the SAFD. This fact is the fundamental reason for choosing the first incoming value of each parameter measurement as the basis for determining the actual mean value to be used by the SAFD during its first two-second operation rather than using a precomputed value.

6.1.1.1 SAMPLE INCIDENT DESCRIPTIONS

A sample of recent incidents are described in the following paragraphs:

1. Test No. 902-428

Scheduled Duration (SDUR) = 700 seconds
Achieved Duration (ADUR) = 204.12 seconds
Engine NO. 2106
Date: July 1, 1987

Engine performance was nominal until engine start plus 163 seconds. At 163 seconds, HPOT discharge temp in Channel A (CHA) began to rise indicating the presence of a hot streak in the OPB injector, HPOT discharge temp in Channel B (CHB) did not respond. The hot streak was localized and due to the rotating effect of the turbine, only a CHA sensor responded.

Posttest examination revealed erosion of the oxidizer preburner injector face and localized burn-through of the HPOTP turbine sheet metal adjacent to the injector erosion area. There was no external engine damage and heating was isolated to the areas noted above.

REDLINE PARAMETER - HPFT discharge temp sensors (231,232) dropped below their lower limit. Pneumatic shutdown was initiated because a hydraulic lockup was in effect (part of the test plan).

OTHER PARAMETERS SHOW CHANGES

879	HX INT TEMP
459-480	HPFP DS PR-PREBURNER PC = ΔP_1
459-410	HPFP DS PR-PREBURNER PC = ΔP_1
743	HPOP SPEED
200	
201	MCC PC AVG (new redline on this parameter was put <u>after</u> this incident)
327-328	HPOP BAL CAV ΔP

2. Test No. 902-471
SDUR = 700 seconds
ADUR = 147.06 seconds
DATE: June 2, 1989

The LPFD #3 flex joint bellows expanded due to a D/S tripod legs break. The tripod missile ruptures a .035" wall in the LPF duct and a leak is initiated. Missile impacts flow straightener and comes to rest. At start plus 147.43 sec. a fire is observed and at 147.58 sec. the lower east thermocouple temp exceeds redline of 635°R. The cutoff was initiated at 147.64 seconds.

REDLINE PARAMETER - Facility cutoff initiated by PID 1493, lower east powerhead thermocouple redline resulting from hydrogen fire originating in the region of the low pressure fuel duct near the HPFTP.

OTHER PARAMETERS THAT SHOW CHANGES

270	Fuel density
203,204	LPFP discharge Pr A,B
2035	
827	Eng F1 in Pr 3
821	Eng F1 in Pr 1
233	HPOT ds temp A
234	HPOT ds temp B
86	HPFP in Pr avg
1021	Eng F1 in T
819	Eng F1 in Pr 2
43	MCC PC avg
873	LOX Tank disch Pr

3. Test No. 904-044

SDUR = 1337 seconds

ADUR = 1270.72 seconds

Date: June 23, 1989

A bearing in the HPOTP failed. Non-flight configuration HPOTP post shutdown hydraulic/H2 fire due to rupture of OPB preburner bowl D below girth weld. Pneumatic control assembly damage and main oxidizer valve actuator neck fracture prevented valve closure, propellant shutoff by prevalues. No facility damage, engine external minor fire damage, no expelled fragments, FPB/OPB, HPFTP, LPTPs, nozzle, MCC and main injector showed no damage. Powerhead damage was isolated to oxidizer preburner heat exchanger bowl. Data and hardware assessment pinpoint source of failure to HPOTP pump and bearings.

REDLINE PARAMETER - MCC PC CH AVG 400 PSI less than Pc Ref.

OTHER PARAMETERS THAT SHOW CHANGES

40	OPOV ACT POS
42	FPOV ACT POS
371	MCC HG IN PR
52	HPFP DS PR
656	PBP BRG BK PR
232	HPFT DS TMP

6.1.1.2 PRELIMINARY SELECTION OF TESTS FOR SAFD IMPLEMENTATION

From the list in the previous Table (6.1.1) and from test histories, a preliminary selection of incident tests was derived for the purpose of implementation on the SAFD algorithm with real-test data. The selection was based on the need to cover a wide range of failure types. Thus, failures that have been simulated on the SAFD algorithm previously, failures that were representative of the most critical and most recurrent anomalies, as well as those that represented fast or slow occurring failures, were selected. The selected list of incidents is presented in a Table (Table 6.1.3) with their corresponding test numbers.

6.1.2 PARAMETER IDENTIFICATION (PID) NUMBER ASSOCIATION WITH TESTS

Every individual measurement parameter is associated with a PID number for each specific engine test. These PID numbers often change from test to test and from engine to engine, since in some cases, new sensors are added and in others, existing ones are removed. Thus, the redistribution of the measurement sensors create the need to identify the PID numbers for each test use in order to apply test data to the SAFD algorithm.

Failure modes, according to the line replaceable units in the Failure Modes Effects Analysis (FMEA), are listed in Table 6.1.4.

Test data processing of the SSME includes storage of measurement data in computer files that only accommodate 9 PIDs per file (meaning 9 measurements). This is apparently necessary for the failure mode effects analysis (FMEA) that is carried out after every failure occurrence.

In order to make the above mentioned files compatible with the SAFD algorithm and make more than 9 measurements available to the SAFD algorithm, a conversion computer code is required.

A computer program was written entitled CONVDAT (see Table 6.1.5), that can combine up to four (4) data files into one file (36 measurements) accessing them on the CDC computer NOS operating system. Each of the original data files must be transferred to the CDC system by using a special procedure and then edited as follows: 1) remove all blank lines, 2) edit descriptions into the following format - first line should give the description of the test (engine number, date, etc.) using a maximum of 60 characters. The second line should have the first PID number with descriptions, using a maximum of 30 characters. The third line should have the second PID number with descriptions, and so on, until the last PID number is covered, each using 30 characters or less.

Once all the files have been converted the CONVDAT routine can be used in the following manner: 1) attach the first file to TAPE20, the second file to TAPE21, the third file to TAPE22, and the fourth file to TAPE23; 2) change the first four lines to reflect the correct accounting information. Following these steps the output file is generated in TAPE31. Change the name of this file; 3) update the values of the parameters on the namelist \$GIVEN. The parameters in the latter are defined as follows:

NPID1 = number of PIDs on TAPE20
NPID2 = number of PIDs on TAPE21
NPID3 = number of PIDs on TAPE22
NPID4 = number of PIDs on TAPE23
TSTART = data start time
TMAX = data stop time

Following the above mentioned steps, the CONVDAT routine can be executed and all of the four files will be combined into one file.

6.1.3 UPDATING AND FINALIZATION OF SAFD MONITORED PARAMETERS

Presently, SAFD uses 24 distinct outputs from SSME instruments. In the original list of SAFD monitored parameters there were some parameters that were totally removed from engine instrumentation or eliminated as a redline. Such parameters are: 1) injector coolant pressure (PID No. 366 non-existent), 2) HPOTP primary seal drain pressure (PID No. 951, eliminated as a redline). From the SSME FMEAs list of the highest ranking failures, 48 engine parameters were selected that encompass measurements related to HPFTP, HPOTP, LPFTP, LPOTP, HEX, MCC, HGM, OPB, FPB, Main Injector, OPOV, FPOV, CCV, and Nozzle. From these parameters a list of 24 of those parameters that have the potential of indicating a failure in the shortest possible time was selected as the final list for SAFD monitoring. The lists of the original and current SAFD monitored parameters are shown in Tables 6.1.6 and 6.1.7, respectively.

Nine of the original parameters were deleted and eleven new ones were added. Those deleted were: 1) injector coolant pressure (366), 2) MCC HG in Pc (367), 3) FPB Pc (410), 4) OPB Pc (480), 5) MCC CLNT Dis. Temp. (18), 6) engine OX injector pressure (858-859), 7) LPOTP pump dis. pressure (302), 8) HEX inlet pressure (878), 9) HEX inlet temp. (879).

6.1.4 SSME CRITICAL OPERATING PARAMETERS: A COMPARISON BETWEEN NOMINAL (PREDICTED) VALUES AND ACTUAL ENGINE DATA

In Table 6.1.8, the engine parameters that are predicted prior to a test and compared with actual data from several tests on each of three SSMEs (2107, 2011 and 2024), are summarized. The values herein are at 109% power level and are selected at specific time instants as indicated in the Table. The last two columns list the corresponding nominal values (those values that are picked when a brand new engine is tested) and their engine-to-engine standard deviations (SD) calculated from a randomly selected set of actual hot-fire test data (the very last column). As can be seen in several of these parameters, the difference between the actual and nominal values could be greater than three times SD (3 sigma). Examples of these are: 1) HPFP speed, difference between nominal and actual value is about 753 rpm while the SD is 107; 2) HPOT DS TMP, difference between actual and nominal is about 104 and the SD is 33; 3) OPOV position, difference between actual and nominal is about 6.24 and SD is 1.89. The reason for evaluating such differences is the fact that the SAFD algorithm presently needs a precomputed mean value for each parameter to check on failures during the first 2-second interval after the algorithm starts. Two of the five simulations that was performed during the Phase I and II studies, test 901-340 was shut off due to a "false alarm" for the only reason that the input mean values were much further off from the actual values than 3 sigma. Thus, if such false alarms are to be avoided as much as possible, it is more judicious to choose a mean value that is closest to the first incoming measurement output for each parameter that can be picked up at the very start of the SAFD algorithm, as soon as the measurements are sensed. The final approach to such a choice of the starting mean value should be decided upon after careful analyses of existing mean value predictions and their corresponding SDs.

6.1.5 CHARACTERISTIC EFFECTS OF PRESURIZATION AND VENTING ON SAFD PARAMETERS

During SSME testing, the LOX tank or the fuel tank, or both are either pressurized or vented several times during the course of a test in virtually every test. These pressurizations/ventings effect some of the parameter values over and above the power level variation effects. Thus, at least eleven of the 24 new SAFD monitored parameters are effected by the venting/pressurization of especially the oxygen tank. Moreover, closure of the fluid or the GOX repressurization valves also has some effects on parameters such as the HPOP and the low pressure fuel pump speed, as well as the FPOV actuator position (see Figures 1 and 2). Analyses on various engine data with and without LOX venting was carried out and the results are summarized in Table 6.1.9. Clearly, almost all parameters are effected, but only about half are significantly influenced to be considered in simulations. Well-defined plans exist to incorporate the effects of such venting and pressurizations as well as of repressurization valve closures on the SAFD parameters using existing SSME "influence coefficients." Thus, a special formula exists that will provide the actual value of any SSME parameter under a given power level and at steady-state conditions. This formula will be utilized to compute varying averages (in a piecewise linear manner) for those parameters effected and a safety band will then be placed around the actual average value of the parameters. This will provide a much healthier approach to failure detection under the above mentioned perturbations.

6.1.5.1 TIME-SLICE TO TIME-SLICE STANDARD DEVIATION VARIATIONS DUE TO LOX VENTING

A separate study was undertaken to assess the influence of LOX venting on various SSME parameters under various time interval calculations of the standard deviations (SD). As expected, when the SD of most parameters were calculated during very short time intervals (less than 1 second) the values obtained were low. However, the SD steadies as it is calculated during intervals longer than 1 second. Some parameters show an increase in SD due to transient effects, such as LOX venting, while others show a decrease. Moreover, all parameters show a level of stabilization of the SDs after two

seconds. This is a relevant result, since in the present SAFD algorithm the SD for each parameter will be calculated on-line during the first two seconds from the start of the algorithm. Thus, the two-second interval calculated SD should be close to the actual slice-to-slice engine SD.

6.2 SAFD ALGORITHM AND SIMULATIONS

The original configuration of the SAFD algorithm encompassed three approaches to failure detection. The first, Approach 1, used during the first two-second period from the termination of a transient, involves utilizing precomputed average values and standard deviations (SD) for each parameter and setting up a 3-times-the-standard-deviation band above and below the average values for limit checking. Thus if a signal violates these band limits then a warning would be flagged out. If several of such flags are available at any instant, engine cutoff is initiated.

In Approach 2, the average value calculated for each parameter during the first two-second period after a power transient was fixed at the end of the two-second interval for the rest of the steady-state operating regime. Moreover, the moving average (MA) taken during the first two-second interval was continuously updated every 80 milliseconds during the course of algorithm operation (by dropping its last/earliest measurement and picking up and adding the current value of the incoming measurement and thus, calculating the new MA). The last MA for each parameter value was compared with its corresponding limits for faults. The limits herein were narrowed down to one precomputed SD above and below the averages. The third, Approach 3, also used the same safety band of one SD on each side of the average for limit checking but it utilized the on-line real-time running average instead of the fixed one as a mean value. Herein actual data was used for comparison with the limits. The latter two approaches were active after the first two-second interval of algorithm start.

The above three approaches were carefully studied and analyzed and it was concluded that the two-second long running average is too insensitive to changes in the SSME. Thus, it was decided to compute MAs at each measurement step (40 milliseconds in CADS output with an option of 20 milliseconds, hardware permitting), for five (or 10) of the last consecutive measurements and to continuously update it by dropping the very last (earliest) of the measurements and adding on the current value to get the average of each parameter. Moreover, a standard deviation is also computed on-line real-time during the first two-second interval after algorithm start

and that value is used to arrive at a $2N \times SD$ bandwidth for limit/trend checking ($N \times SD$ above and one below the average value). However, to determine the validity of such an approach, values of SDs (engine-to-engine, run-to-run, slice-to-slice) from actual test data were evaluated by computing them from various time slices, with different sampling intervals, to find out about their variations. This helped determine if the standard deviation from an initial two-second data of a steady-state condition does actually reflect the true standard deviation of the whole steady-state period of the monitored parameters and if such an approach will not lead to premature cutoff. It was found that N has to be quite large in some cases in order to provide a sufficiently large bandwidth that will avoid false alarms. This is due to the fact that the calculated SD reflects only the sensor noise levels and does not include the effects of other excursions due to transients (such as repressurization or venting) and nonlinear behavior. Also, work was performed on sensitivity studies regarding the effect of averaging intervals on the average values and the overall performance of the SAFD algorithm.

6.2.1 SAFD OBJECTIVE AND SCOPE

The main objective of the Real-Time Failure Control contract is to develop a real-time failure detection algorithm that is signal-based and that detects anomalous behavior of the SSME earlier than the existing redline system.

The SAFD works, as it currently stands, only during SSME steady-state test conditions. It utilizes both low and high frequency measurement signals from 24 key parameters that are currently monitored. However, the option of expanding the monitored parameter list would not require extensive effort. Eight of these parameters are facility and 16 are CADs. All major redline parameters are included in the SAFD, based on the fact that all these are key to a safe engine operation.

6.2.2 THE CURRENT SAFD ALGORITHM

The SAFD algorithm in its present configuration starts at 5 seconds after a start transient or 2 seconds after the completion of a scheduled power transient. As a safety feature, the first measurement values (after algorithm start) of all the 24 monitored parameters are checked against safety limits formed by placing a safety band of $N \cdot SD_p$, where N is a predetermined multiplying factor (normally 4) and SD_p is the precomputed SD. If several parameters (the number of which should be decided prior to a test, usually between 3 and 6) violate these limits then an engine shutdown is signalled. This check will detect any anomalous behavior that could have developed during start or a power transient. If no failures are detected at the first instant then the measurement values of the 24 parameters are chosen as the mean values for the next 2-second interval of the algorithm operation. During this time an on-line real-time SD and a moving average (MA) is calculated that is the average of 200 milliseconds worth of data for each parameter. This MA is updated at every sampling interval (40 milliseconds for the CADS and 20 milliseconds for the facility) by dropping the last value of the measurements and picking up and adding on the most recent one. This MA is checked against a safety band formed by placing safety limits around the above mentioned fixed average (the first incoming measurement value) of $N_1 \cdot SD_p$ bandwidth (where N_1 is a weighting factor normally taken to be 3). If several parameters simultaneously indicate anomalous behavior then engine shutdown is signalled.

If no anomalies are detected during this two-second interval then the last computed MA is fixed as the mean value (MV) for each particular parameter for the rest of the algorithm operation (until another scheduled power transient). A safety band is formed around this fixed MV by placing limits above and below it of $N_2 \cdot SD_c$ (where N_2 is a weighting factor and SD_c is the calculated SD). Then the on-line MA, that is continuously being updated, is checked against these safety limits at every sampling interval. If several parameters indicate violation of the safety limits then engine shutdown is signalled.

This process is stopped at every scheduled power transient and is re-started two seconds after the completion of these power transients. For a visual picture of the algorithm operation see the schematic in Figure 3.

6.2.3 SAFD REFINEMENTS

The SAFD algorithm was further modified (from its Phase I and II condition) to incorporate all the 24 newly selected parameters (Table 6.1.7) and to accommodate the 200 millisecond MA and the SD calculated during the first two-second interval. Moreover, actual test data from incident tests was transferred to the CDC system and all the errors and discrepancies in the data files were eliminated for processing. Most of these tests resulted in a premature redline cutoff due to a failure. Test data was then combined into two data files, one for the facility data and the other for the controller data. A SAFD input file that included most of the 24 SAFD parameters, was also prepared for each test and the algorithm was executed. Several adjustments are always needed (during SAFD simulations with real test data) for the data to be completely usable by the SAFD under all power levels.

Modifications to the model were made to incorporate new failure detection shutdown criteria over the first two-second interval following a scheduled transient. The new approach involves using the first measurement data as the mean value of each parameter in the shutdown logic for this interval. A set of precomputed SD values for the new parameter list must be selected and incorporated into the model for each test. These SD values are required for the one-time comparison with the "nominal" (to check for anomaly) and for the shutdown logic over the two-second interval following a transient. Moreover, the only time nominal values for key SAFD parameters will be needed is during the first instant when the actual measurement data is received. Here the nominal will be compared with the actual and if the difference is greater than 4 SD, this will be considered anomalous behavior. During the follow-on work logic will be included so that the model will accommodate transient behavior, occurring as a result of scheduled LOX and fuel venting, without interpreting these transient behavior occurrences as failures.

The above mentioned (Phase I and II) three fundamental approaches were considered in the refinement the SAFD algorithm, as was described earlier. The underlying purpose of these refinements was to enhance the algorithm performance, especially for avoidance of premature cutoff. One of the principal reasons for premature engine cutoff is sensor failure. The SAFD currently does not address this type of failure. Thus, special algorithmic

and software tools need to be studied that can increase the capability of the SAFD algorithm to address sensor failures. One way to accomplish detection of sensor failures is to consider a single anomalous output as due to the failure of the corresponding instrument while all the remaining outputs are normal. This approach needs to be studied further and such cases should be simulated with the transient model.

Additional refinements to the SAFD algorithm were also looked at. One such refinement is the new "slope-average approach," which entails monitoring the slopes between consecutive averages. Thus, the difference between each pair of consecutive averages is divided by the time interval separating them and the answer is considered as the slope-average. The advantage of such an approach is that it produces very sensitive outputs of signals that have minimal noise (since the sensor noise is "filtered" out by taking averages). Moreover, anomalous trends can easily be detected through evaluation of the sign of the slope-average and whenever there is a trend of positive or negative slopes for a few consecutive intervals, then there is a potential failure. This approach needs to be carefully simulated for evaluation relative to failure detection and sensitivity to failures.

Preliminary simulations were carried out on actual incident test data and plots were generated for various parameters. The plots show the parameter signal, the on-line average, and the fixed average, as well as the slope-average. Moreover, the plots indicate that the slope-average could be used as a reliable indicator of anomalous behavior with the potential of earlier detection compared to the SAFD algorithm in some cases. For example, the increasingly positive trend of the slope-average of the three parameters shown in Figures 4A, 4B, and 4C beginning at about 209 seconds, indicate that the slope-average approach could provide detection of the particular transient at an earlier time than the SAFD algorithm. The slope-average profiles suggest that this test could have been shut down earlier, perhaps at about 209 seconds, as opposed to the SAFD algorithm cutoff time of 214.79 seconds.

6.2.3.1 SAFD REFINEMENT COMPARISONS

In order to compare the performance of the SAFD algorithm with and without refinements, two SSME hot-fire tests (901-284 and 901-364) were considered. Three cases for each test were simulated (Cases I,II,III). The first of these tests was a failure that occurred during the first 10-second period due to a Lee Jet anomaly. This caused the measurement values of parameters to be off nominal and eventually the redlines cut the engine off at 9.88 seconds. The original SAFD simulation had used a recomputed nominal MV and SDs as well as actual test values for five of the parameters as follows:

Parameter	Precomputed Mean	Actual Value	SD
1. HG Inj. delta P	255	151.28	24.53
2. HPFT delta P	1860	1270.5	20.
3. HPOTP delta P	1800	918.58	46.5
4. MCC Pc	2995	1829.5	21.2
5. MCC clnt dis. temp.	420	757.97	6.3

Variations between the actual values and the precomputed mean for each of these parameters being larger than three (3) times SD, the original SAFD algorithm cut off the engine after the first iteration. A similar "false alarm" occurred in test 901-340 simulations with the SAFD algorithm. In order to evaluate the algorithm performance, Approach 1 (working during the first 2-second interval) was shut off and Approach 2 and 3 were used. With the original SAFD algorithm, engine cutoff occurred at 8.86 seconds while with a 200 msec running average and an on-line computed SD, the cutoff was at 7.94 sec and 7.14 sec respectively. Similarly for test 901-364 (see Table 6.2.1).

In the above mentioned three cases for each test, the following were performed:

- 1) In Case I, a precomputed SD and the 2-second (50 measurement) MA were used for limit checking at each 40 millisecond interval.

- 2) In Case II, a precomputed SD was used during the first 2-second interval and a band of 3-SD was put below and above the precomputed MV (as in Case I); but after the 2 seconds the SD, that was computed during the first 2 seconds, was weighted and used for assigning similar but lower limits. The limit checks were again performed by the 2-second (50 measurement) MA every 40 milliseconds.

- 3) Case III involves a 200 millisecond MA (every 5 measurements) but also a calculated (during the first 2-seconds) SD weighted appropriately and used to assign limits around the calculated mean value.

Test 901-364 was used once again, to compare performance of SAFD with and without refinements. Thus, even though there was no failure at 216.71 seconds (the original point of SAFD Phase II simulation cutoff), the signals were showing a trend that provided a good base to check the algorithm performance. It should be pointed out that there was a LOX tank pressurization at 200 sec. and this was the reason for the trending of many of the parameters that were used to test SAFD. However, there was a real failure that was detected by the engine redlines at 293.15 sec., which was or was not related to this transient effect. As far as the algorithm is concerned, these kinds of transient signals are similar to actual failures in behavior and can be used to do some performance and sensitivity analysis. The actual failure was also analyzed through the algorithm to compare with the redline.

In Tables 6.2.1 and 6.2.2A,B,C,D,E,F, a comparison can be made of the $N2*\sigma$ values (upper/lower signal limits defined by $\text{mean} \pm N2*\sigma$) between Case I and Cases II and III. For most parameters, the $N2*\sigma$ values are larger for Case I compared to Cases II and III, yielding more generous upper and lower signal limits. Upper/lower signal limits as close to the signal mean as possible, without being so restrictive as to trigger a false alarm, are desired to facilitate SAFD failure detection at the earliest possible time. The simulation results for the three cases, for each of the two tests, are presented in the above mentioned Tables.

6.2.4 SAFD ALGORITHM SIMULATIONS

Several cases of real-test data from major incidents were applied to the SAFD algorithm to evaluate and understand its strengths and weaknesses. Also, sensitivity studies were carried out to evaluate the effects of: 1) averaging at 40 msec., 80 msec., 120 msec., intervals; 2) the weighting factor N for the determination of the safety bandwidth for each parameter; and 3) the number of anomalous parameters required for a decision for engine shutdown. The results of the simulations are presented in what follows.

6.2.4.1 ALGORITHM SIMULATION OF TEST 750-285

SAFD model simulation results of SSME hot-fire test 750-285 are presented herein. Tests 750-285 experienced a premature engine shutdown due to the development of a small fuel leak downstream of the main fuel valve in downcomer #8 around 204 seconds following start. The fuel leak resulted in a fire and was detected by a powerhead thermocouple redline, triggering an engine shutdown at 223.56 seconds. This test was conducted over a single power level (109%) and did not involve propellant venting and repressurization, or propellant transfer.

SAFD model simulation was initiated at 100 seconds following engine start. Since the fuel leak was small, only a small number of parameters were affected. Seventeen of the twenty-four SAFD parameters were available for simulation. About eight of these parameters appear to reflect the failure. For each set of figures, the Figure 5-1 shows the measurement signal, and the Figure 5-2 shows the SAFD signal average and upper/lower signal limits. Several simulation runs were made while varying the signal upper/lower limits (i.e., variations in n) for each of the eight parameters which appear to reflect the failure. The best of the simulation runs obtained resulted in SAFD shutdown at 212.48 seconds, compared to the redline shutdown at 223.56 seconds, due to detected anomalies in the oxidizer preburner oxidizer valve (OPOV) actuator position, the HPFTP coolant liner pressure, and the HPOTP intermediate seal purge pressure. Table 6.2.3 shows the composition of the signal limits (defined by $AVG \pm n*SD$) for selected parameters, i.e., the average, standard deviation, and n values. The average and standard deviation values are computed over the first two seconds of the algorithm

operation and are fixed at the end of this interval. The signal limits can be adjusted by varying the values for n. A careful review of Figures 5A-1 through 5H-2 will reveal that an attempt to reduce the SAFD signal limit bandwidths will result in a false alarm. This is the case when an attempt is made to reduce the signal limit bandwidths for those parameters that appear to reflect the failure (Figures 5A1 through 5H2). A false alarm would result due to signal average variations prior to the real anomaly occurrence.

As an example, consider the parameter of Figure 5F1-2, the low pressure oxidizer pump discharge pressure. While Figure 5F1 indicates the anomaly should be detectable sometime following 205 seconds, Figure 5F2 reveals that because of the signal limit values in relation to the signal average, reducing the signal limits by lowering the value for n would result in a false alarm by the upper limit prior to detection of the real anomaly by the lower limit. This of course is a direct result of the particular average value used in the signal limit definition of this parameter.

Values for two of the algorithm variables - #P (number of simultaneously occurring anomalous parameters required for shutdown) and n (factor which determines signal limits) - must be predetermined. The values selected for these variables can affect the algorithm's performance dramatically, in terms of both its reliability and its advantage over the redline technique. Selection of the #P value should be large enough to insure a reliable and accurate failure detection, yet small enough to allow the algorithm to respond to a potential failure early. Selection of the n value is critical to reasonable signal limits for the parameters. If the selection for n is too small, the signal limit bandwidths will be too small, possibly resulting in a false anomaly detection. An unnecessarily large selection for n will not facilitate early anomaly detection and may even prevent detection of anomalous behavior. Selection of a value for n to serve all parameters optimally is difficult since the signal amplitudes and frequencies of oscillation vary greatly among the parameters. However, ideas exist that will lead to the development of an automated approach to the selection of n and #P that can be worked on during the next phase of this program.

Simulation results for test 750-285 reveal that a single n value should not be used for all parameters to achieve accurate results. It is necessary to optimally choose an n value appropriate for the behavior of each parameter.

6.2.4.2 ALGORITHM SIMULATIONS OF TESTS 901-340 AND 902-471

SAFD model simulation results of two SSME hot-fire tests which experienced failure are presented herein. Test 901-340 involved failure of the high pressure fuel turbine (HPFT) and was shut down at 405.5 seconds by the HPFT discharge temperature redline. Engine damage incurred included HPFT turnaround duct wall fractures and torn sheet metal, and secondary rotor platform seal fractures. The results of simulating this test with the SAFD algorithm are presented in Table 6.2.4. Four simulation runs, involving algorithm cutoff by Approach 2, are shown for variations in the Approach 2 signal upper/lower limits (i.e., variations in n_2) and in the number of parameters experiencing anomalous behavior simultaneously required for the algorithm to signal a shutdown (i.e., variations in #P). The three cases for $n_2=26$ and #P=6,7 and 8 resulted in test shutdown by Approach 2 (after the first two-second interval) at 279.67 and 295.42 seconds for #P=6 and 7, respectively. The case for #P=8 did not result in a shutdown, however, indicating that fewer than eight parameters had signals outside of their respective upper/lower limits simultaneously at any given time. A case was also simulated with a slightly larger bandwidth around the signal mean ($n_2=27$) with #P=7. For this case, the algorithm signalled a cutoff at 298.7 seconds, later than the comparison case for $n_2=26$ and #P=7, which had a cutoff of 295.42 seconds. The simulation results for selected parameters for the case with $n_2=26$ and #P=7 are shown graphically in Figures 6A1,A2 through 6F1,F2. Both the parameter measurement signals and the algorithm signal means, with the earliest anomaly time, are shown. For the case with $n_2=27$, i.e., larger bandwidths around the means, and #P=7, some of the parameters reached their respective signal limits at slightly later times.

The second simulation was of test 902-471 which involved a hydrogen fire originating in the region of the low pressure fuel duct near the HPFTP due to a leak. This test was shut down prematurely at 147.68 seconds, initiated by the lower east powerhead thermocouple redline. The simulation was performed for the hot-fire test data from 50 seconds, at 100% power level, to the time of the redline cutoff at 147.68 seconds, at 104% power level. The power level change from 100% to 104% was at 140 seconds. Since the algorithm is for steady-state operation only, simulation was performed in two stages corresponding to the two power levels. Simulation for the first

stage was from 50 to 139 seconds, and for the second stage was from 145 to 147.68 seconds. The simulation results are presented in Table 6.2.5. Seven simulation runs are shown for variations in n_1 , i.e., in the Approach 1 signal limits, and in $\#P$. In all cases, the algorithm signalled a shutdown by Approach 1 during the second power level (104%). There are five cases for $n_1=2.5$ and $\#P=4,5,6,7$ and 8 showing the later algorithm shutdown times as a result of increasing the number of simultaneous anomalous parameters required for algorithm shutdown. A simulation run was also made for $n_1=2.0$ and $\#P=6$ which resulted in a premature shutdown by the algorithm. This case indicates the signal limits did not encompass a large enough bandwidth around the mean. A simulation run performed for $n_1=3.5$ and $\#P=6$ in which the algorithm did not trigger a shutdown indicates the bandwidth was too large. The simulation results for selected parameters for the case with $n_1=2.5$ and $\#P=8$ are shown graphically in Figures 7A through 7I. The parameter measurement signals are shown indicating the earliest anomaly time for the respective parameters as detected by the algorithm. Both of the above tests were without venting/pressurization.

6.2.5 HEURISTIC EVALUATIONS AND SENSITIVITY ANALYSIS

Several simulation runs were carried out using the SAFD algorithm on SSME test data from test 901-340. During this test a redline shutdown occurred at 405.5 seconds from start due to a HPFTP failure (HPFTP turnaround duct bulged cracked and tore). The original SAFD algorithm simulations had engine cutoff after 0.08 sec. from the start of the algorithm, which of course, was a "false alarm." The false alarm was apparently due to the large difference between the precomputed mean values for the various engine parameters monitored by SAFD and the actual values from the test data. Thus, in order to avoid such premature cutoff, mean values closer to the actual data were selected and, using three times the standard deviations (SD), safety bands were set around each, to be used for the first two-second interval. Moreover, SDs were computed on-line during the first two seconds of the SAFD running and were used (after multiplication with an appropriate factor N2) to set the safety band around the monitored parameters. The measurement signal averages were also completed during the same interval and the value obtained fixed as the working mean value throughout the simulation. The comparative averages were updated every 40-millisecond interval using the latest 50 values. Presently, the last 5 values will only be utilized for an updating of the above mentioned averages every 200 milliseconds (eventually, when data is available every 20 milliseconds, the last 10 values will be used to update the average every 20-millisecond interval).

Various sensitivity analyses were performed on this test by varying the multiplication factor N2 on the SD as well as the number of parameters, experiencing anomalous behavior that was required for the SAFD algorithm to trigger engine shutdown. Some of the results are presented in Table 6.2.6. The SAFD simulation results for the four different runs are presented in Tables 6.2.7A through 6.2.7D while Figures 8A through 8I show the signal profiles for some of the parameters. As shown in Table 6.2.6, varying N2 and the number of parameters required for shutdown effect the outcome. Thus, appropriate values for each of these should be carefully selected.

6.3 SSME DIGITAL TRANSIENT MODEL FAILURE SIMULATIONS

The SSME digital transient model (DTM) was used to simulate actual SSME test failures. The SSME transient model is a modular digital computer program which is being run on the CONVEX computer using a SUN workstation as the front end system. This particular version of the model has evolved from 25 years of simulating rocket engine transient performance. Several generations of engines have been simulated and great confidence is placed in the predictions of these transient models.

The simulations of real engine failures were done for the following reasons. First, as a preface for the use of the model, on-line with the SAFD algorithm, to create a closed-loop demonstration of the SAFD algorithm's capabilities. Second, to gain increased confidence in the model's ability to simulate engine failures, and third, to use the SSME transient model to simulate certain failure modes that are hypothetical and have not occurred on actual engines.

6.3.1 DTM SIMULATION OF TEST 901-284

Several of the actual engine failures were simulated by the SSME DTM. The description of the failures and examples of the model output for each of these tests are presented with heuristic evaluations.

The effort to simulate measurement and component failures took longer than expected. The fundamental difficulties in simulating actual failures by using the SSME digital transient model entail: 1) imperfect matching of parameter variations caused by actual failures with the simulated values due to the highly nonlinear dynamics of the SSME, 2) errors in the predictions of the actual source or cause of failure from effect. Thus, if the cause of a failure is pinpointed exactly, then the simulations will indicate very closely matched behavior relative to the actuals. However, even if the exact cause of a failure in the system is known, being nonlinear as it is, it is very difficult to get 100% correlation between actual and simulated behavior.

In certain situations, the inverse approach is more efficient. Namely, to start with the effects and to try to get to the cause, as in the case of efficiency variations. However, the SSME, being very complex and having nonlinear dynamics, there are multiple causes that could result in certain effects and vice versa.

6.3.2 TEST 901-284

During the incident test 901-284 the following failure was experienced:

1. Channel B of the controller cut itself off at 3.25 seconds. Channel B shutdown was caused by failure of electronic components in the facility power supply.
2. At 3.9 sec, the Lee Jet orifice, used to purge Channel A Pc transducer passage, became dislodged and caused the Pc transducer to sense MCC coolant flow pressure instead of Pc. This erroneously high reading (3800 psi) caused the controller to close the OPOV to reduce Pc to the desired 3012 psi. A few milliseconds later, the controller calculated a mixture ratio of 9.0 and commanded the FPOV full open in an attempt to reduce the MR to 6.0.
 - a. The immediate results of the controller action, based on an erroneous Pc, was operation in an abnormal mode, characterized by high fuel flow and low turbine inlet temperatures of the OPB and FPB. In fact, the OPB inlet temperature fell quickly to about 440°R (-20°F) which assured freezing of the water which makes up 10% of the total 40 lbs/sec.
 - b. The ultimate result of the controller actions was a fire in the HPOTP at 9.7 sec due to rubbing in the area of the LOX primary seal slinger. The rubbing was caused by a high axial load which displaced the rotor assembly at the pump end of the HPOTP housing. This high axial load was caused by ice formation in the cavity between the housing and the 2nd stage turbine wheel which resulted in reduction in the cavity pressure from about

2500 psi to near ambient. This reduced pressure on one side of the turbine wheel and caused an estimated increase in rotor axial force of about 31,000 lbs, which far exceeded the control capability of the balance pistons to control the position of the rotor.

Plots were generated from simulated data of the above mentioned test and overlayed on actual plots from real-test data (see Figures 9A-9L). The parameters indicate very close matching of real data with simulated data, thus indicating the accuracy of the DTM.

6.3.3 TEST 902-428

Computer simulation results of the incident test 902-428 are presented in this subsection. At the 163rd-second from engine start of this test, the OPB injector experienced a hot streak. Thus, the HPOT discharge temperature channel B (PID No. 234) sensor indicated significantly higher than normal temperature reading throughout the test.

Figure 10A shows the main combustion chamber pressure model with the test data overlaid. Figure 10B has the overlays of the HPOT discharge temperature, channel A. Figure 10C has the HPOT discharge temperature channel B reduced by 170°R (due to it running 170°R over normal) overlaid with the Digital Transient Model (DTM) results. The heat exchanger interface temperature (HXIT) was one of the parameters where the failure was dramatically exhibited. The present configuration of the DTM output does not include this parameter. But for this case, the DTM was modified to include this parameter as an output. The actual HXIT is measured during hot-fire tests only after oxidizer coolant is mixed into the flow, which then reflects a slightly different value. Hence, the model value only is shown in Figure 10D. For a comparison between the actual HXIT and the model, Table 6.3.1 below represents the percentage change of the parameter value during the time interval shown (column 1), the value calculated by the model (column 2), the net percentage change occurring from first to the second time-instant (column 3), the actual measurement values (column 4) and the net percentage change (column 5). In Figures 10E, 10F, and 10G, overlays of chamber mixture ratio, fuel preburner and oxidizer preburner pressures are presented, respectively.

TABLE 6.3.1

TIME	MODEL TOT2MIX		TEST HX TEMP 879	
	Value	Δ%	Value	Δ%
160	1335	----	915	----
170	1340	0.37	920	0.55
180	1350	1.12	930	1.64
185	1355	1.50	934	2.08
190	1320	-1.12	940	2.73
195	1225	-8.24	910	-0.55
200	1165	-12.73	847	-7.43

6.3.4 TEST 750-285

Simulations of the incident test 750-285 that occurred on the SSME on May 21, 1987, on engine 0210 while operating at 109% power level are presented herein. The test was cut off prematurely at 223.6 seconds of a planned 295 seconds, when the powerhead temperatures at the CCV and HPFP exceeded the redline setting of 660°R. At approximately 204 seconds into the test, the nozzle #8 downcomer began to leak hydrogen. The posttest analysis indicated leakage flow to be between .5 and 1 lb/sec, but because of the complex geometry and difficult access to the downcomer, an accurate leak size assessment was precluded. The nozzle was replaced before the next test.

In order to model this failure, a flow path was added to the calculation of flow exiting the downcomer area. This additional flow was set to equal the leakage flow. The leakage flow that was included in the pre-test notes of the next test was initially input in the model. This flow had a maximum leakage of .6 lb/sec. This amount of leakage had a negligible effect on the DTM engine parameters and did not match the test data. Next, the leakage flow was doubled and the model was re-run. The amount of leakage the model experienced is shown in Figure 11A. This has a maximum of 1.2 lbs/sec, close to what the posttest analysis indicated. This amount of leakage caused the model engine parameters to match better with the test data.

Figure 11B shows the high pressure fuel turbine discharge temperature traces from the test data and the transient model. The transient model trace has 150°R added to it. This was done because the test 750-285 ran at a higher temperature than is nominal for this power level. The relevant part of this plot is the temperature trend. Figure 11C shows the high pressure oxidizer turbine discharge temperature traces from the test data and the transient model. The transient model trace has 90°R added to it, for the same reason as mentioned above. Figure 11D shows the oxidizer preburner oxidizer valve position traces from the test data and the transient model. The dead band for this valve is a few tenths, so this is a good correlation between the test and the model. Figure 11E shows the main combustion chamber pressure traces from the transient model and the test data. Figure 11F shows the engine mixture ratio traces from the test data and the transient model.

6.4 SSME DTM HYPOTHETICAL FAILURE SIMULATIONS

There are various potential failures that have never occurred. It would be desirable for the SAFD algorithm to have the capability of detecting any such failure. Thus, a study was performed that entails use of the SSME DTM to simulate the aforementioned types of failures. The intent is to utilize the resulting simulation on the closed-loop (DTM-SAFD) system and assess the performance of the SAFD algorithm in detecting such hypothetical failures. While the DTM provides on-line engine data to the algorithm.

Leakage of fuel or oxidizer is one of the major incidents that could be catastrophic and that is hard to detect. Moreover, the quantity of fuel/oxidizer leakage that can be tolerated, so that the engine could continue to run satisfactorily, depends on the location of the leak. Thus, if a fuel leak is just downstream of the main fuel valve (MFV) its effect will be divided among the three parallel flow paths that branch from the MFV discharge duct. These include the main combustion chamber and the nozzle cooling channels, and the coolant control valve. Therefore, quite a large leak can sometimes occur without having a major impact on any one flow parameter. If, on the other hand, a leak occurs just upstream of the low pressure fuel turbine, its effect will be significant on one flow path. Hence, small leaks can only be tolerated in such instances. It should be noted that any fuel leaks are hazardous and should be detected as early as possible.

6.4.1 RUPTURE IN OXIDIZER PREBURNER PUMP AREA

Simulating leaks with the DTM requires some effort of modifying several parts of the model by introducing additional flow paths. In such an undertaking, a rupture in the SSME oxidizer preburner pump area was simulated. The rupture was assumed to take place on the oxidizer side, downstream of the preburner pump (see Figure 12). An additional flow path for the leak, that would flow from the ruptured area, was incorporated in the model.

Three separate runs of the model were made, with a leakage of 1 lb/sec and 5 lb/sec leakage. The results of each run are presented in Figures 12A through 12J and 12K through 12T, respectively. The engine power level was assumed to be 104% during the leakage initiation time at 30.0 seconds, after system steady-state is reached. The engine control system compensated for the leakage flow by opening the OPOV and FPOV (see Figures 7,8,17, and 18). The engine was back up to nominal value in a short time, about 1 second. The following is a list of the parameter descriptions and the figure numbers of the attached traces.

<u>PARAMETER DESCRIPTION</u>	<u>FIGURE NUMBER</u>	
	1 LB/SEC	5 LB/SEC
Fuel Preburner Temperature	12A	12K
Oxidizer Preburner Temperature	12B	12L
Oxidizer Preburner Pressure	12C	12M
Main Combustion Chamber Pressure	12D	12N
HPOP Discharge Pressure	12E	12O
HPFP Discharge Pressure	12F	12P
FPOV Position	12G	12Q
OPOV Position	12H	12R
Boost Pump Discharge Pressure	12I	12S
Main Chamber Mixture Ratio	12J	12T

A Table (Table 6.4.1) was compiled that shows the effect of each leakage flow (1 lb/sec, and 5 lb/sec) on each of the parameters studied. The effect is defined as the percent change from nominal.

6.4.2 HPFT DISCHARGE FLOW BLOCKAGE

One such failure that involves the HPFT discharge flow blockage, taken from FMEA files, was simulated with the DTM. The blockage was assumed to occur between the High Pressure Fuel Turbine and the Main Injector (see Figure 13A). The amount of blockage was initially set to five times the resistance of the flow path. The engine power level was assumed to be 104% prior to the failure. The failure was initiated at 30.5 seconds, and the model was run from 29 to 39 seconds. The engine control system compensated for the blockage by changing the OPOV and FPOV positions (see Figures 13M, 13N). The following is a list of the parameter descriptions and the Figure numbers of the attached traces:

<u>PARAMETER DESCRIPTION</u>	<u>FIGURE</u>
Fuel Preburner Temperature	13B
Oxidizer Preburner Temperature	13C
Fuel Preburner Pressure	13D
Oxidizer Preburner Pressure	13E
Main Combustion Chamber Pressure	13F
HPOP Discharge Pressure	13G
HPFP Discharge Pressure	13H
LPFP Speed	13I
HPFP Speed	13J
LPOP Speed	13K
HPOP Speed	13L
FPOV Position	13M
OPOV Position	13N
HPFT Discharge Temperature	13O
HPOT Discharge Temperature	13P
Main Chamber Mixture Ratio	13Q
Main Chamber Temperature	13R

6.5 CLOSED-LOOP DTM - SAFD SIMULATIONS

In order to demonstrate the operability of the failure detection algorithm the SAFD was combined with the DTM in such a way that the DTM output was used as inputs to the SAFD algorithm. Any anomalous behavior that effects some of the parameter values can thus be detected by the SAFD if these values are over the limits of the safety bands that are set for each of the parameters. For this purpose, the SAFD failure detection model was combined with the SSME transient model to form a closed-loop system model. The idea behind creating the closed-loop system model is to be able to simulate any failures with the transient model and monitor the parameter signals for anomalous behavior with the SAFD algorithm on-line and real-time. Modifications to the code of both models were required for their combination. For example, subroutine SENSOR of the SAFD model, which reads in the SSME hot-fire test data from input files, has been eliminated as it has no purpose in the closed-loop model. The parameter signals generated by the transient simulation model subroutines will be available to the SAFD subroutines through common blocks and can, therefore, be monitored for anomalies with the SAFD algorithm. Table 6.5.1 correlates the transient model parameter variables with the SAFD parameter variables.

6.5.1 CLOSED-LOOP LEAKAGE SIMULATION

An artificial 5 lb/sec leakage of liquid oxidizer (LOX) was introduced downstream of the HPOTP preburner boost pump as a simulation of a FMEA external rupture (mentioned in the previous section). A non-zero start model run at 104% power level was made with a start time of 29 seconds. The leakage (failure) was initiated at 30 seconds, resulting in anomalous behavior of many parameters. The SAFD algorithm signalled a shutdown during the first two-second interval, by Approach 1 at 30.10 seconds. Seven parameters registered exceedence of the safety band, thus signalling the cutoff.

These parameters include the HPOTP discharge pressure, the HPOTP boost pump discharge pressure, the main combustion chamber pressure, the HPOT discharge temperatures 1 and 2, the LPOTP pump discharge pressure, and the HPFTP discharge pressure. The results of the transient failure detection

simulation are presented in the plots of Figures 14A - 14I. Each plot displays four signals which represent the parameter simulated signal, the signal average, the signal Approach 1 upper limit, and the signal Approach 1 lower limit.

<u>Parameter Description</u>	<u>Figure</u>
HPOTP Discharge Pressure	14A
HPOTP Boost Pump Discharge Pressure	14B
Main Combustion Chamber Pressure	14C
HPFT Discharge Temperature 2	14D
HPOT Discharge Temperature 2	14E
LPOP Discharge Pressure	14F
HPFTP Discharge Pressure	14G
HPFTP Coolant Liner Pressure	14H
FPOV Actuator Position	14I

6.5.2 CLOSED LOOP BLOCKAGE SIMULATION

A failure was simulated which involved increasing the resistance (by a factor of two) of the duct between the HPFT and the main injector as a simulation of a FMEA HPFT discharge flow blockage (mentioned in the previous section). A non-zero start transient model run at 104% power level was made, with a start time of 29. seconds. The failure was implemented three seconds later at 32. seconds, resulting in rapidly occurring anomalies in many of the parameters.

The SAFD algorithm signalled a shutdown with Approach 2 at 32.06 seconds due to detected anomalies in five parameters. Recall that Approach 1 is in operation during the first two seconds of the algorithm operation, while Approach 2 is in operation thereafter. The five parameters include the HPFT discharge temperatures, the HPFTP discharge pressure, the FPOV actuator position, the HPFTP coolant liner pressure, and the fuel flowmeter. The results of the transient-failure detection simulation are presented in the plots of Figures 15A - 15I. Each plot displays four signals which represent the parameter simulated signal, the signal average, the signal Approach 2 upper limit, and the signal Approach 2 lower limit. The plots indicate clearly the engine steady-state behavior followed by anomalous behavior as a result of the blockage, and the subsequent recovery to steady-state due to the engine controller's command of the FPOV and OPOV actuator positions.

The SAFD algorithm detected an anomaly in the HPFT discharge temperature signal far earlier than the potential time of the redline temperature of 1960°R.

Parameter Description

Figure

Main Combustion Chamber Pressure	15A
High Pressure Fuel Turbopump Discharge Pressure	15B
High Pressure Fuel Turbopump Coolant Liner Pressure	15C
High Pressure Fuel Turbine Discharge Temp 1	15D
High Pressure Oxidizer Turbine Discharge Temp 1	15E
High Pressure Fuel Pump Speed	15F
Low Pressure Fuel Pump Speed	15G
Fuel Flowmeter	15H
FPOV Actuator Position	15I

6.6 LESSONS LEARNED

During the course of the present contract, several features of the SSME were investigated in detail and information, useful for future failure detection algorithm development, was analyzed and recorded. Thus, transient effects other than the start and power transients, were found to significantly influence parameter values. If these effects are not compensated for, the failure detection algorithm will lose some of its sensitivity to failures and thus be more sluggish. Two of these effects are due to the repressurization and venting (of fuel and oxidizer) that are carried out during SSME ground tests to simulate actual flight conditions on the engine. These effects are apparent in over half of the 24 SAFD monitored parameters. Some of the effects of GOX and fuel repressurization valve closure are presented in Figure 16 and the effect of venting/repressurization are shown in Figure 17. Moreover, nonlinear behavior of several SSME parameters, that is inherent to engine characteristics, were also identified. These effects were termed nonlinear because of the characteristic shape that each parameter takes in time even in the absence of any venting/repressurization or other transient phenomena. Thus, it takes over 75 seconds for the HPOT turbine discharge temperature, the MCC liner cavity pressure, and the HPOT seal cavity pressure to reach steady-state. While the HPOP intermediate seal purge pressure is totally nonlinear (see Figures 18A,B,C,D,E). If these parameters are to be monitored, then it is necessary to develop estimates of their normal mean values that are piecewise linear or that are represented by predetermined curves that are close to the real parameter value such that the bandwidth placed around such a line can be made less restrictive. For, if the average (mean value) line can be closely represented then the safety band around it can be made smaller and thus provide an increased sensitivity to the algorithm.

In order to evaluate the possibility of a predetermined piecewise linear mean value profile for the parameters that are effected by the repressurization and venting procedures, the planned versus accomplished profile of the engine LOX inlet net positive suction pressure (NPSP) were studied. It was found that the planned profile is very closely traced by

the achieved profile (see Figure 19). Hence, it is possible to determine a piecewise linear average for the effected SAFD parameters by using a predetermined NPSP profile in combination with existing computational routines that calculate the "influence coefficients" that reflect the effects of a given degree of repressurization/venting on a given engine parameter. In this manner, the new piecewise linear average profiles for these parameters will be close representations of their actual values. This will lead to a more sensitive algorithm and thus catch failures in the early stages.

These and other work can be carried out to enhance the SAFD performance and expand its scope significantly.

7. CONCLUSION

Extensive computer simulations with the SAFD algorithm on real SSME incident test data indicate significantly earlier cutoffs than achieved with the existing redline system. Cutoffs were found to be a function of the kind of failure that occurred, the speed with which it progressed and the location and degree of localization of the anomalies. Thus, in fast occurring failures, such as ruptures or breakage of structural areas, the SAFD showed only a slight gain over the redlines. While for slow occurring failures the SAFD algorithm showed significantly earlier shutdown capability.

The performance of the SAFD algorithm depends heavily on the choice of the weighting factor N that determines the bandwidth of the safety limits placed around the average value of each signal for monitoring purposes. Moreover, the added safety feature that the algorithm has is the requirement for multiple anomalous signals for an engine cutoff command. Thus, three, four, five, six or more signals exceeding the safety limits simultaneously leads to a cutoff command. This number should be predetermined for each signal prior to each test. Hence, two factors are important in the decision for engine cutoff. Namely, the weighting factor N and the number of anomalous parameters signalling failures simultaneously. There is no procedure for the selection of these factors other than experience and trial and error presently. However, work has been performed on finding ways of automatically determining these numbers at the start of the algorithm during a test.

The SAFD, as it currently stands, can only handle steady-state test operating conditions and it is turned off during the start transient, as well as during power transients. However, the first instant check that the algorithm is equipped with (that checks the value of each of the first incoming measurement signals against a precomputed nominal expected value) is for detection of anomalous behavior that might have occurred during a transient. This feature provides some degree of fault detection capability at start or power transients. Moreover, the option of expanding the capability to handle transients, as well as other nonlinear and excursion effects are under consideration and plans for such augmentation exist. The

algorithm monitors more parameters than the redlines, with the option of expanding the list even further. Also, the SAFD avoids "false alarms" by the above mentioned requirement of the anomalous behavior of several parameters prior to a decision for engine shutdown.

There are transient effects that effect several engine parameters due to repressurization and venting, as well as to GOX/fuel repressurization valve closures. These effects are presently compensated for by increasing the safety bandwidth to cover parameter excursions due to such transients, thus reducing the sensitivity of the algorithm to actual failures. However, plans to accommodate such behavior have been worked upon and can be implemented in follow-on work. Also lacking is sensor failure detection (except for negative readings). These and other limitations of the SAFD can be worked on and its effectiveness and scope can be enhanced given appropriate planning, analyses, simulations, and judicious approaches.

8. RECOMMENDATIONS

By all means, it is highly desirable to develop a failure detection algorithm for the SSME that can operate under all conditions (steady-state and transient) and that is sensitive enough to detect slow and fast failures at such an early stage that damage to the engine is minimized. There are certain approaches that, if taken, can lead to the above mentioned enhanced and expanded algorithm. In this section a few tasks are outlined that will accomplish some of the enhancements.

8.1 FAILURE DETECTION

The fault detection problem involves a thorough and realistic understanding and specification of the given system. The various failure modes that may occur can be described as either fast occurring and progressing or as incipient (slow developing) faults. Fault detection is approached either via model-based or signal-based techniques. For analytical redundancy purposes some kind of validation of nominal relationships of the given system, using the actual input and the measured output, are carried out and the dynamics of the system are evaluated on-line in a real-time manner (Figure 20).

Most advanced fault detection schemes suffer from complexity and often from inherent weakness in reliability. However, it is usually possible to develop simple fault detection schemes that do not require extensive analytical development and that work reliably and efficiently. Such an approach involves the use of the SSME DTM.

Analytical redundancy, especially when applied to key engine parameters, can provide significant reliability and enhanced performance, especially under sensor failures. A good analytical model of the engine is required that can predict the expected outputs very closely (to that of the actual values) and thus provide analytical values to compare actual outputs with and make a decision regarding the status of the sensor. The SSME DTM is a very effective tool that can be utilized (perhaps piecewise linearization will be required in order to make it real-time on-line applicable) for such analytical redundancy purposes. There are many key sensors that need such

redundancy and that when implemented can enhance engine performance, avoid engine shutdowns due to false alarms, and that can minimize damage from failures.

8.2 SENSOR FAILURE DETECTION

Throughout the history of the Space Shuttle program, the only SSME in-flight shutdown occurred during flight 51F July 30, 1985, due to the malfunction of the HPFT discharge temperature sensors. This type of failure can be easily avoided given a good (simple) sensor failure detection approach.

Such an approach was evaluated using the information from past engine data as well as simulations via the SSME DTM. It is clearly indicated in the sensor outputs from flight 51F (see Figure 21) that the only parameters that showed anomalous behavior were the two HPFT discharge temperature sensors, while all the other parameters were nominal. This is sufficient cause to believe that it is a sensor failure. Moreover, computer simulations by the DTM of the same sensor output (as was shown in Figure 21) was artificially induced and the effects on other parameters were plotted. Figure 22 shows the dramatic influence of a sudden temperature rise of the HPFT discharge flow on several other parameters. Since no such effects were recorded during flight 51F the "failure" was a false alarm. Similar indications are shown in Figure 23. Herein, a change in any one of the parameters shown, results in a corresponding change in each of the other sensor outputs. Thus, sensor outputs can be correlated in such a manner as to generate useful information regarding the status of sensors.

The implementation of such a scheme is straight forward, does not require extensive computational effort and can significantly enhance the performance of the SAFD algorithm.

8.3 SAFD PERFORMANCE ENHANCEMENTS

In accordance with the observations made in the previous pages, it is highly recommended that work be continued on the SAFD algorithm development and enhancements directed towards expanding the capabilities of the algorithm. These expansions should address SAFD operation during start and power transients, accommodations and compensations for nonlinear effects and transient effects due to fuel/oxidizer repressurization/venting and fuel/GOX repressurization valve closures. In addition, sensor failure detection schemes should be simulated that are simple and easy to implement in order to study their feasibility and effectiveness.

The capability exists at Rocketdyne to evaluate the SSME from a systems point of view and develop failure detection schemes based on practical implementation and feasibility issues and formulated on sound mathematical and advanced fault detection knowledge. Advanced observer-based estimation routines can be utilized, using the DTM, that can provide analytical redundancy and enhanced failure detection capability. Various options have already been studied and their feasibility has been evaluated.

This useful effort should continue without the slow-down of unnecessary contractual breaks in order to have the engineers devote their full attention to the important task of SSME failure detection.

9. REFERENCES

1. R. Isermann, "Process Fault Detection Based on Modeling and Estimation Methods. A survey," Automatica, Vol. 20, pp. 387-409, 1984.
2. A. S. Willsky, "A survey of Design Methods for Failure Detection in Dynamic Systems," Automatica, Vol. 12, pp. 601-611, 1976.
3. E. Y. Shapiro, H. V. Panossian, "Analytical Redundancy for Aircraft Flight Control Sensors," NATO/AGARD, 43rd Symposium on Advanced Guidance and Control Systems Technology, pp. 53-1, 53-20, England, October, 1986.
4. H. V. Panossian, "Algorithms for System Fault Detection through Modeling and Estimation Techniques," Control and Dynamics Systems, C. T. Leondes (Ed.), Academic Press, NY, pp. 47-66, 1988.
5. H. L. Jones, "Failure Detection in Linear Systems," Ph.D. Thesis, MIT, Department of Aeronautics and Astronautics, Cambridge, Mass., 1973.
6. T. Weiss, et al, "Robust Detection/Isolation Accommodation for Sensor Failures - Final Report," NASA-CR-164797, NA53-24078, September, 1984.
7. J. J. Gertler, "Survey of Model Based Failure Detection and Isolation in Complex Plants," IEEE Control Systems Magazine, Vol. 8, pp. 3-11, 1988.
8. H. V. Panossian, "Stochastic Optimal Linear Feedback Control Systems Using Available Measurements," Journal of Optimization Theory and Application, Vol. 7, pp. 248-250, 1984.
9. H. Panossian, "State and Parameter Estimation in Electrohydraulic Actuation Systems for Failure Analysis," Proceedings of International Symposium on Test and Failure Analysis, Long Beach, CA, pp. 228-231, 1975.
10. J. W. Willsky, "Failure Detection in Dynamic Systems," NATO AGARD-ograph No. 190, 1980.
11. W. C. Merrill, "Sensor Failure Detection for Jet Engines Using Analytical Redundancy," J. Guidance, Vol. 8, No. 6, pp. 517-526, 1988.
12. W. C. Merrill, J. C. DeLaat, and W. M. Bruton, "Advanced Detection, Isolation, and Accommodation of Sensor Failures-Real-Time Evaluation," J. Guidance, Vol. 11, No. 6, pp. 517-526, 1988.
13. M. H. Taniguchi, RI/RD 87-109, "Failure Control Techniques for the SSME," NAS8-36305, Phase II final report, Rockwell International, Rocketdyne Division, Canoga Park, CA, 1988.
14. M. H. Taniguchi, RI/RD 87-109, "SSME Failure Mode and Effects Analysis and Initial Items List," Rockwell International, Rocketdyne Division, Canoga Park, CA, 1988.

APPENDIX I

TABLES

TABLE 6.1.1 DETAILED COMPARISON OF SOME FAILURES

TEST #	ENGINE #	DATE	DURATION	POWER LEVEL	DESCRIPTION OF FAILURE	FAILURE CLASSIFICATION	TYPE OF FAILURE	RELINE PARAMETER	OTHER PARAMETERS THAT SHOW CHANGES *** SEE CODE	CODE FOR PARAMETERS LISTED ABOVE
01-116	0003	3-24-77	74.07	75	SPOT FAILURES, MOTOR /SEAL SUPPORT, EXT DAM	MAJOR, CRITICALITY ONE	SPOT	SPOT SHAFT SPEED	1.2,3,4	1
01-136	0004	9-9-77	390.23	90	SPOT BEARING FAILURES, MOTOR /SEAL SUPPORT, EXT DAM	MAJOR, CRITICALITY ONE	SPOT	CONTROLLER, LOSS OF ELECTRICAL	1.2,3,4	1
01-147	0005	11-17-77	31.09	70	SPOT FAILURES, POWER TRANSMFER, TURBINE BLADES	MAJOR	SPOT	PRESURER PUMP RADIAL ACCEL	NONE	2
01-147	0005	12-31-77	31.26	81	SPOT FAILURES, POWER TRANSMFER, TURBINE BLADES	MAJOR	SPOT	PRESURER BOOST PUMP ACCEL	NONE	2
01-172	0002	3-3-78	281.17	92	HAIRY INJECTOR FAILURES, LOX POST FRACTURE, REPLACED INJECTOR	MAJOR	INJECTOR	SPOT DIS TEMP	5,6,7,8,9,10,11,3,4	3
01-183	0003	6-8-77	31.06	100	MAIN INJECTOR FAILURES, LOX POST FRACTURE, INJECTOR MISC	MAJOR	INJECTOR	EXCESSIVE SPOT RADIAL ACCEL	6,11,16,8,9,12,13,3,4,7,13	4
02-113	0101	6-16-78	5.74	92	FACILITY MALFUNCTIONS, GRT ICING BLOCKED FUEL PUMP INLET DOCK	MAJOR	PUMP INLET DOCK	EXCESSIVE SPOT RADIAL ACCEL	8,12,10,3,4,16,13,19	5
02-113	0101	7-18-78	6.84	92	EXTREME WIGGLING IN TURBOBOSS MANIFOLD	MAJOR, CRITICALITY ONE	SPOT	SPOT DIS TEMP	12,13,16,17,3,4,20,26,18	6
02-130	0101	7-21-78	41.81	100	FIRE IN THE SPOT, HEAT ADDITION TO LOX	MAJOR, CRITICALITY ONE	CONTROLLER	SPOT RADIAL ACCEL	1	7
02-132	0006	10-3-78	1.34	20	NOV GRT POSITION AT PLATEAU, EXT DAM	MAJOR	CONTROLLER	SPOT DIS TEMP, MCC IGNITION	NONE	8
01-222	0007	12-8-78	4.25	90	SEAL EXCHANGER FAILURES, WELD FRACTURE	MAJOR, CRITICALITY ONE	SEAL EXCHANGER	HEAT EXC OUTLET PRESSURE	NONE	9
01-325	2001	13-27-78	258.83	100	SEAL FRICTION, FIRE, EXT DAM	MAJOR, CRITICALITY ONE	WELD EX VALVE	SPOT DIS TEMP	21,23,22,24,25,18	10
176-01	0001	9-14-79	4.22	100	MOBILE STEERBOSS FAILED	MAJOR, CRITICALITY ONE	MAIN FUEL VALVE	SPOT DIS TEMP	8,12,13,3,4	11
176-01	0002	7-3-79	18.49	100	SEAL FAILURES, FUEL LEAK	MAJOR, CRITICALITY ONE	STEERBOSS	SPOTS AND SEAL CAVITY PR	NONE	12
176-01	0004	11-4-79	9.78	100	STEERBOSS FAILURES, FUEL LEAK	MAJOR, CRITICALITY ONE	INJECTOR	FIRE DETECTORS	3,4,1,12,13	13
176-01	0006	7-13-80	105.28	102	SOLE BURNED IN PPS, INJECTOR FAILURES	MAJOR, CRITICALITY ONE	INJECTOR	SPOT DIS TEMP	6,9,11,9,3,4,15,13,19,13	14
102-198	2004	7-23-80	9.33	102	SOLE IN INJECTOR, LOX POST FAILURES	MAJOR, CRITICALITY ONE	CONTROLLER	SPOT RADIAL ACCEL	7,10	15
102-284	0010	7-30-80	9.89	60	LEE JET DISPLACED, EXCESSIVE SENSOR, EXT DAM	MAJOR, CRITICALITY ONE	SPOT	MA	11,9,3,13,3,19	16
902-309	2008	11-16-80	8709.82	90	SEAL GAS IMPRESSION TO MOTOR COOLING	MAJOR	INJECTOR	LOOP INLET DOCK	13,1,19,14,3,4,20,13	17
901-307	0009	1-28-81	78.03	109	LOX POST FRACTURES, PPS EMISSION	MAJOR	INJECTOR	SPOT DIS TEMP	19,9,7,11,9,19,19,10,14,13	18
901-331	2106	7-13-81	221.14	100	LOX POST FRACTURES, MCC EMISSION, MAIN INJECTOR SUPPORT, EXT DAM	MAJOR	INJECTOR	SPOT DIS TEMP	13,2,3,4	19
750-148	0110	9-3-81	14.00	109	HAIRY INJECTOR SUPPORT, SEVERE DAMAGE	MAJOR	INJECTOR	SPOT DIS TEMP	8,11,10,18,7,8,18,14,13	20
902-249	0284	9-21-81	450.37	109	TURBINE BLADE FAILURES, VOLTAJE WIGGLING, EXT DAM	MAJOR, CRITICALITY ONE	SPOT	SPOTS ACC	12,13,18,26,3,4	21
901-246	0107	11-19-81	8709.82	109	LOCALIZED, TURBINE BLADES	MAJOR	SPOT	SPOT DIS TEMP	20,22,23,26,3,4,16,17,18	22
901-246	0107	11-19-81	8709.82	109	LOCALIZED, TURBINE BLADES	MAJOR, CRITICALITY ONE	INJECTOR	SPOT DIS TEMP	20,23,3,4,12,13,26	23
750-140	0110	3-13-82	3.16	20	SEAL FROM ERM BLOCKED FUEL, EXT DAM	MAJOR, CRITICALITY ONE	SPOT	MA	NONE	24
901-242	2013	3-27-82	8709.82	109	POWER TRANSMFER FAILURES	MAJOR, CRITICALITY ONE	SPOT	MA	12,13,18,16,26	25
901-263	2013	3-30-82	8709.82	109	SPOT TORN AROUND DOCK FAILURES	MAJOR, CRITICALITY ONE	SPOT	MA	20,22,23,17,18,26,3,4,16	26
901-264	2013	4-7-82	392.16	109	HAIRY EXL, TURBINE BEARING FAILURES, EXT DAM	MAJOR, CRITICALITY ONE	SPOT	MA	20,17,3,4,26,16,12,13,18	27
750-140	0107	4-21-82	8709.82	80	NOV GAS IMPRESSION TO MOTOR COOLING	MAJOR	SPOT	MA	NONE	28
750-175	2100	9-27-82	116.06	113	HIGH PRESSURE OXIDIZER DOCK SUPPORT, EXT DAM	MAJOR, CRITICALITY ONE	SPOT	MA	12,13,18,16,26	29
901-410	2014	9-30-82	8709.82	104	POWER TRANSMFER FAILURES	MAJOR, CRITICALITY ONE	SPOT	MA	14,18,19,12,13,19,3,4	30
901-438	0108	3-14-84	611.06	109	COOLANT LINDER SHELLS, TURBINE EXT DAM	MAJOR, CRITICALITY ONE	SPOT	MA	16,8,19,13,13,13,28,19,3,4	31
750-259	2308	7-27-85	281.54	109	MCC OUTLET MANIFOLD WIGGLING, EXT DAM	MAJOR, CRITICALITY ONE	MOBILE TUBE	POWERHEAD THERMOCOUPLE	28,1,29,3,4,30,21	32
901-485	2108	7-24-85	281.54	109	HIGH EFFICIENCY SPOT, MOBILE TUBE SUPPORT	CRITICALITY ONE	FIXED LINE	POWERHEAD THERMOCOUPLE	29,6,33,4,12,13,28,21,21,26,26,28,19,40,30,31,39,41	33
902-438	2104	5-21-87	281.54	109	SEAL CRACK AT STOP WELD	MAJOR, CRITICALITY ONE	INJECTOR	SPOT DIS TEMP	5,18	34
902-471	2204	7-1-87	284.12	104	NOV STEAK IN OPR INJECTOR	MAJOR, CRITICALITY ONE	DOCK, FLEX JOINT	POWERHEAD THERMOCOUPLE	8,23,37,34	35
904-044	0213	6-23-89	1370.73	94	LOW PRESSURE FUEL DOCK BELLOW LEAK, EXT DAM	MAJOR, CRITICALITY ONE	SPOT	MCC PC AVG	1,26,41,30,39	36

TABLE 6.1.2 MEAN VALUES AND STANDARD DEVIATIONS

SAFD SLICE TO SLICE SIGMA ENGINE VARIATION STUDY (E0211.1047PL) [SL2210]
GENSTAT PROGRAM VERSION - 1.0Y
TOTAL ENGINES - 1 TOTAL RUNS - 1 TOTAL SLICES - 100
DATE - 11/20/00

Table with 6 columns: ID #, PARAMETER TITLE, MEAN, SIGMA EE, SIGMA SL A, SIGMA SL B. Contains engine parameter data for study E0211.1047PL.

ORIGINAL PAGE IS OF POOR QUALITY

A1544 B

T027 A1539

SAFD SLICE TO SLICE SIGMA ENGINE VARIATION STUDY (E2206.1047PL) [SL2206]
GENSTAT PROGRAM VERSION - 1.0Y
TOTAL ENGINES - 1 TOTAL RUNS - 1 TOTAL SLICES - 100

Table with 6 columns: ID #, PARAMETER TITLE, MEAN, SIGMA EE, SIGMA SL A, SIGMA SL B. Contains engine parameter data for study E2206.1047PL.

104% SL

T02A2471

100% SL

SAFD SLICE TO SLICE SIGMA ENGINE VARIATION STUDY (F2029.1047PL) [SL2029A]
GENSTAT PROGRAM VERSION - 1.0X
TOTAL ENGINES - 1 TOTAL RUNS - 1 TOTAL SLICES - 100

Table with 6 columns: ID #, PARAMETER TITLE, MEAN, SIGMA EE, SIGMA SL A, SIGMA SL B. Contains engine parameter data for study F2029.1047PL.

A2439

A2449

A2441 C

A2441 B

(E2029.109XPL)

TABLE 6.1.3

PRELIMINARY CHOICE OF TESTS FOR SAFD SIMULATIONS

TEST #	REASON FOR CHOICE
901-173	RE-RUN OF TESTS FROM SAFD PHASE 2
901-225	RE-RUN OF TESTS FROM SAFD PHASE 2
901-285	RE-RUN OF TESTS FROM SAFD PHASE 2
901-340	RE-RUN OF TESTS FROM SAFD PHASE 2
901-364	RE-RUN OF TESTS FROM SAFD PHASE 2
750-285	ONLY FEEDLINE FAILURE
901-485	ONLY NOZZLE TUBE FAILURE
750-259	ONLY MCC NECK FAILURE
750-175	OXIDIZER DUCT FAILURE
902-471	FUEL DUCT FAILURE
902-428	OPB INJECTOR FAILURE
901-307	FPB INJECTOR FAILURE
902-249	TURBINE BLADE FAILURE (HPFTP)
901-436	COOLANT LINER BUCKLE (HPFTP)
901-136	BEARING FAILURE (HPOTP)
904-044	BEARING FAILURE (HPOTP)
SF6-01	MAIN FUEL VALVE FAILURE

TABLE 6.1.4 - SSME FAILURE MODES FROM FMEA

Item No.	Failure Mode	Failure Effect	Failure Cause	Failure Mode	Failure Effect	Failure Cause
1110-11	1110-11
1110-12	1110-12
1110-13	1110-13
1110-14	1110-14
1110-15	1110-15
1110-16	1110-16
1110-17	1110-17
1110-18	1110-18
1110-19	1110-19
1110-20	1110-20
1110-21	1110-21
1110-22	1110-22
1110-23	1110-23
1110-24	1110-24
1110-25	1110-25
1110-26	1110-26
1110-27	1110-27
1110-28	1110-28
1110-29	1110-29
1110-30	1110-30
1110-31	1110-31
1110-32	1110-32
1110-33	1110-33
1110-34	1110-34
1110-35	1110-35
1110-36	1110-36
1110-37	1110-37
1110-38	1110-38
1110-39	1110-39
1110-40	1110-40
1110-41	1110-41
1110-42	1110-42
1110-43	1110-43
1110-44	1110-44
1110-45	1110-45
1110-46	1110-46
1110-47	1110-47
1110-48	1110-48
1110-49	1110-49
1110-50	1110-50
1110-51	1110-51
1110-52	1110-52
1110-53	1110-53
1110-54	1110-54
1110-55	1110-55
1110-56	1110-56
1110-57	1110-57
1110-58	1110-58
1110-59	1110-59
1110-60	1110-60
1110-61	1110-61
1110-62	1110-62
1110-63	1110-63
1110-64	1110-64
1110-65	1110-65
1110-66	1110-66
1110-67	1110-67
1110-68	1110-68
1110-69	1110-69
1110-70	1110-70
1110-71	1110-71
1110-72	1110-72
1110-73	1110-73
1110-74	1110-74
1110-75	1110-75
1110-76	1110-76
1110-77	1110-77
1110-78	1110-78
1110-79	1110-79
1110-80	1110-80
1110-81	1110-81
1110-82	1110-82
1110-83	1110-83
1110-84	1110-84
1110-85	1110-85
1110-86	1110-86
1110-87	1110-87
1110-88	1110-88
1110-89	1110-89
1110-90	1110-90
1110-91	1110-91
1110-92	1110-92
1110-93	1110-93
1110-94	1110-94
1110-95	1110-95
1110-96	1110-96
1110-97	1110-97
1110-98	1110-98
1110-99	1110-99
1110-100	1110-100

ORIGINAL PAGE IS OF POOR QUALITY

TABLE 6.1.5 DATA 'ERSION ROUTINE

CONVAT PROGRAM

PROGRAM MAIN 74/990 OPT-1 TRACE FTN 4.8+670 89/08/08. 14.33.01 PAGE 1

```

1      *
2      *
3      * THIS ROUTINE IS USED TO COMBINE DATA FILES BEFORE THEY *****
4      * ARE INPUT TO THE SAFO ALGORITHM. *****
5      * S. J. ECKERLING 12 JULY, 1989 *****
6      *
7      *
8      * PROGRAM MAIN(INPUT, OUTPUT, TAPE31, TAPES=INPUT, TAPE6=OUTPUT,
9      * +TAPE20, TAPE21, TAPE22, TAPE23)
10     * DIMENSION DUMMY(100), DESC1(6,27), DESC2(6,27), COM1(8)
11     * DIMENSION COM2(8), TEMP(10), COM3(8), DESC3(6,27), TEMP2(10)
12     * DIMENSION COM4(8), TEMP3(10), DESC4(6,27)
13     * NAMELIST /GIVEN/ NPID1, NPID2, NPID3, NPID4, TSTART, TMAX
14     *
15     * ***** READ AND WRITE NAMELIST *****
16     *
17     * READ(5,GIVEN)
18     * IF(EOF(5))10,20
19     * 10 PRINT *, "NO NAMELIST INPUT FOUND"
20     * GO TO 500
21     * 20 WRITE(6,GIVEN)
22     *
23     * ***** READ AND WRITE TITLES AND DESCRIPTIONS FROM DATA FILES *****
24     *
25     * READ(20,50)(COM1(I), I=1,6)
26     * READ(21,50)(COM2(I), I=1,6)
27     * 50 FORMAT(6A10)
28     * READ(20,50)((DESC1(J,K), J=1,6), K=1, NPID1)
29     * READ(21,50)((DESC2(J,K), J=1,6), K=1, NPID2)
30     * WRITE(6,50)(COM1(I), I=1,6)
31     * WRITE(6,50)((DESC1(J,K), J=1,6), K=1, NPID1)
32     * WRITE(31,50)((DESC1(J,K), J=1,6), K=1, NPID1)
33     * WRITE(6,50)((DESC2(J,K), J=1,6), K=1, NPID2)
34     * WRITE(31,50)((DESC2(J,K), J=1,6), K=1, NPID2)
35     * IF (NPID3.EQ.0) GO TO 60
36     * READ (22,50)(COM3(I), I=1,6)
37     * READ (22,50)((DESC3(J,K),J=1,6), K=1, NPID3)
38     * WRITE (6,50)((DESC3(J,K),J=1,6), K=1, NPID3)
39     * WRITE (31,50)((DESC3(J,K),J=1,6), K=1, NPID3)
40     * 60 CONTINUE
41     * IF (NPID4.EQ.0) GO TO 65
42     * READ (23,50)(COM4(I), I=1,6)
43     * READ (23,50)((DESC4(J,K),J=1,6), K=1, NPID4)
44     * WRITE (6,50)((DESC4(J,K),J=1,6), K=1, NPID4)
45     * WRITE (31,50)((DESC4(J,K),J=1,6), K=1, NPID4)
46     * 65 CONTINUE
47     *
48     * ***** READ DATA FROM DATA FILES *****
49     *
50     *
51     * NPID11=NPID1+1
52     * NPID21=NPID2+1
53     * NPIDTOT=NPID1+NPID2+1
54     * NPID12=NPID1+2
55     * NPID31=NPID3+1
56     * NPIDTOT3=NPID1+NPID2+NPID3+1
57     * NPIDTOT1=NPIDTOT+1

```

ORIGINAL PAGE IS
OF POOR QUALITY

```

NPIDA1-NPIDA+1
NPIDT04-NPID1+NPID2+NPID3+NPIDA+1
NPIDT02-NPIDT03+1
180 READ(20,200)(DUMMY(I),I=1,NPID11)
IF(DUMMY(1).LT.TSTART)GO TO 380
READ(21,200)(TEMP(I),I=1,NPID21)
X=2
DO 100 I-NPID12,NPIDTOT
DUMMY(I)=TEMP(X)
X=X+1
100 CONTINUE
IF(TEMP(1).NE.DUMMY(1))GO TO 400
IF(NPID3.EQ.0)GO TO 80
READ(22,200)(TEMP2(I),I=1,NPID31)
Z=2
DO 70 I-NPIDT01,NPIDT03
DUMMY(I)=TEMP2(Z)
Z=Z+1
70 CONTINUE
IF(TEMP2(1).NE.DUMMY(1))GO TO 400
80 CONTINUE
IF(NPID4.EQ.0)GO TO 85
READ(23,200)(TEMP3(I),I=1,NPID41)
Z=2
DO 75 I-NPIDT02,NPIDT04
DUMMY(I)=TEMP3(Z)
Z=Z+1
75 CONTINUE
IF(TEMP3(1).NE.DUMMY(1))GO TO 400
85 CONTINUE
*
* *** WRITE COMBINED DATA TO TAPE 31 AND PRINTOUT ***
C
WRITE(6,250) DUMMY(1)
WRITE(31,250)DUMMY(1)
C
WRITE(6,230)(DUMMY(I),I=2,NPIDT04)
WRITE(31,230)(DUMMY(I),I=2,NPIDT04)
200 FORMAT(F9.2,9F13.4)
230 FORMAT(9F13.4/9F13.4/9F13.4)
250 FORMAT(F9.2)
IF(DUMMY(1).EQ.TMAX)GO TO 500
GO TO 180
100 *
* *** ERROR MESSAGES ***
*
380 PRINT *,"DATA START TIME NOT EQUAL TO TSTART"
GO TO 500
400 PRINT *,"TIMES ON THE FILES DO NOT MATCH"
500 CONTINUE
WRITE(6,250)DUMMY(1)
END
    
```

ORIGINAL PAGE IS OF POOR QUALITY

TABLE 6 (cont.)

\$GIVEN	
NPID1	= 4.
NPID2	= 4.
NPID3	= 3.
NPID4	= 1.
TSTART	= .1088E+04.
TMAX	= .1271E+04.
\$END	
SME	CONTROLLER DATA FOR TEST 904 44 ENGINE 0212 CNTRLR
18	MCC CLNT DS TMP
84	HPFP CLNT LNR
231	HPFT DS TMP
280	HPFP SPEED
210	HPFP INLET PR B
232	HPFT DS TMP
233	HPOT DS TMP
234	HPOT DS TMP
88	HPFP IN PR AVG
140	OPOV ACT POS
142	FPOV ACT POS
200	MCC PC AVG
	1271.00

ORIGINAL PAGE IS
OF POOR QUALITY

SSME Real-Time Failure Control Algorithm

Original SAFD Monitored Parameters (Phase I & II)

No.	SAFD Parameters	Facility PID No.	Controller
1	Inj clnt PR	Old PID = 366	24
2	MCC HIG IN PR	367	63
3	MCC Pc	129/162 161/130	53, 54, channel A, B
4	HPFP Cl Lur PR	A/53 - B/54	58, 158
5	FPB Pc	Old = 410, New = 8500	
6	OPB Pc	Old = 480, New = 8458	
7	MCC OX Inj PR	8684 (395)	
8	Main inj LOX inj PR	8076 (459)	29, 52, 152
9	HPFP DS PR		
10	MCC clnt dis temp	260/261	
11	HPFP speed	231	18
12	HPFT dis temp T1 A	232	19
13	HPFT dis temp T1 B	233	
14	HPOTP dis temp T1	234	
15	HPOTP dis temp T2	854	
16	FAL OC FM DS PR	858 - 859	209-210, LPOTP IN press.
17	Eng OX IN pressure	302 (A/209-B/210)	70/71 channel A/B
18	LPOP DS PR	8354 (878)	
19	HX int PR	8355 (879)	
20	HX int temp	8352 (883)	
21	HX vent ΔP		40 FL PID
22	OPOV act pos		42 FL PID
	FPOV act pos		

SSME Real-Time Failure Control Algorithm

Current SAFD Monitored Parameters

No.	Parameter	PID TTB	Flight PID	Facility PID	Redline
1	HPFTP shaft speed		260, 261	764	Start Redline
2	HPFTP turbine discharge temperature channel A		231		Redline
3	HPFTP turbine discharge temperature channel B		232		
4	HPFTP discharge pressure		52, 152	459	Redline
5	HPFTP radial accel			1944, 1954	
6	HPFTP coolant liner pressure		53, 54	1981, 1985	Redline
7	HPFTP balance cavity pressure			457	
8	HPOTP discharge pressure		90, 140		Redline
9	HPOTP turbine discharge temperature channel A		233		Redline
10	HPOTP turbine discharge temperature channel B		234		Redline
11	HPOTP intermediate seal purge pressure		211-212		
12	HPOTP secondary seal drain pressure		91-92		
13	HPOTP boost pump discharge pressure	1989, 1996, 1988, 1984, 1999	59, 159		Redline
14	HPOTP boost pump radial accel				
15	HPOTP boost pump bearing coolant discharge temperature	8251, 8255			Redline
16	LPFTP shaft speed		32	754, 755	
17	LPOTP pump discharge pressure			302	
18	HEX venturi delta pressure	8352			
19	HEX bypass mix temperature	8359			
20	MCC pressure bridge 1, 2		129, 130 161, 162 1951		
21	MCC liner cavity pressure		40		Redline
22	OPOV ACT position		42		
23	FPOV ACT position		251/253 (1)	721/722 (3)	
24	Fuel flowmeter		258/133 (2)		

TABL 1.8

SSME CRITICAL OPERATING PARAMETERS

TEST NUMBER	ENGINE 2107				ENGINE 2011				ENGINE 2024				NOMINAL VALUES	ENGINE TO ENGINE				
	902-465		902-466		902-467		902-473		902-474		902-475				902-477		902-478	
	109X @ 400 SECS FL VENT, 140 NPSP		109X @ 400 SECS FL VENT, 140 NPSP		109X @ 400 SECS FL VENT, 140 NPSP		109X @ 400 SECS FL VENT, 140 NPSP		104X @ 45 SECS NOMINAL		109X @ 445 SECS FL VENT, 140 NPSP				109X @ 400 SECS FL VENT, 140 NPSP		109X @ 400 SECS FL VENT, 140 NPSP	
POWER LEVEL	PRED.	ACTUAL	PRED.	ACTUAL	PRED.	ACTUAL	PRED.	ACTUAL	PRED.	ACTUAL	PRED.	ACTUAL	PRED.	ACTUAL	ACTUAL	ACTUAL		
LPOP SPEED	5240	5360	5290	5390	5380	5370	5220	5180	5300	5315	5300	5315	5300	5250	5260	5260		
HPOP SPEED	28500	29200	29000	28800	29200	28750	27600	27850	28900	28700	28900	28700	29150	28300	28500	28500		
LPPP SPEED	16500	15020	15900	15930	15750	16130	15850	15780	16350	16250	16350	16250	17350	16670	16570	16570		
HPFP SPEED	36350	36000	36400	36420	36050	35950	34950	35150	36550	36675	36550	36675	36600	36220	35600	35600		
HPOT DS TMP CH A	1370	1630	1370	1390	1440	1450	1360	1300	1300	1300	1300	1300	1250	1320	1370	1370		
HPOT DS TMP CH B	1370	1630	1370	1390	1450	1450	1360	1300	1300	1300	1300	1300	1280	1350	1355	1424.95		
HPFT DS TMP CH A	1720	1715	1730	1765	1760	1775	1730	1765	1830	1830	1770	1830	1730	1735	1740	1740		
HPFT DS TMP CH B	1740	1815	1750	1850	1860	1790	1750	1780	1850	1820	1850	1820	1750	1785	1780	1780		
OPDV POSITION	68	72	70	70.5	71	73	70	66.5	73	69	69	69	68	70.5	71	71.5		
FPDV POSITION	84	81	83	85.0	85	84	82	82.0	84	84	84	84	84	84.5	85	83.8		
HPOP NSS	11000	10800	11400	10800	11100	10900	11400	11300	10600	10600	10600	10600	10600	10600	10700	10500		
HPFP NSS	6600	6840	6600	7200	7500	6700	6800	5900	6500	6640	6500	6640	6800	6200	6400	6200		
MIXTURE RATIO	6.011*	6.35	6.011*	6.03	6.011*	6.05	6.011*	6.04	6.011*	6.015*	6.011*	6.015*	6.011*	5.94	6.011*	6.00		
FPI (PSIA)	22	24	22	24	23	24	38	39	24	24	24	24	22	24	22	24		
OP1 (PSIA)	158	157	158	159	158	158	96	97	158	157	157	157	158	160	158	160		
LPPF UNIT NO.	2120	4266	4009	4302	4010	4006	4006	4011	4301	2322	4011	4301	2322	4006	2131	6007		
HPFP UNIT NO.	2020	2020	2020	2020	2020	2020	2020	2020	2020	2020	2020	2020	2020	2020	2020	2020		
LPOP UNIT NO.	2020	2020	2020	2020	2020	2020	2020	2020	2020	2020	2020	2020	2020	2020	2020	2020		
HPOP UNIT NO.	4306	4306	4302	4302	2126R1	2126R1	4205	4205	4205	4107	4205	4205	4205	2323	4107	4107		

* COMMANDER MR

TABLE 6.1.9
LOX Venting Effects on Engine Parameters

SAFD SLICE TO SLICE SIGMA VARIATION STUDY (E2206.104XPL) [SL478ST]
 TEST 9820479, 120-170 SEC
 GENSTAT PROGRAM VERSION - 1.0Y0
 TIME - 11:25:10 TOTAL ENGINES - 1 TOTAL RUNS - 1 TOTAL SLICES - 2500

ID #	PARAMETER TITLE	MEAN		SIGMA SL	
		W/O	LOX VENT	W/O	LOX VENT
24	MCC HG INJ PR A	3358.530000	7.424200	3361.164000	7.932800
53	HPFP CLNT LNR A	3418.478000	6.122985	3419.583000	6.289600
54	HPFP CLNT LNR B	3420.993000	5.847053	3422.872000	5.686497
410	FPB PC NFD 7K PSIA	5226.430000	8.563354	5199.320000	7.123161
480	OPB PC 10K PSIS	5199.605000	8.953334	5205.344000	8.418725
395	MCC OX INJ PR 5K PSIS	3689.450000	5.116195	3688.150000	5.594066
450	HPFP DS PR NFD 9500 PSI	6230.496000	8.410079	6242.445000	8.957813
200	MCC PC A AVG (MCPA)	3129.450000	3.794997	3129.479000	4.007133
201	MCC PC B AVG (MCPB)	3123.417000	4.100808	3122.822000	4.136481
18	MCC CLNT DS TMP B	419.369600	0.129922	419.388400	0.250929
260	HPFP SPEED A	35671.460000	182.274200	35719.340000	190.672200
261	HPFP SPEED B	35672.380000	184.865500	35718.340000	193.844400
231	HPFT DS TMP A	1743.885000	3.020531	1734.308000	2.908910
232	HPFT DS TMP B	1793.342000	2.358172	1791.759000	2.243026
233	HPOT DS TMP A	1213.202000	4.290950	1226.649000	18.773500
234	HPOT DS TMP B	1225.651000	3.937029	1239.988000	9.369440
854	FAC OX FM DS PR 350 PSIS	80.128950	0.194576	83.974030	0.410670
850	ENG OX IN PR 1 250 PSIS	81.709070	0.176293	85.816530	0.361681
850	ENG OX IN PR 2 250 PSIS	81.894150	0.394484	85.975070	0.273270
200	LPOP DISCHG PR A	355.929400	1.020331	331.221200	13.834740
210	LPOP DISCHG PR B	356.633300	1.056745	331.847900	13.880640
870	HX INT PR 5K PSIS	3301.594000	4.079388	3305.602000	4.152877
870	HX INT T 160/1900	798.222200	0.924097	801.521500	2.494000
883	HX VENT DP 250PSID	120.795400	0.425036	122.448400	0.153301
140	OPOV ACT POS A (OPV2)	66.702950	0.212270	67.734830	0.385368
141	OPOV ACT POS B (RVDB-1)	66.152190	0.186293	67.159850	0.373177
142	FPOV ACT POS A (FPV2)	84.766460	0.151954	84.721850	0.164692
143	FPOV ACT POS B (RVDB-2)	84.388140	0.175358	84.315580	0.179500
203	LPFP DISCHG PR A	242.203100	1.139864	238.324400	2.776806
204	LPFP DISCHG PR B (P10)	242.375600	1.166406	238.413700	2.802386
821	ENG FL IN PR 1 100 PSI	23.446910	0.187962	21.056670	1.636252
819	ENG FL IN PR 2 100 PSI	23.474410	0.173840	21.084610	1.636756
334	HPOP DS PR NFD 7K PSIA	4046.910000	5.511643	4045.992000	5.814549
341	HPD DS PR NFD 9500 PSI	7201.841000	12.087000	7204.449000	13.231340

SAFD SLICE TO SLICE SIGMA VARIATION STUDY (E2029.104XPL) [SL44910]
 NO LOX VENT
 (E2019.104XPL) [SL40010]
 TIME - 10:09:28 GENSTAT PROGRAM VERSION - 1.0Y0
 TOTAL ENGINES - 1 TOTAL RUNS - 1 TOTAL SLICES - 500

ID #	PARAMETER TITLE	MEAN		SIGMA SL	
		W/O	LOX VENT	WITH LOX VENT	SIGMA SL
24	MCC HG INJ PR A	3414.170000	7.597303	3359.750000	7.010504
53	HPFP CLNT LNR A	3483.085000	5.930776	3415.322000	7.299684
54	HPFP CLNT LNR B	3481.936000	6.378578	3421.910000	6.128956
410	FPB PC NFD 7K PSIA	5218.273000	7.613472	5155.039000	6.180888
480	OPB PC 10K PSIS	5259.555000	8.801890	5184.922000	6.574975
395	MCC OX INJ PR 5K PSIS	3714.312000	5.484037	3717.699000	5.481334
450	HPFP DS PR NFD 9500 PSI	6187.762000	11.264220	6176.307000	8.027305
200	MCC PC A AVG (MCPA)	3130.245000	4.575542	3127.474000	4.049453
201	MCC PC B AVG (MCPB)	3122.960000	4.647684	3125.301000	3.380368
18	MCC CLNT DS TMP B	444.851000	1.603500	477.030300	0.557341
260	HPFP SPEED A	35132.020000	964.518300	35341.360000	451.590600
261	HPFP SPEED B	35127.340000	957.677200	35327.310000	450.100600
231	HPFT DS TMP A	1751.530000	8.563097	1646.938000	5.386970
232	HPFT DS TMP B	1786.972000	10.842100	1687.157000	3.984813
233	HPOT DS TMP A	1387.077000	7.075738	1317.067000	4.393735
234	HPOT DS TMP B	1404.864000	2.354313	1333.535000	3.680635
854	FAC OX FM DS PR 350 PSIS	80.367430	0.425190	51.577030	1.604575
850	ENG OX IN PR 1 250 PSIS	81.183100	0.572645	51.980470	1.800270
850	ENG OX IN PR 2 250 PSIS	81.273500	0.575450	52.626140	1.864007
200	LPOP DISCHG PR A	355.053000	1.637205	314.231900	3.464459
210	LPOP DISCHG PR B	354.163300	1.670046	315.787000	3.404008
870	HX INT PR 5K PSIS	3007.715000	5.019732	3712.677000	3.805730
870	HX INT T 160/1900	915.102100	0.707595	785.300600	1.457747
883	HX VENT DP 250PSID	80.381890	0.003282	78.484700	0.073770
140	OPOV ACT POS A (OPV2)	70.626350	0.133506	66.010310	0.165753
141	OPOV ACT POS B (RVDB-1)	70.514370	0.116327	65.854610	0.138066
142	FPOV ACT POS A (FPV2)	82.185620	0.163748	81.468000	0.156630
143	FPOV ACT POS B (RVDB-2)	81.907330	0.166048	81.433000	0.137637
203	LPFP DISCHG PR A	238.403200	2.047325	227.678700	1.260090
204	LPFP DISCHG PR B (P10)	238.504100	2.022556	226.492000	1.305388
821	ENG FL IN PR 1 100 PSI	7.648723	0.219018	7.627837	0.217851
819	ENG FL IN PR 2 100 PSI	7.586492	0.223712	7.570885	0.222751
334	HPOP DS PR NFD 7K PSIA	4088.483000	7.482929	4079.622000	5.723232
341	HPD DS PR NFD 9500 PSI	7123.242000	14.242000	7340.066000	11.357020

ORIGINAL PAGE IS
OF POOR QUALITY

Table 0.2.1

SAFD Simulation Of Hot-Fire Test 901-364
Values For N2*σ

	Case I N2 * σ σ - SD pre-computed N2 = 1	Cases II,III N2 * σ σ - SD computed on line N2 = 8
1	Sec Injector Faceplate ΔP	---
2	Prim Injector Faceplate ΔP	---
3	Hot Gas Injector ΔP	22.08
4	Coolant Liner ΔP	20.48
5	HPFT ΔP	27.12
6	HPOT ΔP	31.44
7	MCC Ox Inj P - MCC PC	21.28
8	HPFP Ds P - MCC PC	34.0
9	MCC PC	28.0
10	MCC Coolant Ds T	1.6
11	HPFP Speed	130.72
12	HPFT Ds T1 A	24.64
13	HPFT Ds T1 B	17.36
14	HPOT Ds T1	14.56
15	HPOT Ds T2	8.96
16	Facility Ox Flowmeter Ds P	6.32
17	Engine Ox Inlet P	3.12
18	LPOP Ds P	4.8
19	HEX Int P	15.68
20	HEX Int T	3.36
21	HEX Vent ΔP	0.32
22	OPOV Act Position	0.68
23	FPOV Act Position	0.864

Case I Simulation cutoff at 214.553 seconds
Cases II,III Simulation cutoff at 206.75 and 205.75 seconds, respectively

SD - Standard Deviation
N2 - Multiplying factor for Approach-2

SAFD Simulation Results Test 901-284, Case I

6.2.2 A

A CUTOFF SIGNAL HAS BEEN INITIATED BECAUSE OF THE FOLLOWING MEASUREMENTS AND APPROACH OPTION FLAG(S)-----

APPROACH OPTION FLAG KEY: (TIME)...TIME APPROACH DETECTS AN ANOMALY.
(0.)...THE APPROACH DOES NOT DETECT AN ANOMALY.

SENSOR MEASUREMENT	DATA	AVG1	AVG2	AVG3	AVGINC	APPROACH-1	APPROACH-2	APPROACH-3
HEAT EXCH INT PR	1.7729E+03	3.5500E+03	1.7264E+03	1.6411E+03	1.7729E+03	0.	8.8600E+00	0.
HEAT EXCH INT TEMP	3.3447E+02	6.3000E+02	3.5802E+02	4.5855E+02	3.3447E+02	0.	8.8600E+00	0.

NUMBER OF SENSORS INDICATING AN ANOMALY--- 2
INTERIM FROM END TIME OF SCHEDULED TRANSIENT--- 3.76000E+00
TIME FROM START (T=0. SECONDS) ----- 8.85999E+00

-----NOTE: ANY ASTERISKS (*) ABOVE INDICATE THE PARAMETER IS NOT COUNTED BECAUSE OF LOGIC CHECKS.

SENSOR MEASUREMENT IDENTIFICATION	AVERAGE VALUE	STANDARD DEV.	N1--MULTIPLIER	N2--MULTIPLIER	N3--MULTIPLIER
HEAT EXCH INT PR	3.55000E+03	2.79500E+01	3.00000E+00	3.00000E+00	3.00000E+00
HEAT EXCH INT TEMP	6.30000E+02	1.00800E+01	3.00000E+00	3.00000E+00	3.00000E+00

SENSOR MEASUREMENT IDENTIFICATION APP-1 EARLY TIME APP-2 EARLY TIME APP-3 EARLY TIME

HOT-GAS INJECTOR DELTA-P	0.	0.	0.
HI PR FU TURBINE-HPFT DELTAP	0.	0.	0.
HI PR OX TURBINE-HPOT DELTAP	0.	0.	0.
MCC OX INJ PR - MCC PC	0.	0.	0.
HI PR FU PUMP DS PR - MCC PC	0.	0.	0.
MCC PC	0.	0.	0.
MCC CLNT DS TEMP	0.	0.	0.
HI PR FU PUMP SPEED	0.	0.	0.
HI PR FU TURBINE DS TEMP A	0.	0.	0.
HI PR FU TURBINE DS TEMP B	0.	0.	0.
HI PR OX TURBINE DS TEMP A	0.	0.	0.
HI PR OX TURBINE DS TEMP B	0.	0.	0.
FAC OX FLOWMETER DS PR	0.	0.	0.
ENG OX INLET PR	0.	0.	0.
LOW PR OX PUMP DS PR	0.	0.	0.
HEAT EXCH INT PR	0.	0.	0.
HEAT EXCH INT TEMP	0.	7.46000E+00	7.14000E+00
HEAT EXCH VENT DELTA-P	0.	0.	0.
OX PREBURN. OX VALVE ACT POS	0.	0.	0.
FU PREBURN. OX VALVE ACT POS	0.	0.	0.

THE END TIME FOR PLOTTING DATA IS 8.98000E+00
THE START TIME FOR PLOTTING IS--- 3.50000E+00
THE TIME INCREMENT IS----- 2.00000E-02

Table 2B
SAFD Simulation Results For Unit 901-284, Case II

A CUTOFF SIGNAL HAS BEEN INITIATED
BECAUSE OF THE FOLLOWING MEASUREMENTS AND APPROACH OPTION FLAG(S)-----
APPROACH OPTION FLAG KEY: (TIME)...TIME APPROACH DETECTS AN ANOMALY.
(0.)...THE APPROACH DOES NOT DETECT AN ANOMALY.

SENSOR MEASUREMENT	DATA	AVG1	AVG2	AVG3	AVGINC	APPROACH-1	APPROACH-2	APPROACH-3
HI PR FU TURBINE-HPFT DELTAP	1.1771E+03	1.2270E+03	1.1916E+03	1.2272E+03	1.1771E+03	0.	7.9400E+00	0.
HEAT EXCH VENT DELTA-P	4.7935E+01	4.2000E+01	4.4400E+01	4.2094E+01	4.7935E+01	0.	7.9400E+00	0.

NUMBER OF SENSORS INDICATING AN ANOMALY-- 2
INTERIM FROM END TIME OF SCHEDULED TRANSIENT--- 2.84000E+00
TIME FROM START (T=0. SECONDS) ----- 7.94000E+00

----NOTE: ANY ASTERISKS (*) ABOVE INDICATE THE PARAMETER IS NOT COUNTED BECAUSE OF LOGIC CHECKS.

SENSOR MEASUREMENT IDENTIFICATION	AVERAGE VALUE	STANDARD DEV.	N1-MULTIPLIER	N2-MULTIPLIER	N3-MULTIPLIER
HI PR FU TURBINE-HPFT DELTAP	1.22700E+03	4.40000E+00	8.00000E+00	8.00000E+00	8.00000E+00
HEAT EXCH VENT DELTA-P	4.20000E+01	2.30000E-01	8.00000E+00	8.00000E+00	8.00000E+00

SENSOR MEASUREMENT IDENTIFICATION	APP-1 EARLY TIME	APP-2 EARLY TIME	APP-3 EARLY TIME
HOT-GAS INJECTOR DELTA-P	0.	0.	0.
HI PR FU TURBINE-HPFT DELTAP	0.	0.	0.
HI PR OX TURBINE-HPOT DELTAP	0.	0.	0.
MCC OX INJ PR - MCC PC	0.	0.	0.
HI PR FU PUMP DS PR - MCC PC	0.	0.	0.
MCC PC	0.	0.	0.
MCC CLNT DS TEMP	0.	0.	0.
HI PR FU PUMP SPEED	0.	0.	0.
HI PR FU TURBINE DS TEMP A	0.	0.	0.
HI PR FU TURBINE DS TEMP B	0.	0.	0.
HI PR OX TURBINE DS TEMP A	0.	0.	0.
HI PR OX TURBINE DS TEMP B	0.	0.	0.
FAC OX FLOWMETER DS PR	0.	0.	0.
ENG OX INLET PR	0.	0.	0.
LOW PR OX PUMP DS PR	0.	0.	0.
HEAT EXCH INT PR	0.	0.	0.
HEAT EXCH INT TEMP	0.	0.	0.
HEAT EXCH VENT DELTA-P	0.	7.78000E+00	0.
OX PREBURN. OX VALVE ACT POS	0.	0.	0.
FU PREBURN. OX VALVE ACT POS	0.	0.	0.

Table 6
SAFD Simulation Results For Test 901-284, Case III

A CUTOFF SIGNAL HAS BEEN INITIATED
BECAUSE OF THE FOLLOWING MEASUREMENTS AND APPROACH OPTION FLAG(S)-----
APPROACH OPTION FLAG KEY: (TIME)...TIME APPROACH DETECTS AN ANOMALY.
(0.)...THE APPROACH DOES NOT DETECT AN ANOMALY.

SENSOR MEASUREMENT	DATA	AVG1	AVG2	AVG3	AVGNC	APPROACH-1	APPROACH-2	APPROACH-3
HI PR FU TURBINE-HPFT DELTAP	1.1888E+03	1.2270E+03	1.1916E+03	1.2272E+03	1.1888E+03	0.	7.1400E+00	0.
HEAT EXCH INT TEMP	3.8413E+02	4.5900E+02	3.8857E+02	4.5855E+02	3.8413E+02	0.	7.1400E+00	0.
HEAT EXCH VENT DELTA-P	4.4654E+01	4.2000E+01	4.4931E+01	4.2094E+01	4.4654E+01	0.	7.1400E+00	0.

5
20
21

NUMBER OF SENSORS INDICATING AN ANOMALY--- 3
INTERIM FROM END TIME OF SCHEDULED TRANSIENT--- 2.040000E+00
TIME FROM START (T=0. SECONDS) ----- 7.140000E+00

-----NOTE: ANY ASTERISKS (*) ABOVE INDICATE THE PARAMETER IS NOT COUNTED BECAUSE OF LOGIC CHECKS.

SENSOR MEASUREMENT IDENTIFICATION	AVERAGE VALUE	STANDARD DEV.	N1-MULTIPLIER	N2-MULTIPLIER	N3-MULTIPLIER
HI PR FU TURBINE-HPFT DELTAP	1.22700E+03	4.40000E+00	8.00000E+00	8.00000E+00	8.00000E+00
HEAT EXCH INT TEMP	4.59000E+02	8.40000E+00	8.00000E+00	8.00000E+00	8.00000E+00
HEAT EXCH VENT DELTA-P	4.20000E+01	2.30000E-01	8.00000E+00	8.00000E+00	8.00000E+00

SENSOR MEASUREMENT IDENTIFICATION	APP-1 EARLY TIME	APP-2 EARLY TIME	APP-3 EARLY TIME
HOT-GAS INJECTOR DELTA-P	0.	0.	0.
HI PR FU TURBINE-HPFT DELTAP	0.	0.	0.
HI PR OX TURBINE-HPOT DELTAP	0.	0.	0.
MCC OX INJ PR - MCC PC	0.	0.	0.
HI PR FU PUMP DS PR - MCC PC	0.	0.	0.
MCC PC	0.	0.	0.
MCC CLNT DS TEMP	0.	0.	0.
HI PR FU PUMP SPEED	0.	0.	0.
HI PR FU TURBINE DS TEMP A	0.	0.	0.
HI PR FU TURBINE DS TEMP B	0.	0.	0.
HI PR OX TURBINE DS TEMP A	0.	0.	0.
HI PR OX TURBINE DS TEMP B	0.	0.	0.
FAC OX FLOWMETER DS PR	0.	0.	0.
ENG OX INLET PR	0.	0.	0.
LOW PR OX PUMP DS PR	0.	0.	0.
HEAT EXCH INT PR	0.	0.	0.
HEAT EXCH INT TEMP	0.	0.	0.
HEAT EXCH VENT DELTA-P	0.	0.	0.
OX PREBURN. OX VALVE ACT POS	0.	0.	0.
FU PREBURN. OX VALVE ACT POS	0.	0.	0.

THE END TIME FOR PLOTTING DATA IS 8.98000E+00
THE START TIME FOR PLOTTING IS--- 3.50000E+00
THE TIME INCREMENT IS----- 2.00000E-02

Tab 1 .2D
SAFD Simulation Results For Test 1-364, Case I

A CUTOFF SIGNAL HAS BEEN INITIATED
BECAUSE OF THE FOLLOWING MEASUREMENTS AND APPROACH OPTION FLAG(S)-----
APPROACH OPTION FLAG KEY: (TIME)...TIME APPROACH DETECTS AN ANOMALY.
(0.)...THE APPROACH DOES NOT DETECT AN ANOMALY.

SENSOR MEASUREMENT	DATA	AVG1	AVG2	AVG3	AVGINC	APPROACH-1	APPROACH-2	APPROACH-3
FAC OX FLOWMETER DS PR	1.0313E+02	9.0000E+01	1.0117E+02	7.6313E+01	1.0313E+02	0.	2.1455E+02	0.
ENG OX INLET PR	1.0193E+02	9.0000E+01	1.0006E+02	7.5331E+01	1.0193E+02	0.	2.1455E+02	0.
LOW PR OX PUMP DS PR	3.4272E+02	3.2000E+02	3.4215E+02	3.2116E+02	3.4272E+02	0.	2.1455E+02	0.
OX PREBURN. OX VALVE ACT POS	7.0625E+01	7.2550E+01	7.0658E+01	7.1727E+01	7.0625E+01	0.	2.1455E+02	0.

NUMBER OF SENSORS INDICATING AN ANOMALY---
INTERIM FROM END TIME OF SCHEDULED TRANSIENT--- 5.44800E+01
TIME FROM START (T=0. SECONDS) ----- 2.14553E+02

-----NOTE: ANY ASTERISKS (*) ABOVE INDICATE THE PARAMETER IS NOT COUNTED BECAUSE OF LOGIC CHECKS.

SENSOR MEASUREMENT IDENTIFICATION	AVERAGE VALUE	STANDARD DEV.	N1-MULTIPLIER	N2-MULTIPLIER	N3-MULTIPLIER
FAC OX FLOWMETER DS PR	9.00000E+01	5.88000E+00	3.00000E+00	1.00000E+00	1.00000E+00
ENG OX INLET PR	9.00000E+01	4.75000E+00	3.00000E+00	1.00000E+00	1.00000E+00
LOW PR OX PUMP DS PR	3.20000E+02	2.09400E+01	3.00000E+00	1.00000E+00	1.00000E+00
OX PREBURN. OX VALVE ACT POS	7.25500E+01	7.59000E-01	3.00000E+00	1.00000E+00	1.00000E+00

SENSOR MEASUREMENT IDENTIFICATION	APP-1 EARLY TIME	APP-2 EARLY TIME	APP-3 EARLY TIME
HOT-GAS INJECTOR DELTA-P	0.	0.	0.
COOLANT LINER DELTA-P	0.	0.	0.
HI PR FU TURBINE-HPFT DELTAP	0.	0.	0.
HI PR OX TURBINE-HPOT DELTAP	0.	0.	0.
MCC OX INJ PR - MCC PC	0.	0.	0.
HI PR FU PUMP DS PR - MCC PC	0.	0.	0.
MCC PC	0.	0.	0.
MCC CLNT DS TEMP	0.	0.	0.
HI PR FU PUMP SPEED	0.	0.	0.
HI PR FU TURBINE DS TEMP A	0.	0.	0.
HI PR FU TURBINE DS TEMP B	0.	0.	0.
HI PR OX TURBINE DS TEMP A	0.	0.	0.
HI PR OX TURBINE DS TEMP B	0.	0.	0.
FAC OX FLOWMETER DS PR	0.	2.06554E+02	2.09473E+02
ENG OX INLET PR	1.60117E+02	2.06114E+02	2.07634E+02
LOW PR OX PUMP DS PR	0.	0.	0.
HEAT EXCH INT PR	0.	0.	0.
HEAT EXCH INT TEMP	0.	0.	0.
HEAT EXCH VENT DELTA-P	0.	0.	0.
OX PREBURN. OX VALVE ACT POS	0.	1.70356E+02	0.
FU PREBURN. OX VALVE ACT POS	0.	0.	0.

THE END TIME FOR PLOTTING DATA IS 3.1998E+02
THE START TIME FOR PLOTTING IS--- 1.0000E+02
THE TIME INCREMENT IS----- 2.0000E-02

SAFD Simulation Results For Test 901-364, Case II

A CUTOFF SIGNAL HAS BEEN INITIATED BECAUSE OF THE FOLLOWING MEASUREMENTS AND APPROACH OPTION FLAG(S)-----
 APPROACH OPTION FLAG KEY: (TIME)...TIME APPROACH DETECTS AN ANOMALY.
 (0.)...THE APPROACH DOES NOT DETECT AN ANOMALY.

SENSOR MEASUREMENT	DATA	AVG1	AVG2	AVG3	AVGINC	APPROACH-1	APPROACH-2	APPROACH-3
FAC OX FLOWMETER DS PR	8.5953E+01	7.6000E+01	8.2686E+01	7.6313E+01	8.5953E+01	0.	2.0675E+02	0.
ENG OX INLET PR	8.4489E+01	7.5000E+01	8.1576E+01	7.5331E+01	8.4489E+01	0.	2.0675E+02	0.
LOW PR OX PUMP DS PR	3.2850E+02	3.2100E+02	3.2667E+02	3.2116E+02	3.2850E+02	0.	2.0675E+02	0.
HEAT EXCH VENT DELTA-P	1.3144E+02	1.3100E+02	1.3147E+02	1.3093E+02	1.3144E+02	0.	2.0675E+02	0.

NUMBER OF SENSORS INDICATING AN ANOMALY-- 4
 INTERIM FROM END TIME OF SCHEDULED TRANSIENT--- 4.66800E+01
 TIME FROM START (T=0. SECONDS) ----- 2.06754E+02

-----NOTE: ANY ASTERISKS (*) ABOVE INDICATE THE PARAMETER IS NOT COUNTED BECAUSE OF LOGIC CHECKS.

SENSOR MEASUREMENT IDENTIFICATION	AVERAGE VALUE	STANDARD DEV.	N1-MULTIPLIER	N2-MULTIPLIER	N3-MULTIPLIER
FAC OX FLOWMETER DS PR	7.6000E+01	7.9000E-01	8.0000E+00	8.0000E+00	8.0000E+00
ENG OX INLET PR	7.5000E+01	3.9000E-01	8.0000E+00	8.0000E+00	8.0000E+00
LOW PR OX PUMP DS PR	3.2100E+02	6.0000E-01	8.0000E+00	8.0000E+00	8.0000E+00
HEAT EXCH VENT DELTA-P	1.3100E+02	4.0000E-02	8.0000E+00	8.0000E+00	8.0000E+00

SENSOR MEASUREMENT IDENTIFICATION	APP-1 EARLY TIME	APP-2 EARLY TIME	APP-3 EARLY TIME
HOT-GAS INJECTOR DELTA-P	0.	0.	0.
COOLANT LINER DELTA-P	0.	0.	0.
HI PR FU TURBINE-HPFT DELTAP	0.	0.	0.
HI PR OX TURBINE-HPOT DELTAP	0.	0.	0.
MCC OX INJ PR - MCC PC	0.	0.	0.
HI PR FU PUMP DS PR - MCC PC	0.	0.	0.
MCC PC	0.	0.	0.
MCC CLNT DS TEMP	0.	0.	0.
HI PR FU PUMP SPEED	0.	0.	0.
HI PR FU TURBINE DS TEMP A	0.	0.	0.
HI PR FU TURBINE DS TEMP B	0.	0.	0.
HI PR OX TURBINE DS TEMP A	0.	0.	0.
HI PR OX TURBINE DS TEMP B	0.	1.74996E+02	0.
FAC OX FLOWMETER DS PR	0.	0.	0.
ENG OX INLET PR	0.	2.05394E+02	0.
LOW PR OX PUMP DS PR	0.	2.06434E+02	0.
HEAT EXCH INT PR	0.	0.	0.
HEAT EXCH INT TEMP	0.	1.83595E+02	0.
HEAT EXCH VENT DELTA-P	0.	1.80476E+02	0.
OX PREBURN. OX VALVE ACT POS	0.	1.69796E+02	0.
FU PREBURN. OX VALVE ACT POS	0.	0.	0.

Table 6
SAFD Simulation Results For Test 901-364, Case III

A CUTOFF SIGNAL HAS BEEN INITIATED BECAUSE OF THE FOLLOWING MEASUREMENTS AND APPROACH OPTION FLAG(S)-----
 APPROACH OPTION FLAG KEY: (TIME)...TIME APPROACH DETECTS AN ANOMALY.
 (0.)...THE APPROACH DOES NOT DETECT AN ANOMALY.

SENSOR MEASUREMENT	DATA	AVG1	AVG2	AVG3	AVGINC	APPROACH-1	APPROACH-2	APPROACH-3
FAC OX FLOWMETER DS PR	8.3021E+01	7.6000E+01	8.2820E+01	7.6313E+01	8.3021E+01	0.	2.0575E+02	0.
ENG OX INLET PR	8.2360E+01	7.5000E+01	8.1841E+01	7.5331E+01	8.2360E+01	0.	2.0575E+02	0.
LOW PR OX PUMP DS PR	3.2721E+02	3.2100E+02	3.2721E+02	3.2116E+02	3.2721E+02	0.	2.0575E+02	0.
HEAT EXCH VENT DELTA-P	1.3147E+02	1.3100E+02	1.3138E+02	1.3093E+02	1.3147E+02	0.	2.0575E+02	0.

NUMBER OF SENSORS INDICATING AN ANOMALY-- 4
 INTERIM FROM END TIME OF SCHEDULED TRANSIENT--- 4.56800E+01
 TIME FROM START (T=0. SECONDS) ----- 2.05754E+02

-----NOTE: ANY ASTERISKS (*) ABOVE INDICATE THE PARAMETER IS NOT COUNTED BECAUSE OF LOGIC CHECKS.

SENSOR MEASUREMENT IDENTIFICATION	AVERAGE VALUE	STANDARD DEV.	N1-MULTIPLIER	N2-MULTIPLIER	N3-MULTIPLIER
FAC OX FLOWMETER DS PR	7.60000E+01	7.90000E-01	8.00000E+00	8.00000E+00	8.00000E+00
ENG OX INLET PR	7.50000E+01	3.90000E-01	8.00000E+00	8.00000E+00	8.00000E+00
LOW PR OX PUMP DS PR	3.21000E+02	6.00000E-01	8.00000E+00	8.00000E+00	8.00000E+00
HEAT EXCH VENT DELTA-P	1.31000E+02	4.00000E-02	8.00000E+00	8.00000E+00	8.00000E+00

SENSOR MEASUREMENT IDENTIFICATION	APP-1 EARLY TIME	APP-2 EARLY TIME	APP-3 EARLY TIME
HOT-GAS INJECTOR DELTA-P	0.	0.	0.
COOLANT LINER DELTA-P	0.	0.	0.
HI PR FU TURBINE-HPFT DELTAP	0.	0.	0.
HI PR OX TURBINE-HPOT DELTAP	0.	0.	0.
MCC OX INJ PR - MCC PC	0.	0.	0.
HI PR FU PUMP DS PR - MCC PC	0.	0.	0.
MCC PC	0.	0.	0.
MCC CLNT DS TEMP	0.	0.	0.
HI PR FU PUMP SPEED	0.	0.	0.
HI PR FU TURBINE DS TEMP A	0.	2.04834E+02	0.
HI PR FU TURBINE DS TEMP B	0.	1.63877E+02	0.
HI PR OX TURBINE DS TEMP A	0.	0.	0.
HI PR OX TURBINE DS TEMP B	0.	0.	0.
FAC OX FLOWMETER DS PR	0.	2.04594E+02	0.
ENG OX INLET PR	0.	2.05194E+02	0.
LOW PR OX PUMP DS PR	0.	0.	0.
HEAT EXCH INT PR	0.	1.77916E+02	0.
HEAT EXCH INT TEMP	0.	1.73156E+02	0.
HEAT EXCH VENT DELTA-P	0.	1.67236E+02	0.
OX PREBURN. OX VALVE ACT POS	0.	0.	0.
FU PREBURN. OX VALVE ACT POS	0.	0.	0.

THE END TIME FOR PLOTTING DATA IS 3.1998E+02
 THE START TIME FOR PLOTTING IS--- 1.0000E+02
 THE TIME INCREMENT IS----- 2.0000E-02

ORIGINAL PAGE IS
OF POOR QUALITY

Table 6.2.3
Signal Limit Composition, Test 750-285

Parameter	Signal Limit Average (AVG)	Signal Limit Standard Deviation (SD)	n
OPOV Actuator Position	68.	0.2 <i>0.2</i>	63.
HPOTP Coolant Liner Pressure	3614.	5.0	7.8
HPOTP Intermediate Seal Purge Pressure	275.	0.6	38.5
HPOT Dis Temp A	1435.	1.94	7.1
HPOT Dis Temp B	1464.	1.5 <i>1.5</i>	19.7
LPOP Dis Pres	355.	0.83	3.8
Oxidizer Preburner Boost Pump Dis Pres	7944.	16.79	2.5
FPOV Actuator Position	83.	1.0 <i>1.0</i>	5.0

Note: Signal limits, defined by $AVG \pm n*SD$, are shown graphically in Figures 5A1,2 through 5H1,2 for selected parameters

TABLE 6.2.4
Simulation Results For Test 901-340

n2	#P	c/o (seconds)
26	6	279.67
26	7	295.42
26	8	none
27	7	298.7

redline cutoff: 405.5

TABLE 6.2.5
Simulation Results For Test 902-471

n1	#p	c/o (seconds)
2.5	4	146.24
2.5	5	146.28
2.5	6	146.28
2.5	7	146.76
2.5	8	146.76
2.0	6	50.68 (premature)
3.5	6	none
		redline cutoff: 147.68

Where n1,n2 - Multiplying factor which determines signal limits for Approaches-1,2.

*P - The number of parameters experiencing anomalies simultaneously required for algorithm to signal a shutdown.

c/o - The algorithm shutdown (cutoff) time.

TABLE 6.2.6
COMPARISON OF RESULTS, Simulation for Test 901-340

Simulation Run No.	N2	No. Parameters Required For Shutdown	SAFD Shutdown Time (Sec)
1	19	4	22.04
2	17	7	21.0
3	17	4	20.28
4	16	4	19.8

A CUTOFF SIGNAL HAS BEEN INITIATED BECAUSE OF THE FOLLOWING MEASUREMENTS AND APPROACH OPTION FLAG(S)-----

APPROACH OPTION FLAG KEY: (TIME)...TIME APPROACH DETECTS AN ANOMALY.
(0.)...THE APPROACH DOES NOT DETECT AN ANOMALY.

SENSOR MEASUREMENT	DATA	AVG1	AVG2	AVG3	AVGNC	APPROACH-1	APPROACH-2	APPROACH-3
COOLANT LINER DELTA-P	3.0899E+02	1.8870E+02	2.1489E+02	2.0515E+02	3.0899E+02	0.	0.	2.2040E+01
HI PR FU TURBINE DS TEMP A	1.6861E+03	1.7650E+03	1.7037E+03	1.7813E+03	1.6861E+03	0.	2.2040E+01	0.
HI PR FU TURBINE DS TEMP B	1.6773E+03	1.6480E+03	1.6684E+03	1.6574E+03	1.6773E+03	0.	2.2040E+01	0.
*HI PR OX TURBINE DS TEMP A	1.4222E+03	1.4380E+03	1.4482E+03	1.3847E+03	1.4222E+03	0.	2.2040E+01	0.
HEAT EXCH INT TEMP	9.0587E+02	8.6390E+02	9.0384E+02	8.2039E+02	9.0587E+02	0.	2.2040E+01	0.

NUMBER OF SENSORS INDICATING AN ANOMALY--- 4
INTERIM FROM END TIME OF SCHEDULED TRANSIENT--- 9.96000E+00
TIME FROM START (T=0. SECONDS) ----- 2.20400E+01

----NOTE: ANY ASTERISKS (*) ABOVE INDICATE THE PARAMETER IS NOT COUNTED BECAUSE OF LOGIC CHECKS.

SENSOR MEASUREMENT IDENTIFICATION	AVERAGE VALUE	STANDARD DEV.	N1--MULTIPLIER	N2--MULTIPLIER	N3--MULTIPLIER
COOLANT LINER DELTA-P	1.88700E+02	4.02000E+00	3.00000E+00	1.90000E+01	1.90000E+01
HI PR FU TURBINE DS TEMP A	1.76500E+03	4.05000E+00	3.00000E+00	1.90000E+01	1.90000E+01
HI PR FU TURBINE DS TEMP B	1.64800E+03	2.00000E-01	3.00000E-01	1.90000E+01	1.90000E+01
HEAT EXCH INT TEMP	8.63900E+02	1.68000E+00	3.00000E+00	1.90000E+01	1.90000E+01

SENSOR MEASUREMENT IDENTIFICATION	APP-1 EARLY TIME	APP-2 EARLY TIME	APP-3 EARLY TIME
HOT-GAS INJECTOR DELTA-P	0.	0.	0.
COOLANT LINER DELTA-P	0.	0.	2.18800E+01
HI PR FU TURBINE-HPFT DELTAP	0.	0.	0.
HI PR OX TURBINE-HPOT DELTAP	0.	0.	0.
MCC OX INJ PR - MCC PC	0.	0.	0.
HI PR FU PUMP DS PR - MCC PC	0.	0.	0.
MCC CLNT DS TEMP	0.	0.	0.
HI PR FU PUMP SPEED	0.	0.	0.
HI PR FU TURBINE DS TEMP A	0.	0.	2.06000E+01
HI PR FU TURBINE DS TEMP B	0.	1.87600E+01	1.41600E+01
HI PR OX TURBINE DS TEMP A	0.	1.68000E+01	0.
HI PR OX TURBINE DS TEMP B	0.	0.	0.
FAC OX FLOWMETER DS PR	0.	0.	0.
ENG OX INLET PR	0.	0.	0.
LOW PR OX PUMP DS PR	0.	0.	0.
HEAT EXCH INT PR	0.	0.	0.
HEAT EXCH INT TEMP	0.	1.59200E+01	0.
HEAT EXCH VENT DELTA-P	0.	0.	0.
OX PREBURN. OX VALVE ACT POS	0.	0.	0.
FU PREBURN. OX VALVE ACT POS	0.	0.	2.10400E+01

TP 2.7B
SIMULATION RUN NO. 2, Test 901-340

A CUTOFF SIGNAL HAS BEEN INITIATED
BECAUSE OF THE FOLLOWING MEASUREMENTS AND APPROACH OPTION FLAG(S)-----

APPROACH OPTION FLAG KEY: (TIME)...TIME APPROACH DETECTS AN ANOMALY.
(0.)...THE APPROACH DOES NOT DETECT AN ANOMALY.

SENSOR MEASUREMENT	DATA	AVG1	AVG2	AVG3	AVGNC	APPROACH-1	APPROACH-2	APPROACH-3
HI PR FU TURBINE DS TEMP A	1.6671E+03	1.7650E+03	1.7521E+03	1.7813E+03	1.6671E+03	0.	0.	2.1000E+01
HI PR FU TURBINE DS TEMP B	1.6698E+03	1.6480E+03	1.6515E+03	1.6574E+03	1.6698E+03	0.	2.1000E+01	2.1000E+01
HI PR OX TURBINE DS TEMP A	1.4626E+03	1.4380E+03	1.4540E+03	1.3847E+03	1.4626E+03	0.	2.1000E+01	0.
HI PR OX TURBINE DS TEMP B	1.4974E+03	1.4810E+03	1.4918E+03	1.4213E+03	1.4974E+03	0.	2.1000E+01	0.
HEAT EXCH INT PR	3.8640E+03	3.8598E+03	3.8905E+03	3.8371E+03	3.8640E+03	0.	2.1000E+01	0.
HEAT EXCH INT TEMP	9.0366E+02	8.6390E+02	8.9738E+02	8.2039E+02	9.0366E+02	0.	2.1000E+01	0.
FU PREBURN. OX VALVE ACT POS	8.3550E+01	8.2700E+01	8.2249E+01	8.3321E+01	8.3550E+01	0.	0.	2.1000E+01

NUMBER OF SENSORS INDICATING AN ANOMALY-- 7
INTERIM FROM END TIME OF SCHEDULED TRANSIENT--- 8.92000E+00
TIME FROM START (T=0. SECONDS) ----- 2.10000E+01

----NOTE: ANY ASTERISKS (*) ABOVE INDICATE THE PARAMETER IS NOT COUNTED BECAUSE OF LOGIC CHECKS.

SENSOR MEASUREMENT IDENTIFICATION	AVERAGE VALUE	STANDARD DEV.	N1-MULTIPLIER	N2-MULTIPLIER	N3-MULTIPLIER
HI PR FU TURBINE DS TEMP A	1.76500E+03	4.05000E+00	3.00000E+00	1.70000E+01	1.70000E+01
HI PR FU TURBINE DS TEMP B	1.64800E+03	2.00000E-01	3.00000E+00	1.70000E+01	1.70000E+01
HI PR OX TURBINE DS TEMP A	1.43800E+03	2.80000E+00	3.00000E+00	1.70000E+01	1.70000E+01
HI PR OX TURBINE DS TEMP B	1.48100E+03	3.80000E+00	3.00000E+00	1.70000E+01	1.70000E+01
HEAT EXCH INT PR	3.85980E+03	2.95000E+00	1.30000E+01	1.70000E+01	1.70000E+01
HEAT EXCH INT TEMP	8.63900E+02	1.68000E+00	3.00000E+00	1.70000E+01	1.70000E+01
FU PREBURN. OX VALVE ACT POS	8.27000E+01	7.10000E-02	1.00000E+00	1.70000E+01	1.70000E+01

SENSOR MEASUREMENT IDENTIFICATION	APP-1 EARLY TIME	APP-2 EARLY TIME	APP-3 EARLY TIME
HOT-GAS INJECTOR DELTA-P	0.	0.	0.
COOLANT LINER DELTA-P	0.	0.	0.
HI PR FU TURBINE-HPFT DELTAP	0.	0.	0.
HI PR OX TURBINE-HPOT DELTAP	0.	0.	0.
MCC OX INJ PR - MCC PC	0.	0.	0.
HI PR FU PUMP DS PR - MCC PC	0.	0.	0.
MCC PC	0.	0.	0.
MCC CLNT DS TEMP	0.	0.	0.
HI PR FU PUMP SPEED	0.	0.	2.06000E+01
HI PR FU TURBINE DS TEMP A	0.	1.87200E+01	1.41600E+01
HI PR FU TURBINE DS TEMP B	0.	1.62000E+01	0.
HI PR OX TURBINE DS TEMP A	0.	2.02800E+01	0.
HI PR OX TURBINE DS TEMP B	0.	0.	0.
FAC OX FLOWMETER DS PR	0.	0.	0.
ENG OX INLET PR	0.	0.	0.
LOW PR OX PUMP DS PR	0.	2.00400E+01	0.
HEAT EXCH INT PR	0.	1.56800E+01	0.
HEAT EXCH INT TEMP	0.	0.	0.
HEAT EXCH VENT DELTA-P	0.	0.	0.
OX PREBURN. OX VALVE ACT POS	0.	0.	0.
FU PREBURN. OX VALVE ACT POS	0.	0.	0.

ORIGINAL PAGE IS
OF POOR QUALITY

TABLE 1
 SIMULATION RUN NO. 3, Test 901-340

A CUTOFF SIGNAL HAS BEEN INITIATED
 BECAUSE OF THE FOLLOWING MEASUREMENTS AND APPROACH OPTION FLAG(S)-----
 APPROACH OPTION FLAG KEY: (TIME)...TIME APPROACH DETECTS AN ANOMALY.
 (0.)...THE APPROACH DOES NOT DETECT AN ANOMALY.

SENSOR MEASUREMENT	DATA	AVG1	AVG2	AVG3	AVGINC	APPROACH-1	APPROACH-2	APPROACH-3
*HI PR FU TURBINE DS TEMP B	1.6554E+03	1.6480E+03	1.6468E+03	1.6574E+03	1.6554E+03	0.	2.0280E+01	2.0280E+01
HI PR OX TURBINE DS TEMP A	1.4544E+03	1.4380E+03	1.4509E+03	1.3847E+03	1.4544E+03	0.	2.0280E+01	0.
HI PR OX TURBINE DS TEMP B	1.4933E+03	1.4810E+03	1.4859E+03	1.4213E+03	1.4933E+03	0.	2.0280E+01	0.
HEAT EXCH INT PR	3.8880E+03	3.8598E+03	3.8892E+03	3.8371E+03	3.8880E+03	0.	2.0280E+01	0.
HEAT EXCH INT TEMP	8.9922E+02	8.6390E+02	8.9252E+02	8.2039E+02	8.9922E+02	0.	2.0280E+01	0.

NUMBER OF SENSORS INDICATING AN ANOMALY-- 4
 INTERIM FROM END TIME OF SCHEDULED TRANSIENT--- 8.20000E+00
 TIME FROM START (T=0. SECONDS) ----- 2.02800E+01

----NOTE: ANY ASTERISKS (*) ABOVE INDICATE THE PARAMETER IS NOT COUNTED BECAUSE OF LOGIC CHECKS.

SENSOR MEASUREMENT IDENTIFICATION	AVERAGE VALUE	STANDARD DEV.	N1-MULTIPLIER	N2-MULTIPLIER	N3-MULTIPLIER
HI PR OX TURBINE DS TEMP A	1.4380E+03	2.8000E+00	3.0000E+00	1.70000E+01	1.70000E+01
HI PR OX TURBINE DS TEMP B	1.4810E+03	3.8000E+00	3.0000E+00	1.70000E+01	1.70000E+01
HEAT EXCH INT PR	3.8598E+03	2.9500E+00	1.3000E+01	1.70000E+01	1.70000E+01
HEAT EXCH INT TEMP	8.6390E+02	1.6800E+00	3.0000E+00	1.70000E+01	1.70000E+01

SENSOR MEASUREMENT IDENTIFICATION	APP-1 EARLY TIME	APP-2 EARLY TIME	APP-3 EARLY TIME
HOT-GAS INJECTOR DELTA-P	0.	0.	0.
COOLANT LINER DELTA-P	0.	0.	0.
HI PR FU TURBINE-HPFT DELTAP	0.	0.	0.
HI PR OX TURBINE-HPOT DELTAP	0.	0.	0.
MCC OX INJ PR - MCC PC	0.	0.	0.
HI PR FU PUMP DS PR - MCC PC	0.	0.	0.
MCC PC	0.	0.	0.
MCC CLNT DS TEMP	0.	0.	0.
HI PR FU PUMP SPEED	0.	0.	0.
HI PR FU TURBINE DS TEMP A	0.	0.	0.
HI PR FU TURBINE DS TEMP B	0.	1.87200E+01	1.41600E+01
HI PR OX TURBINE DS TEMP A	0.	1.62000E+01	0.
HI PR OX TURBINE DS TEMP B	0.	0.	0.
FAC OX FLOWMETER DS PR	0.	0.	0.
ENG OX INLET PR	0.	0.	0.
LOW PR OX PUMP DS PR	0.	0.	0.
HEAT EXCH INT PR	0.	2.00400E+01	0.
HEAT EXCH INT TEMP	0.	1.56800E+01	0.
HEAT EXCH VENT DELTA-P	0.	0.	0.
OX PREBURN. OX VALVE ACT POS	0.	0.	0.
FU PREBURN. OX VALVE ACT POS	0.	0.	0.

TABLE 'D

SIMULATION RUN NO. 4, Test 901-340

A CUTOFF SIGNAL HAS BEEN INITIATED BECAUSE OF THE FOLLOWING MEASUREMENTS AND APPROACH OPTION FLAG(S)-----

APPROACH OPTION FLAG KEY: (TIME)...TIME APPROACH DETECTS AN ANOMALY.
(0.)...THE APPROACH DOES NOT DETECT AN ANOMALY.

SENSOR MEASUREMENT	DATA	AVG1	AVG2	AVG3	AVGNC	APPROACH-1	APPROACH-2	APPROACH-3
*HI PR FU TURBINE DS TEMP B	1.6526E+03	1.6480E+03	1.6492E+03	1.6574E+03	1.6526E+03	0.	1.9800E+01	1.9800E+01
HI PR OX TURBINE DS TEMP A	1.4544E+03	1.4380E+03	1.4504E+03	1.3847E+03	1.4544E+03	0.	1.9800E+01	0.
HI PR OX TURBINE DS TEMP B	1.4892E+03	1.4810E+03	1.4830E+03	1.4213E+03	1.4892E+03	0.	1.9800E+01	0.
HEAT EXCH INT PR	3.8927E+03	3.8598E+03	3.8847E+03	3.8371E+03	3.8927E+03	0.	1.9800E+01	0.
HEAT EXCH INT TEMP	8.9511E+02	8.6390E+02	8.6934E+02	8.2039E+02	8.9511E+02	0.	1.9800E+01	0.

NUMBER OF SENSORS INDICATING AN ANOMALY--- 4
INTERIM FROM END TIME OF SCHEDULED TRANSIENT--- 7.72000E+00
TIME FROM START (T=0. SECONDS) ----- 1.98000E+01

-----NOTE: ANY ASTERISKS (*) ABOVE INDICATE THE PARAMETER IS NOT COUNTED BECAUSE OF LOGIC CHECKS.

SENSOR MEASUREMENT IDENTIFICATION	AVERAGE VALUE	STANDARD DEV.	N1-MULTIPLIER	N2-MULTIPLIER	N3-MULTIPLIER
HI PR OX TURBINE DS TEMP A	1.43800E+03	2.80000E+00	3.00000E+00	1.60000E+01	1.60000E+01
HI PR OX TURBINE DS TEMP B	1.48100E+03	3.80000E+00	3.00000E+00	1.60000E+01	1.60000E+01
HEAT EXCH INT PR	3.85980E+03	2.95000E+00	1.30000E+01	1.60000E+01	1.60000E+01
HEAT EXCH INT TEMP	8.63900E+02	1.68000E+00	3.00000E+00	1.60000E+01	1.60000E+01

SENSOR MEASUREMENT IDENTIFICATION	APP-1 EARLY TIME	APP-2 EARLY TIME	APP-3 EARLY TIME
HOT-GAS INJECTOR DELTA-P	0.	0.	0.
COOLANT LINER DELTA-P	0.	0.	0.
HI PR FU TURBINE-HPFT DELTAP	0.	0.	0.
HI PR OX TURBINE-HPOT DELTAP	0.	0.	0.
MCC OX INJ PR - MCC PC	0.	0.	0.
HI PR FU PUMP DS PR - MCC PC	0.	0.	0.
MCC PC	0.	0.	0.
MCC CLNT DS TEMP	0.	0.	0.
HI PR FU PUMP SPEED	0.	0.	0.
HI PR FU TURBINE DS TEMP A	0.	1.87200E+01	1.41600E+01
HI PR FU TURBINE DS TEMP B	0.	1.59200E+01	0.
HI PR OX TURBINE DS TEMP A	0.	1.75200E+01	0.
HI PR OX TURBINE DS TEMP B	0.	0.	0.
FAC OX FLOWMETER DS PR	0.	0.	0.
ENG OX INLET PR	0.	0.	0.
LOW PR OX PUMP DS PR	0.	0.	0.
HEAT EXCH INT PR	0.	0.	0.
HEAT EXCH INT TEMP	0.	1.55600E+01	0.
HEAT EXCH VENT DELTA-P	0.	0.	0.
OX PREBURN, OX VALVE ACT POS	0.	0.	0.
FU PREBURN, OX VALVE ACT POS	0.	0.	0.

TABLE 6.4.1

PARAMETER DESCRIPTION	PERCENT CHANGE FROM NOMINAL	
	1 lb-sec leak	5 lb-sec leak
FUEL PREBURNER TEMP	-.279	-1.40
OX PREBURNER TEMP	-.743	-2.16
OX PREBURNER PRESSURE	-.228	-1.18
MAIN CHAMBER PRESSURE	-.192	-0.99
HPOP DISCHARGE PRESSURE	-.255	-1.32
HPFP DISCHARGE PRESSURE	-.188	-0.97
FPOV POSITION	-.182	0.70
OPOV POSITION	-.125	1.20
BOOST PUMP DIS PRESSURE	-.454	-2.32
MAIN CHAMBER MIX RATIO	-.265	-0.76

APPENDIX II

FIGURES

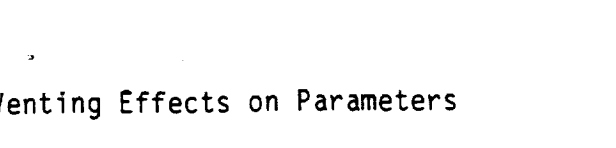
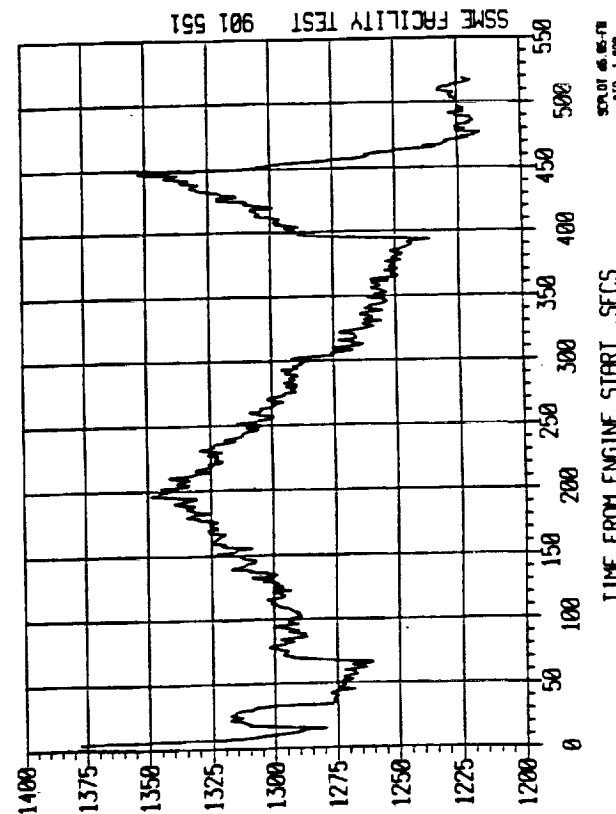
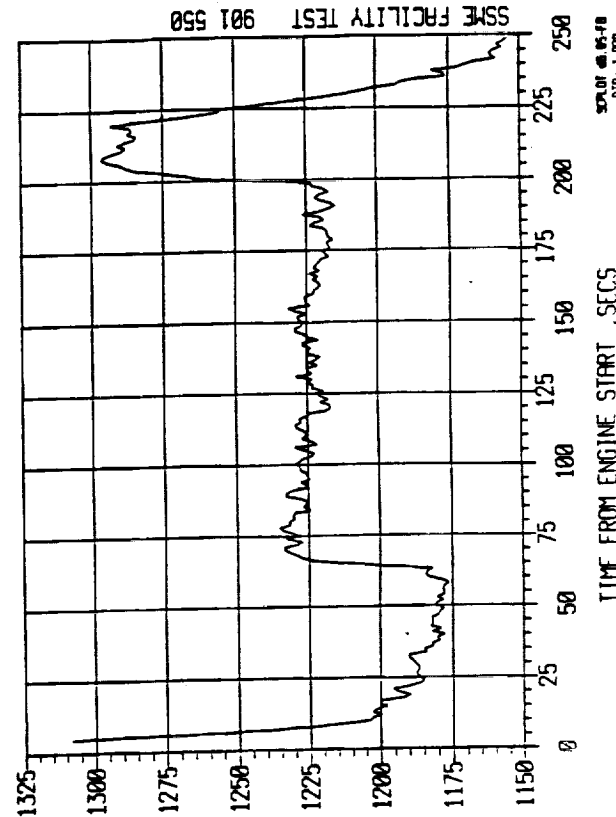
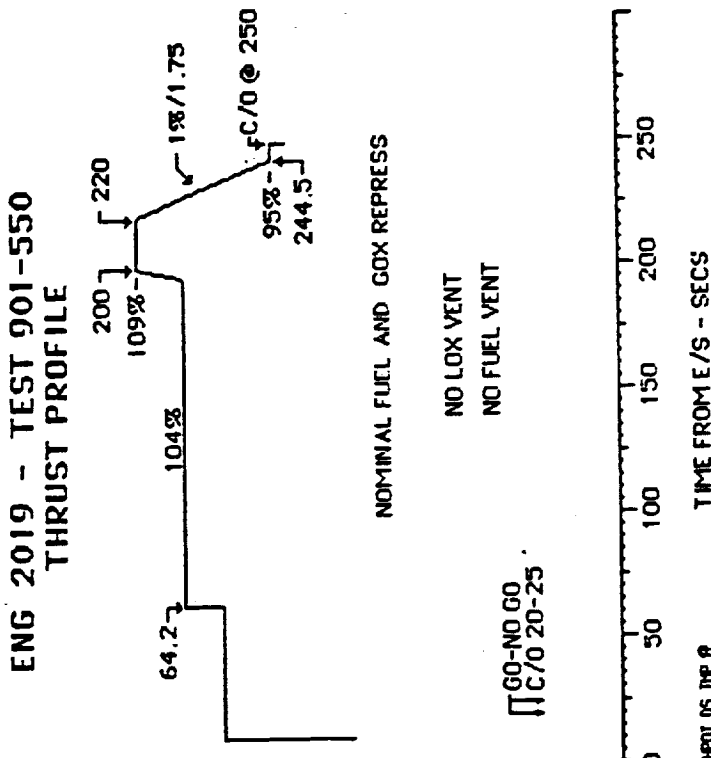
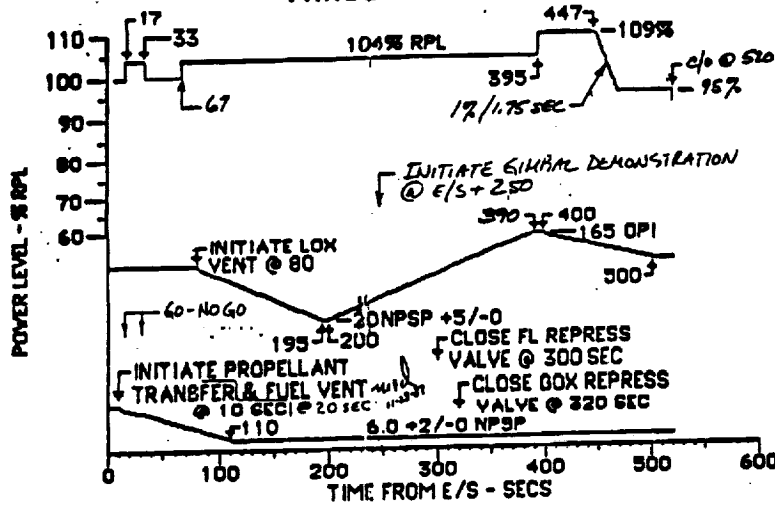
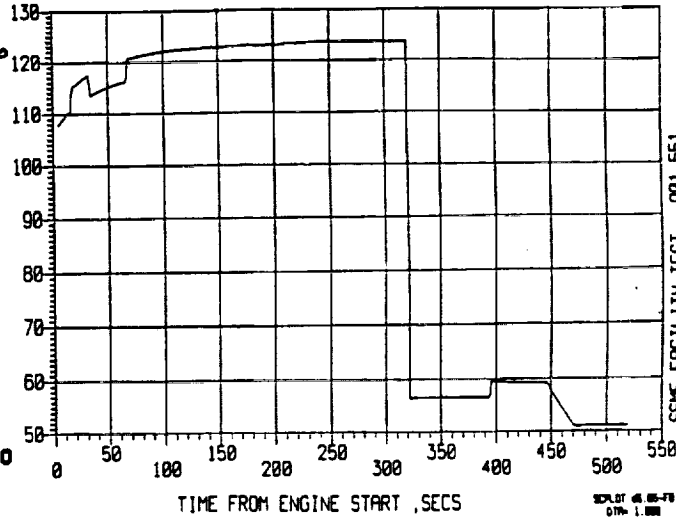


FIGURE 1. Pressurization/Venting Effects on Parameters

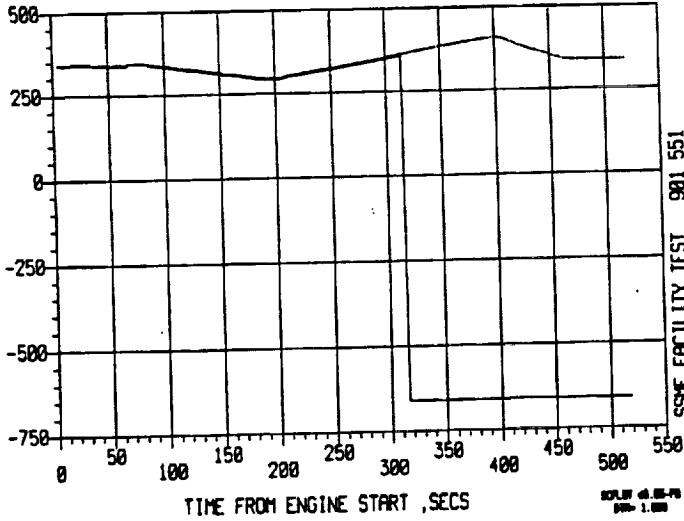
ENG 2019 - TEST 901-551
THRUST PROFILE



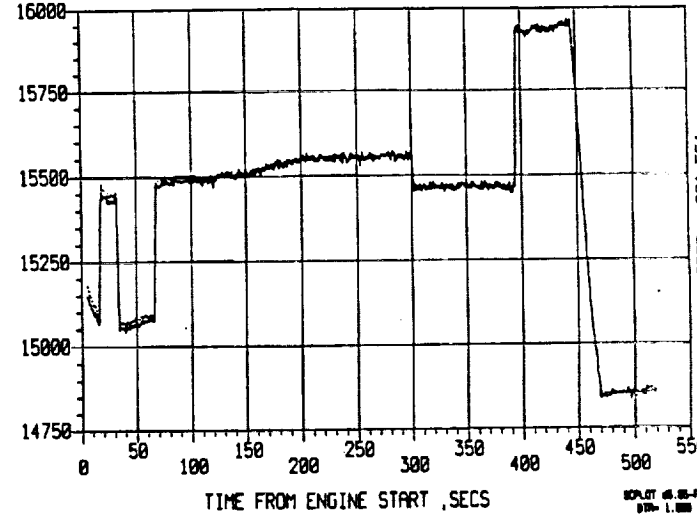
883 HX VENT DP 250 PSID



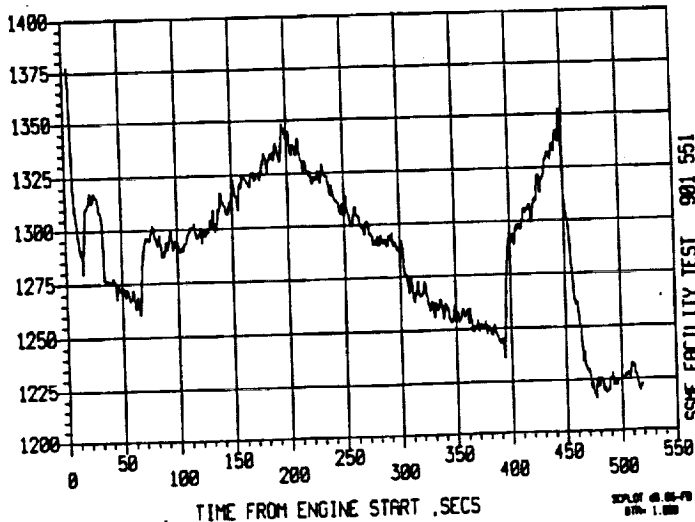
209 HPOP INLET PR A
218 HPOP INLET PR B



32 LFPF SPEED A
754 LFPF SPD IFD 24K RPM



233 HPOP DS TMP A



42 FPOV ACT POS A (FPV1)

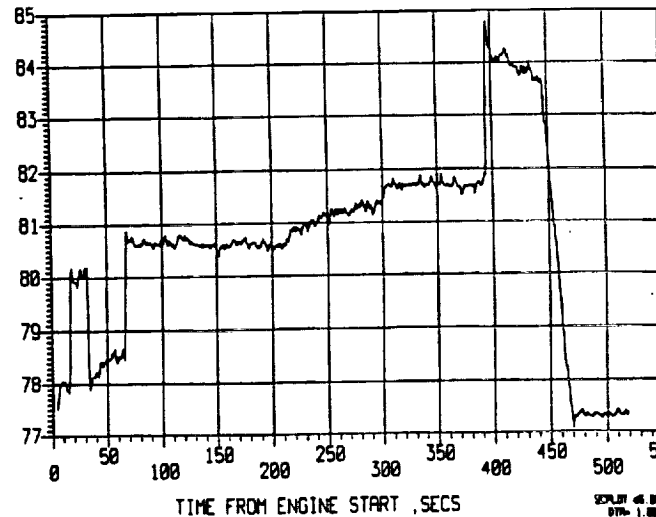
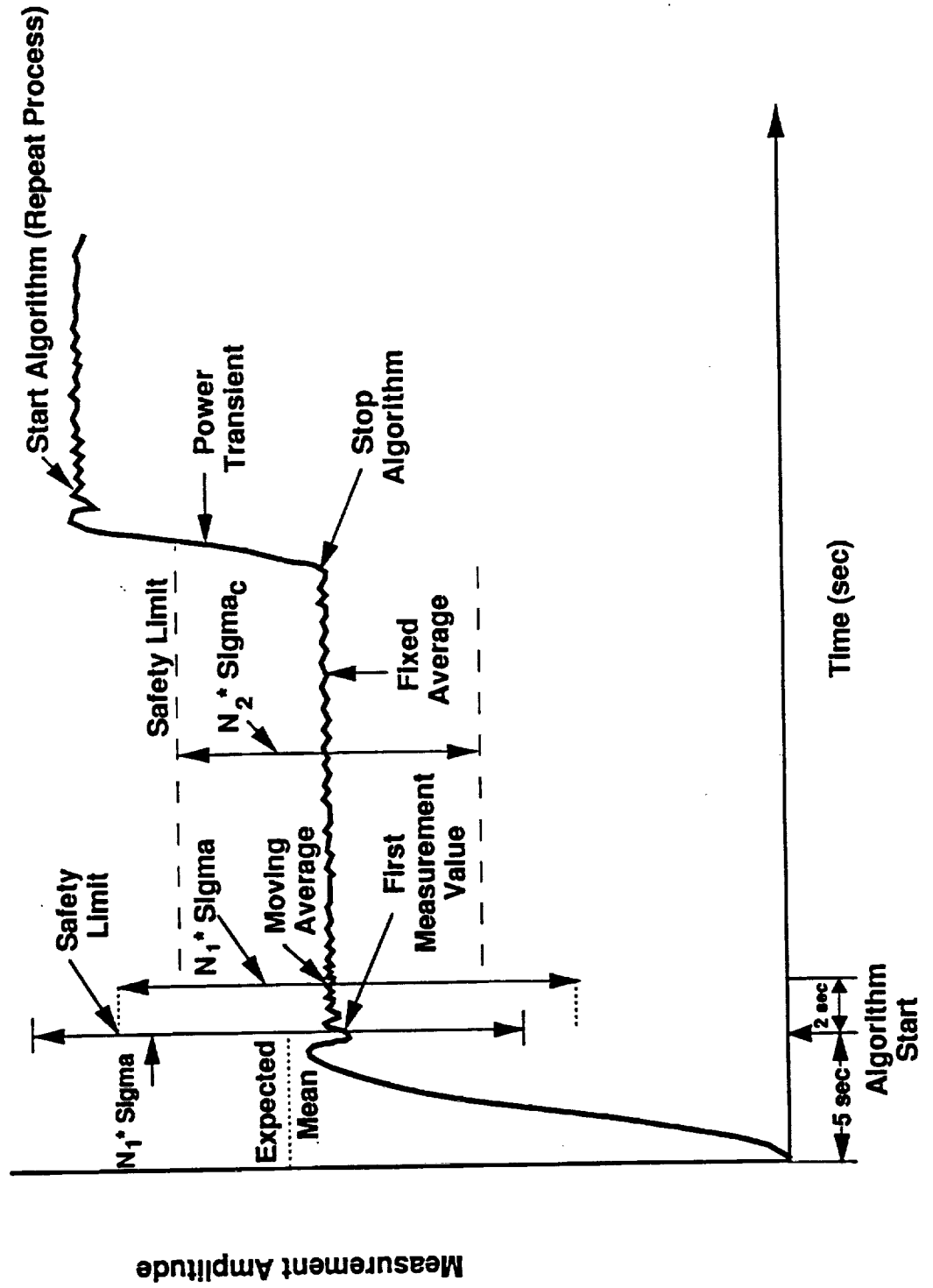


FIGURE 2. Closure of GOX and Fluid Repressurization Valves' Effect on Parameters

FIG. 3

SAFD Algorithm Schematic



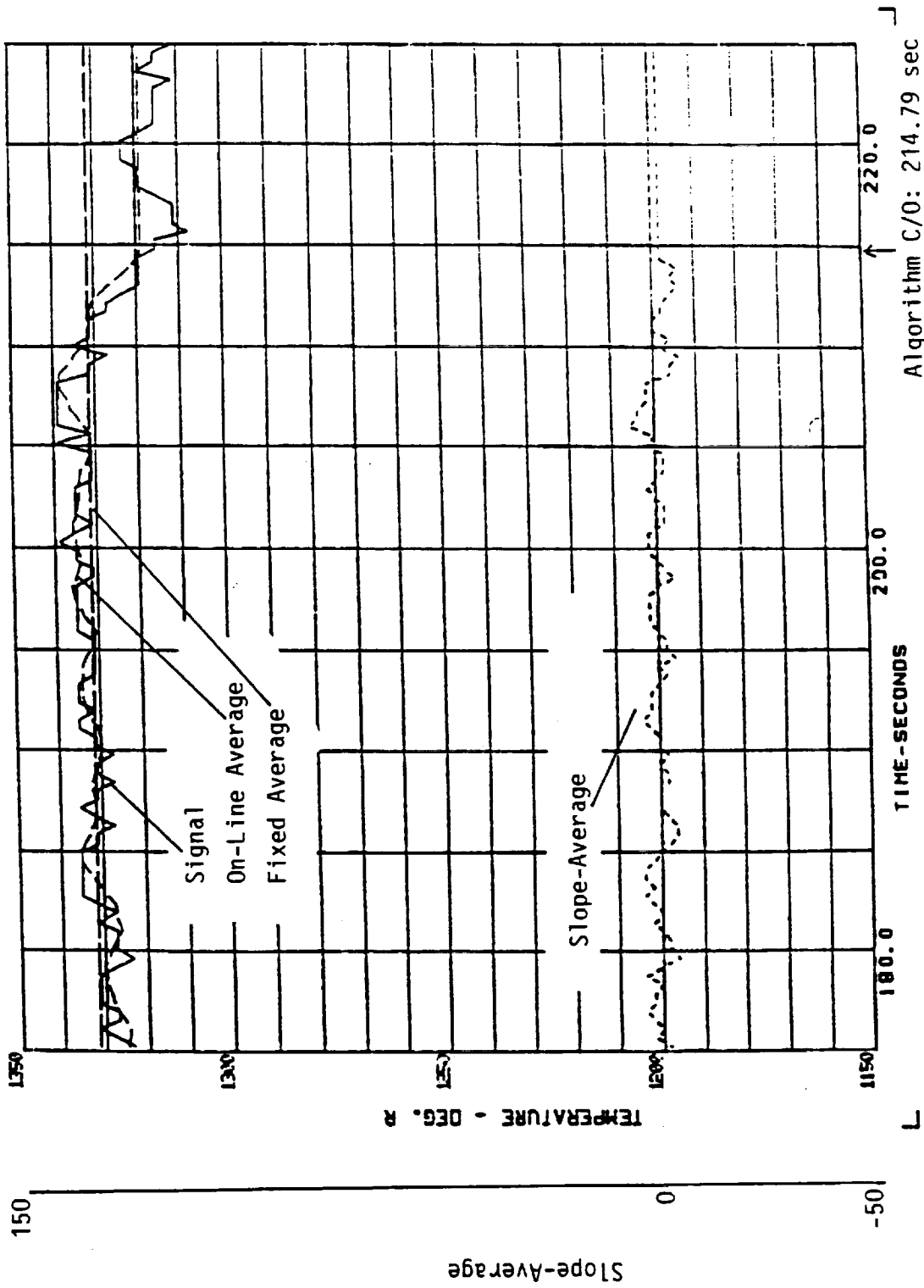
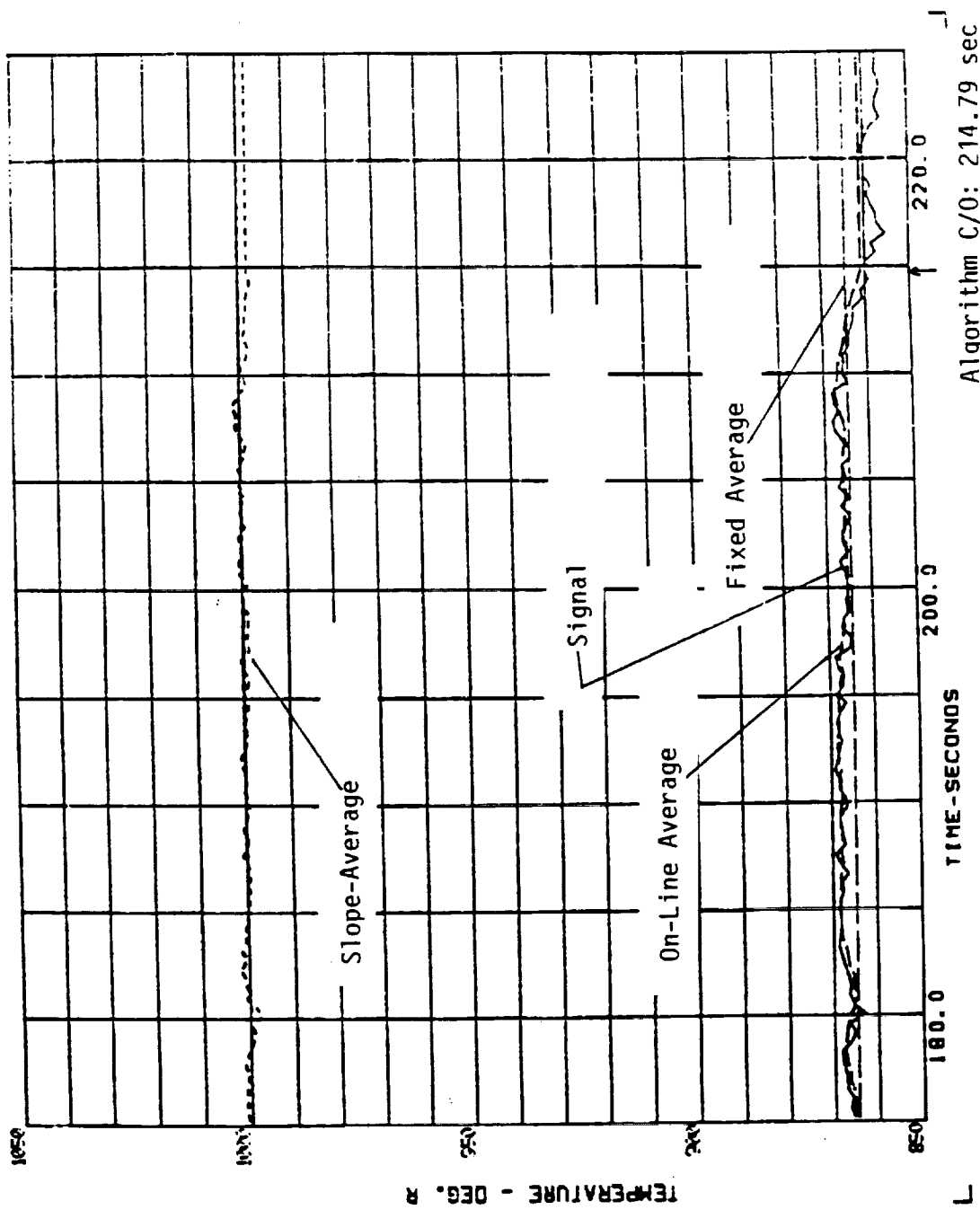


FIGURE 4A - SLOPE-AVERAGE APPROACH

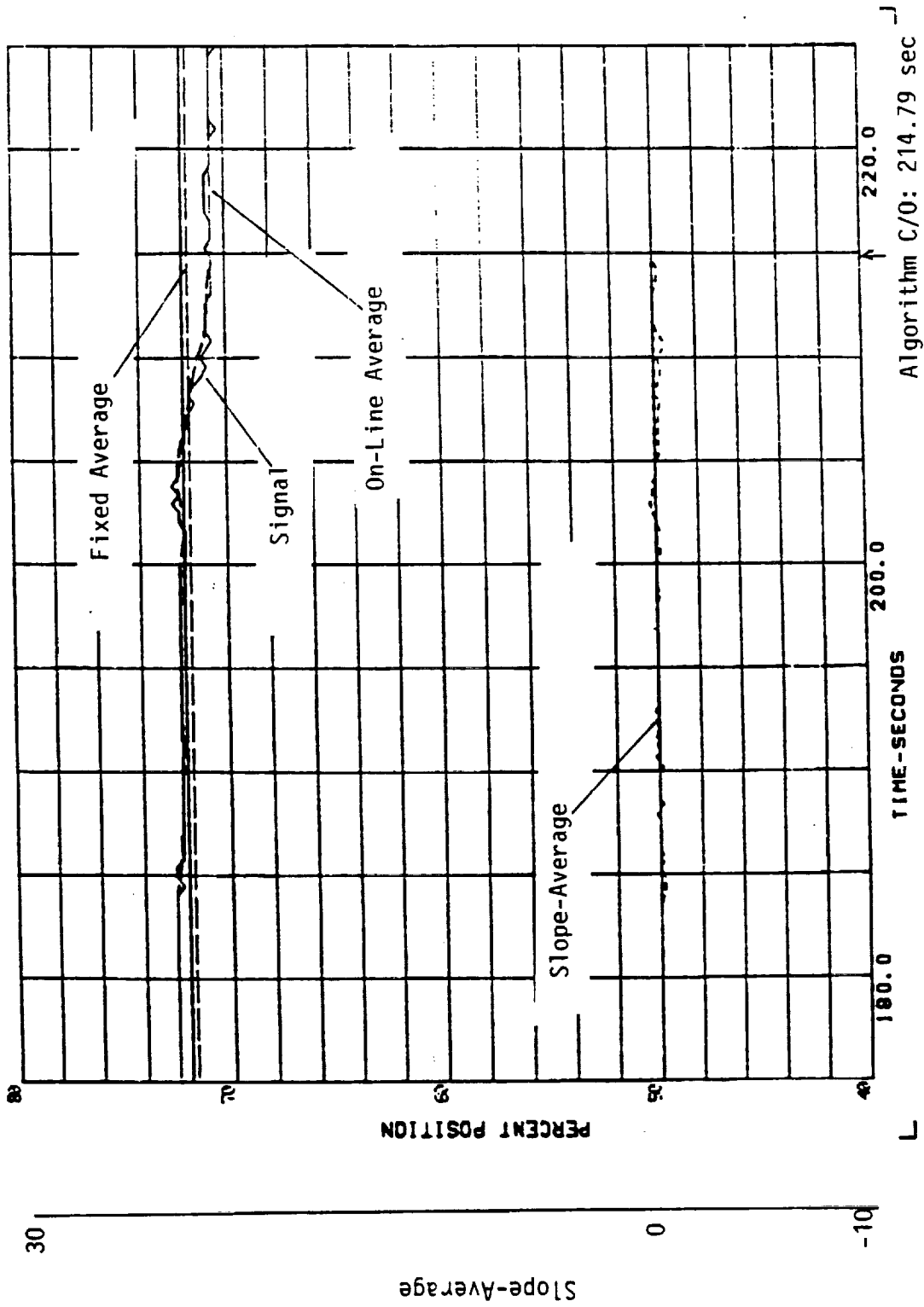
High Pressure Oxidizer Turbine Ds Temp 1, Test 901-364



Algorithm C/O: 214.79 sec
 (Redline C/O: 392.15 sec)

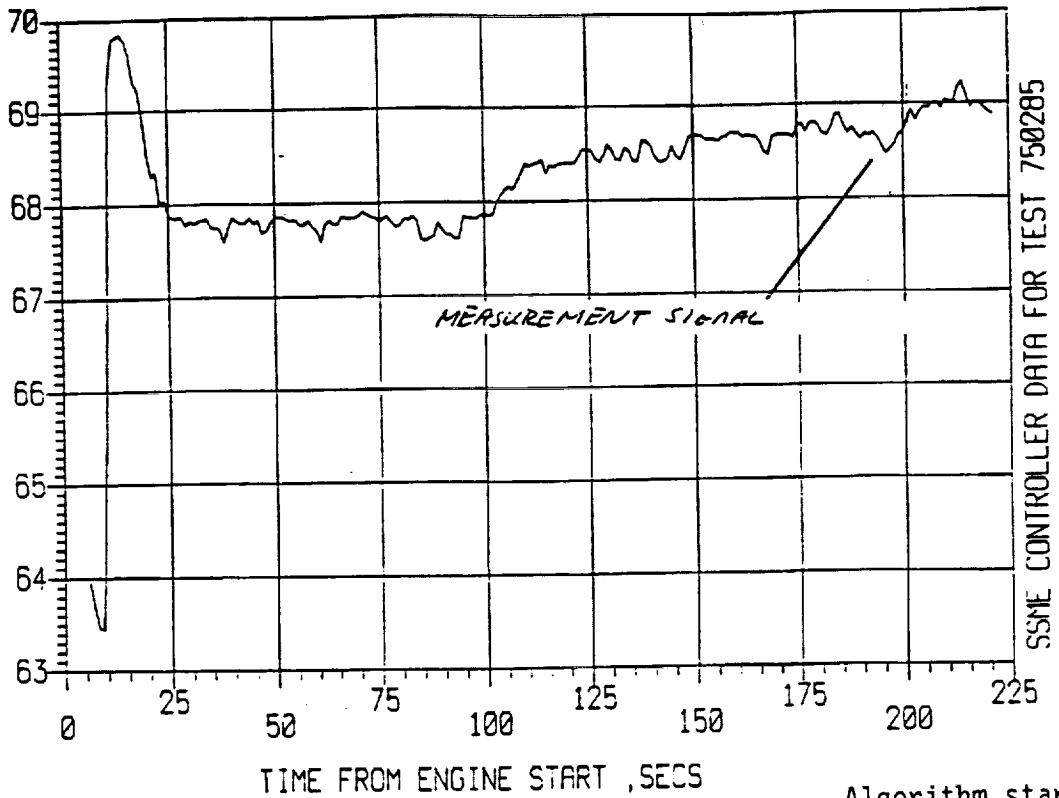
Slope-Average Approach

Figure 4R - Heat Exchanger Interface Temp, Test 901-364



Algorithm C/O: 214.79 sec
 (RedLine C/O: 392.15 sec)

Slope-Average Approach
 Figure 4C - 0POV Actuator Position, Test 901-364



Algorithm start: 100 secs.

Figure 5A1

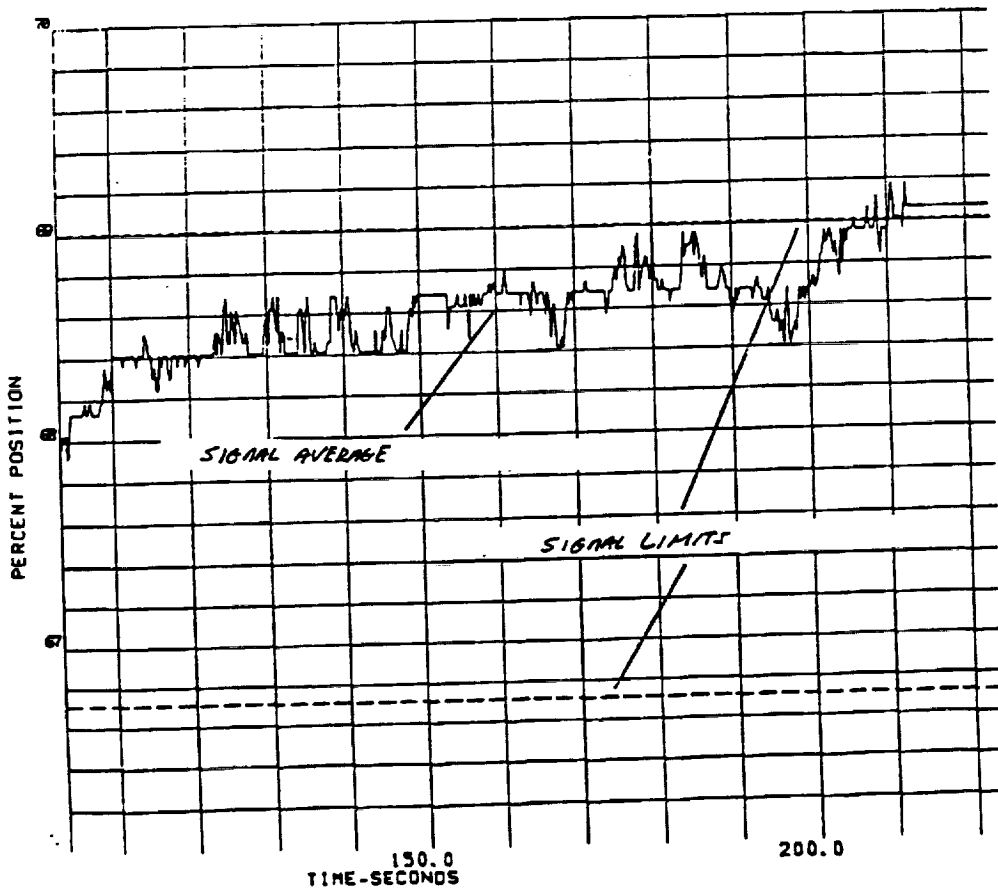


Figure 5A2

Test 750-285

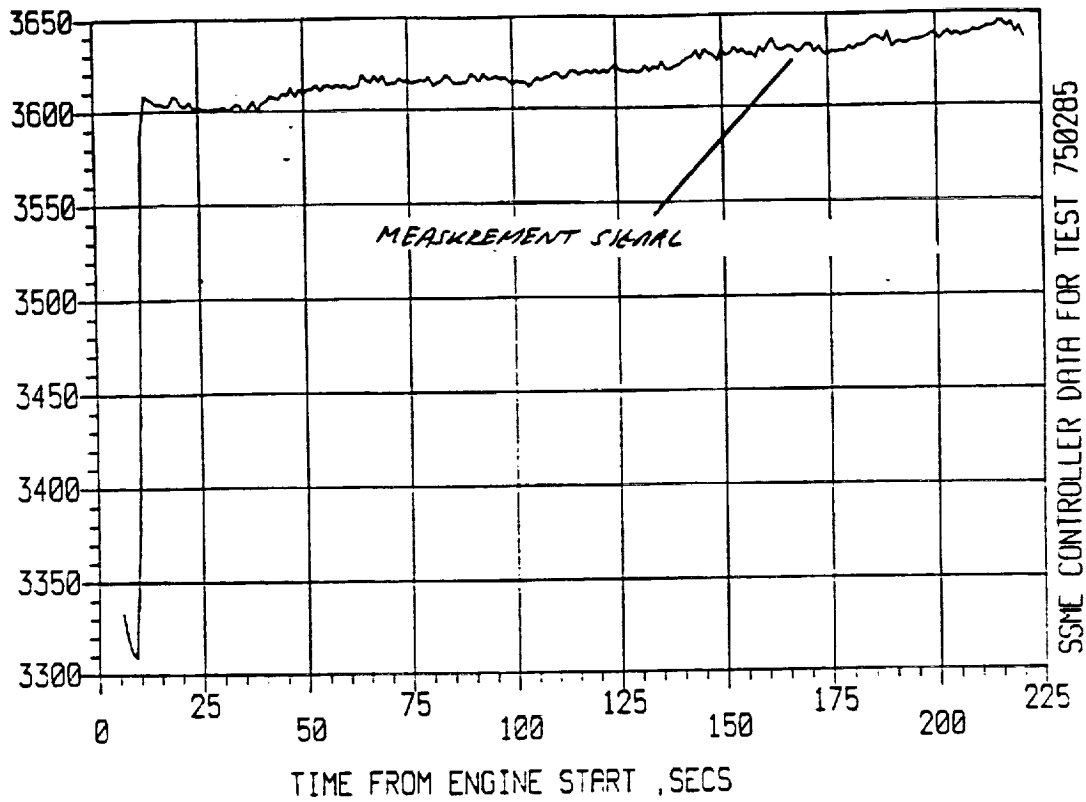


Figure 5B1

Algorithm start: 100 seconds

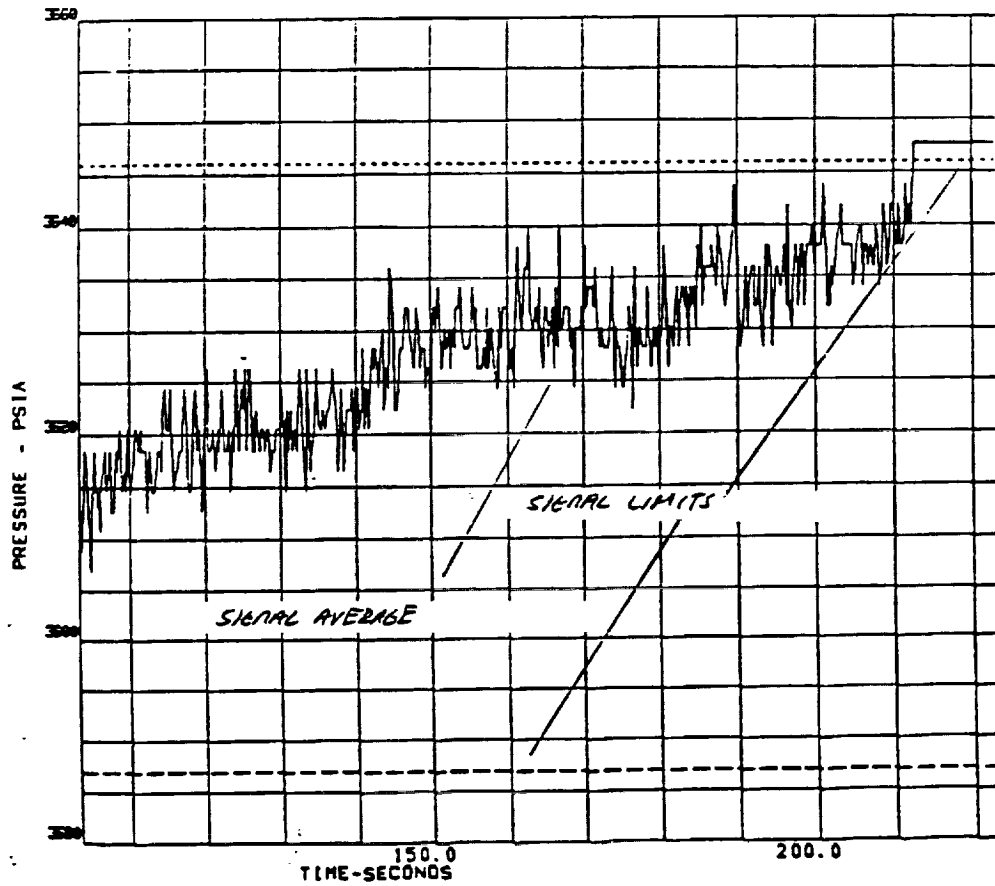


Figure 5B2 - Test 750-285

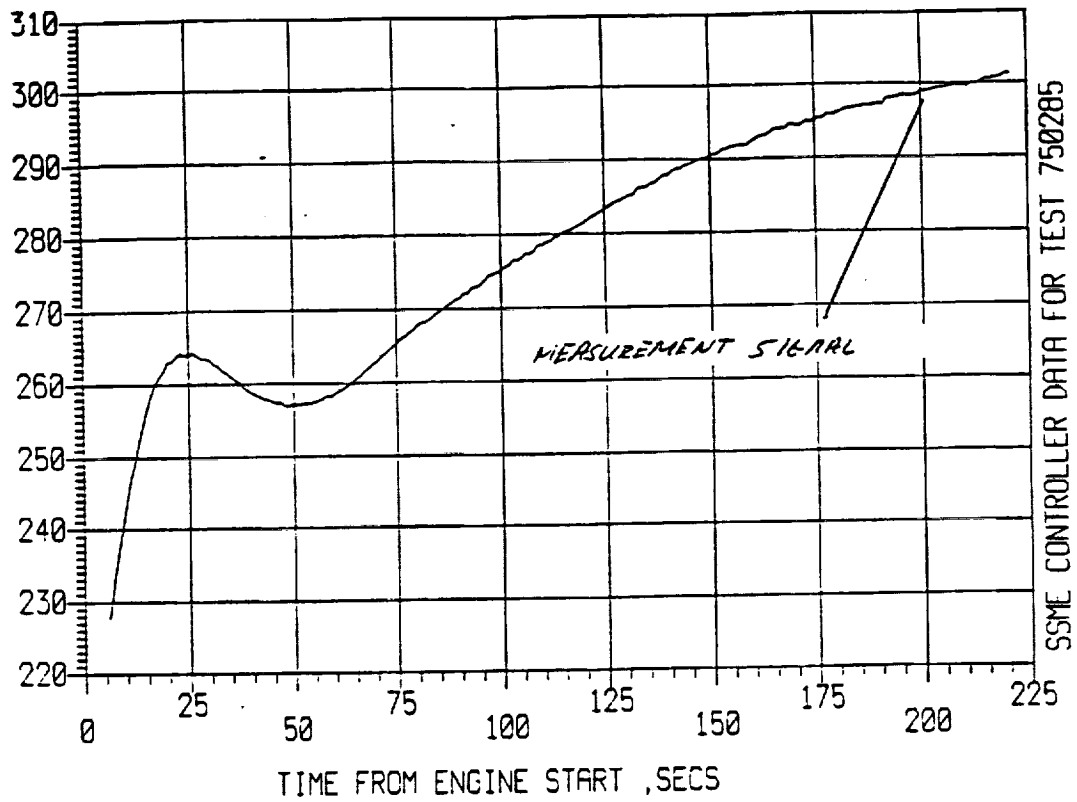


Figure 5C1

Algorithm start: 100 second

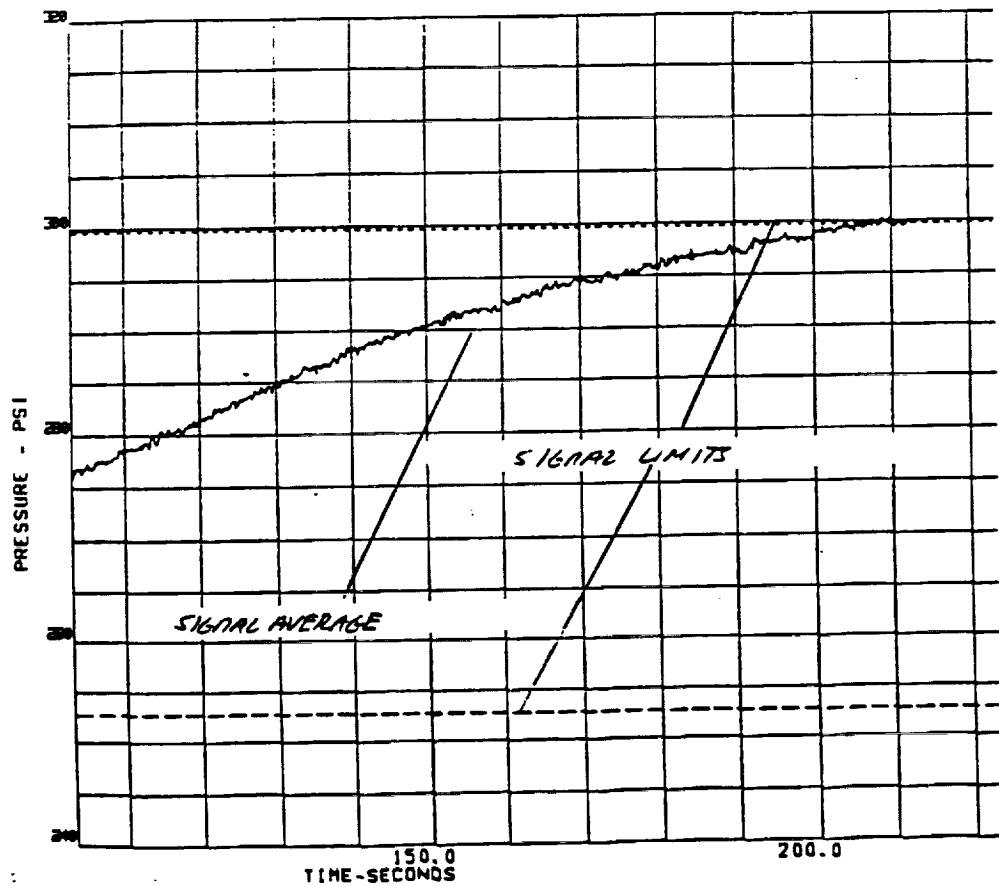


Figure 5C2 - Test 750-285

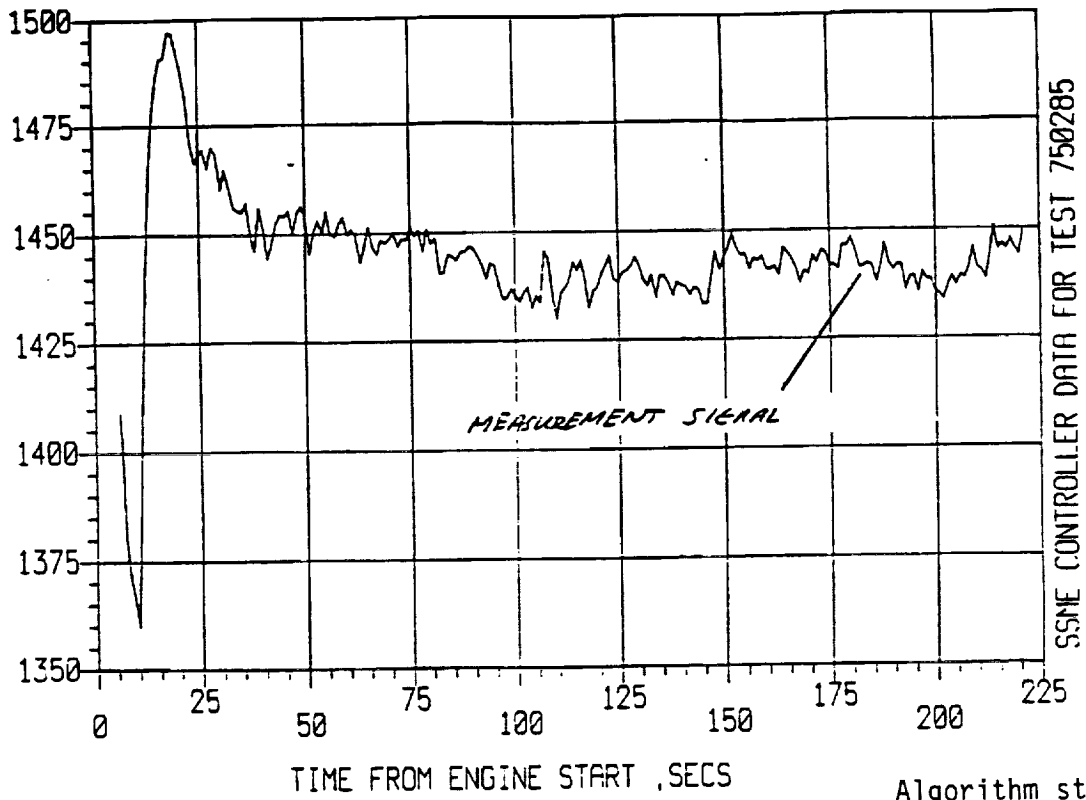


Figure 5D1

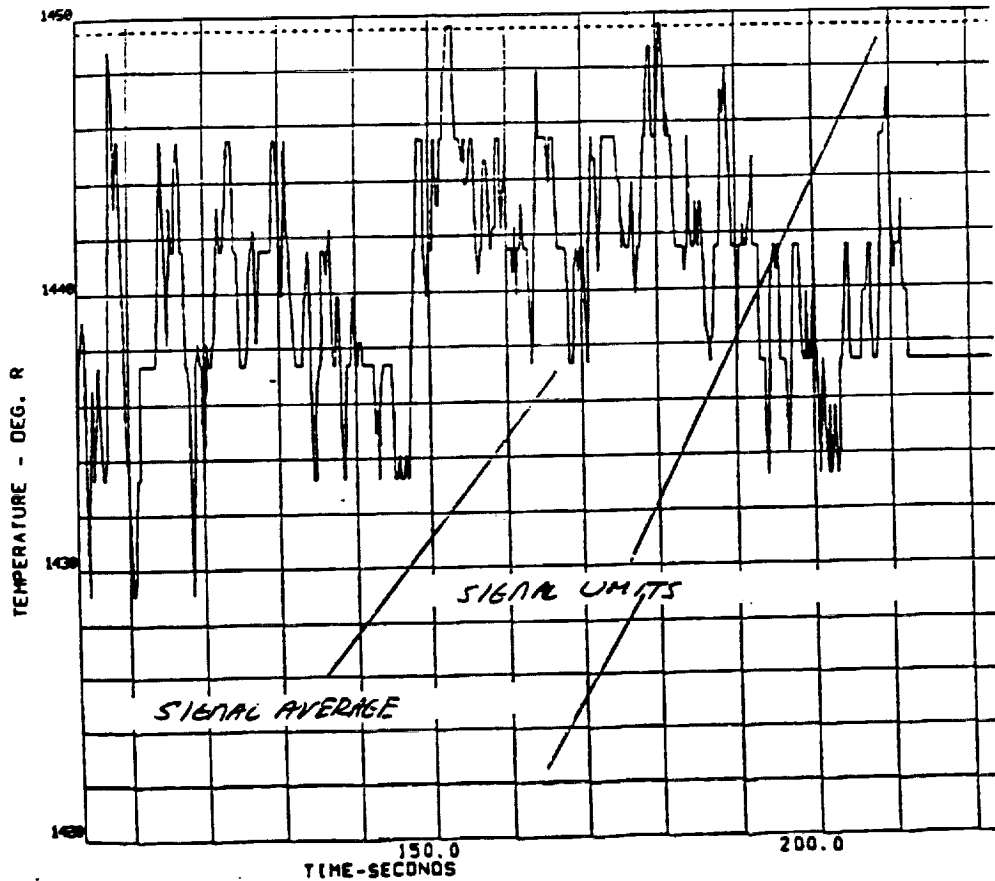
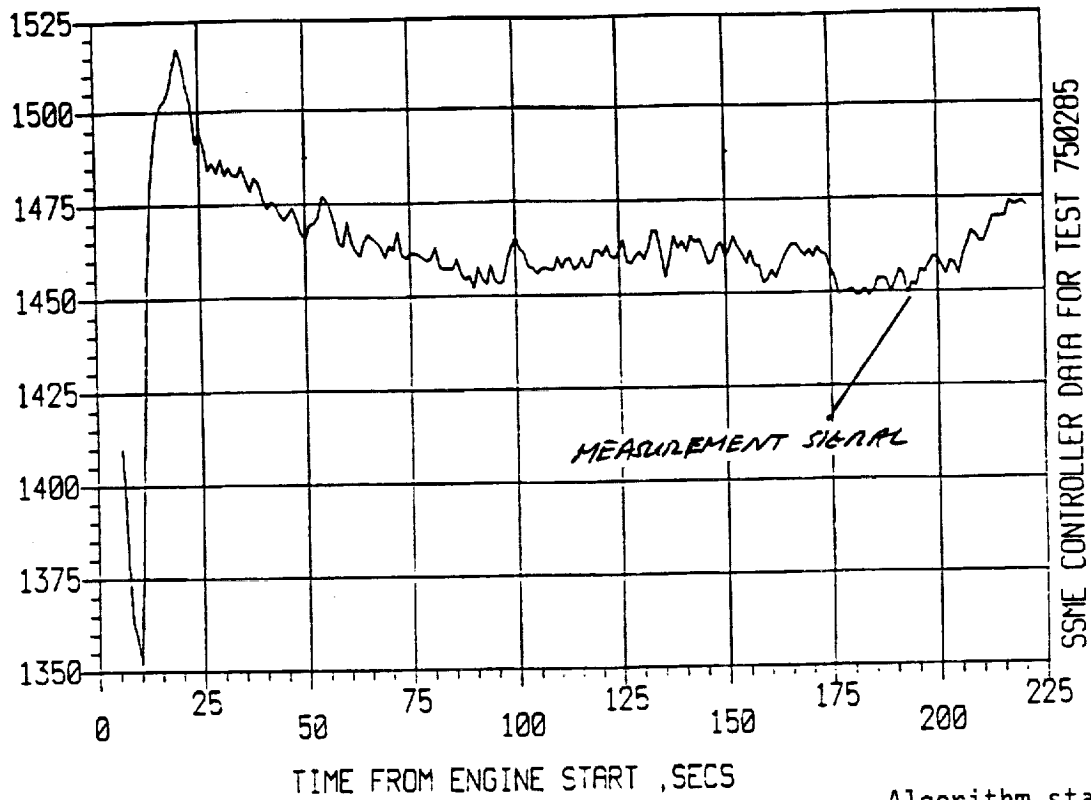


Figure 5D2 - Test 750-285



Algorithm start: 100 second

Figure 5E1

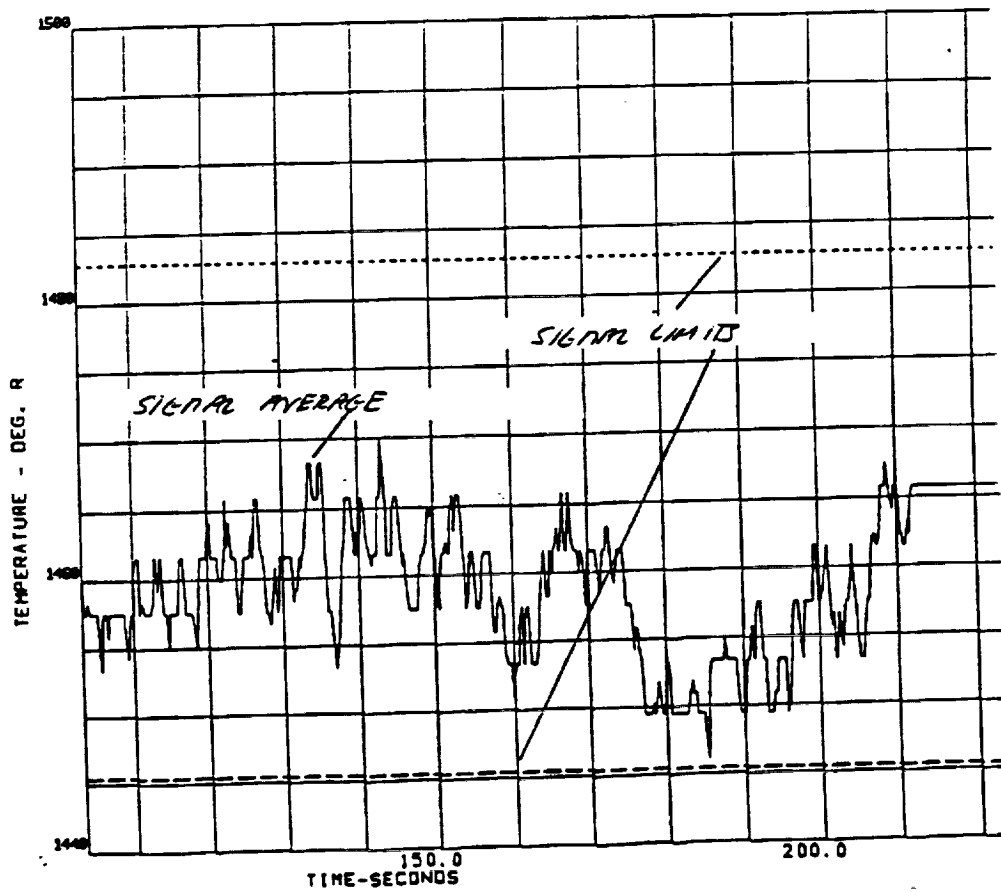


Figure 5E2 - Test 750-285

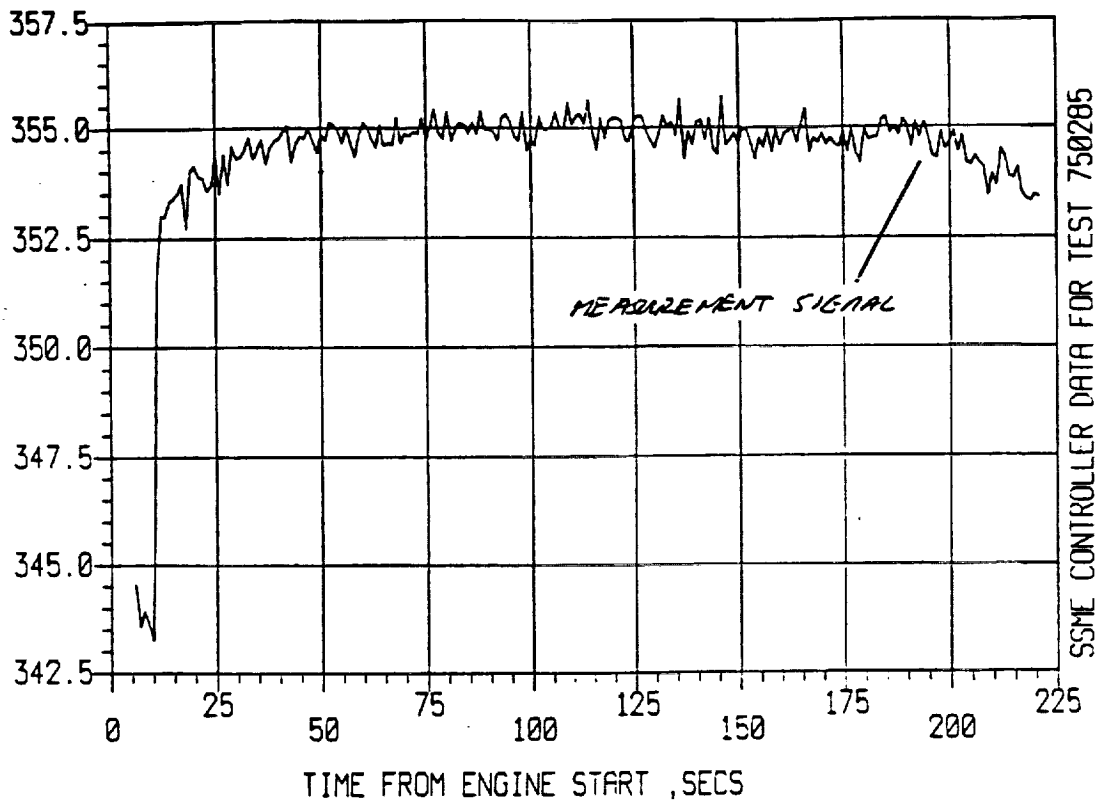


Figure 5F1

Algorithm start: 100 seconds

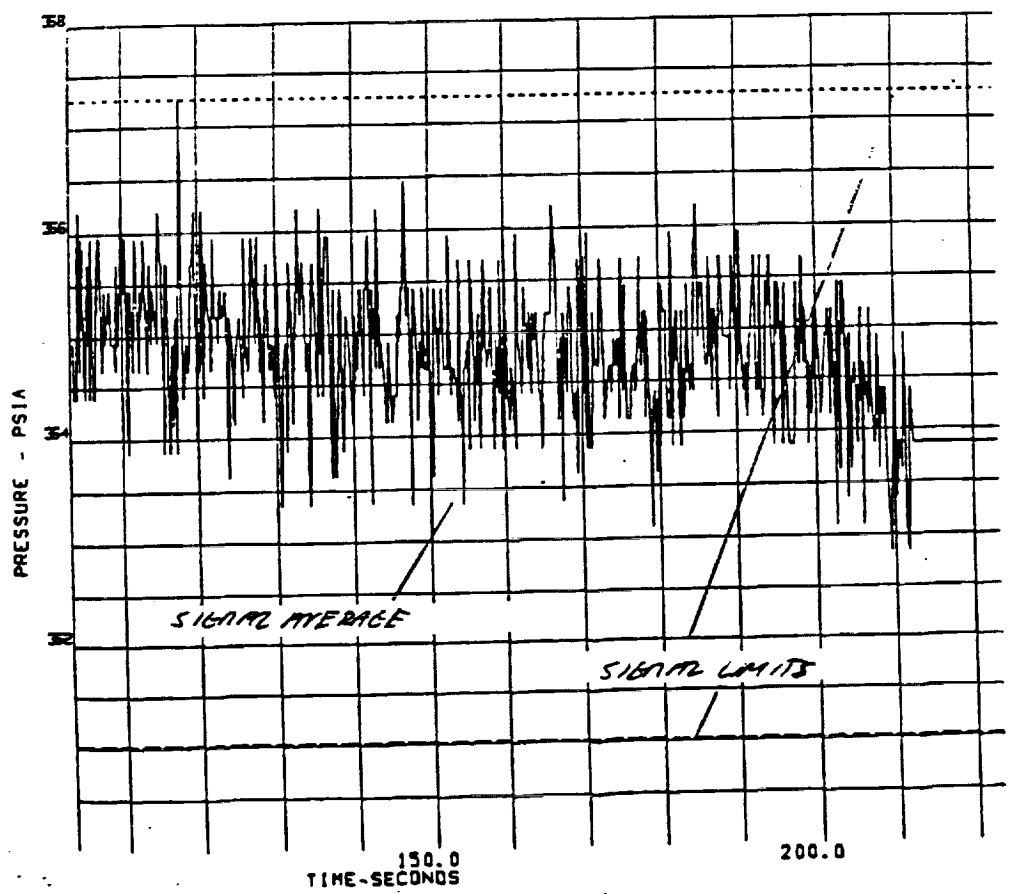


Figure 5F2 TEst 750-285

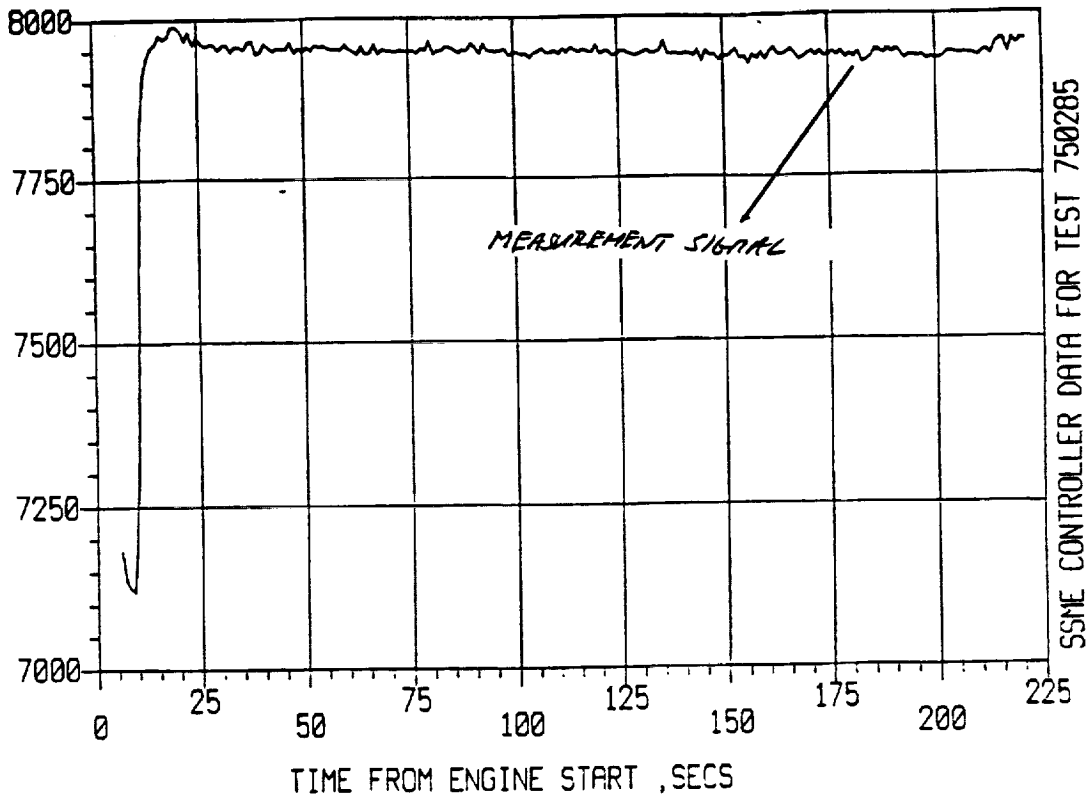


Figure 5G1

Algorithm start: 100 seconds

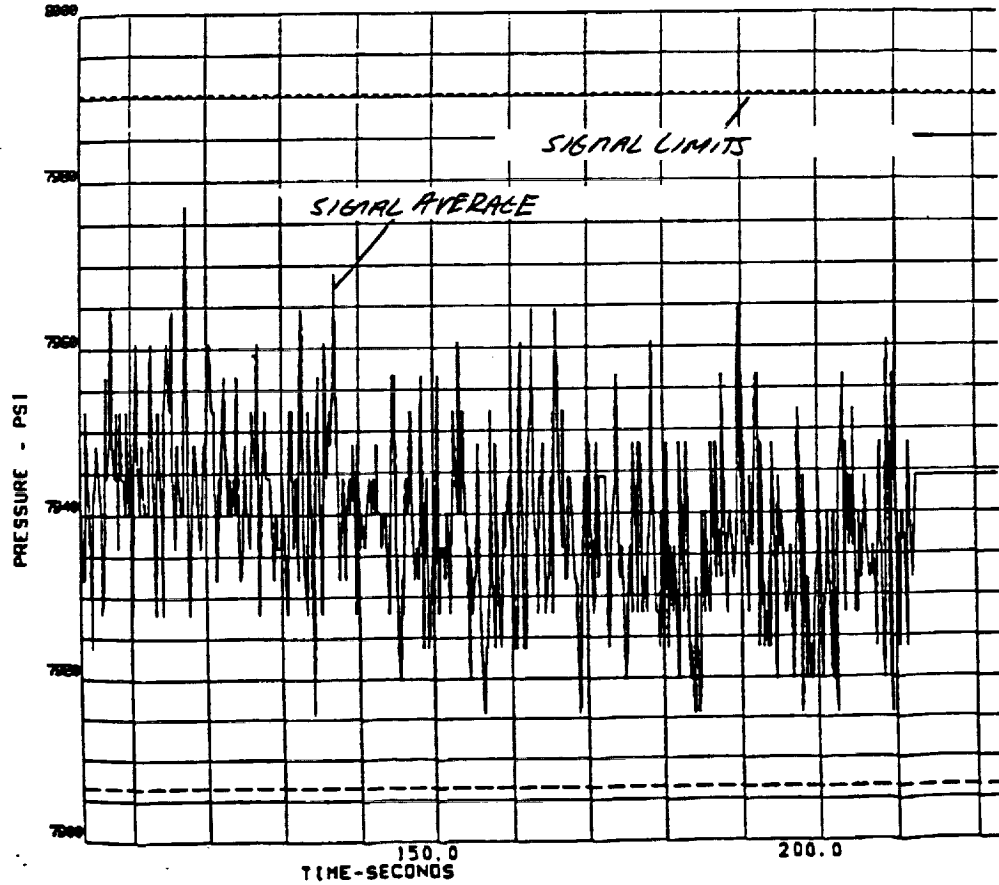
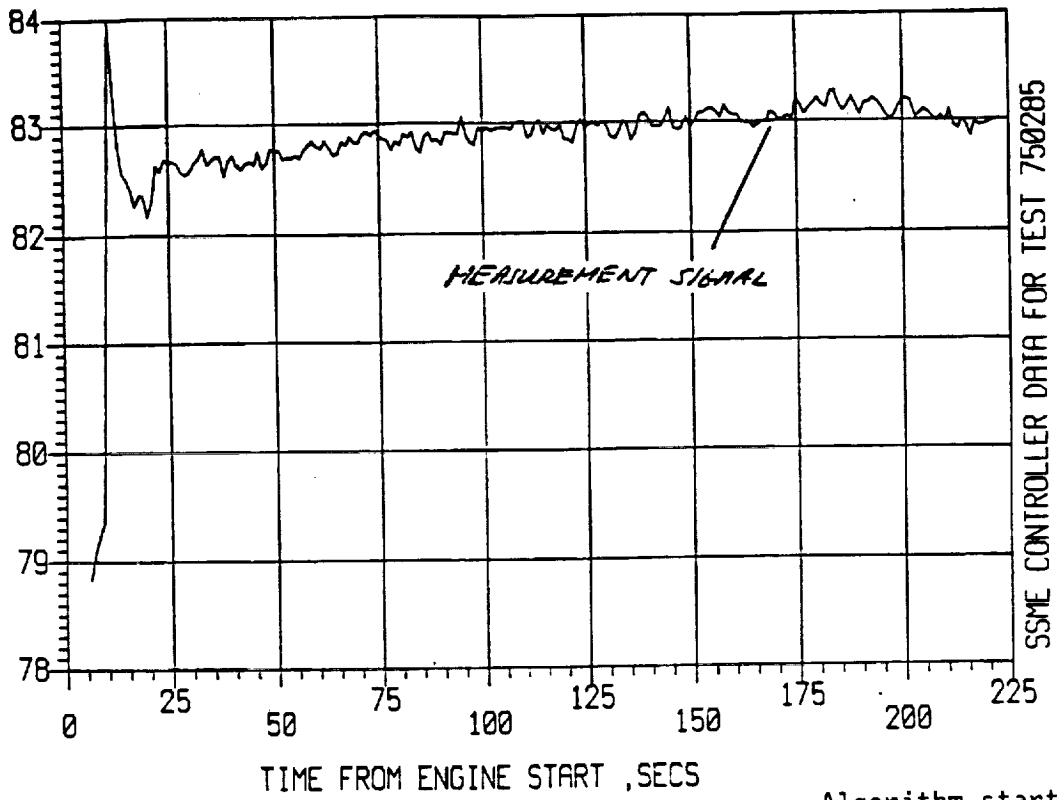


Figure 5G2 - Test 750-285



Algorithm start: 100 seconds

Figure 5H1

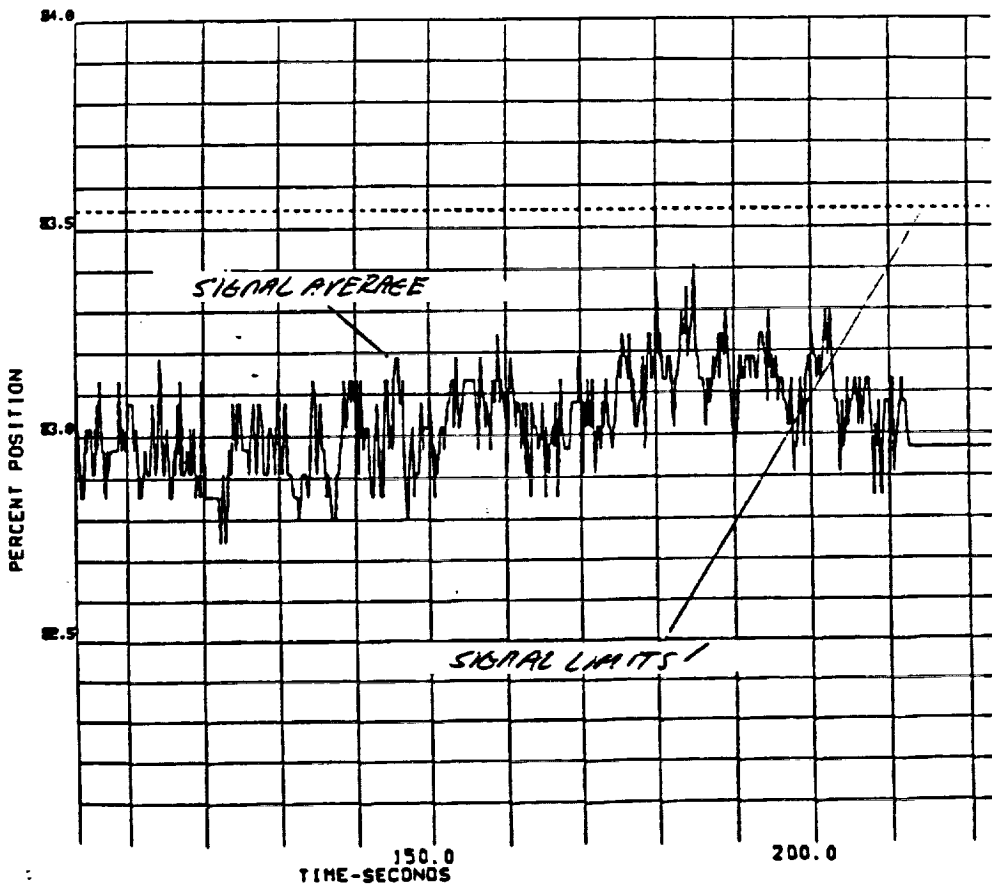


Figure 5H2 - Test 750-285

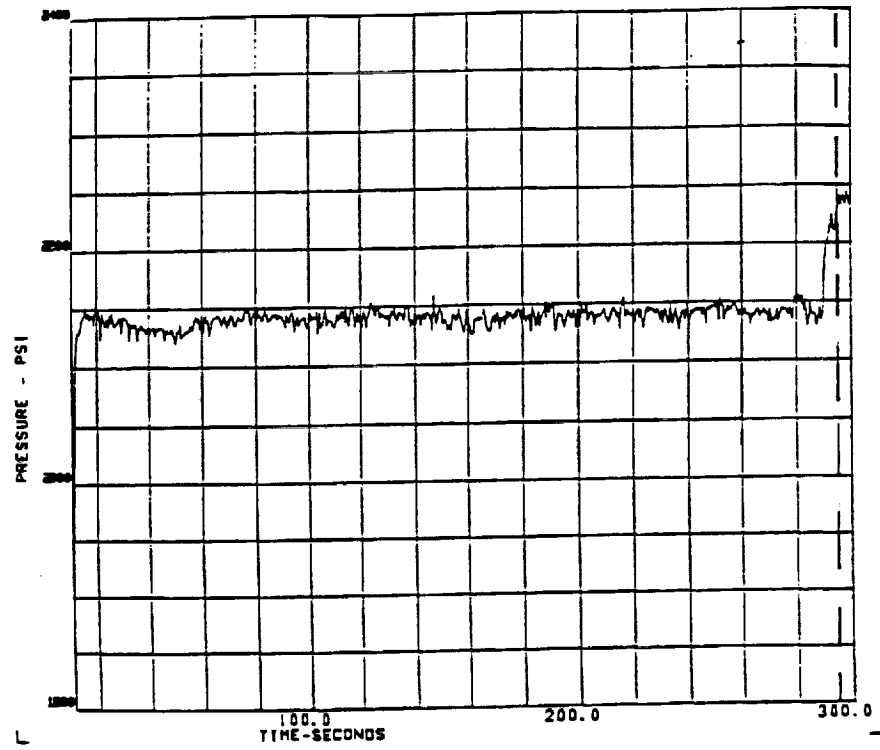


Figure 6A1 High Pressure Oxidizer Turbine Delta-P, Measurement Signal
Test 901-340

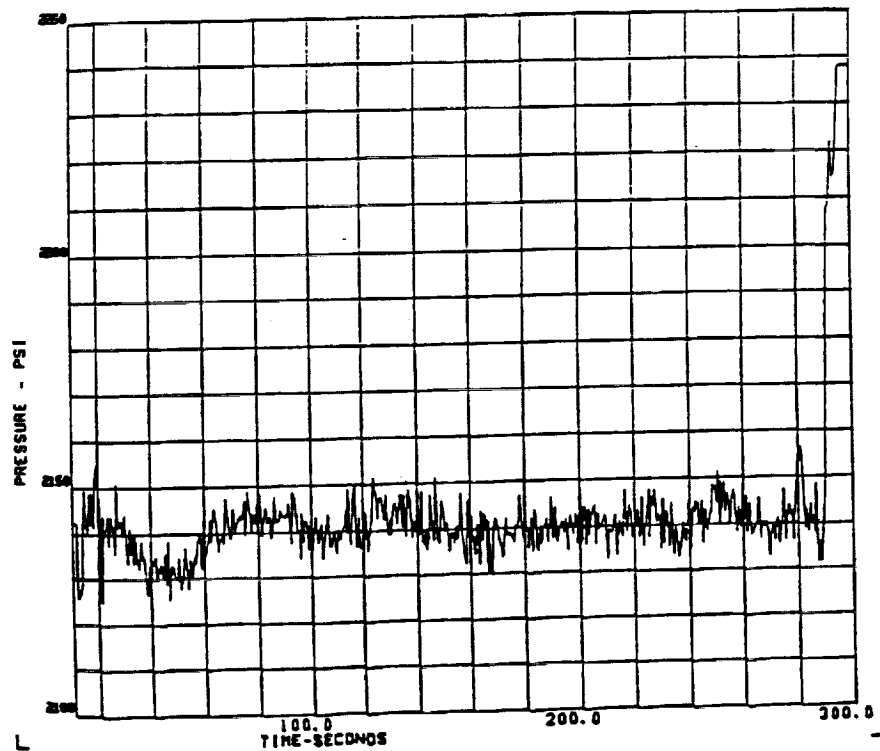


Figure 6A2 High Pressure Oxidizer Turbine Delta-P, SAFD Algorithm Signal Average
Test 901-340

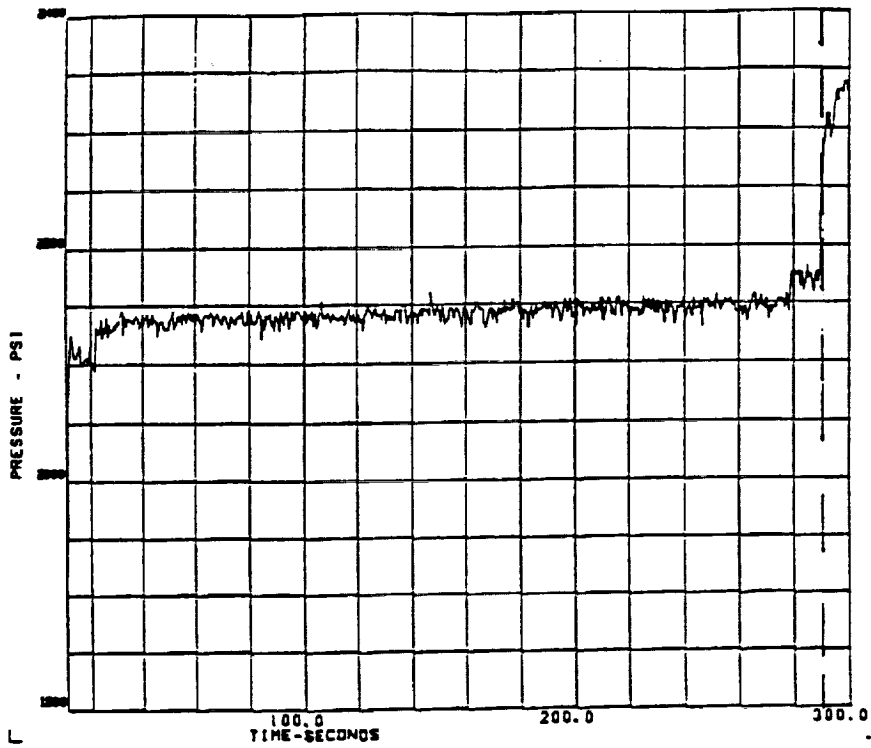
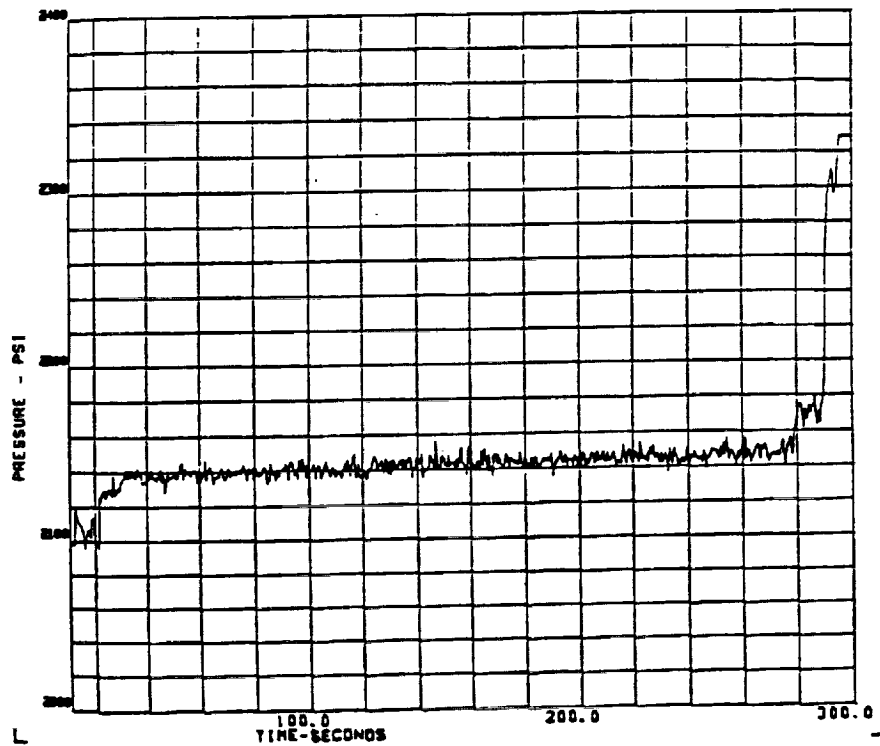


Figure 681 High Pressure Fuel Turbine Delta-P, Measurement Signal
Test 901-340



ORIGINAL PAGE IS
OF POOR QUALITY

Figure 682 High Pressure Fuel Turbine Delta-P, SAFD Algorithm Signal Average
Test 901-340

FPOV ACT POSITION
TEST 901-340 APPROACH-1 BEGINS AT 12-SEC FROM START

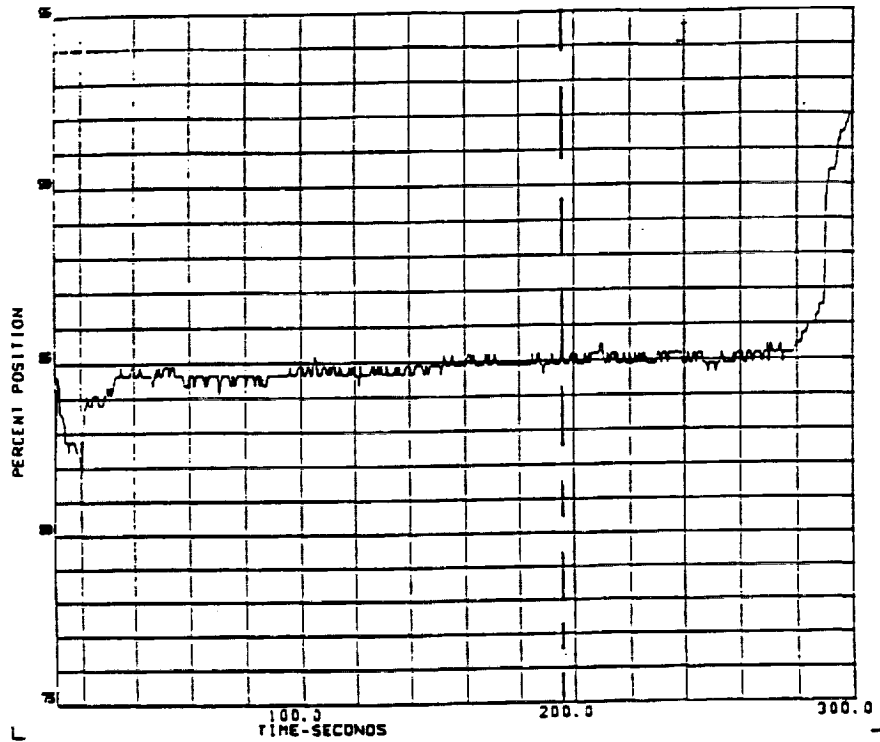


Figure 6C1 FPOV Actuator Position, Measurement Signal
Test 901-340

ORIGINAL PAGE IS
OF POOR QUALITY

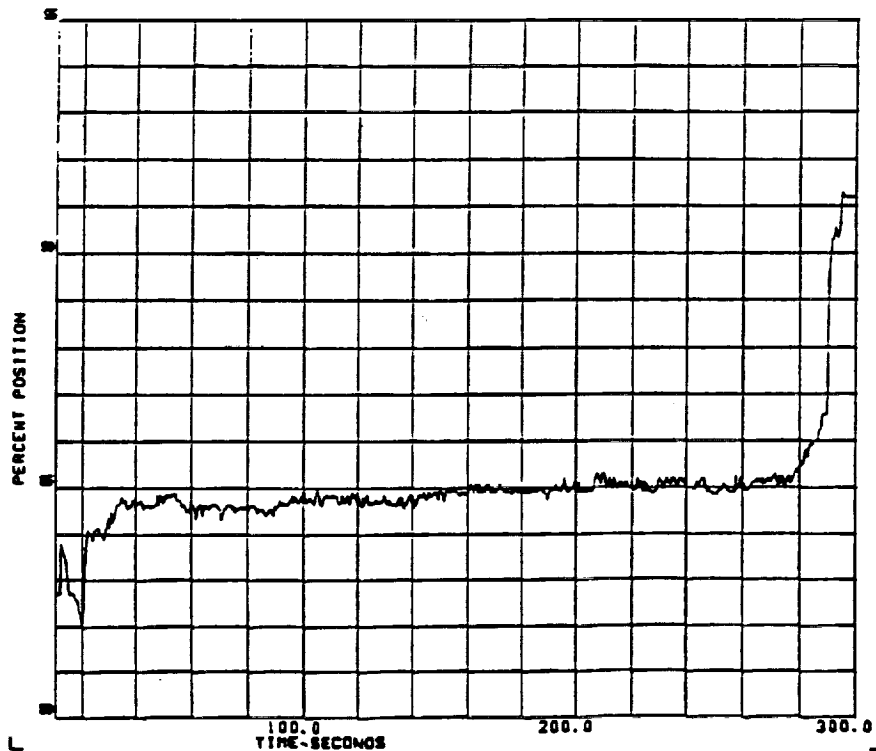


Figure 6C2 FPOV Actuator Position, SAFD Algorithm Signal Average
Test 901-340

HEX VENT DELTA-P
TEST 901-340 (APPROX-1 SECDS AT 12-SEC PREV START)

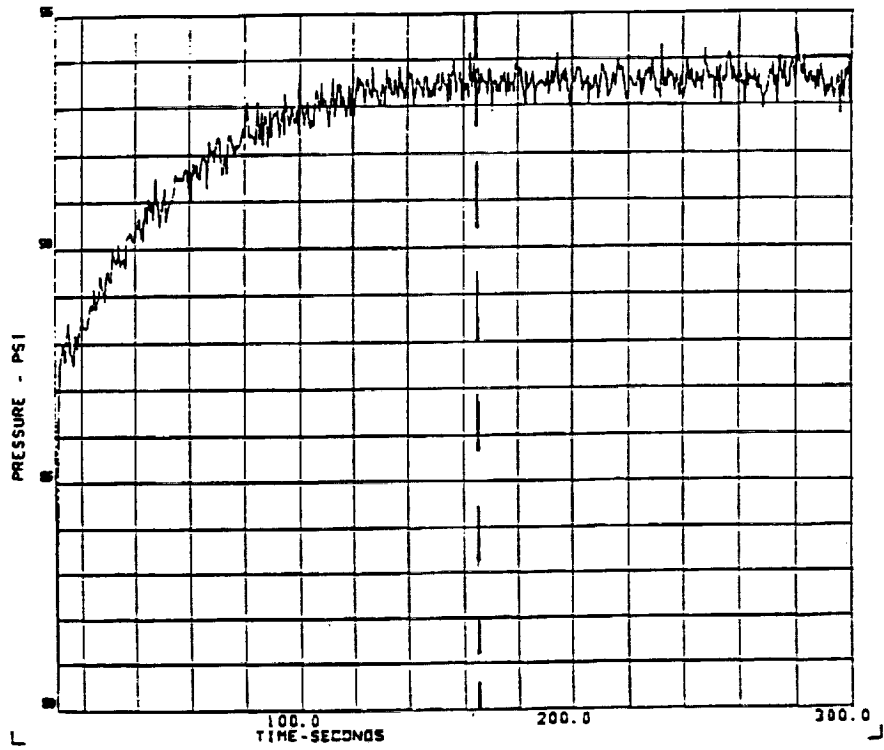


Figure 601 HEX Vent Delta-P, Measurement Signal
Test 901-340

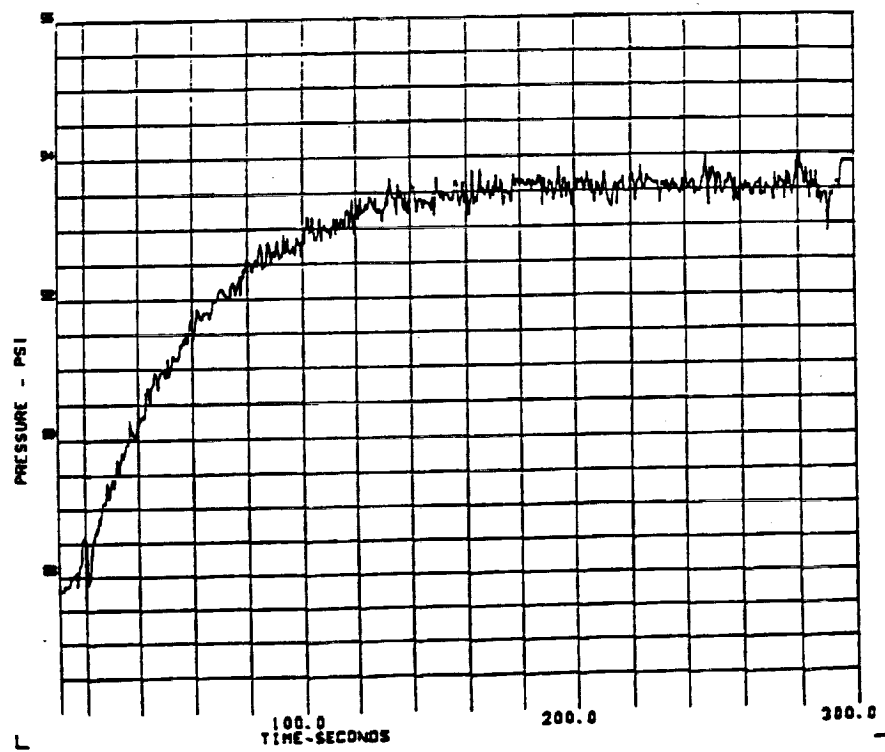


Figure 602 HEX Vent Delta-P, SAFD Algorithm Signal Average
Test 901-340

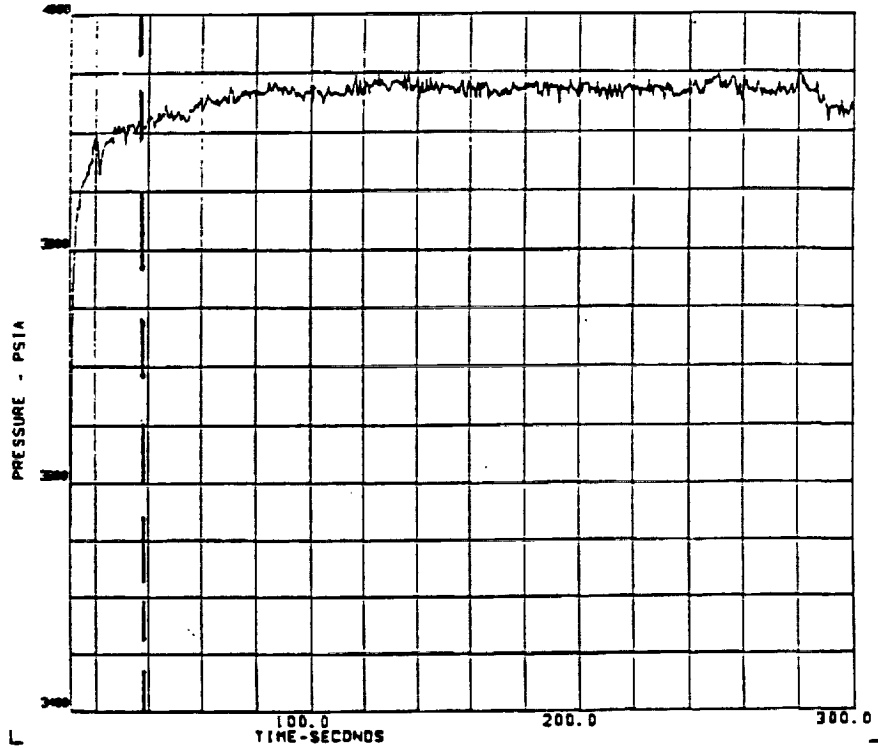
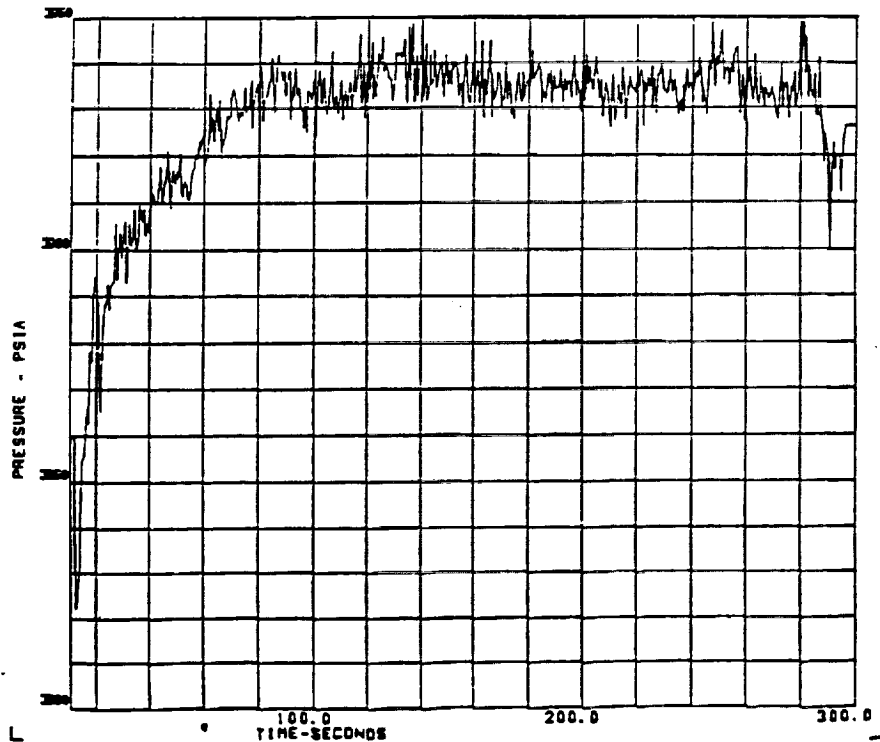


Figure 6E1 HEX Interface Pressure, Measurement Signal
Test 901-340



ORIGINAL PAGE IS
OF POOR QUALITY

Figure 6E2 HEX Interface Pressure, SAFD Algorithm Signal Average
Test 901-340

HPP COOLANT LINER DELTA-P
SERIES TEST 901-340 (APPROX-1 SECS AT 12-SEC FROM START)

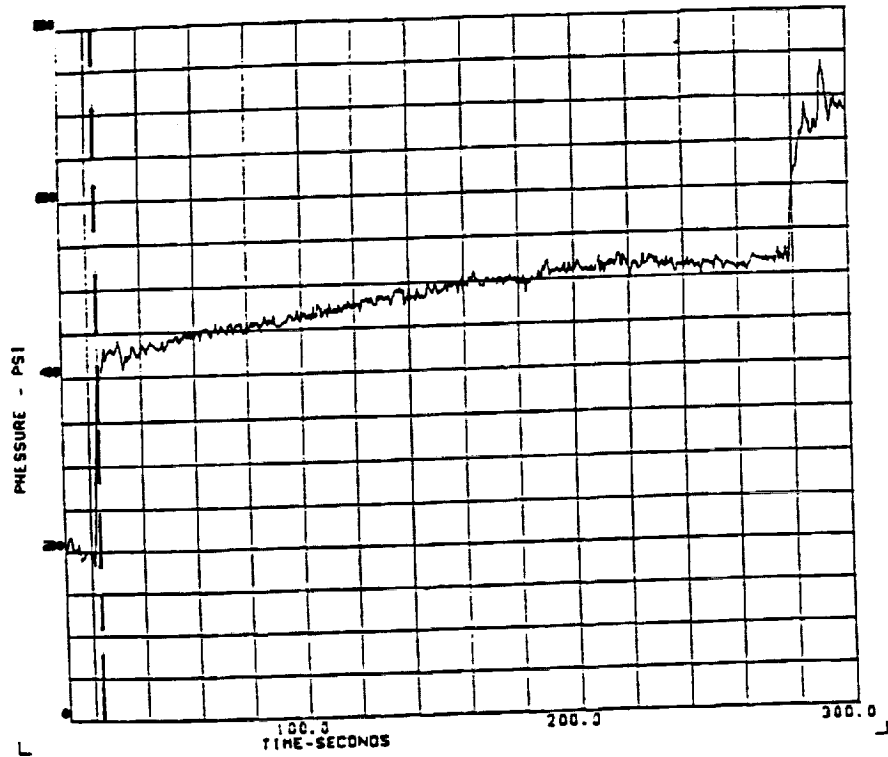
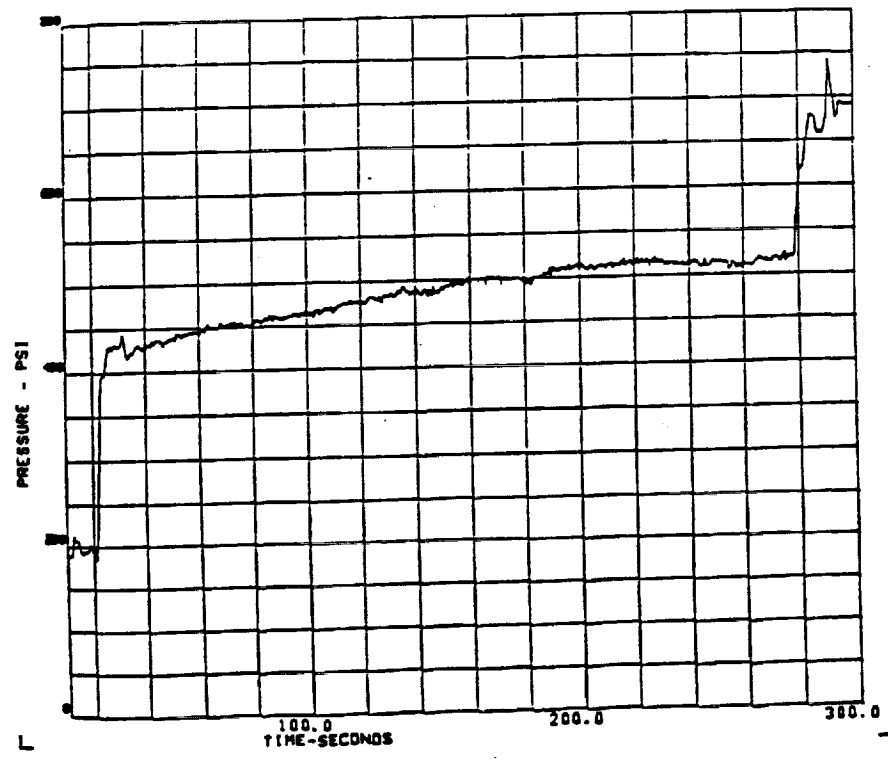


Figure 6F1 High Pressure Fuel Pump Coolant Liner Delta-P, Measurement Signal
Test 901-340



ORIGINAL PAGE IS
OF POOR QUALITY

Figure 6F2 High Pressure Fuel Pump Coolant Liner Delta-P, SAFD Algorithm Signal Average
Test 901-340

HPOT DS TMP A

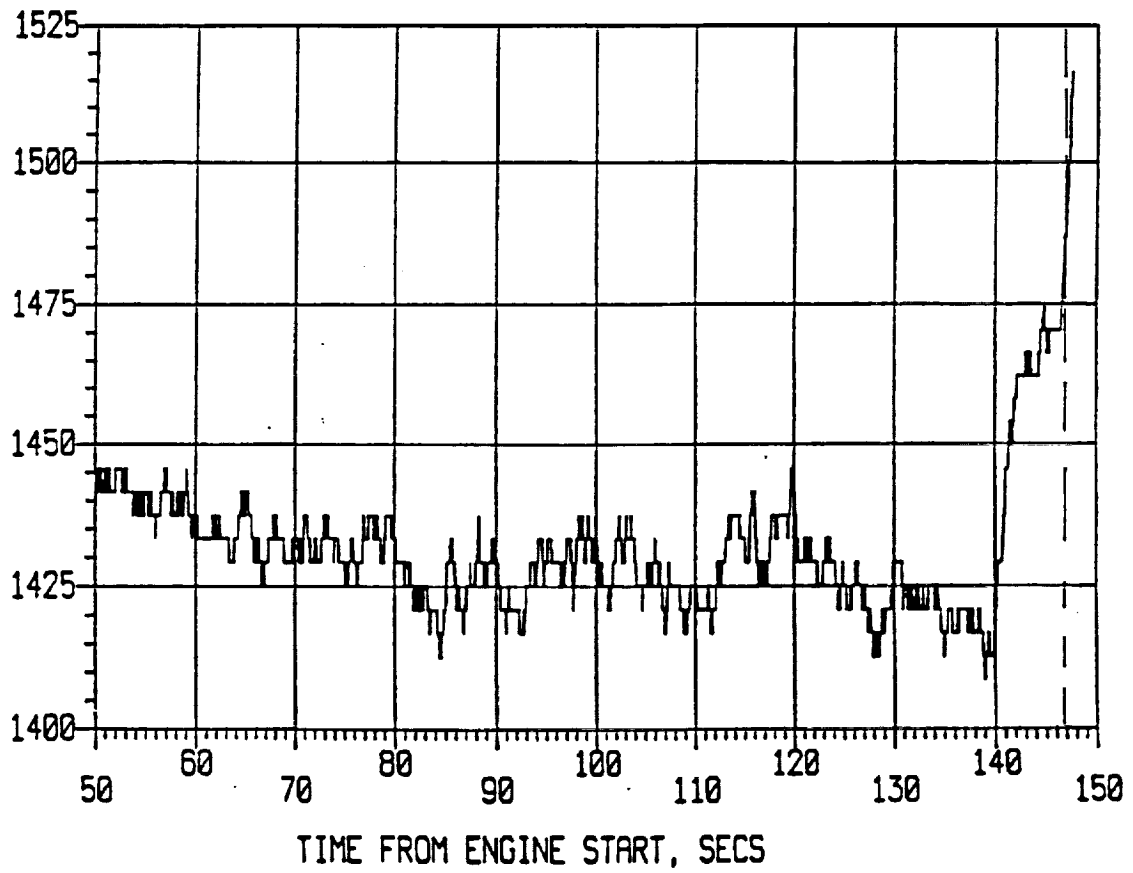


Figure 7A High Pressure Oxidizer Turbine Discharge Temp. A, Measurement Signal
Test 902-471

HPOT DS TMP B

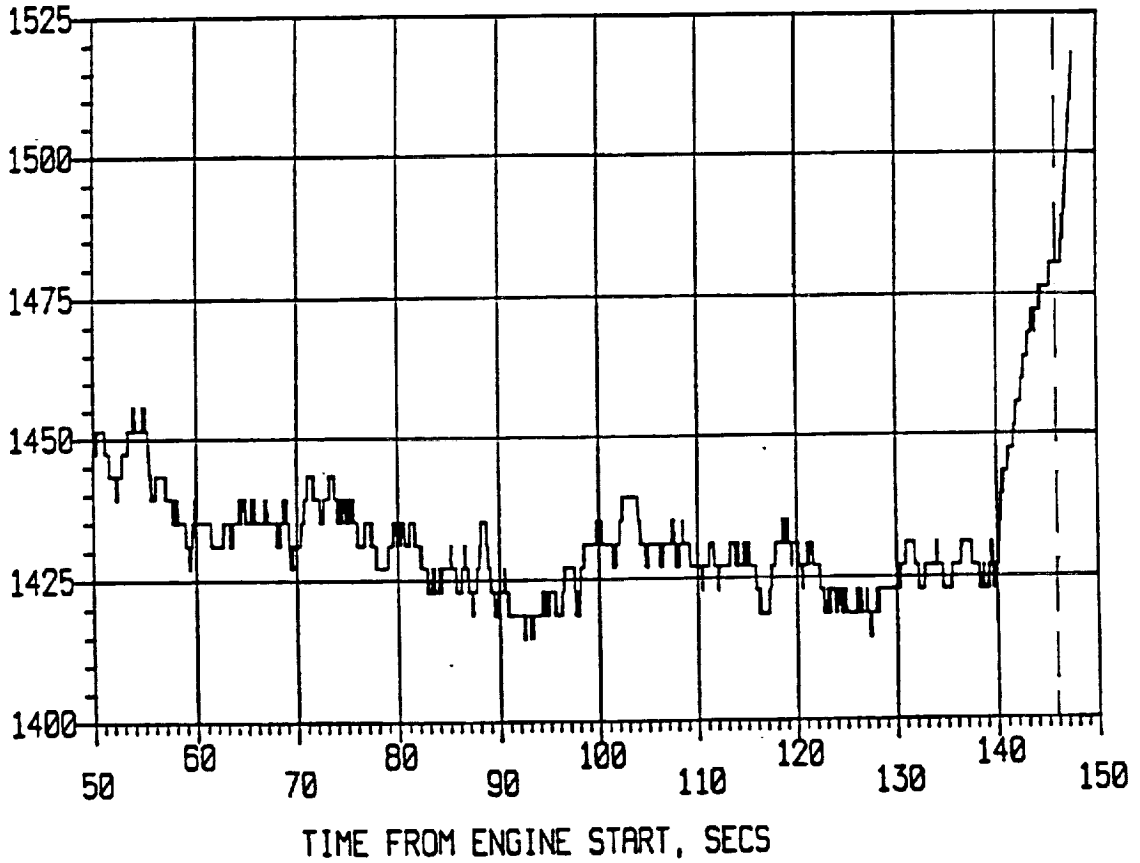


Figure 7B High Pressure Oxidizer Turbine Discharge Temp. B, Measurement Signal
Test 902-471

ENG FL FLOW NFD 27KOPM

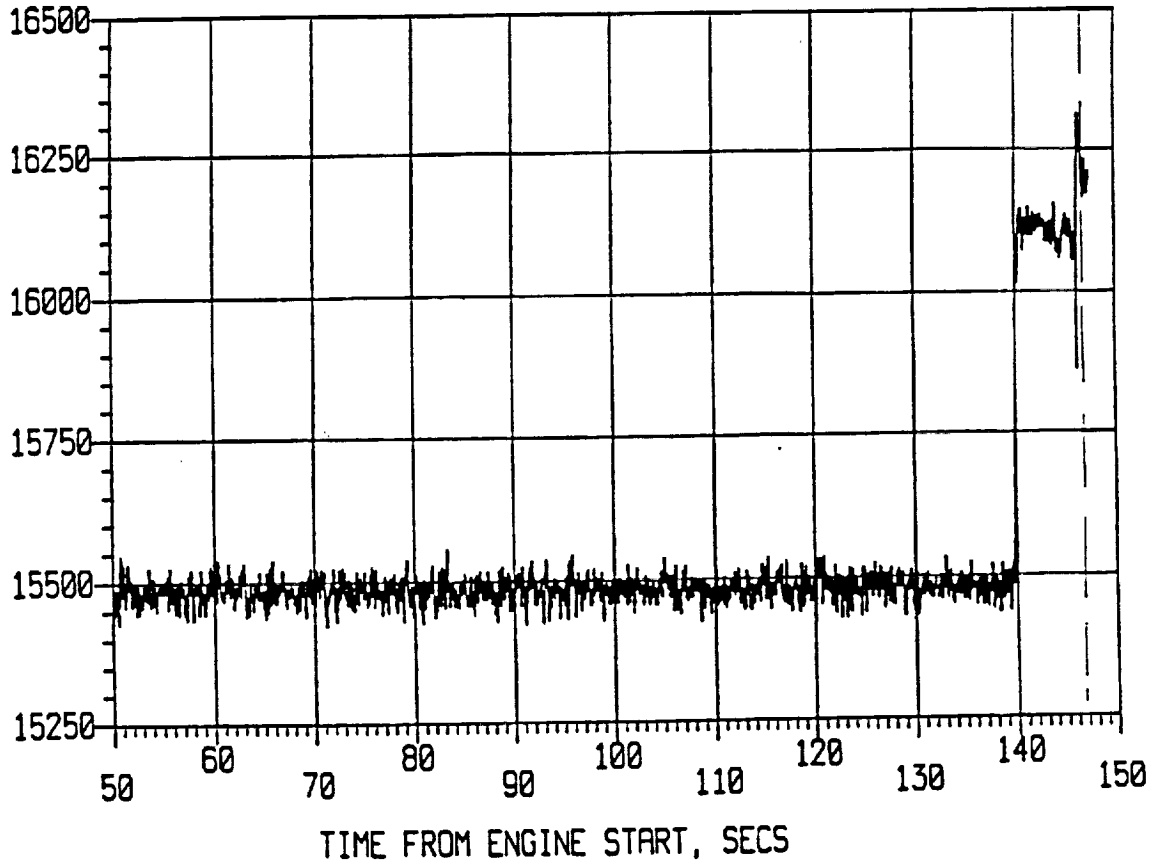


Figure 7C Engine Fuel Flow, Measurement Signal
Test 902-471

HPFP BAL CAV PR 10K PSIS

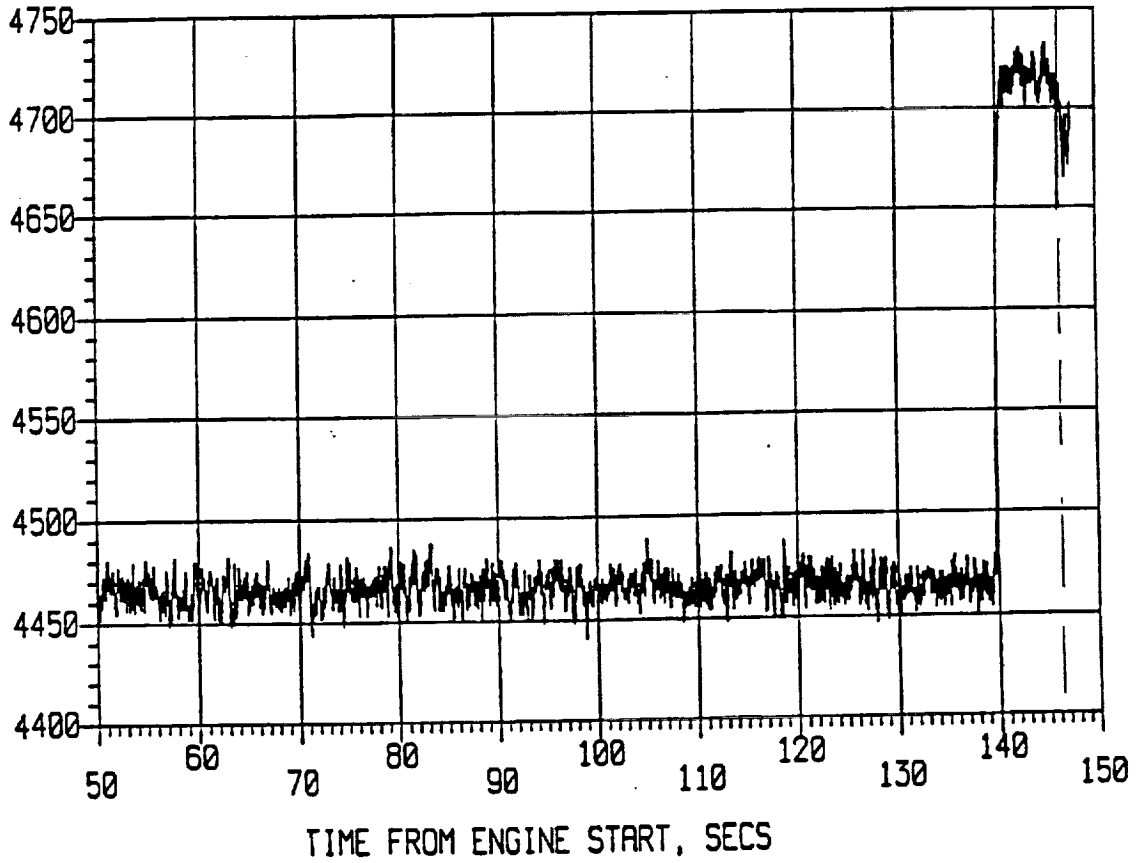


Figure 7D High Pressure Fuel Pump Balance Cavity Pressure, Measurement Signal
Test 902-471

HPOP DS PR A

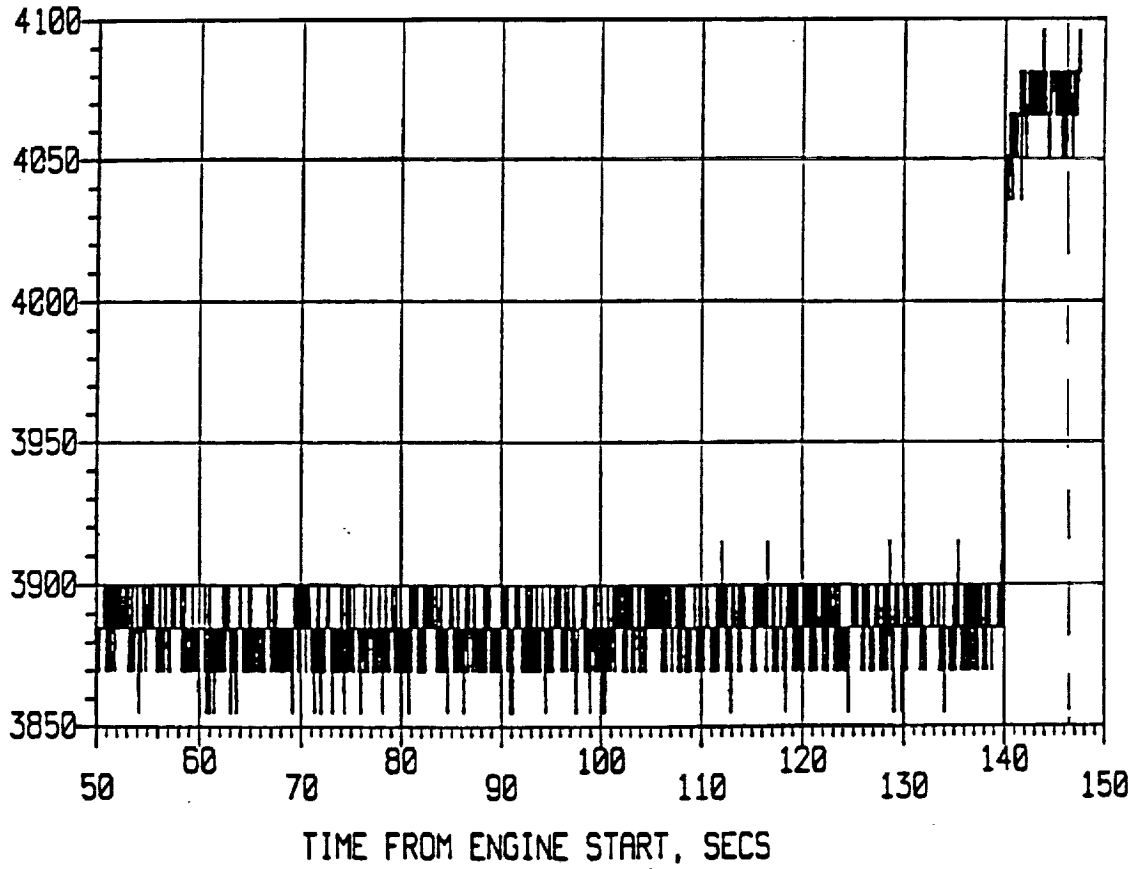


Figure 7E High Pressure Oxidizer Pump Discharge Pressure A, Measurement Signal
Test 902-471

MCC PC B2

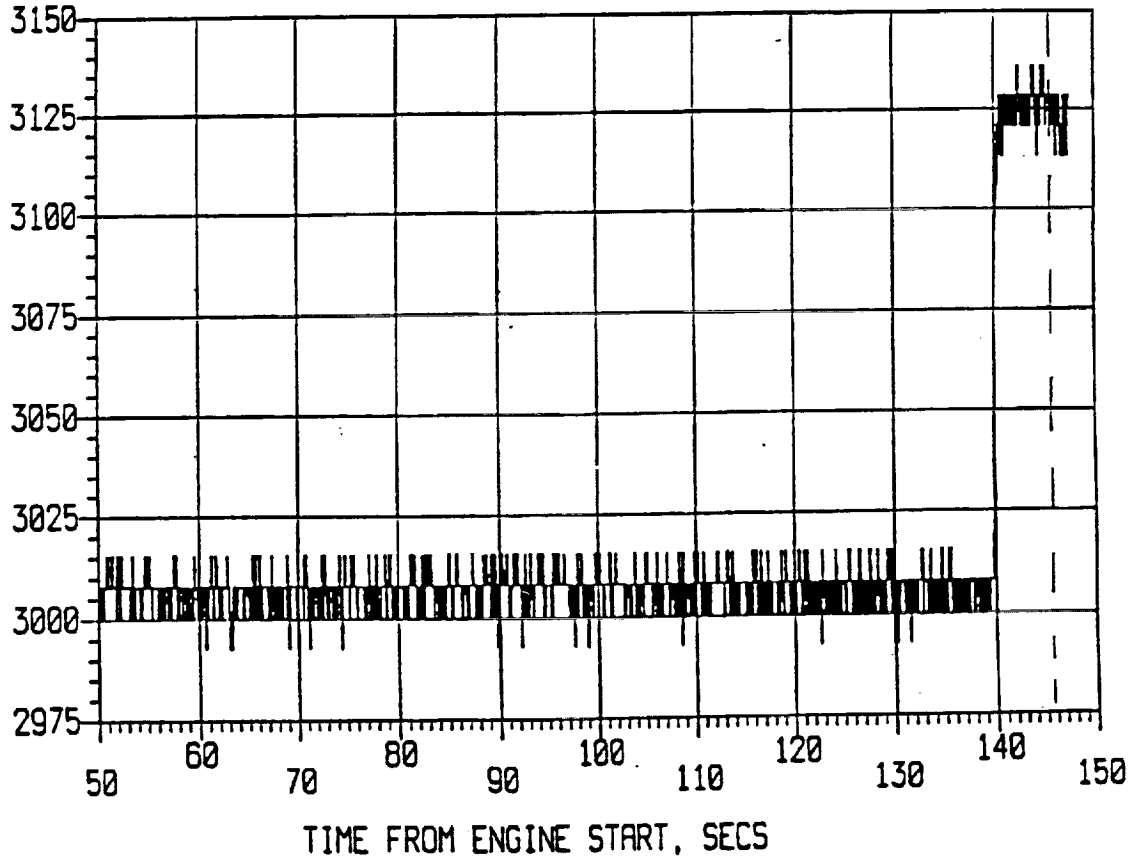


Figure 7F Main Combustion Chamber Pressure, Measurement Signal
Test 902-471

HPFP DS PR A

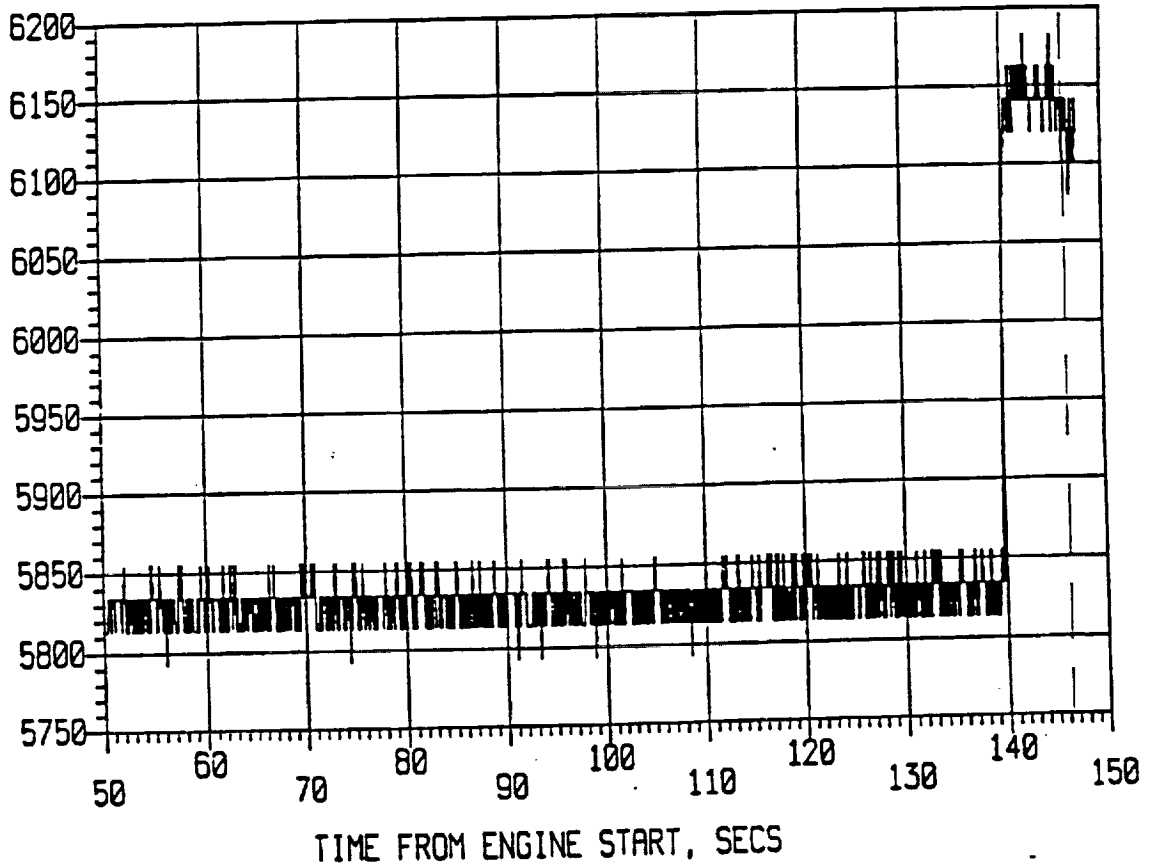


Figure 7G High Pressure Fuel Pump Discharge Pressure A, Measurement Signal
Test 902-471

HPFP CLNT LNR A

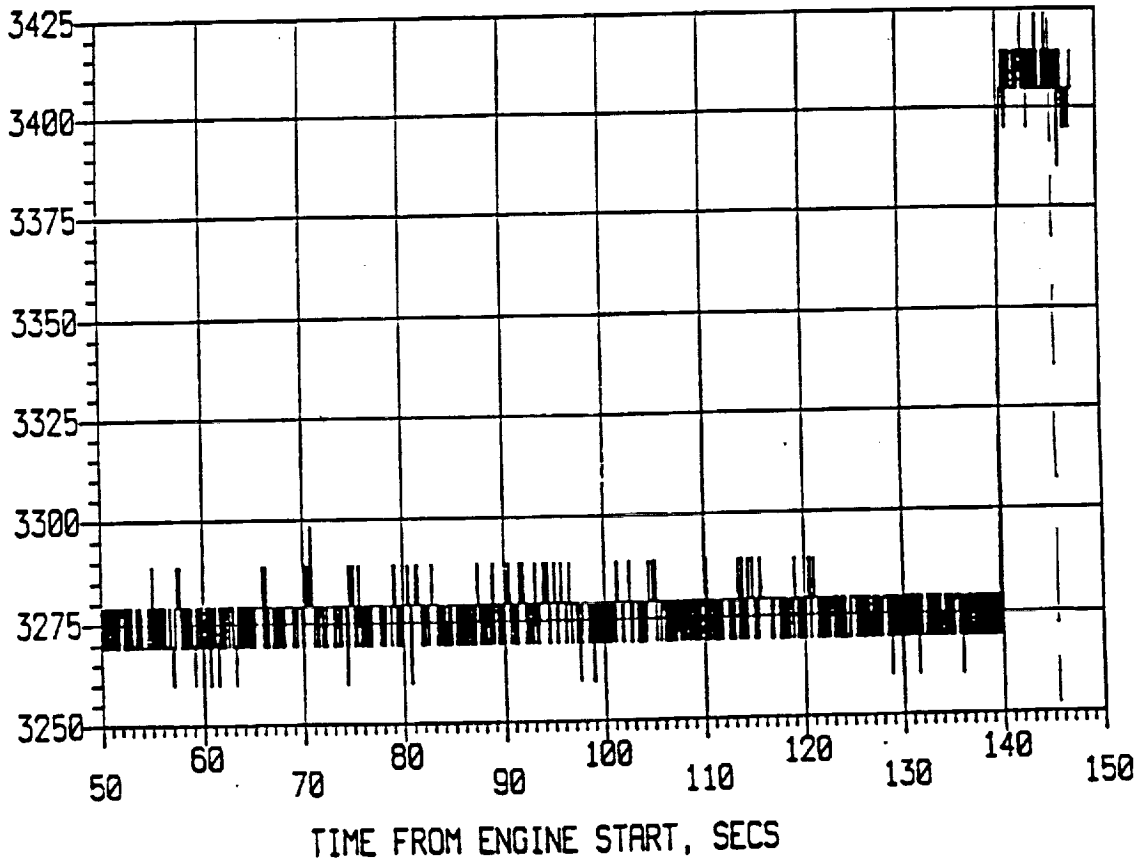


Figure 7H High Pressure Fuel Pump Coolant Liner Pressure A, Measurement Signal
Test 902-471

HX INT T

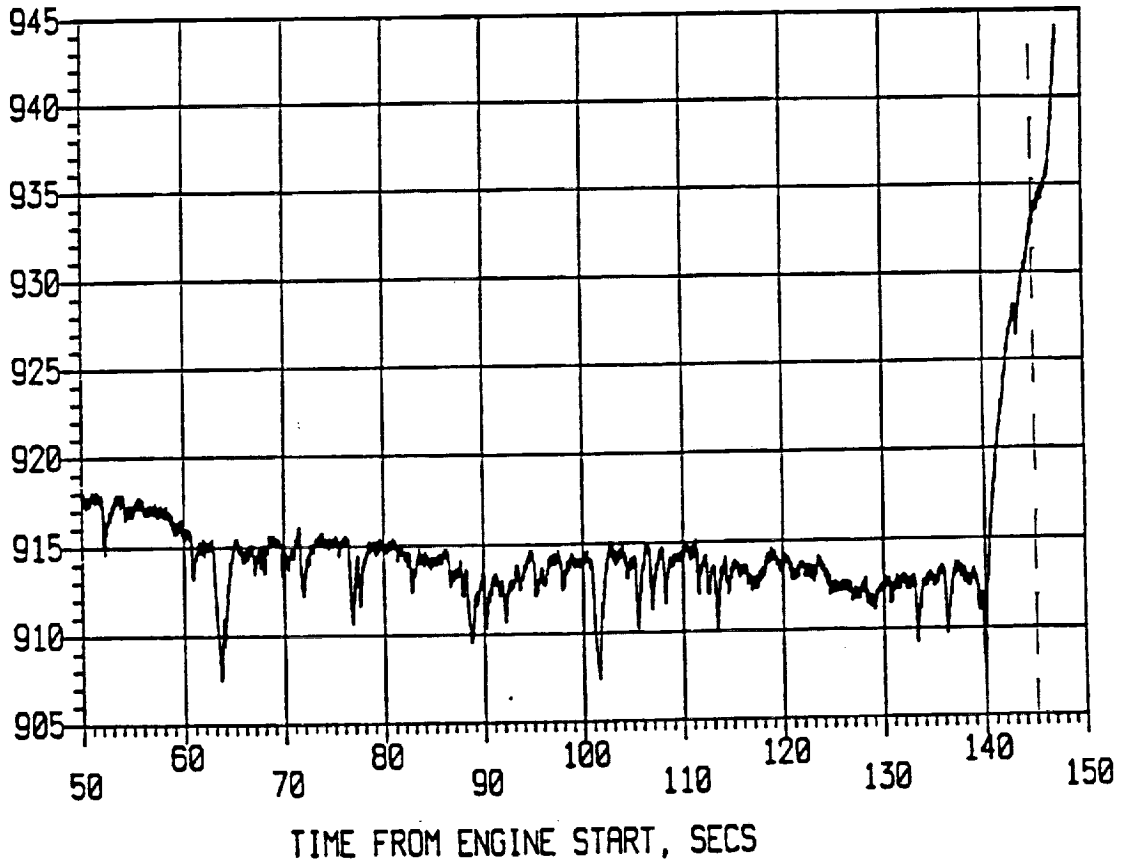
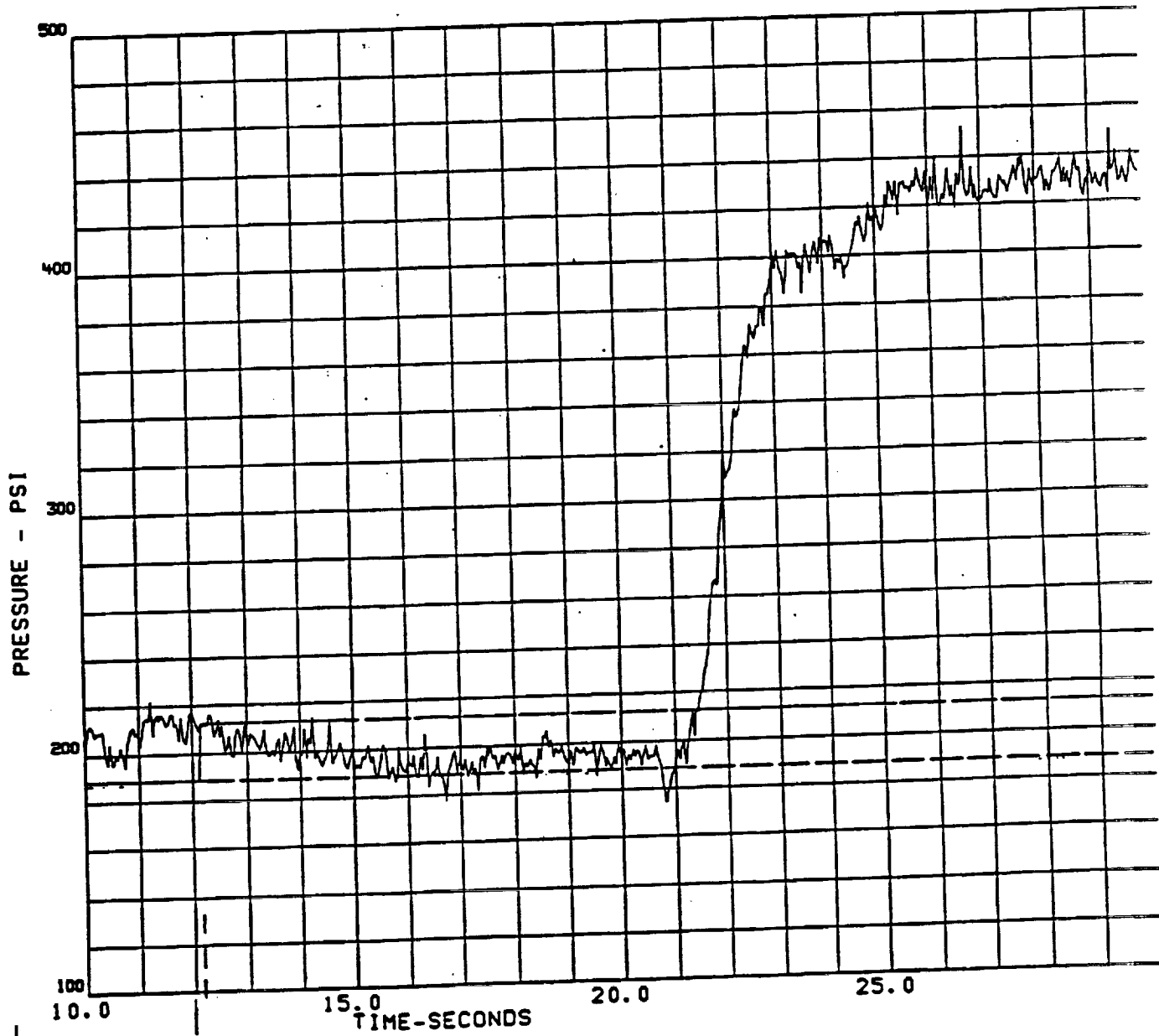


Figure 71 HEX Interface Temperature, Signal Measurement
Test 902-471

HFFP COOLANT LINER DELTA-P

———	SENSOR	TEST 901-340	(APPROACH-1 BEGINS AT 12-SEC FROM START)
-----	AV1ND4	TEST 901-340	(APPROACH-1 BEGINS AT 12-SEC FROM START)
-----	AV2ND4	TEST 901-340	(APPROACH-1 BEGINS AT 12-SEC FROM START)
-----	AV3ND4	TEST 901-340	(APPROACH-1 BEGINS AT 12-SEC FROM START)
-----	AV4ND4	TEST 901-340	(APPROACH-1 BEGINS AT 12-SEC FROM START)



Algorithm start: 12.08 sec.

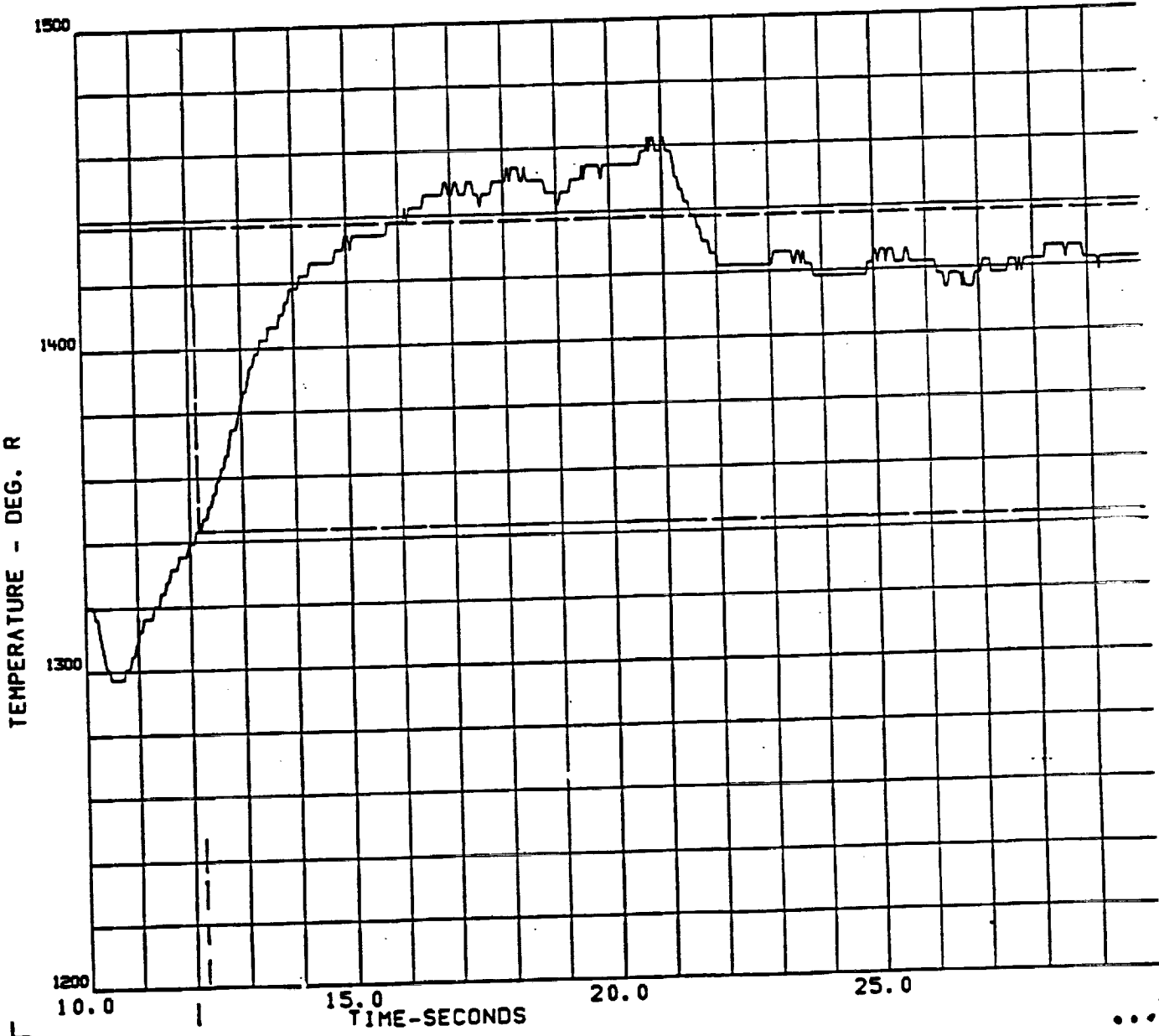
Redline
Cutoff:
405.5

ORIGINAL PAGE IS
OF POOR QUALITY

FIGURE 8A

HIGH PRESSURE OX TURBINE DS TEMP

- SENS14 TEST 901-340 (APPROACH+1 BEGINS AT 12-SEC FROM START)
- - - AVIN14 TEST 901-340 (APPROACH+1 BEGINS AT 12-SEC FROM START)
- - - AV2N14 TEST 901-340 (APPROACH+1 BEGINS AT 12-SEC FROM START)
- - - AV3N14 TEST 901-340 (APPROACH+1 BEGINS AT 12-SEC FROM START)
- - - AVIN14 TEST 901-340 (APPROACH+1 BEGINS AT 12-SEC FROM START)



Algorithm start: 12.08 sec.

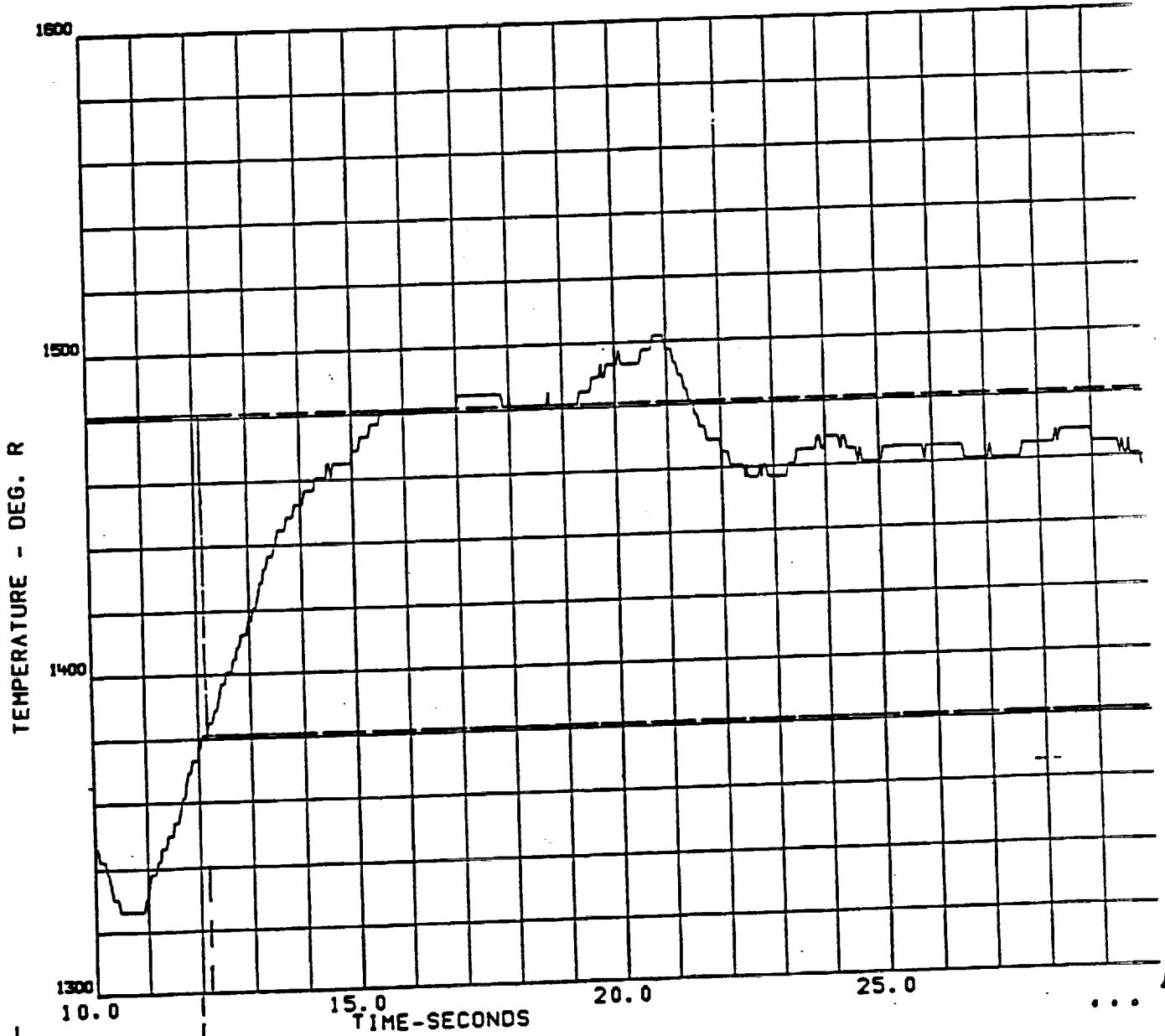
Redline
C/O: 405.5

ORIGINAL PAGE IS
OF POOR QUALITY

FIGURE 8B

HIGH PRESSURE OX TURBINE DS TEMP2

————	SENS15	TEST 901-340	(APPROACH+1 BEGINS AT 12-SEC FROM START)
-----	AV1N15	TEST 901-340	(APPROACH+1 BEGINS AT 12-SEC FROM START)
-----	AV2N15	TEST 901-340	(APPROACH+1 BEGINS AT 12-SEC FROM START)
-----	AV3N15	TEST 901-340	(APPROACH+1 BEGINS AT 12-SEC FROM START)
-----	AVIN15	TEST 901-340	(APPROACH+1 BEGINS AT 12-SEC FROM START)



Algorithm start: 12.08 sec.

Redline
C/O: 405.5

FIGURE 8C

—	SENS19	TEST 901-340 (APPROACH+1 BEGINS AT 12-SEC FROM START)
- - - -	AV1N19	TEST 901-340 (APPROACH+1 BEGINS AT 12-SEC FROM START)
- - - -	AV2N19	TEST 901-340 (APPROACH+1 BEGINS AT 12-SEC FROM START)
- - - -	AV3N19	TEST 901-340 (APPROACH+1 BEGINS AT 12-SEC FROM START)
- - - -	AVIN19	TEST 901-340 (APPROACH+1 BEGINS AT 12-SEC FROM START)

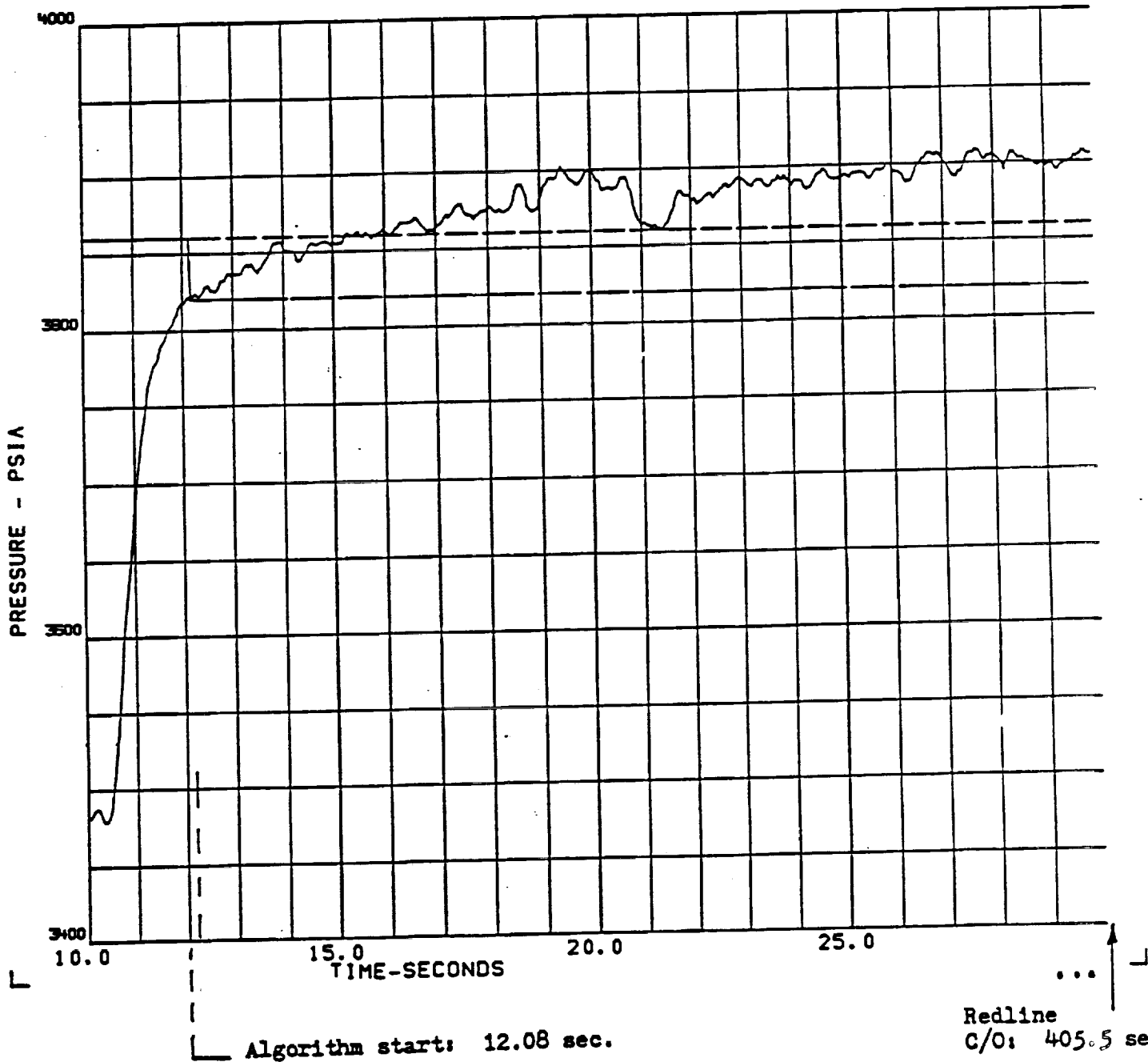
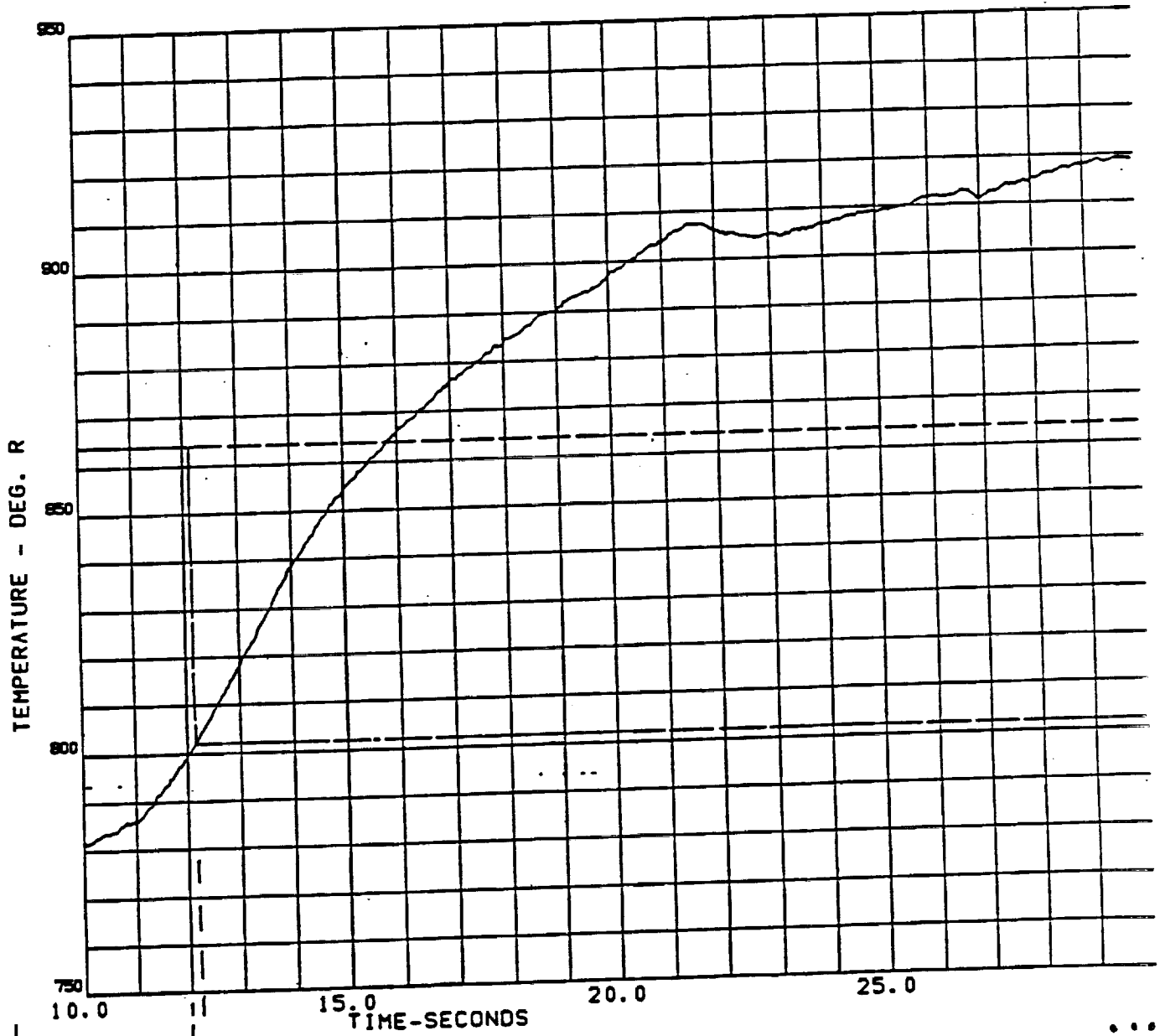


FIGURE 8D :

HX INT TEMP	
-----	TEST 901-340 (APPROACH+1 BEGINS AT 12-SEC FROM START)
-----	TEST 901-340 (APPROACH+1 BEGINS AT 12-SEC FROM START)
-----	TEST 901-340 (APPROACH+1 BEGINS AT 12-SEC FROM START)
-----	TEST 901-340 (APPROACH+1 BEGINS AT 12-SEC FROM START)
-----	TEST 901-340 (APPROACH+1 BEGINS AT 12-SEC FROM START)
-----	TEST 901-340 (APPROACH+1 BEGINS AT 12-SEC FROM START)

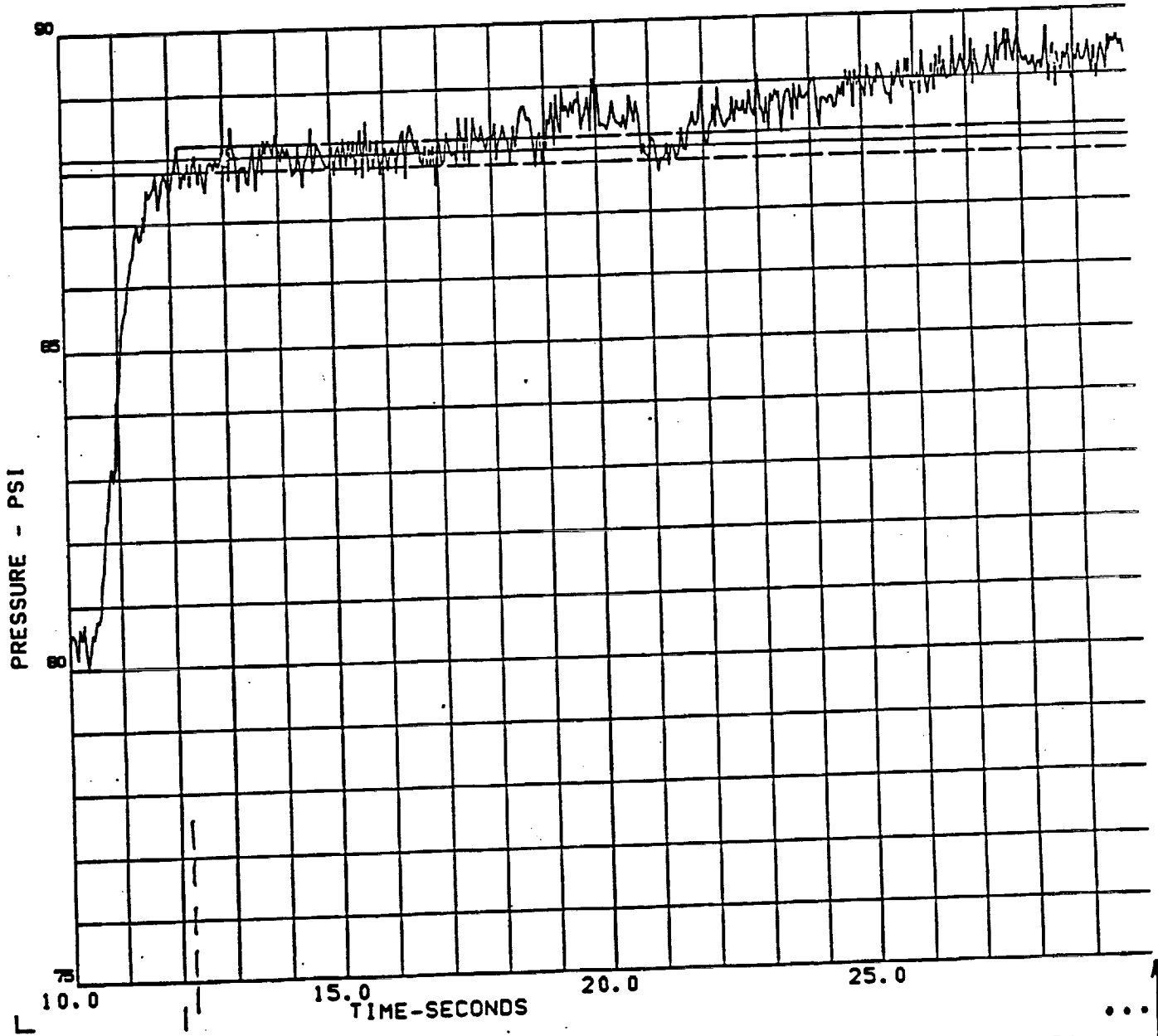


Algorithm start: 12.08 sec.

Redline
C/O: 405.5 se

FIGURE 8E

HX VENT DELTA-P			
—	SEN21	TEST 901-340	(APPROACH+1 BEGINS AT 12-SEC FROM START)
---	AV1N21	TEST 901-340	(APPROACH+1 BEGINS AT 12-SEC FROM START)
---	AV2N21	TEST 901-340	(APPROACH+1 BEGINS AT 12-SEC FROM START)
---	AV3N21	TEST 901-340	(APPROACH+1 BEGINS AT 12-SEC FROM START)
---	AV4N21	TEST 901-340	(APPROACH+1 BEGINS AT 12-SEC FROM START)

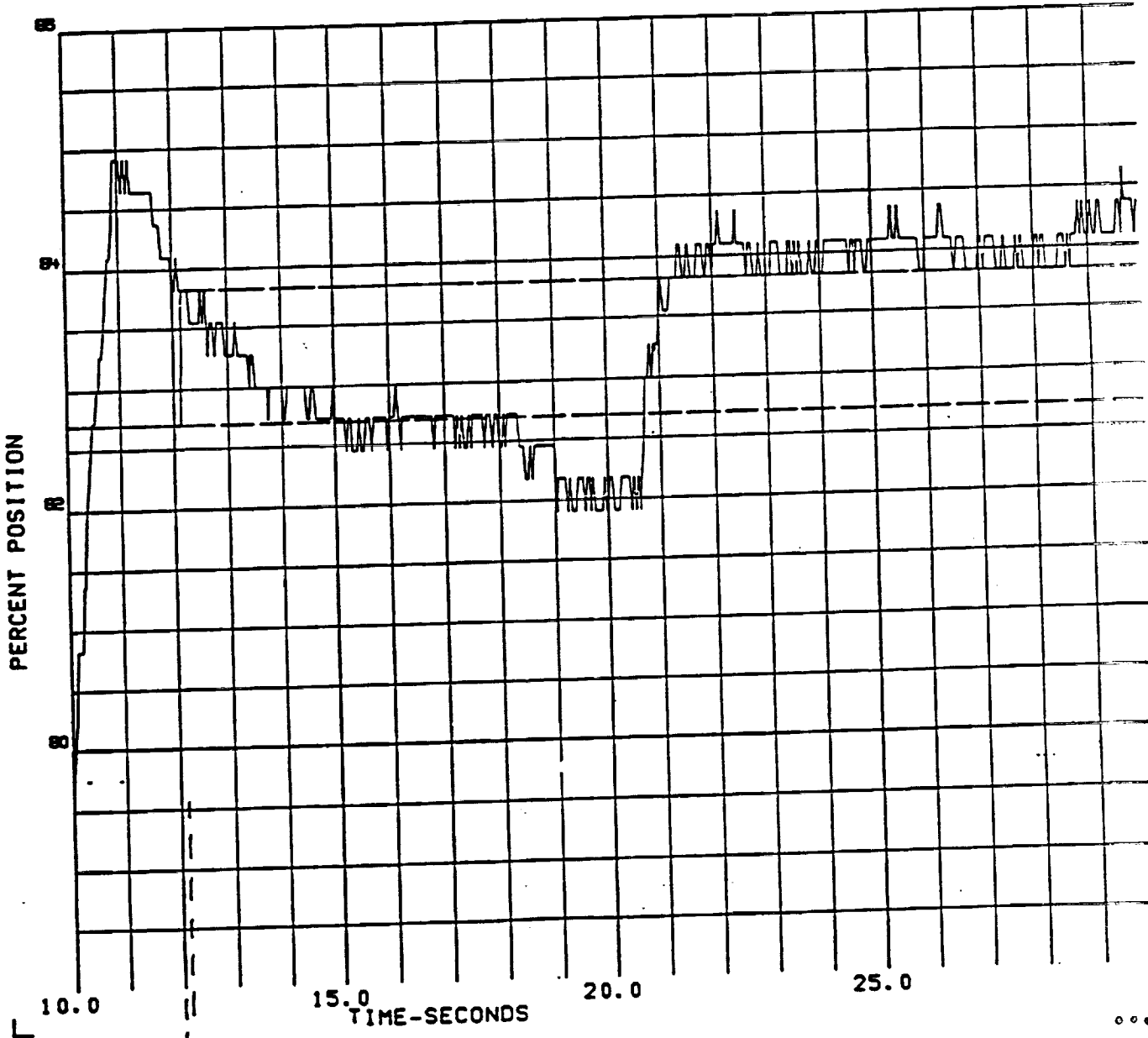


Algorithm start: 12.08 sec.

Redline
C/O: 405.5

FIGURE 8F

FPOV ACT POSITION
 ———— SENSE3 TEST 901-340 (APPROACH+1 BEGINS AT 12-SEC FROM START)
 - - - - AV1N23 TEST 901-340 (APPROACH+1 BEGINS AT 12-SEC FROM START)
 - - - - AV2N23 TEST 901-340 (APPROACH+1 BEGINS AT 12-SEC FROM START)
 - - - - AV3N23 TEST 901-340 (APPROACH+1 BEGINS AT 12-SEC FROM START)
 - - - - AV1N23 TEST 901-340 (APPROACH+1 BEGINS AT 12-SEC FROM START)



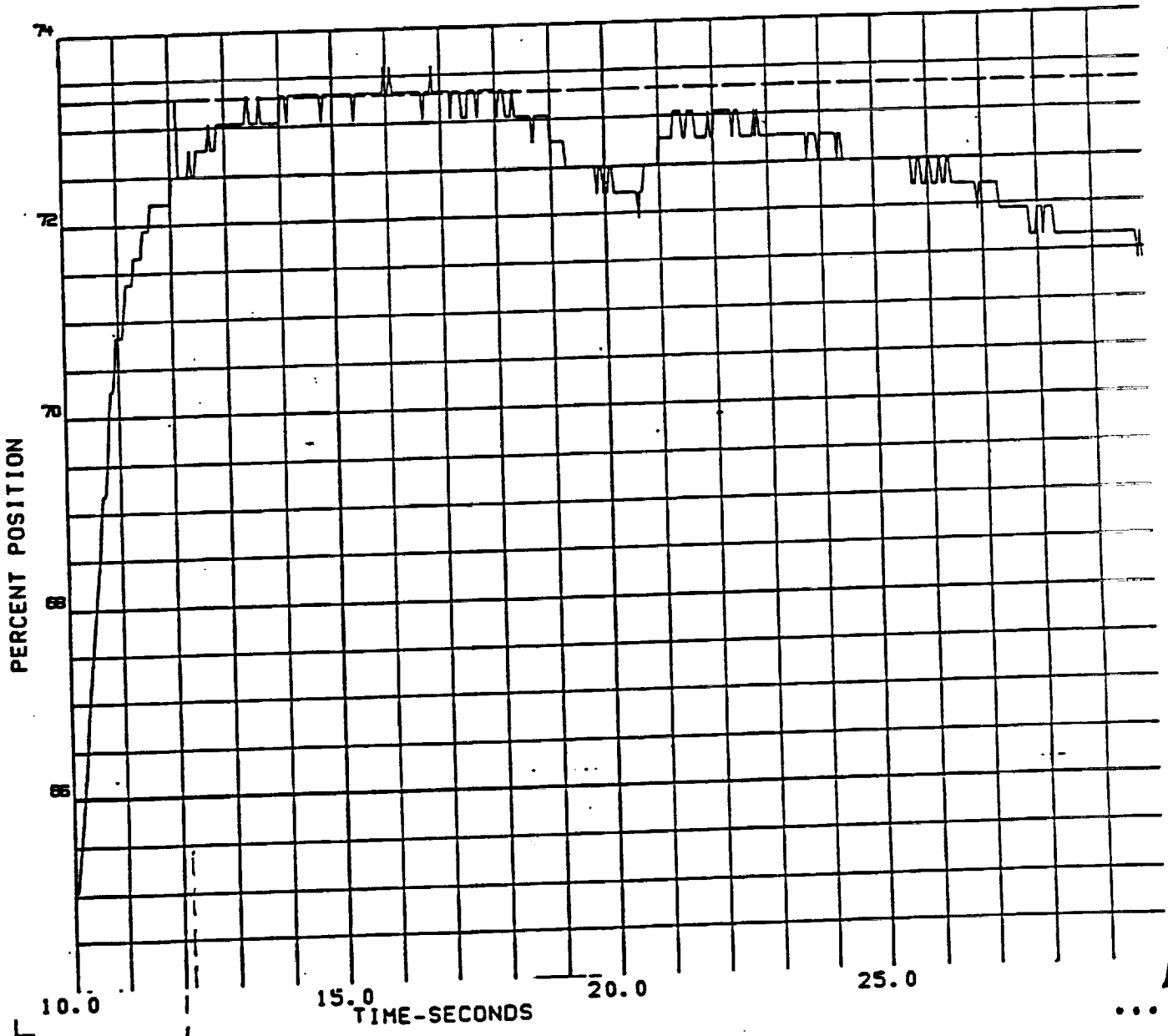
Algorithm start: 12.08 sec.

Redline
C/O: 405.

FIGURE 8G

OPV ACT POSITION

—	SE622	TEST 901-340	(APPROACH-1 BEGINS AT 12-SEC FROM START)
---	AV122	TEST 901-340	(APPROACH-1 BEGINS AT 12-SEC FROM START)
---	AV222	TEST 901-340	(APPROACH-1 BEGINS AT 12-SEC FROM START)
---	AV322	TEST 901-340	(APPROACH-1 BEGINS AT 12-SEC FROM START)
---	AV422	TEST 901-340	(APPROACH-1 BEGINS AT 12-SEC FROM START)



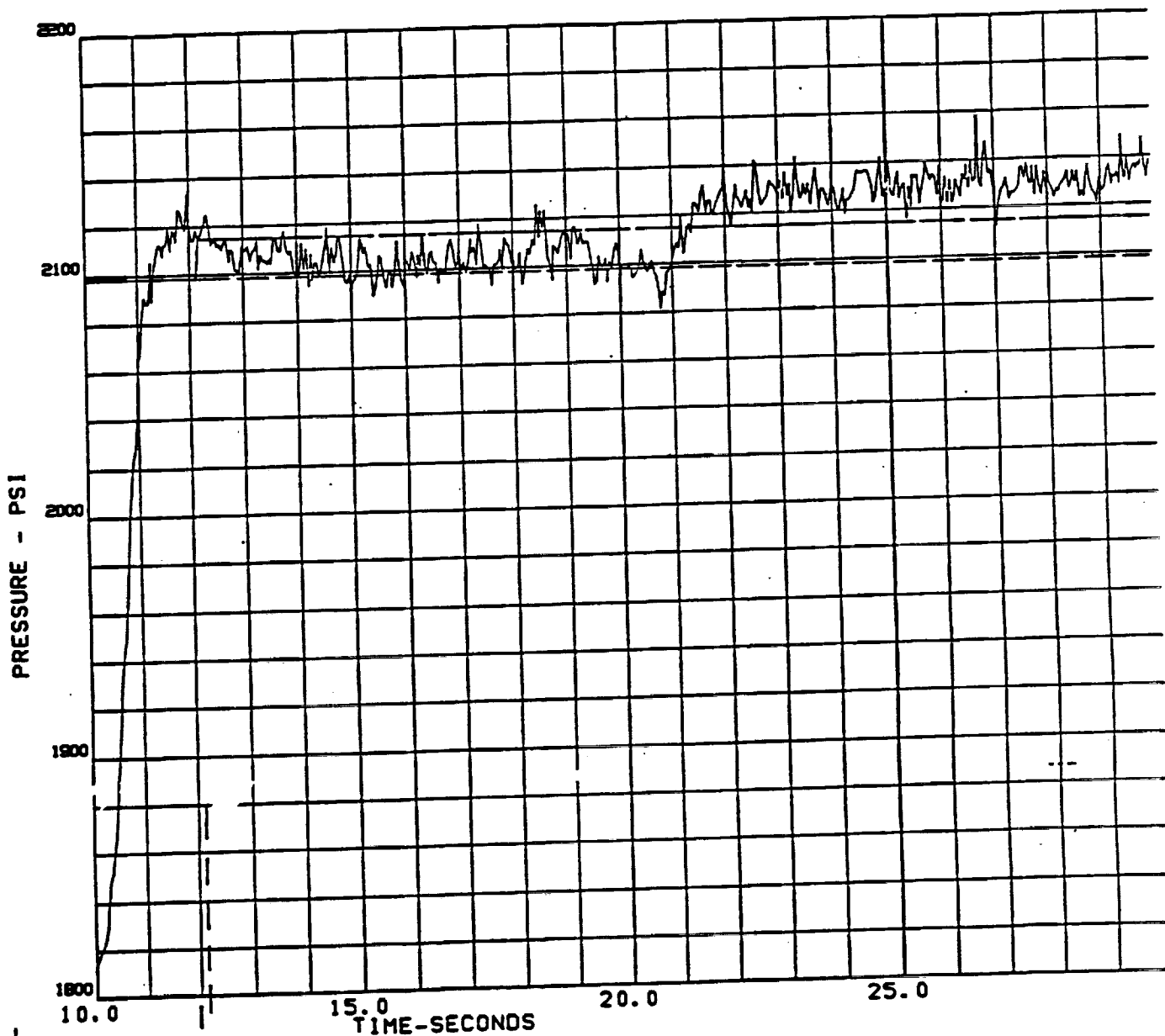
Algorithm start: 12.08 sec.

Redline
C/O: 405.5

FIGURE 8H

HIGH PRESSURE FUEL TURBINE DELTA-P

- SENSOS TEST 901-340 (APPROACH+1 BEGINS AT 12-SEC FROM START)
- - - AV1NOS TEST 901-340 (APPROACH+1 BEGINS AT 12-SEC FROM START)
- - - AV2NOS TEST 901-340 (APPROACH+1 BEGINS AT 12-SEC FROM START)
- - - AV3NOS TEST 901-340 (APPROACH+1 BEGINS AT 12-SEC FROM START)
- - - AVINOS TEST 901-340 (APPROACH+1 BEGINS AT 12-SEC FROM START)



Algorithm start: 12.08 sec.

Redline
C/O: 405.5 sec

FIGURE 81

FPOV ACT POSITION

0 0 0 0 X FPOV ATPDTH START W CNT ADDITION 11/89 SHERRY MODEL DATA
42 FPOV ACT POS SSME CONTROLLER DATA FOR TEST 901284 TEST DATA

89/12-07
CRTLOOK

2

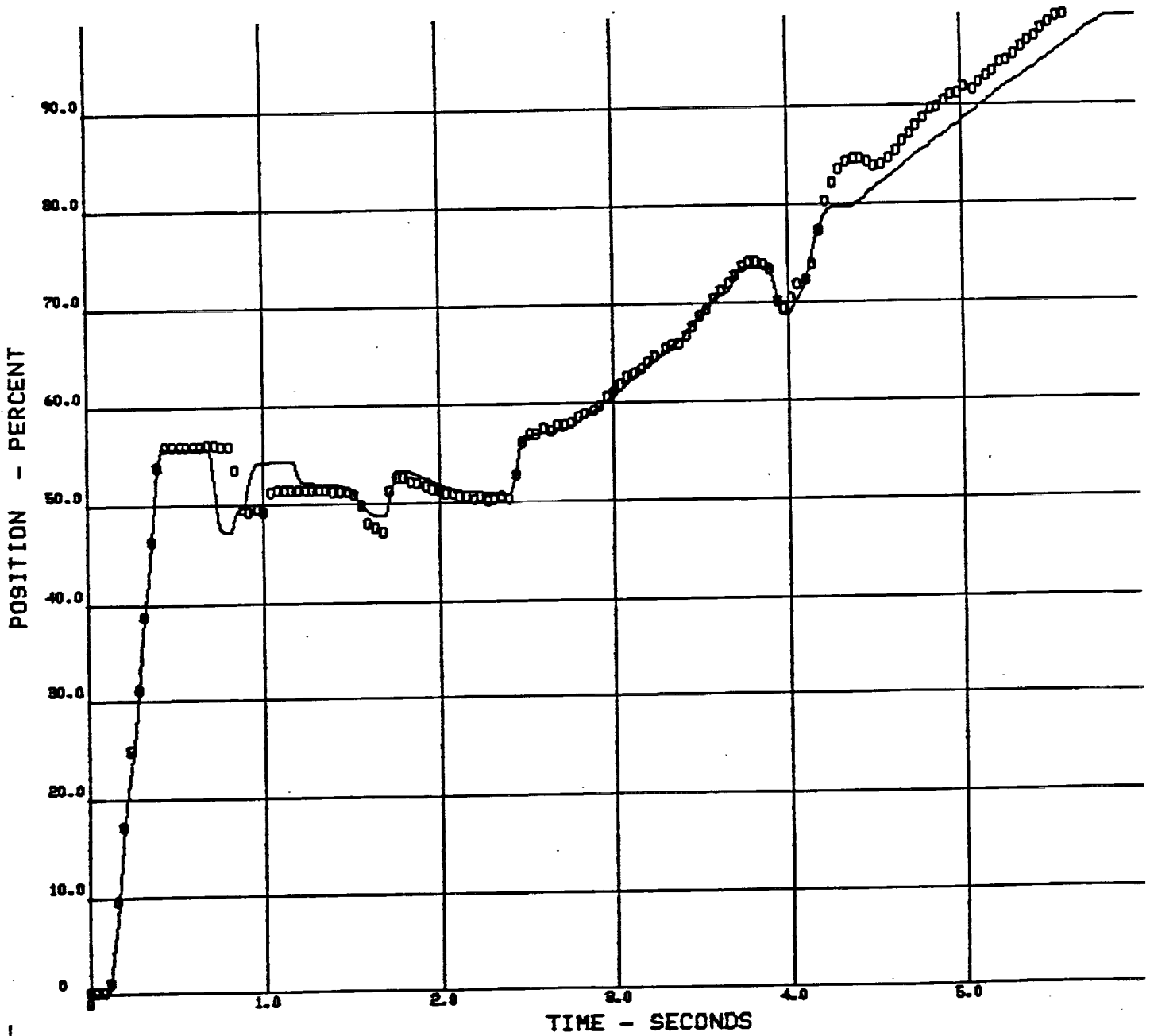


FIGURE 9A-Test 901-284

OPOV ACT POSITION

69/12/07
CRTLOOK

3

0 0 0 0 XOPV ATPDTH START W CNT ADDITION 11/89 SHERRY MODEL DATA
40 OPOV ACT POS SSME CONTROLLER DATA FOR TEST 901284 TEST DATA

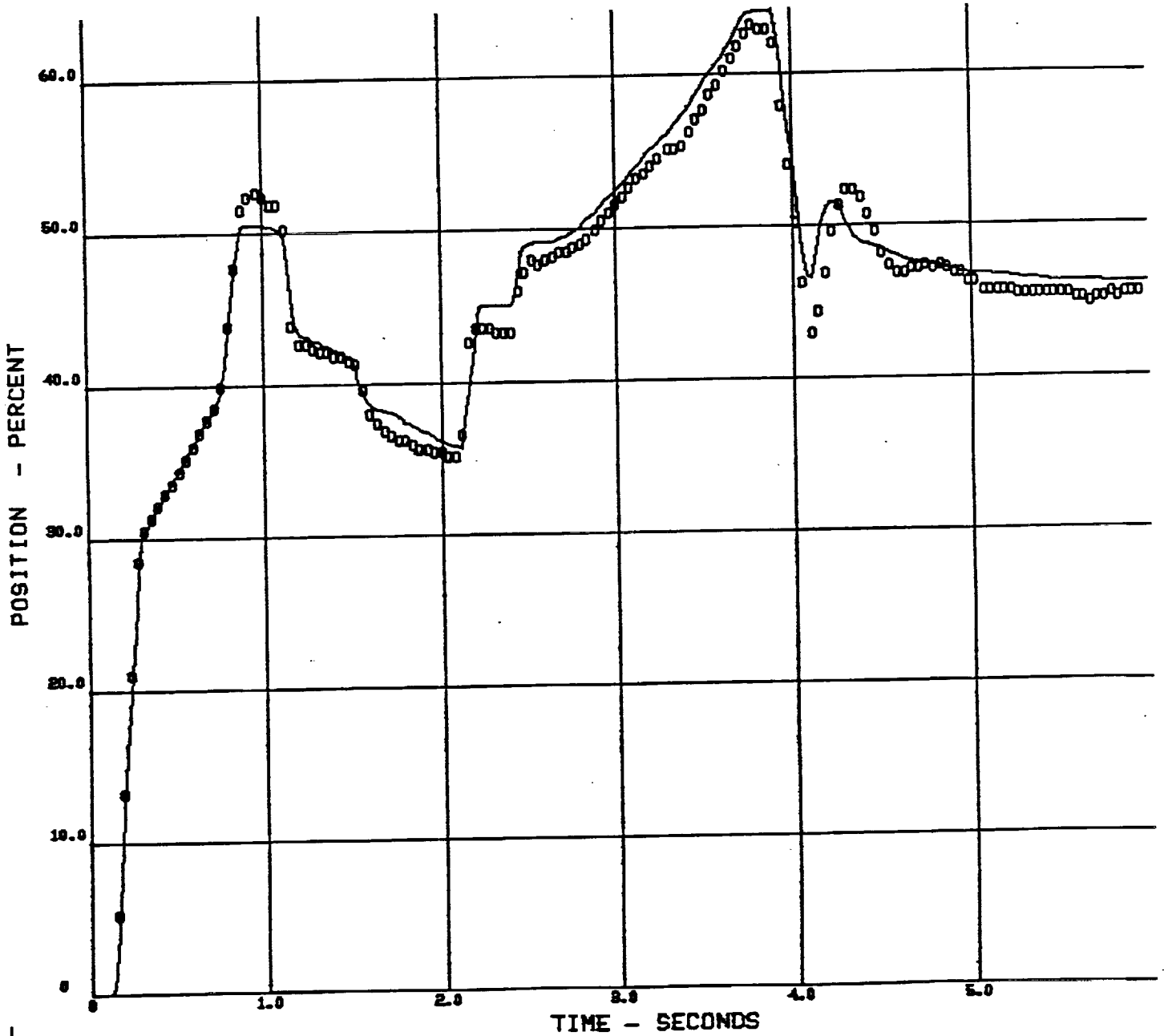


FIGURE 9B - Test 901-284

HPFT TUR DIS T A

0000 A04 ATPOTH START W CNT ADDITION 11/89 SHERRY MODEL DATA
231 HPFT TUR DS SSME CONTROLLER DATA FOR TEST 901284 TEST DATA

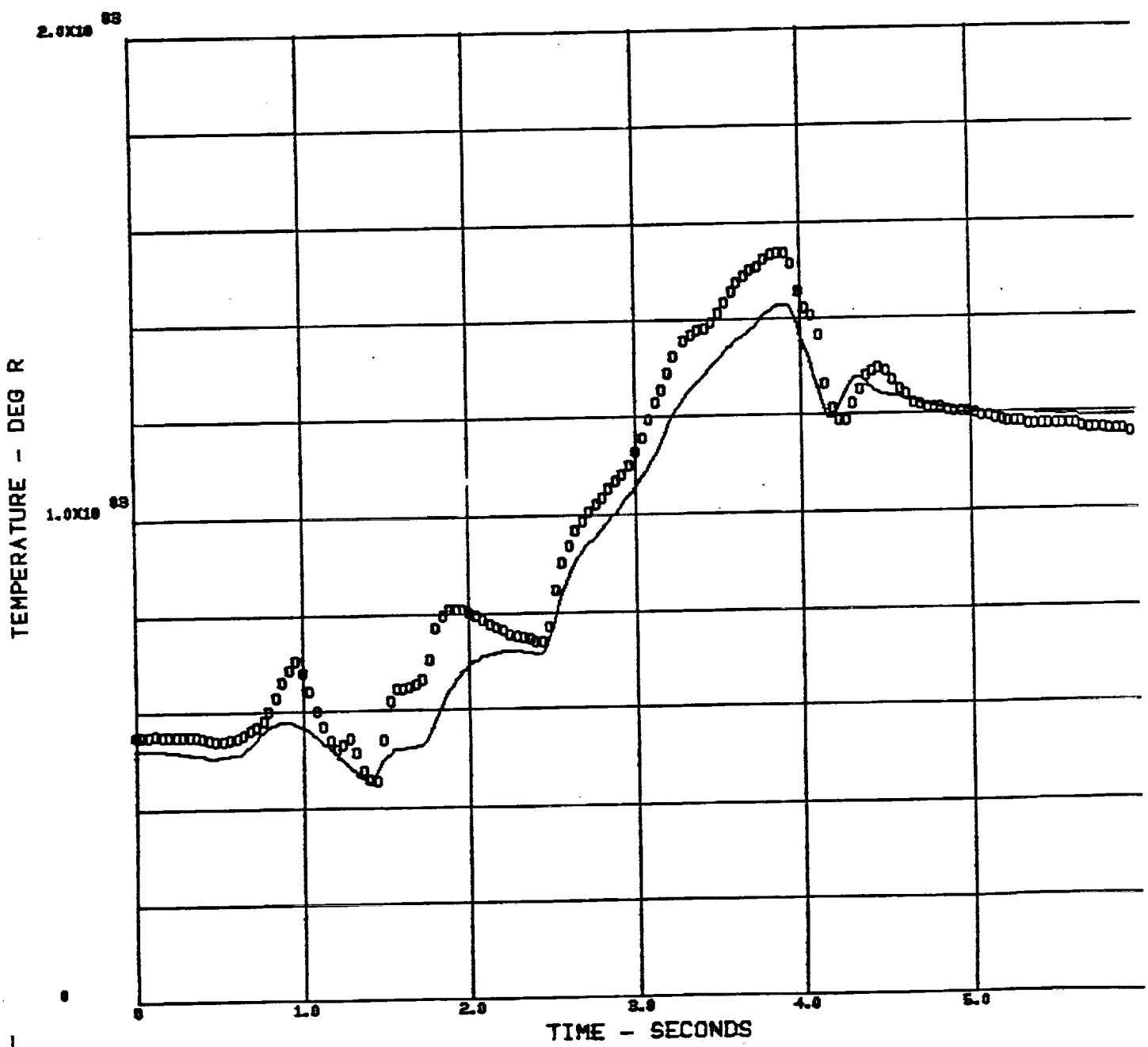


FIGURE 9C - Test 901-284

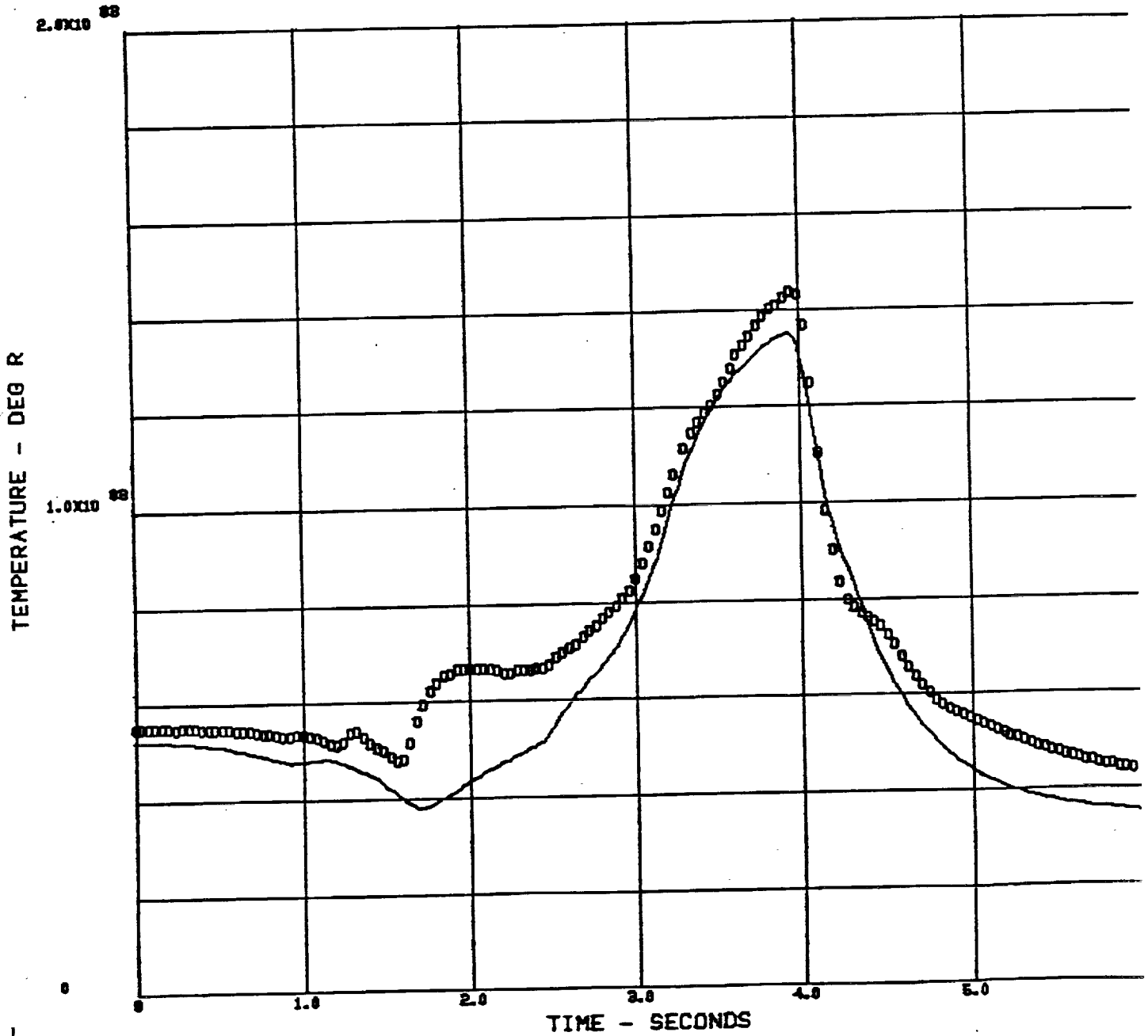
ORIGINAL PAGE IS
OF POOR QUALITY

HPOT TUR DIS T A

89/12-07
CRTLOOK

5

0000 238 HPOT TUR DS SSME CONTROLLER DATA FOR TEST 901284 TEST DATA



ORIGINAL PAGE IS
OF POOR QUALITY

FIGURE 9D - Test 901-284

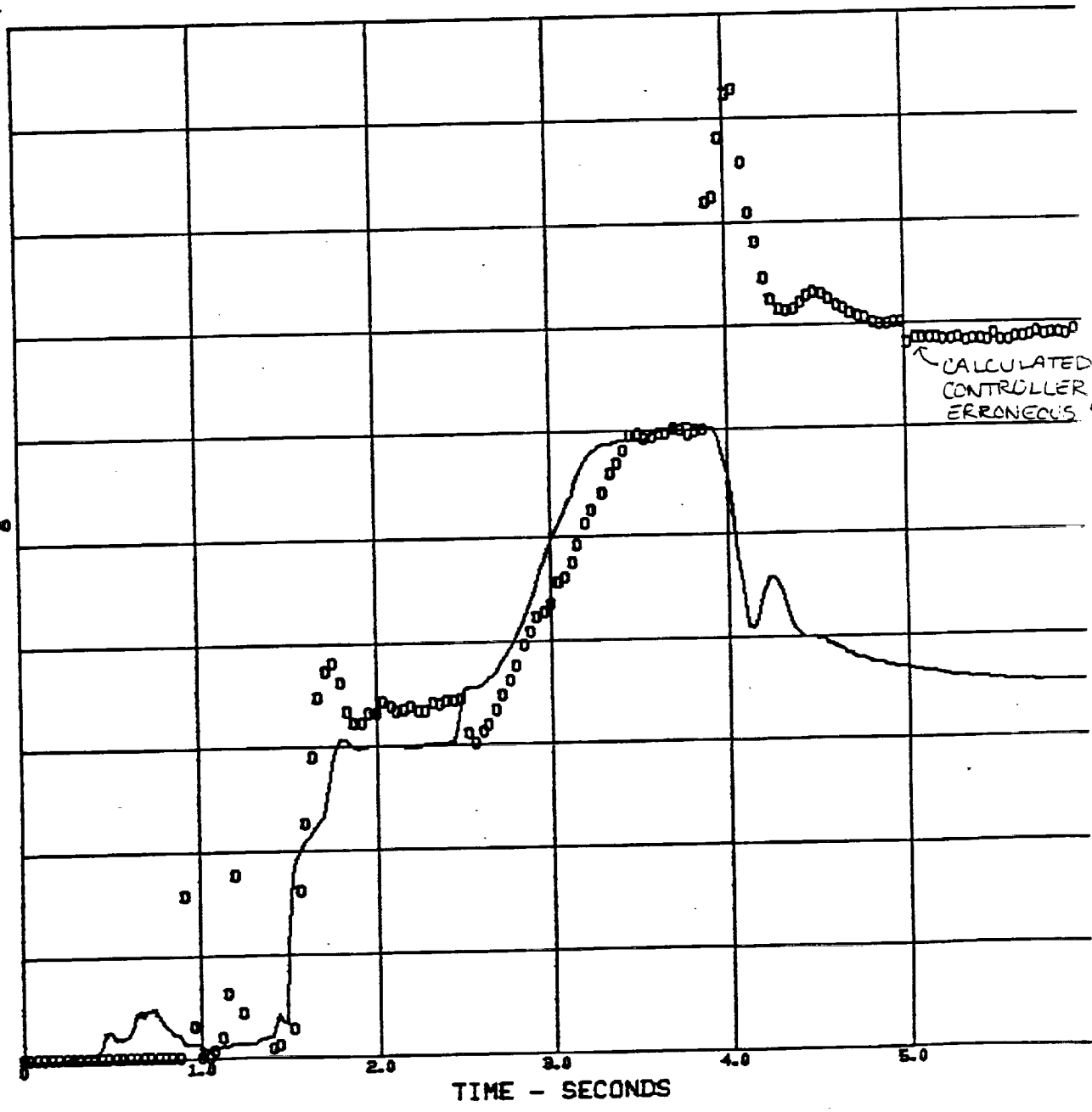
MIXTURE RATIO

0 0 0 0 8 MX RATIO 01 SSNE CONTROLLER DATA FOR TEST 901284 TEST DATA

1.00X10⁰¹

MIXTURE RATIO

5.00X10⁰⁰



CALCULATED BY CONTROLLER USING ERRONEOUS

FIGURE 9F - Test 901-284

MCC CLNT DIS PR

89/12-07
CRTLOOK

0 0 0 0 P(6) 17 ATPOTH START W CNT ADDITION 11/89 SHERRY MODEL DATA
MCC CLNT DS SSME CONTROLLER DATA FOR TEST 901284 TEST DATA

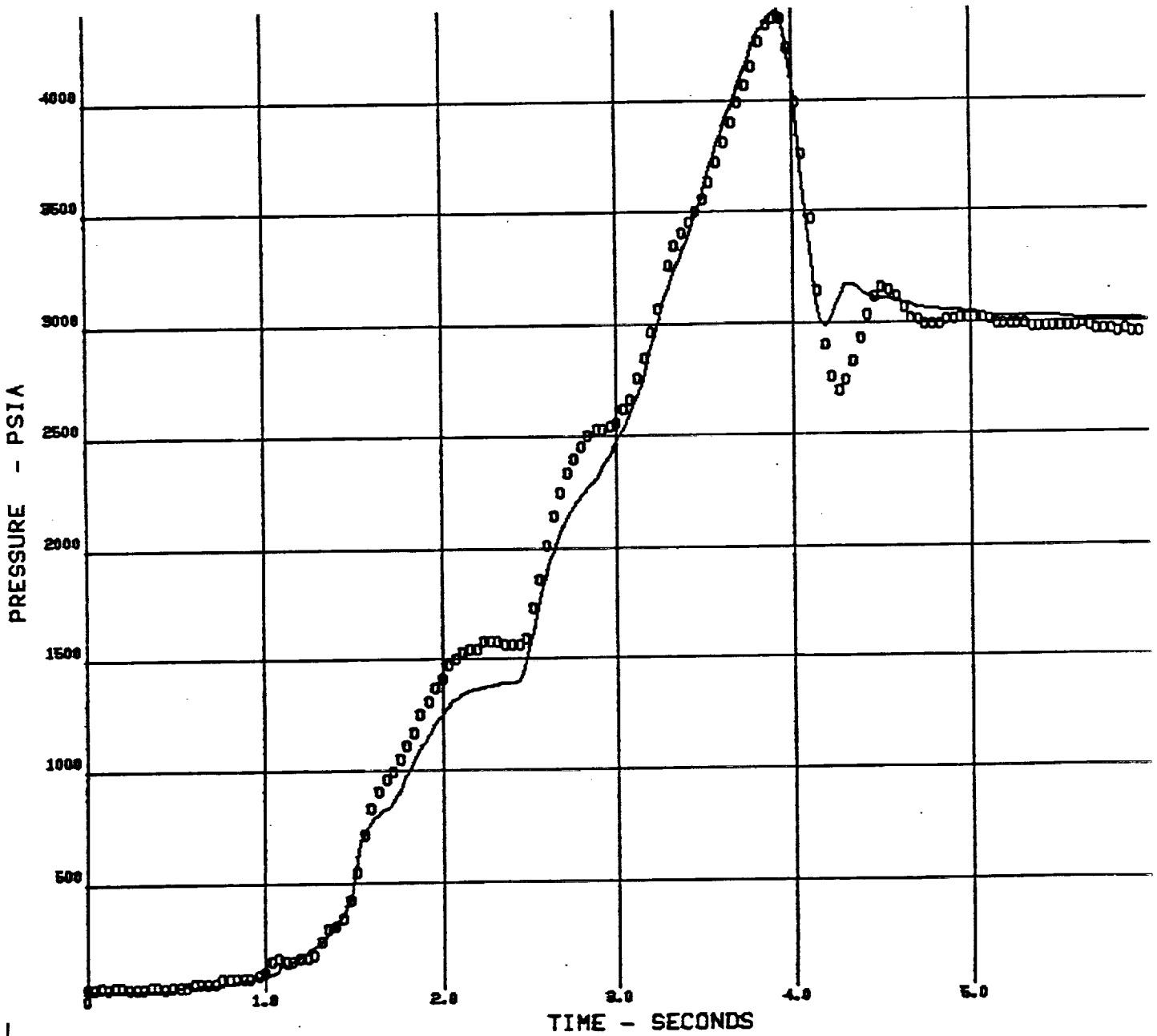


FIGURE 9G -Test 901-284

89/12-07
CRTLOOK

OPB PC
POP
0 0 0 0 480
ATPDM START W CNT ADDITION 11/89 SHERRY MODEL DATA
OPB PC PSIAE SSME CONTROLLER DATA FOR TEST 901284 TEST DATA

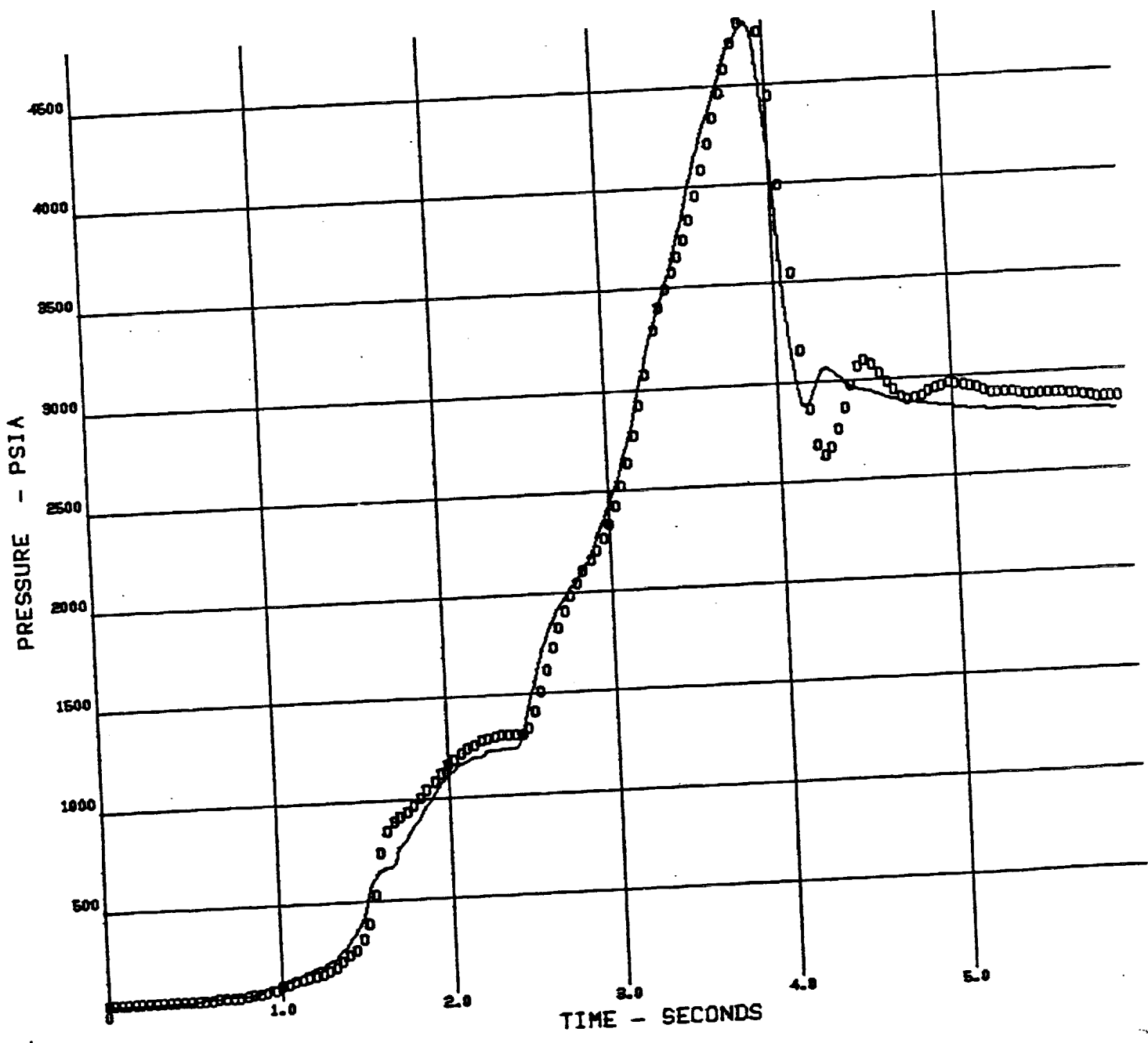


FIGURE 9H - Test 901-284

89/12.07
CRTLOOK

9

HCC PC
PCIE
0 0 0 0 383 HCC PC 1 PSI

ATPOTH START W CNT ADDITION 11/89 SHERRY
SSME CONTROLLER DATA FOR TEST 901284

MODEL DATA
TEST DATA

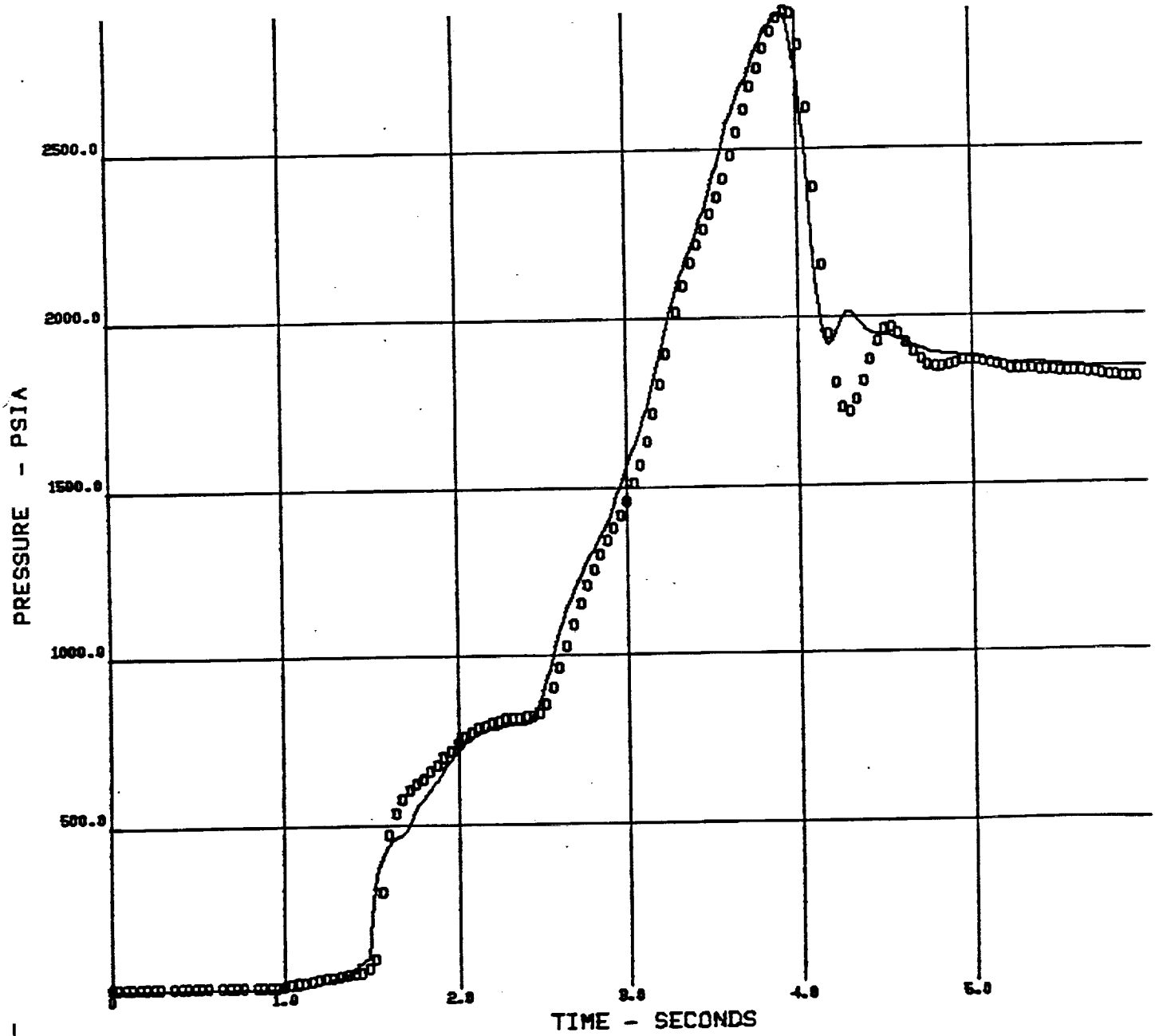


FIGURE 9I - Test 901-284

HPOP DIS PR

POD2

ATPDM START W CNT ADDITION 11/89 SHERRY MODEL DATA

0 0 0 0

334

HPOP DS PR NF

SSME CONTROLLER DATA FOR TEST 901284 TEST DATA

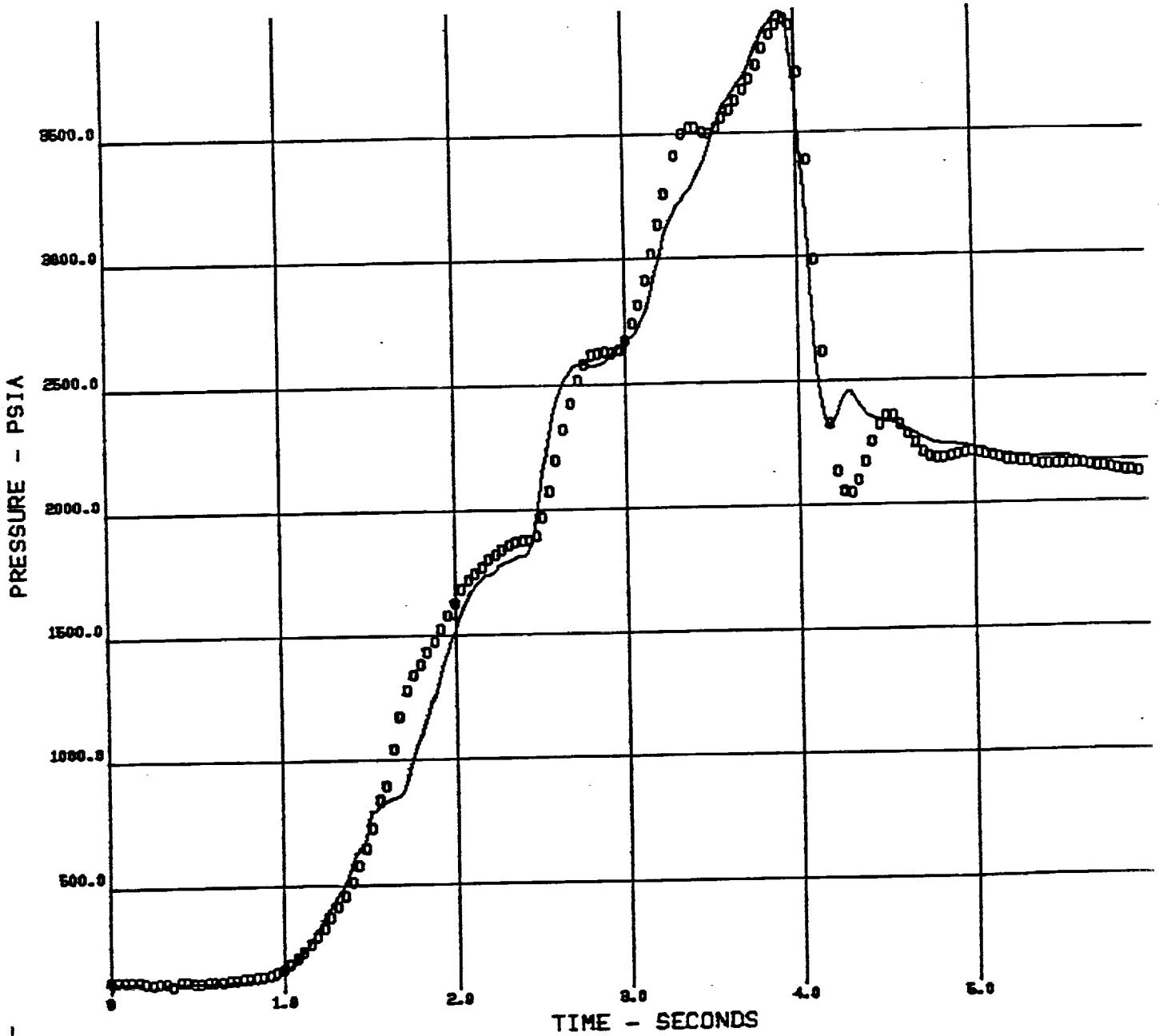


FIGURE 9J - Test 901-284

ORIGINAL PAGE IS
OF POOR QUALITY

89/12-07
CRTLOOK

11

HPFP DIS PR

P(3)

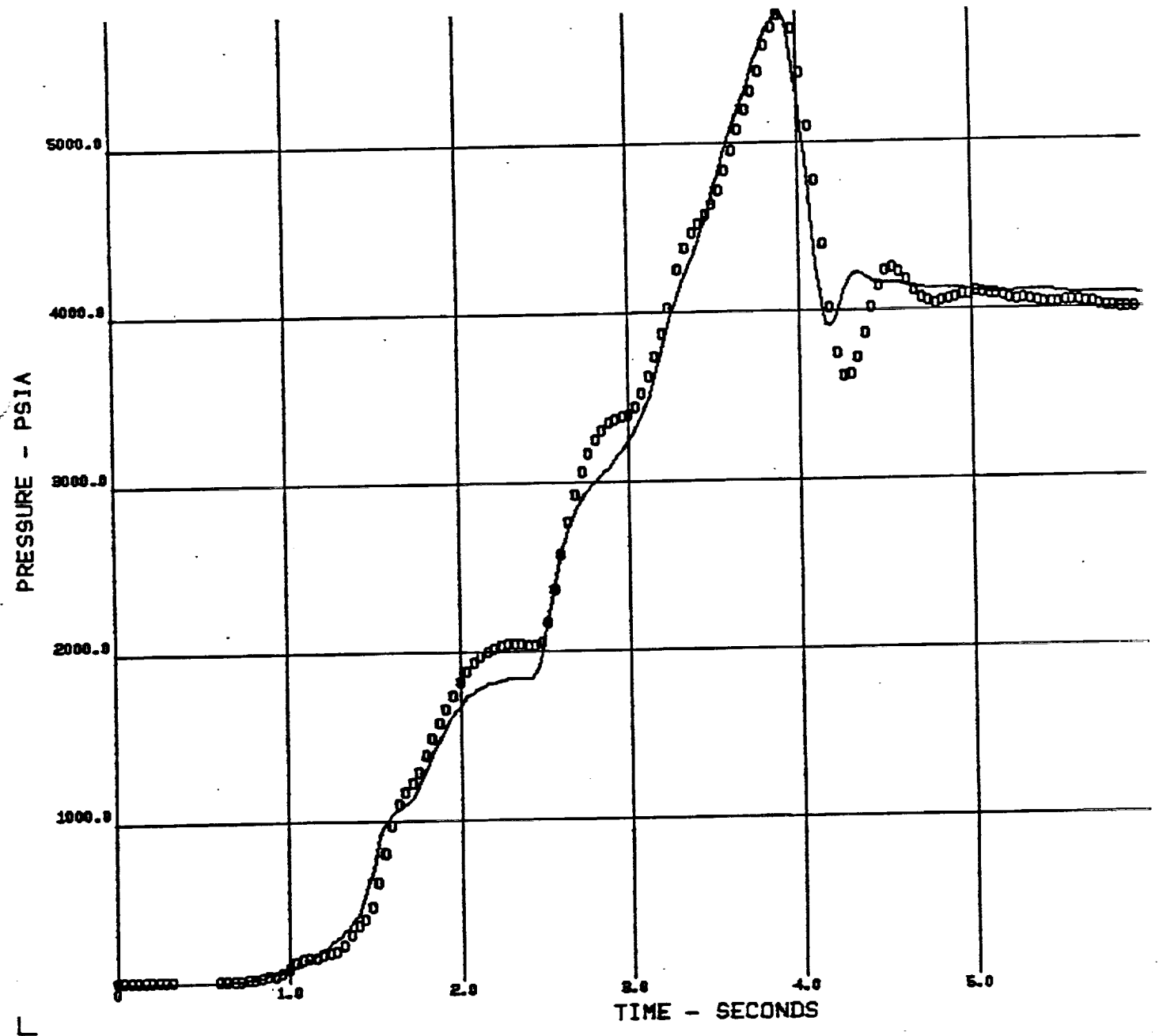
ATPDTM START H CNT ADDITION 11/89 SHERRY MODEL DATA

0 0 0 0

459

HPFP DS PR NF

SSHE CONTROLLER DATA FOR TEST 901284 TEST DATA



ORIGINAL PAGE IS
OF POOR QUALITY

FIGURE 9K - Test 901-284

89/12-07
CRTLOOK

ENG FL FLOW

0 0 0 0 722 ENG FL FLOW N ATPOTH START W CNT ADDITION 11/89 SHERRY MODEL DATA
SSME CONTROLLER DATA FOR TEST 901284 TEST DATA

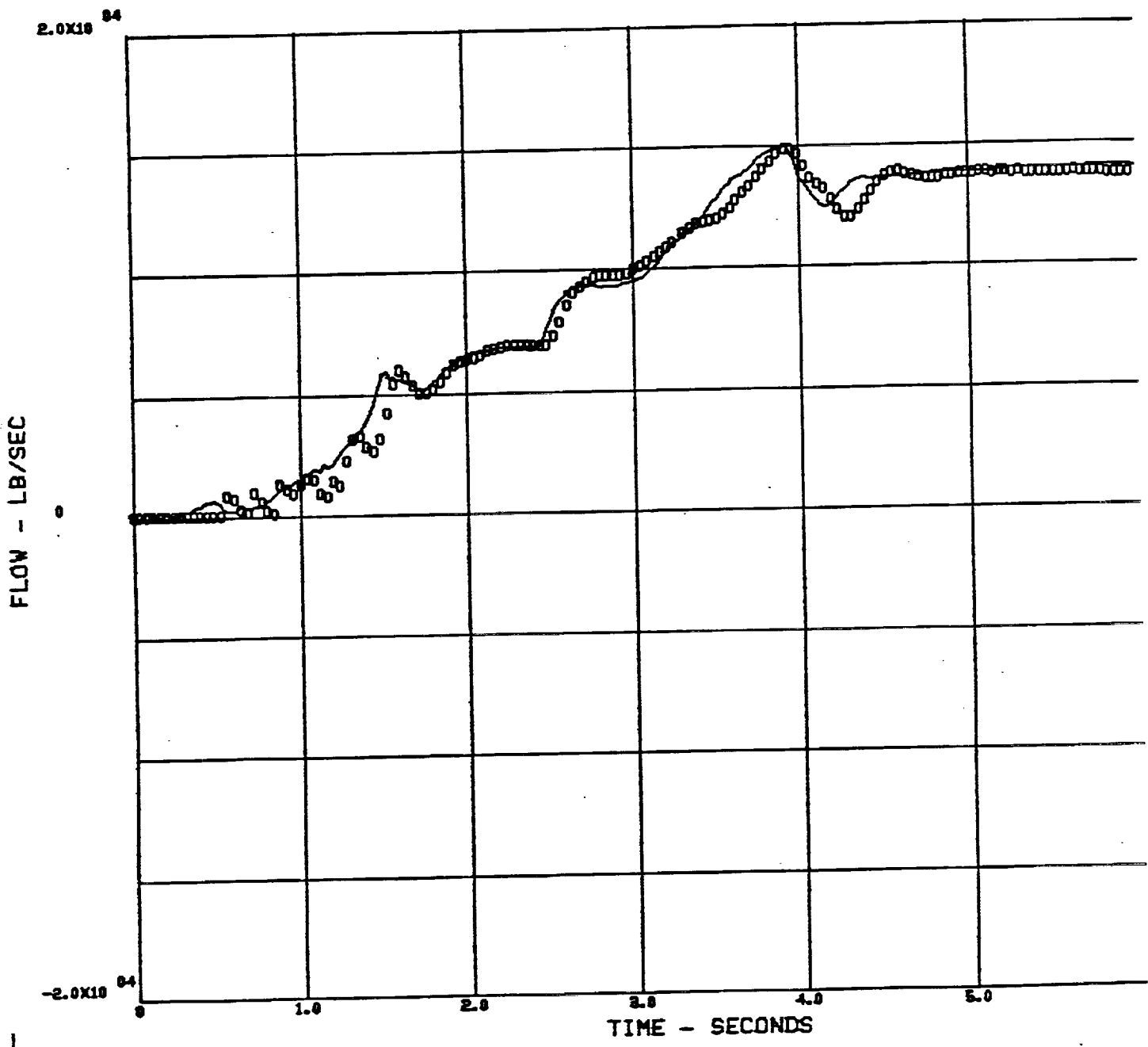
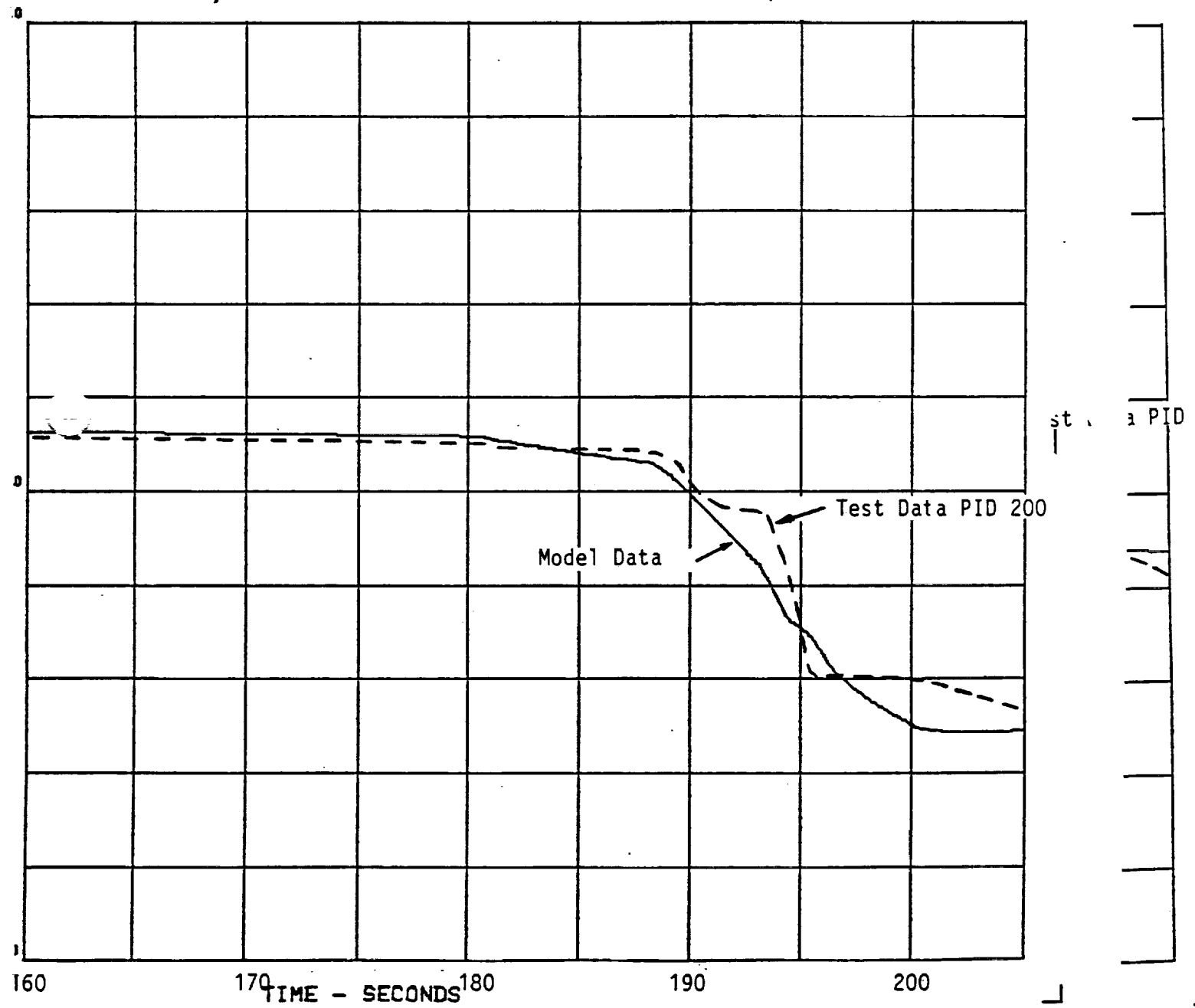
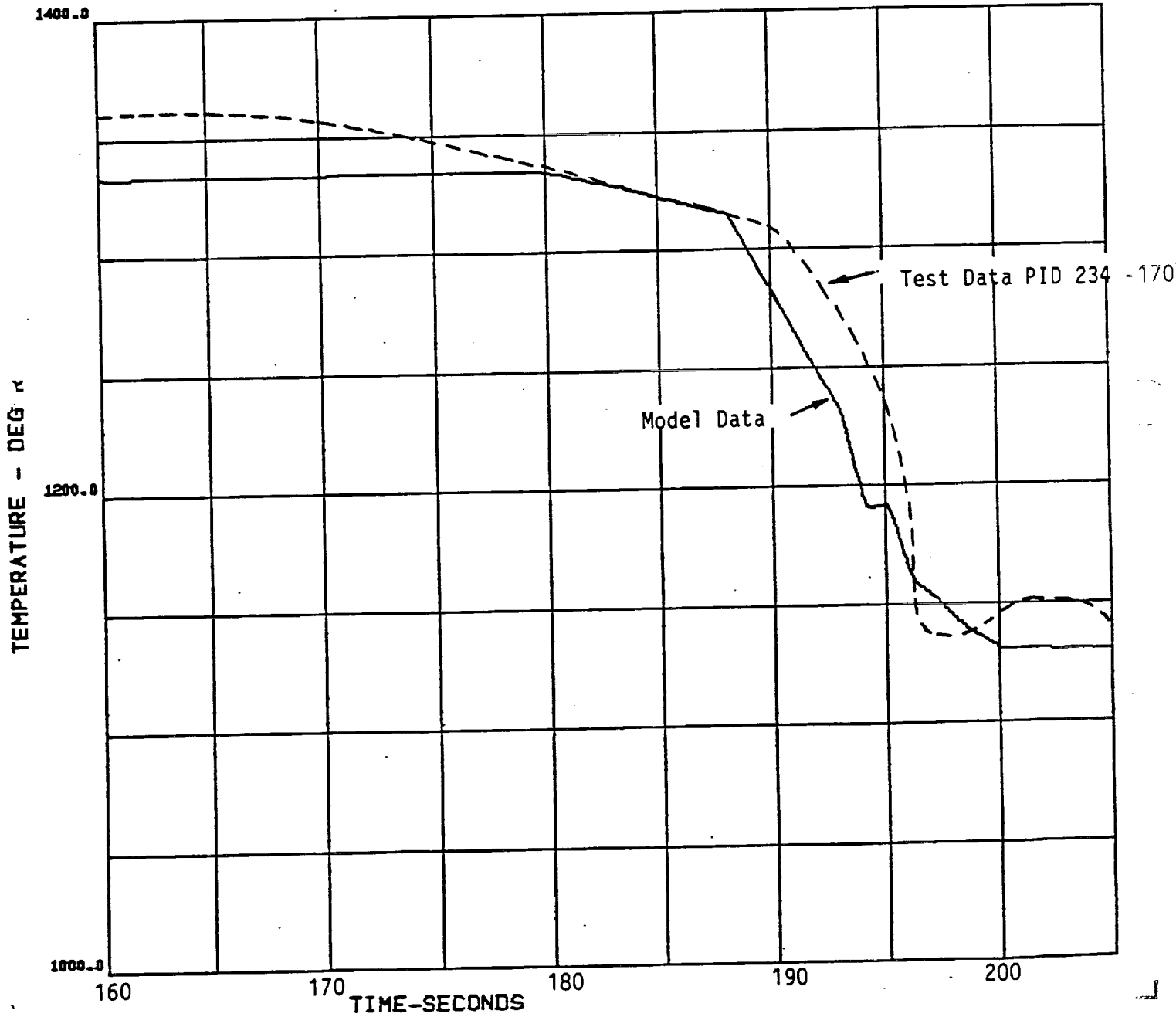


FIGURE 9L - Test 901-284



ORIGINAL PAGE IS
OF POOR QUALITY

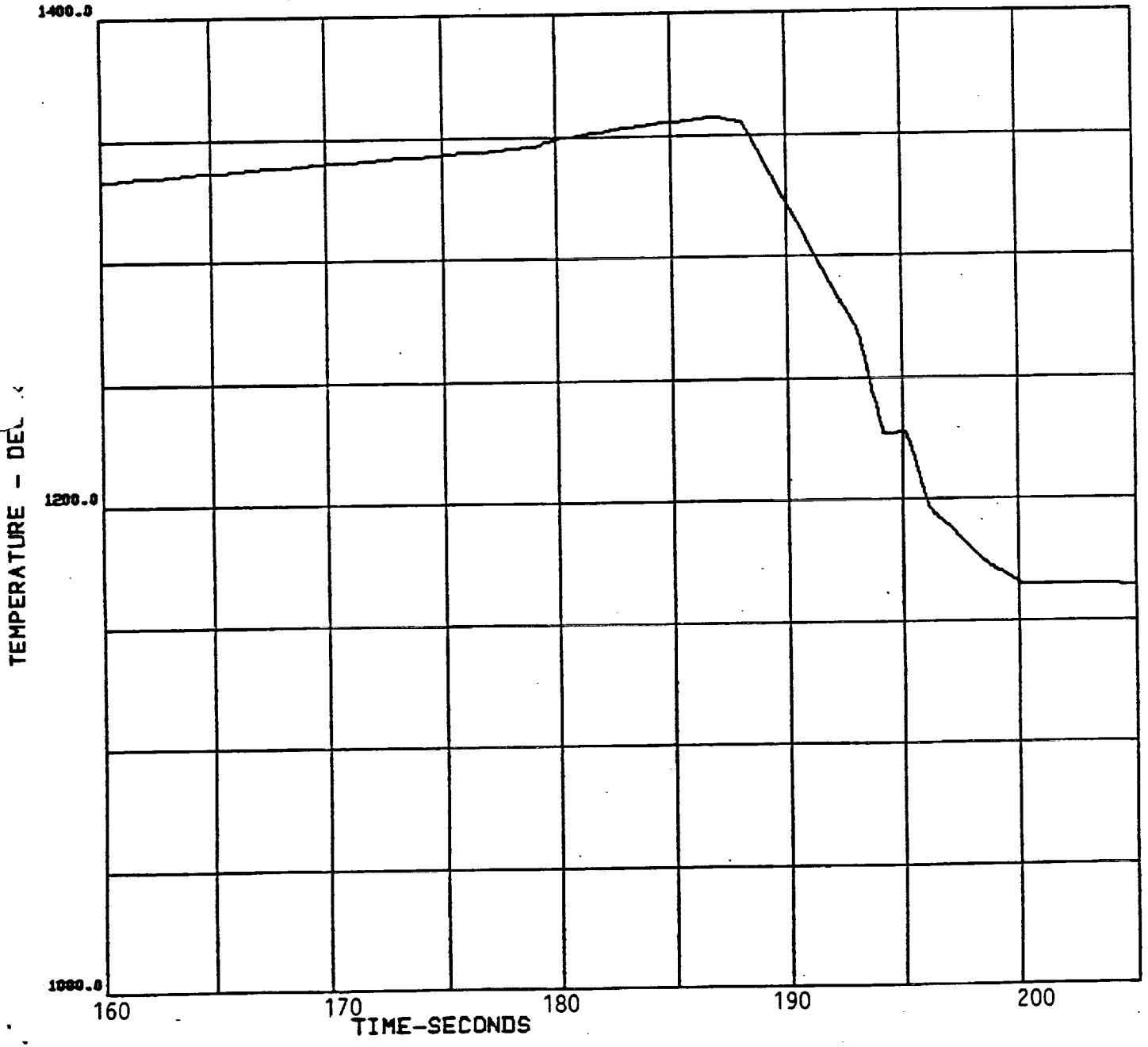
FIGURE 10A - Test 902-428



PRECEDING PAGE BLANK NOT FILMED

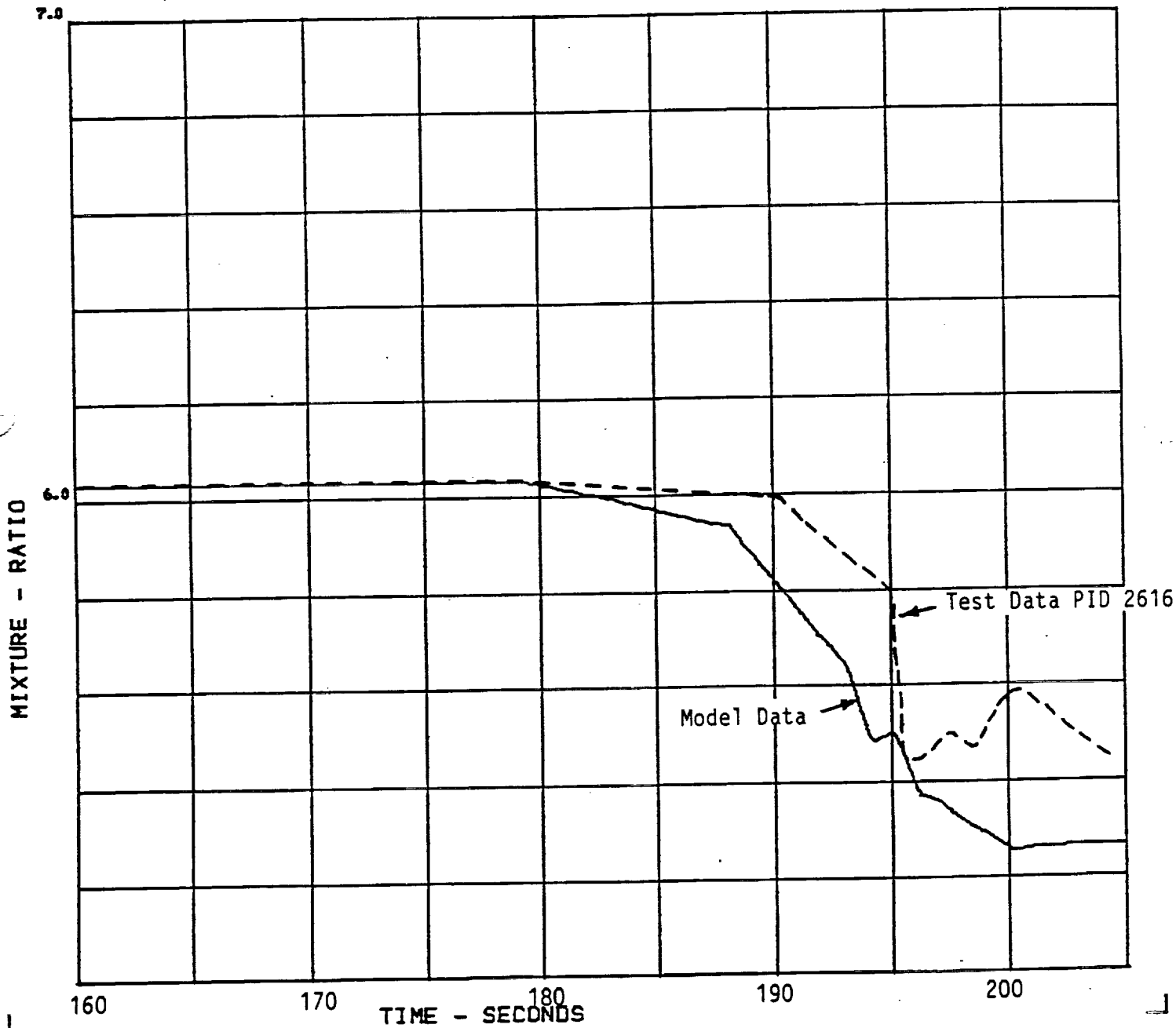
ORIGINAL PAGE IS
OF POOR QUALITY

FIGURE 10C - Test 902-428



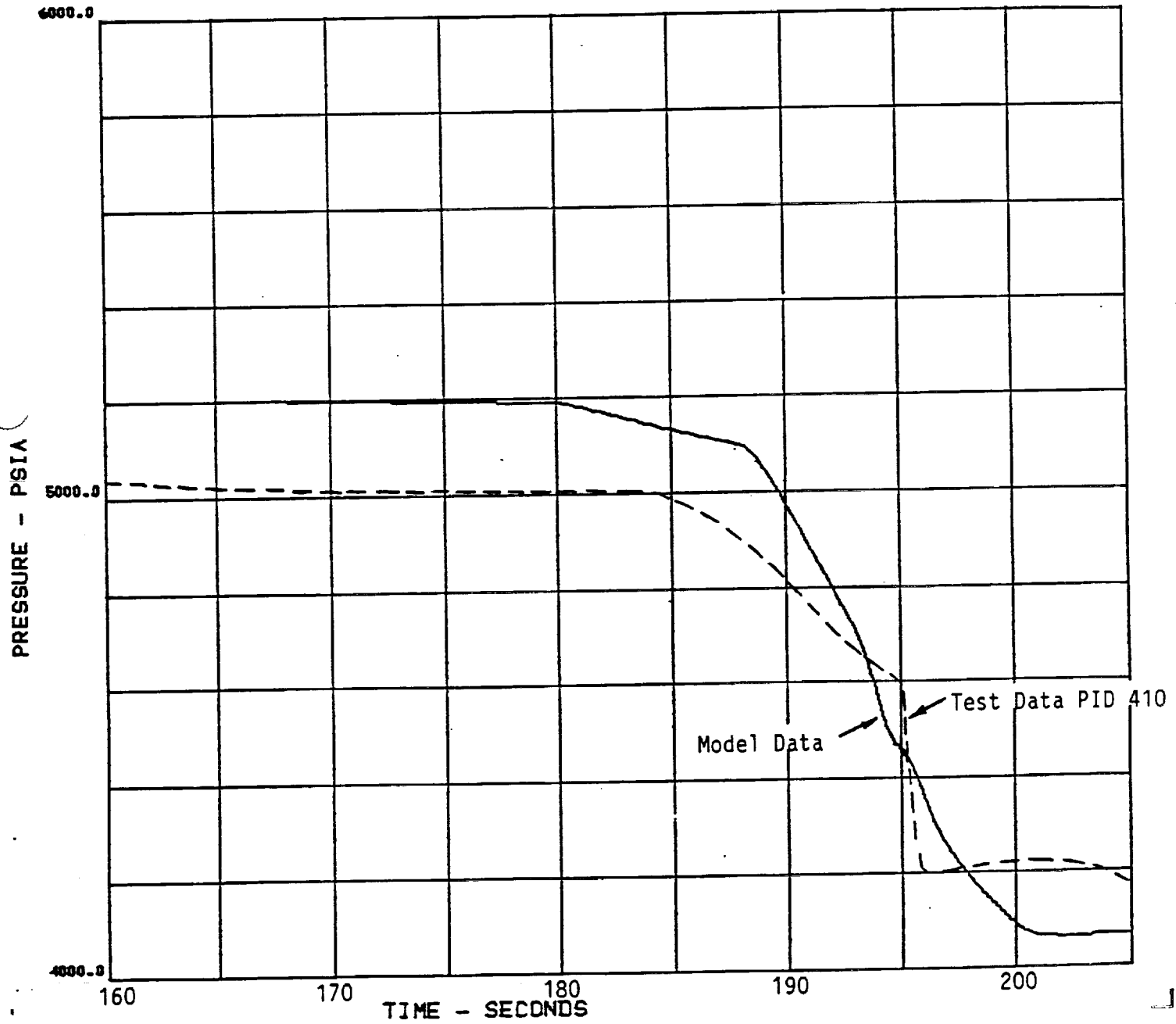
ORIGINAL PAGE IS
OF POOR QUALITY

FIGURE 10D - Test 902-428



ORIGINAL PAGE IS
OF POOR QUALITY

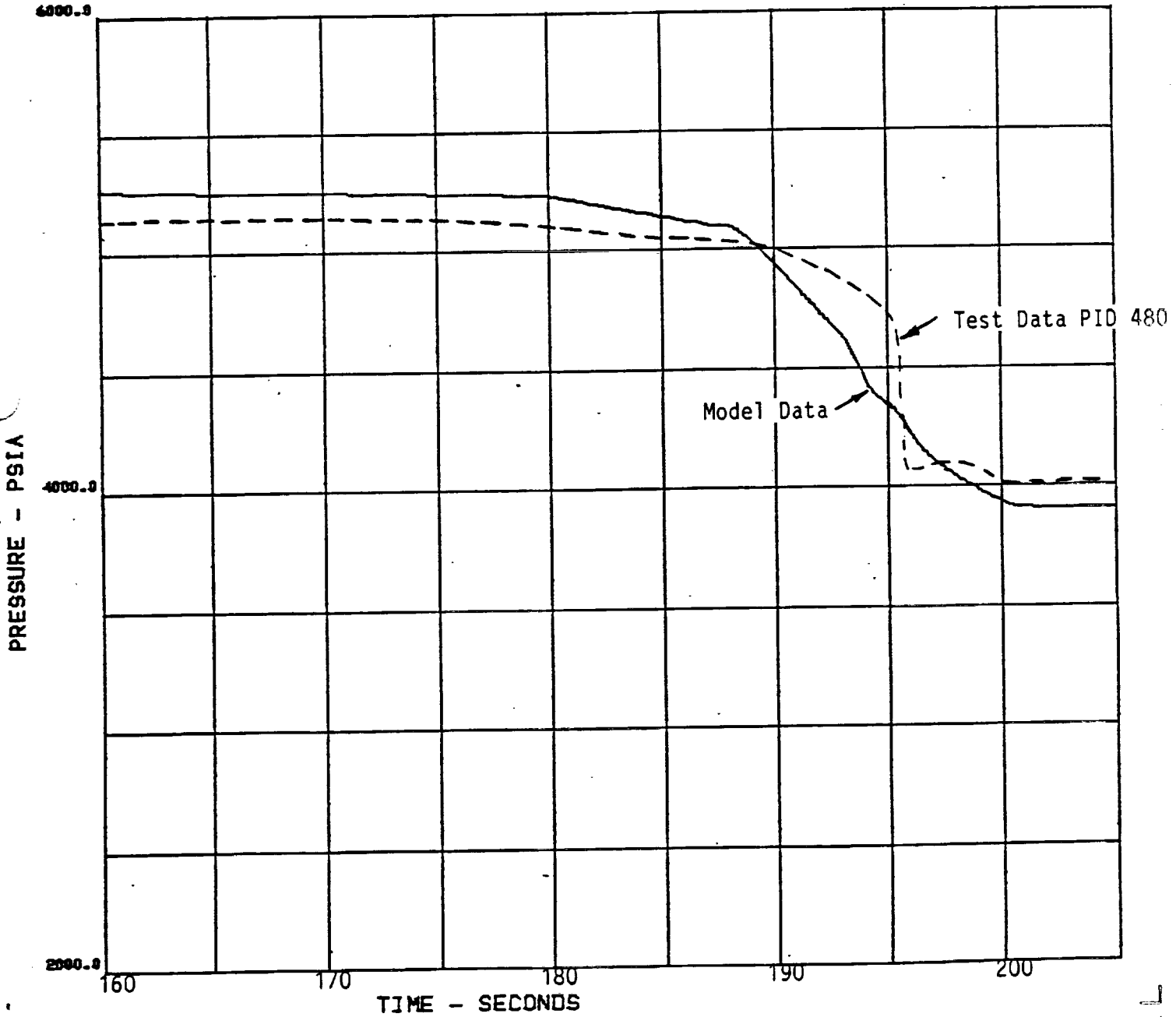
FIGURE 10E - Test 902-428



ORIGINAL PAGE IS
OF POOR QUALITY

ORIGINAL PAGE IS
OF POOR QUALITY

FIGURE 10F - Test 902-428



ORIGINAL PAGE IS
OF POOR QUALITY

ORIGINAL PAGE IS
OF POOR QUALITY

FIGURE 10G - Test 902-428

Figure 11A Fuel Leakage Flow
FUEL LEAKAGE FLOW
 MODEL TEST 750-285

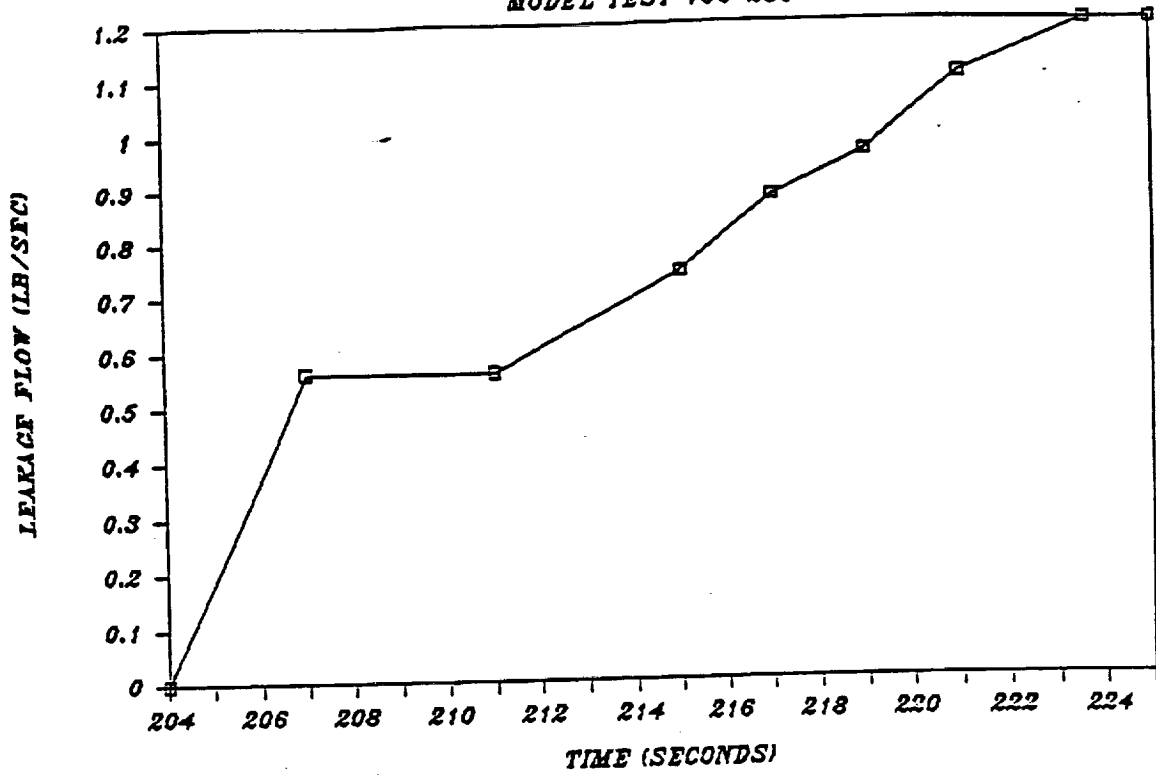
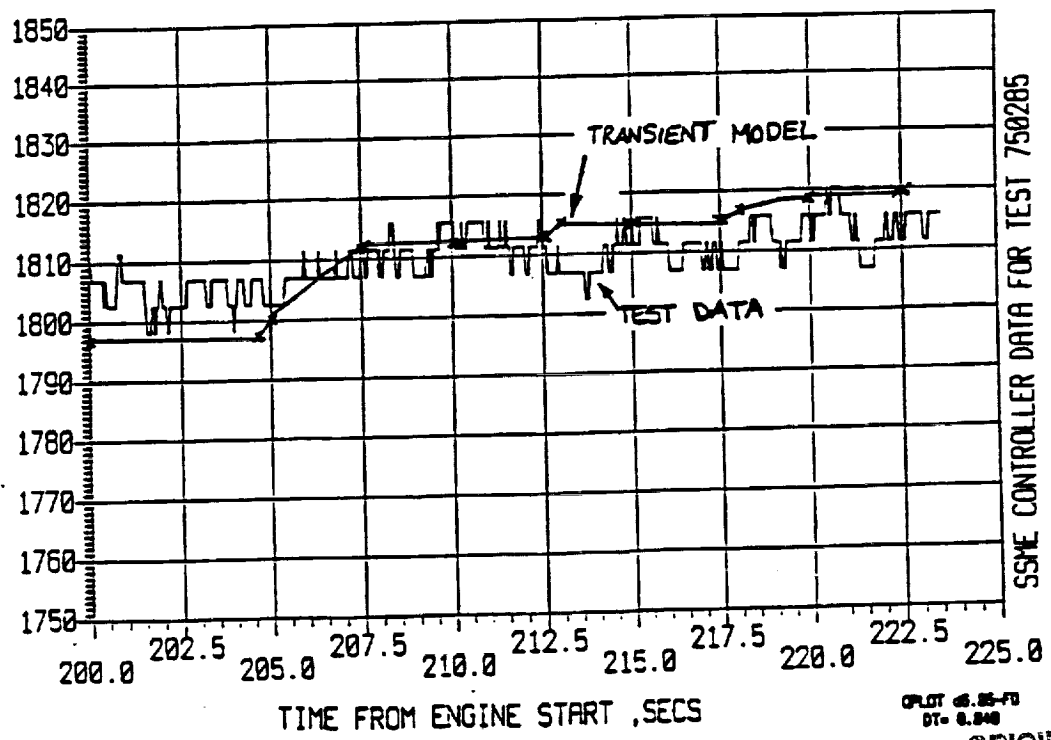


Figure 11B High Pressure Fuel Turbine Discharge Temperature

DETR 232 HPFT TUR DS T B (FTDB)



SSME CONTROLLER DATA FOR TEST 750285

PLT 4.25-73
 DT- 8.248

ORIGINAL PAGE IS
 OF POOR QUALITY

Figure 11G- High Pressure Oxidizer Turbine Discharge Temperature

REF 234 HPOT TUR DS T B (OTDB)

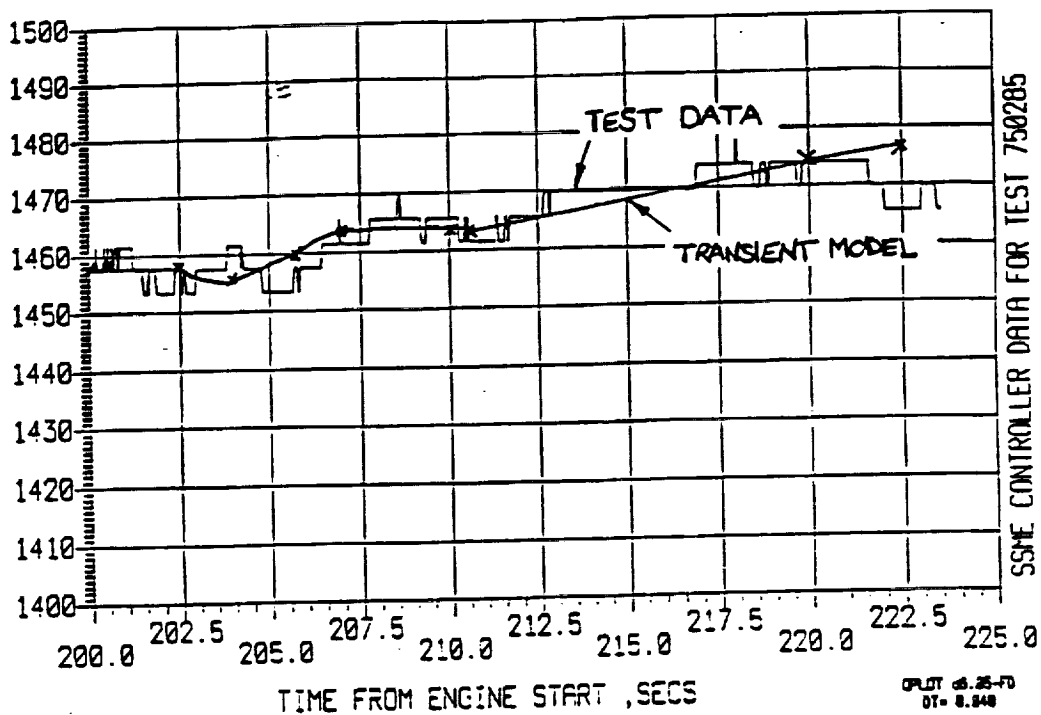
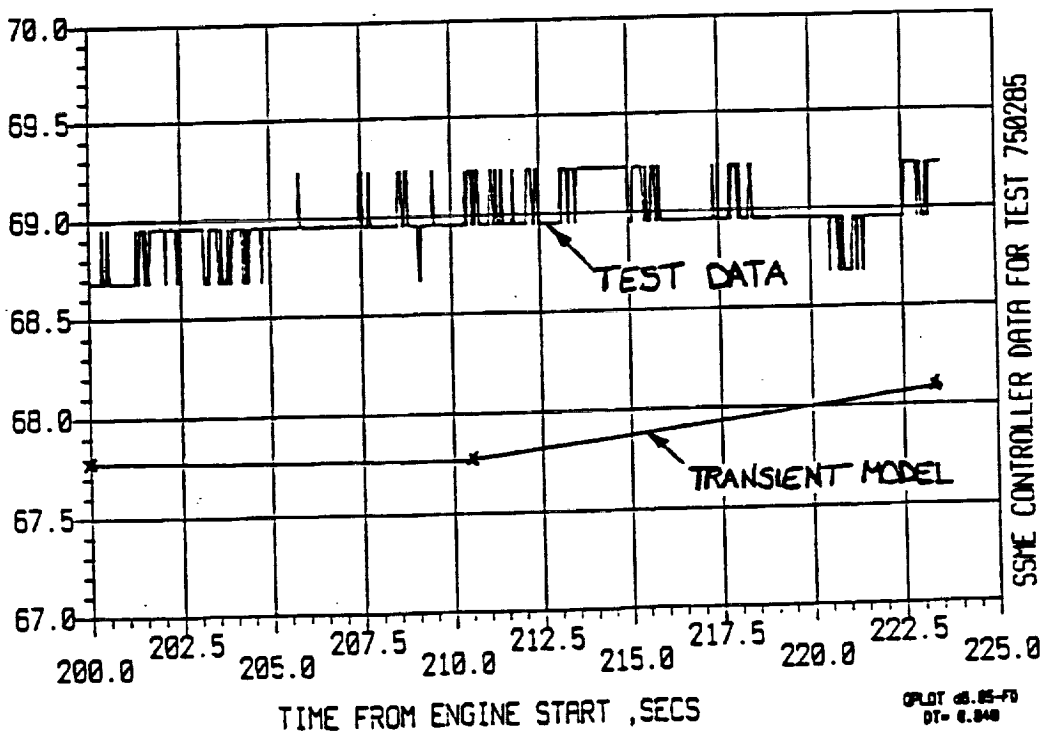


Figure 11D Oxidizer Preburner Oxidizer Valve Position

REF 48 OPOV ACT POSIT (OPV1)



ORIGINAL PAGE IS
OF POOR QUALITY

Figure 11E Main Combustion Chamber Pressure (MCP)

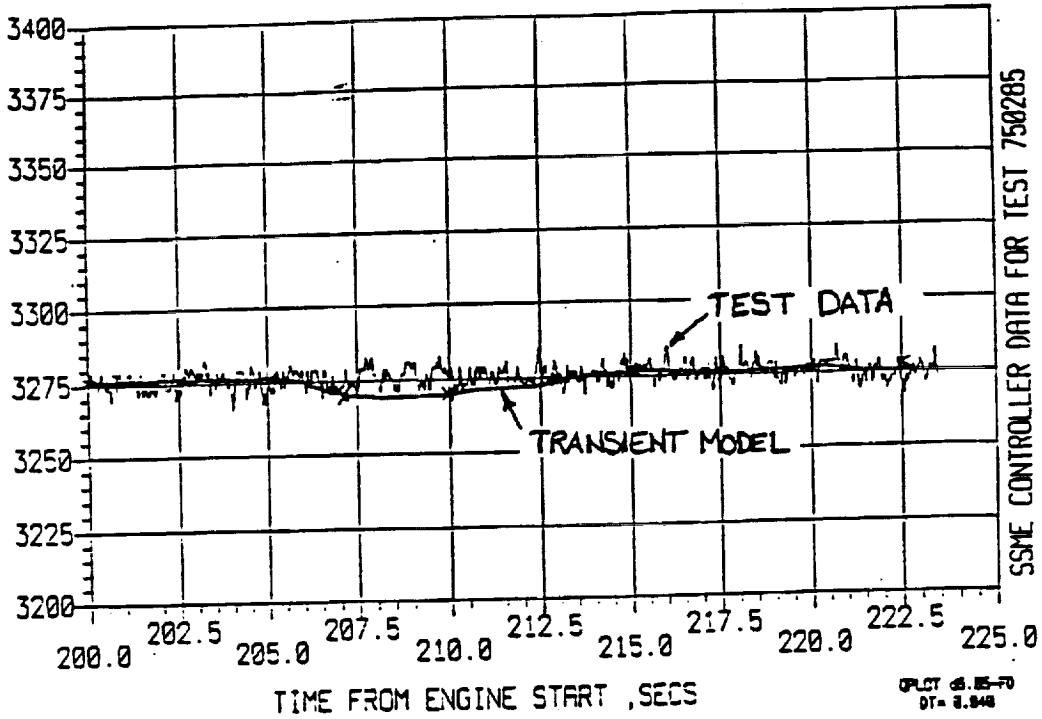
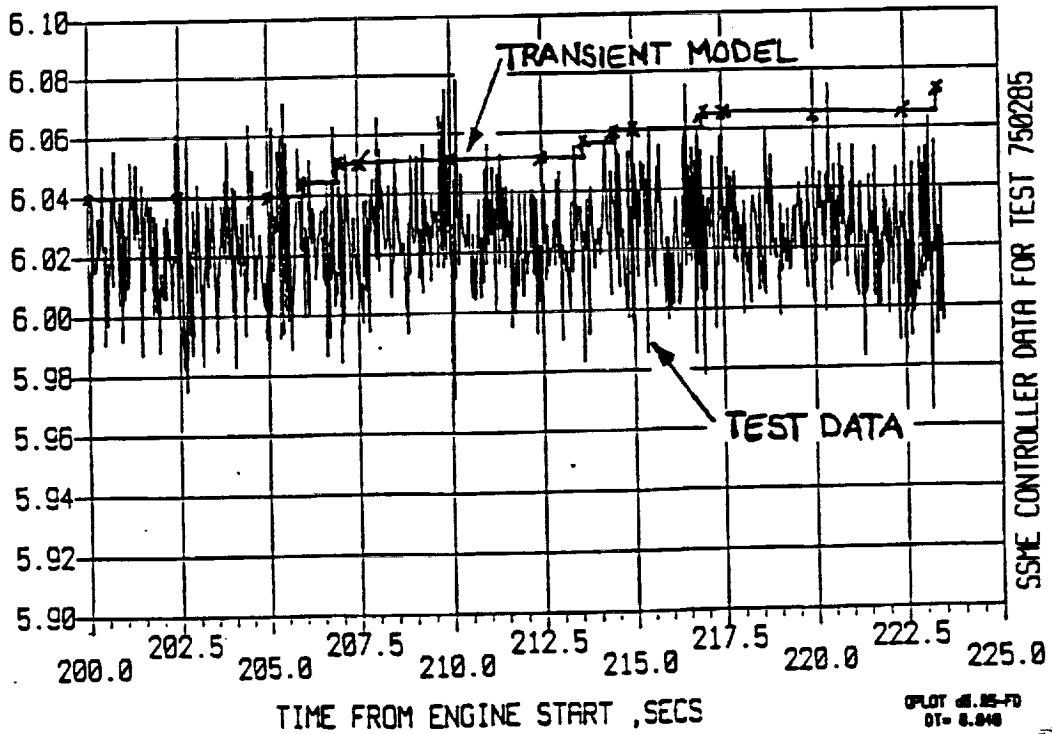


Figure 11F Mixture Ratio (MXRT)



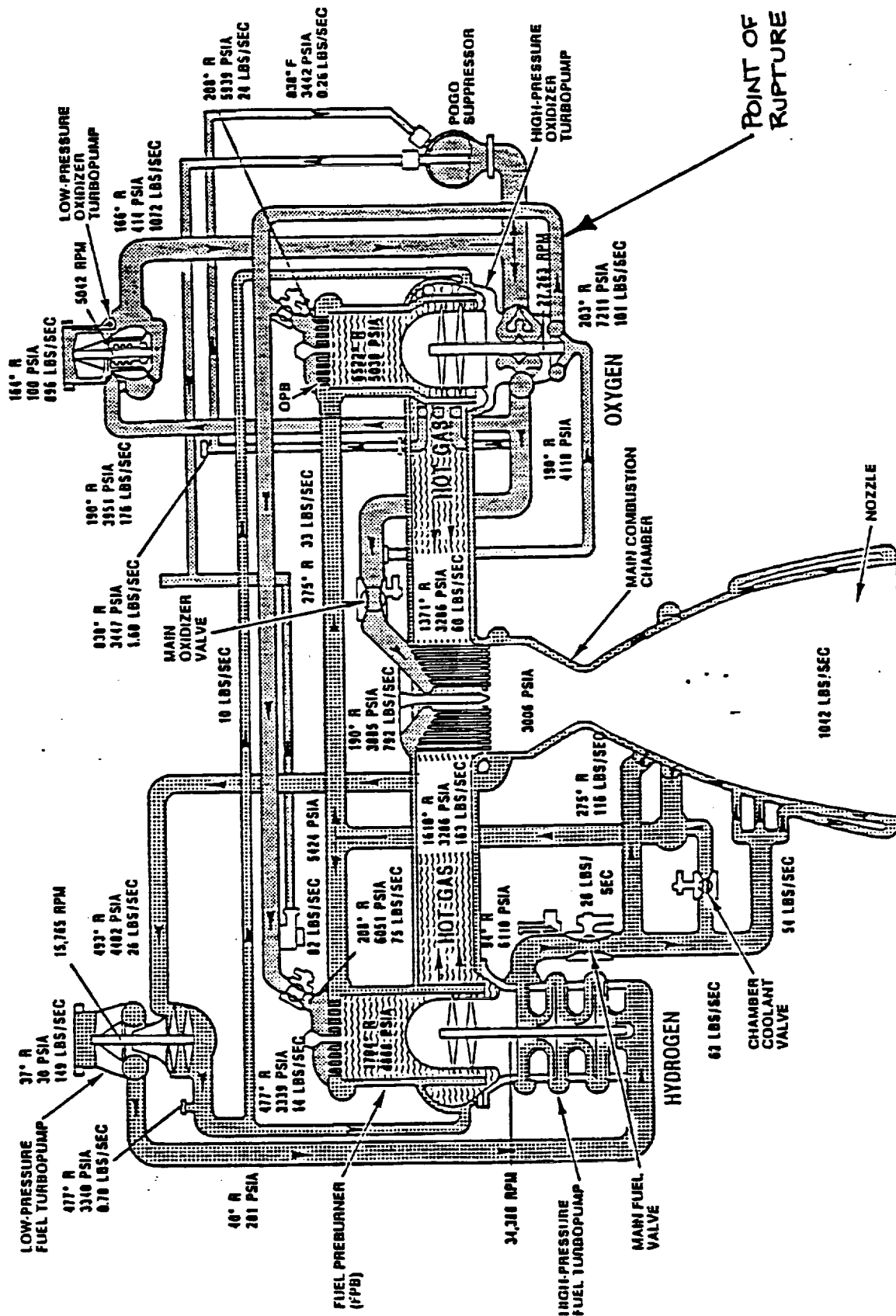


Figure 12 SSME Flow Schematic 100% RPL

FIGURE 12A - Hypothetical Leakage Effect

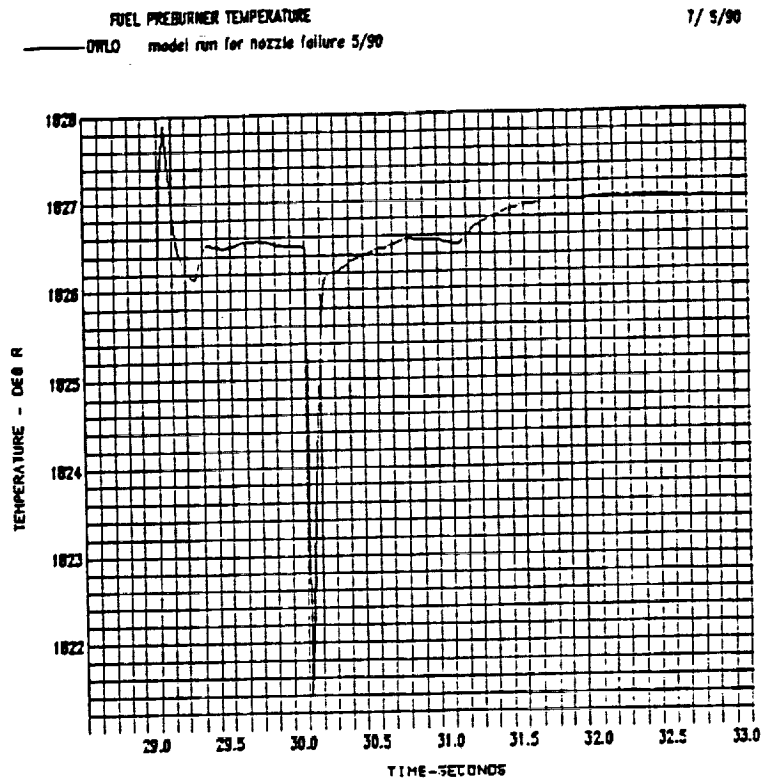


FIGURE 12B - Hypothetical Leakage Effect

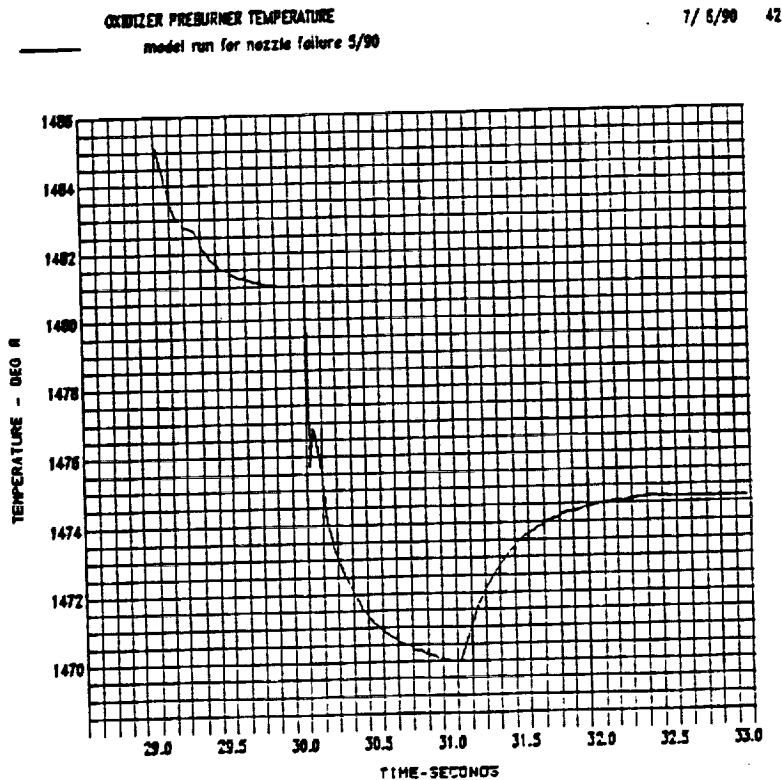


FIGURE 12C - Hypothetical Leakage Effect

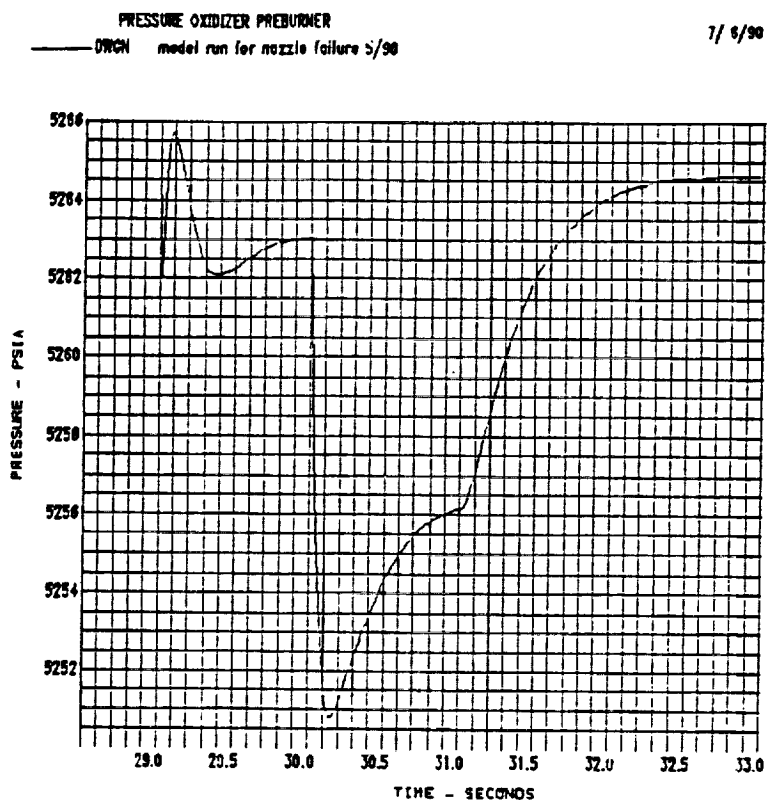


FIGURE 12D - Hypothetical Leakage Effect

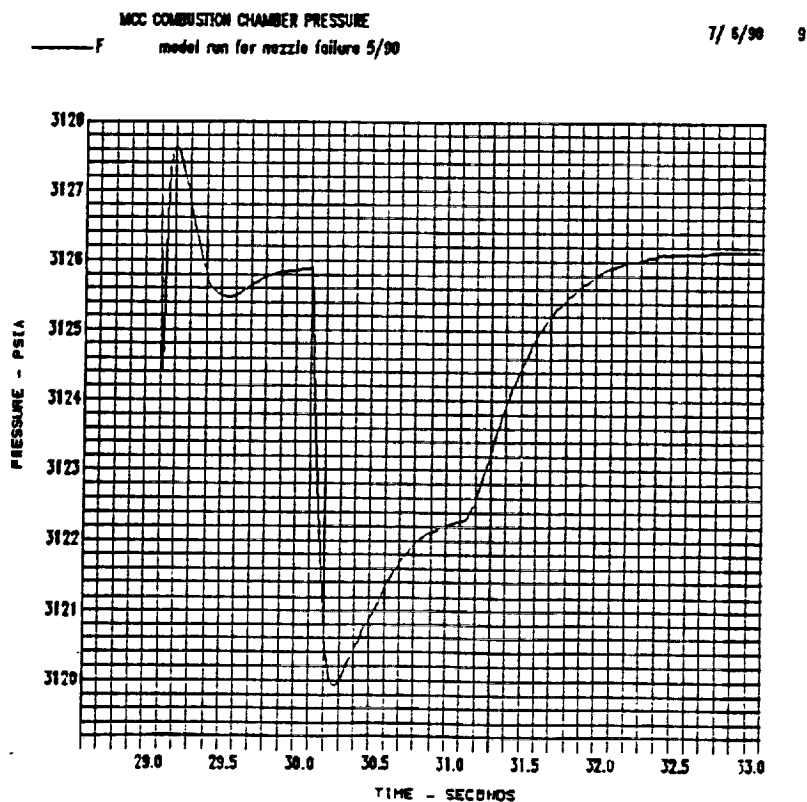


FIGURE 12E - Hypothetical Leakage Effect

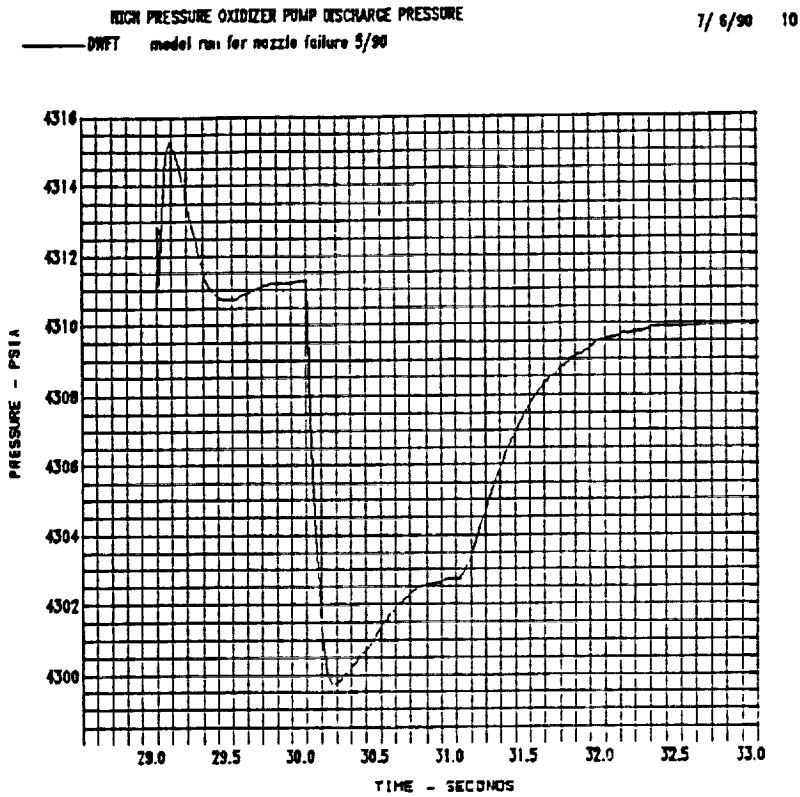
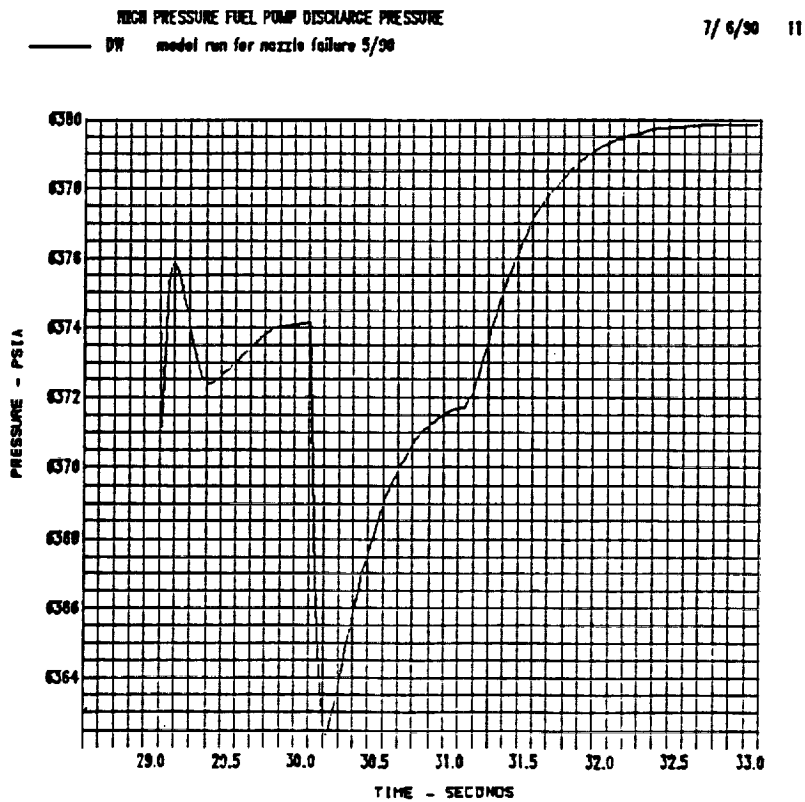


FIGURE 12F - Hypothetical Leakage Effect



ORIGINAL PAGE IS
OF POOR QUALITY

FIGURE 12G - Hypothetical Leakage Effect

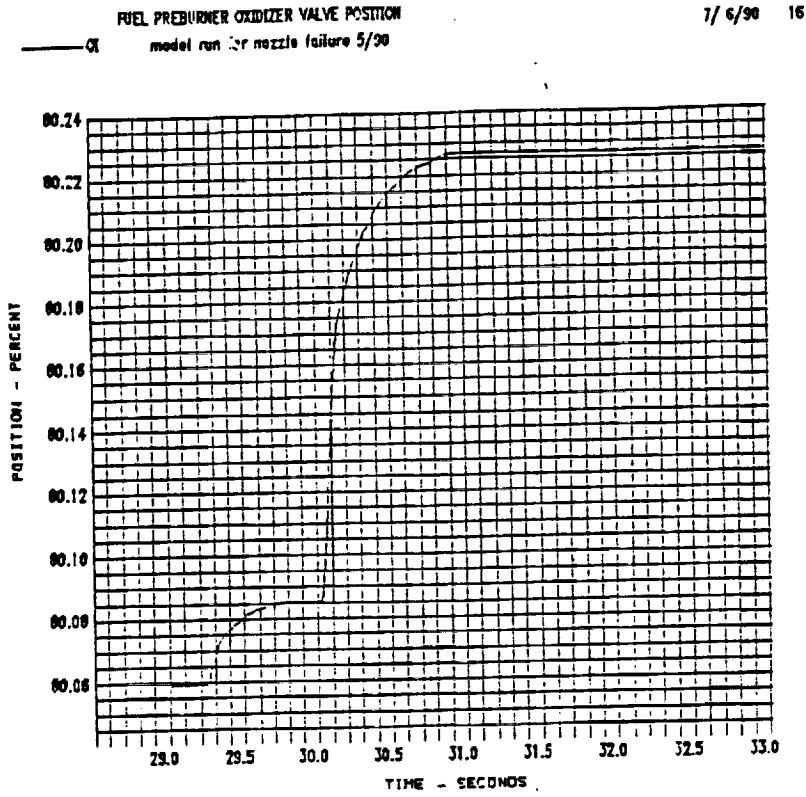
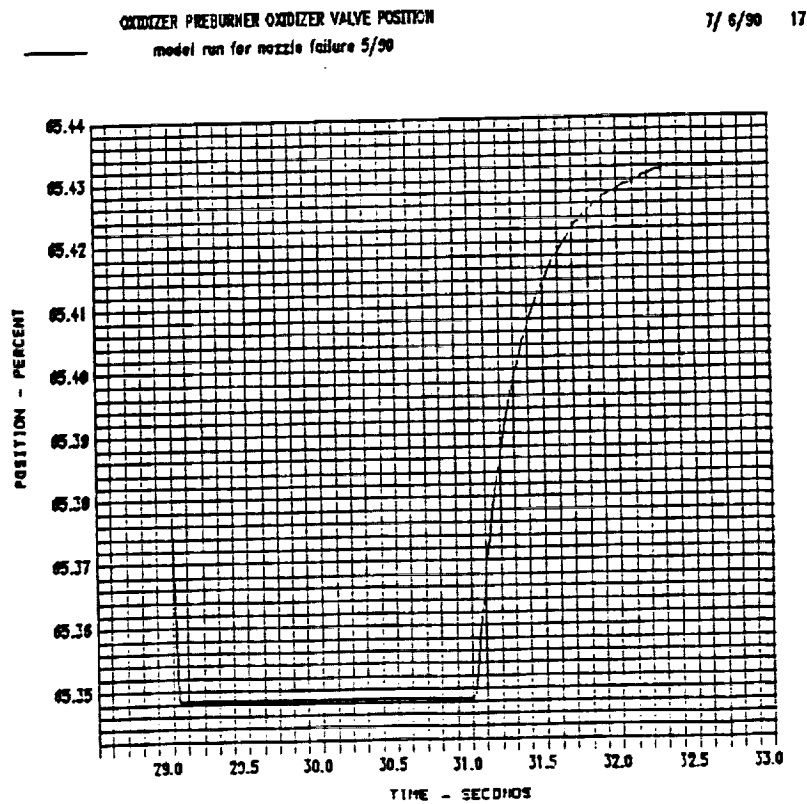


FIGURE 12H - Hypothetical Leakage Effect



ORIGINAL PAGE IS
OF POOR QUALITY

FIGURE 12I - Hypothetical Leakage Effect

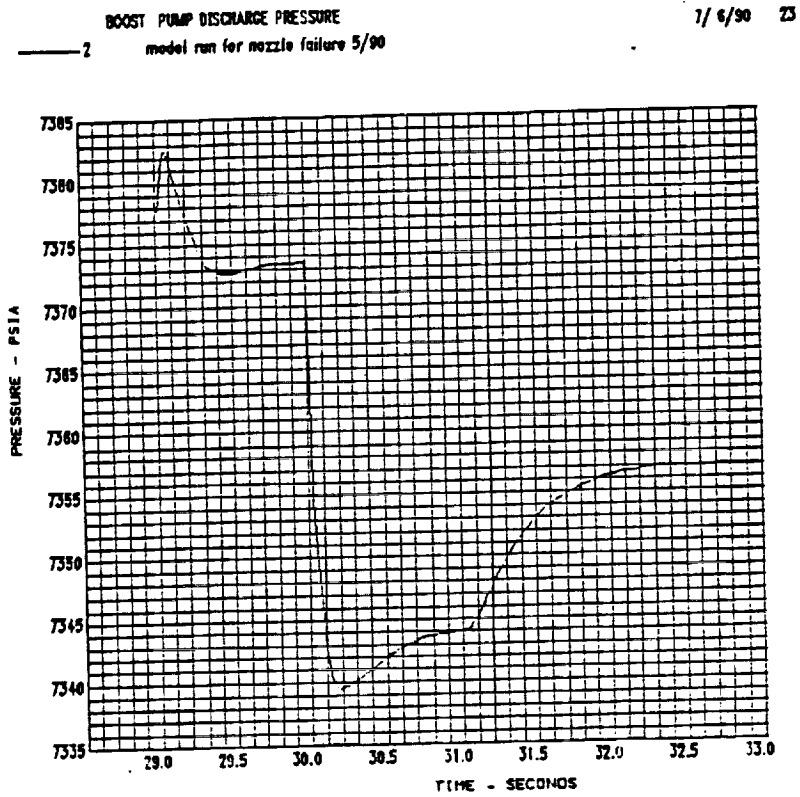
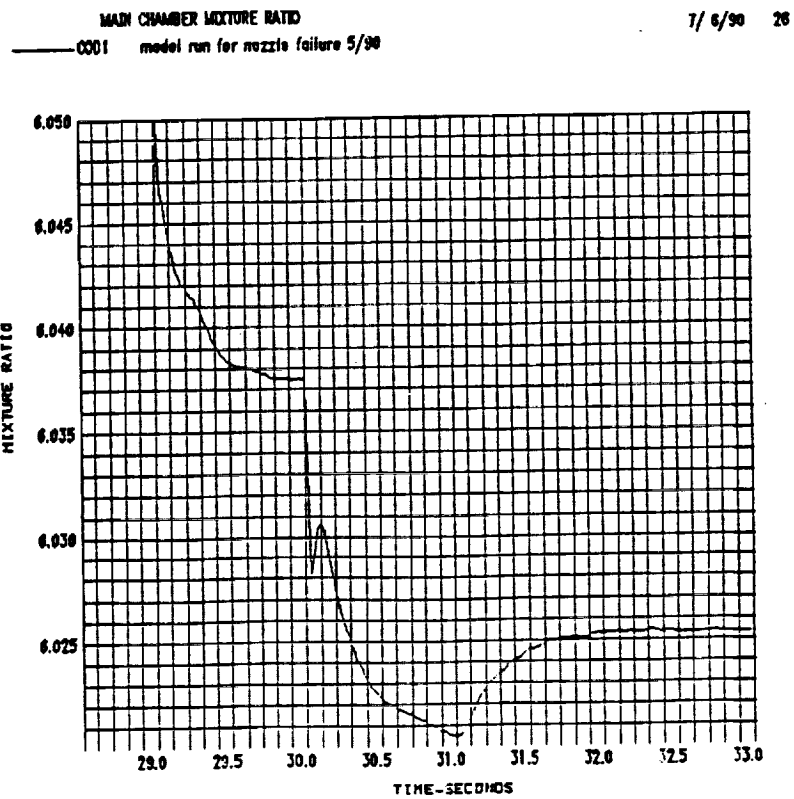


FIGURE 12J - Hypothetical Leakage Effect



ORIGINAL PAGE IS
OF POOR QUALITY

Figure 12K - Hypothetical Leakage Effect

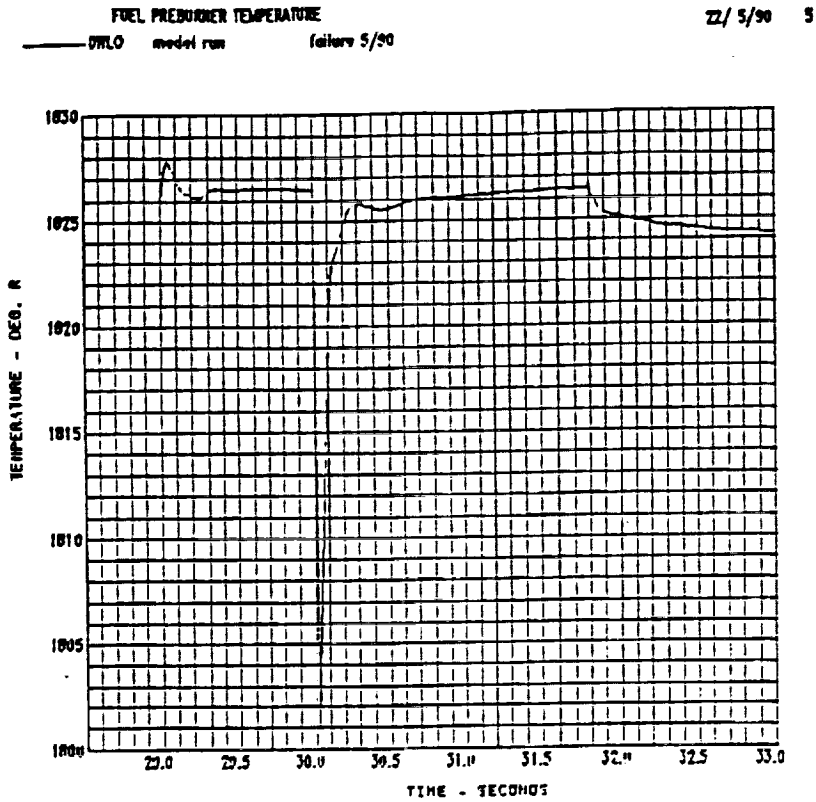
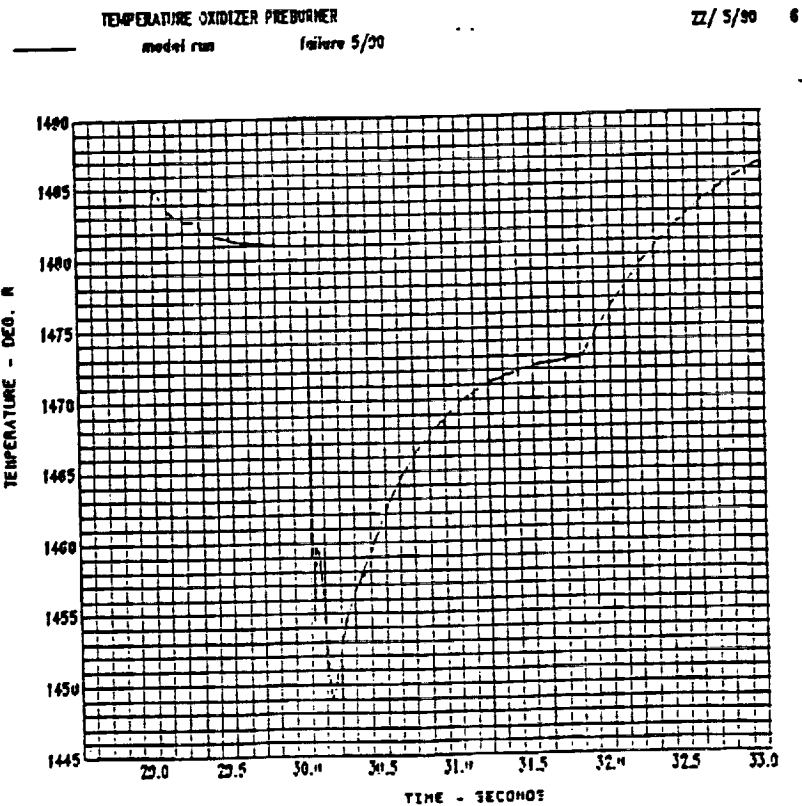


Figure 12L - Hypothetical Leakage Effect



ORIGINAL PAGE IS
 OF POOR QUALITY

Figures Showing the Effects of a 5 lb/sec Lox
 Leak Downstream of the Preburner Pump

Figure 12M - Hypothetical Leakage Effect

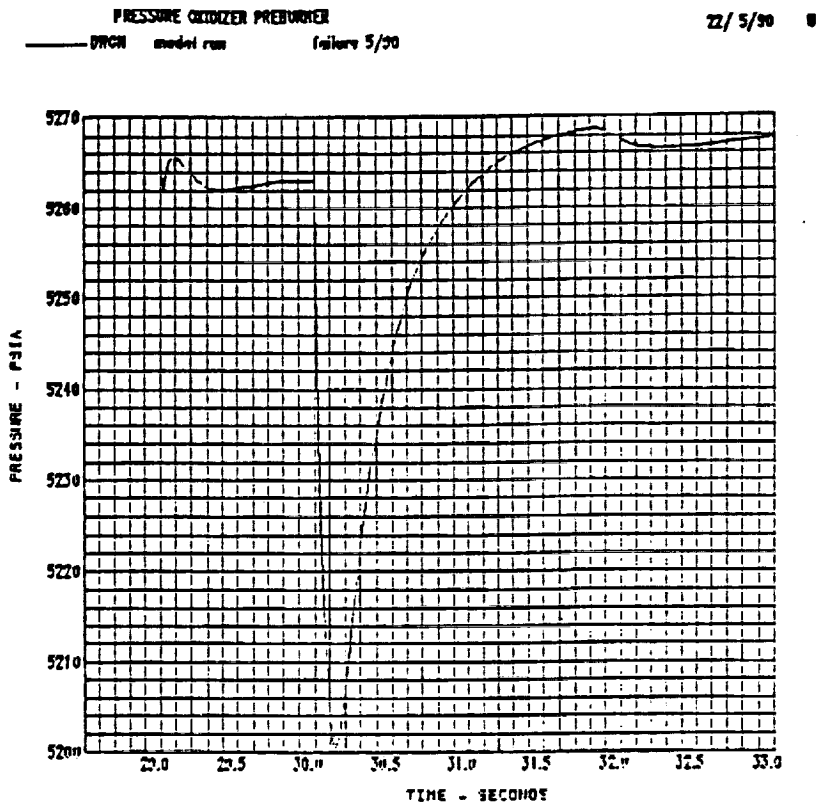
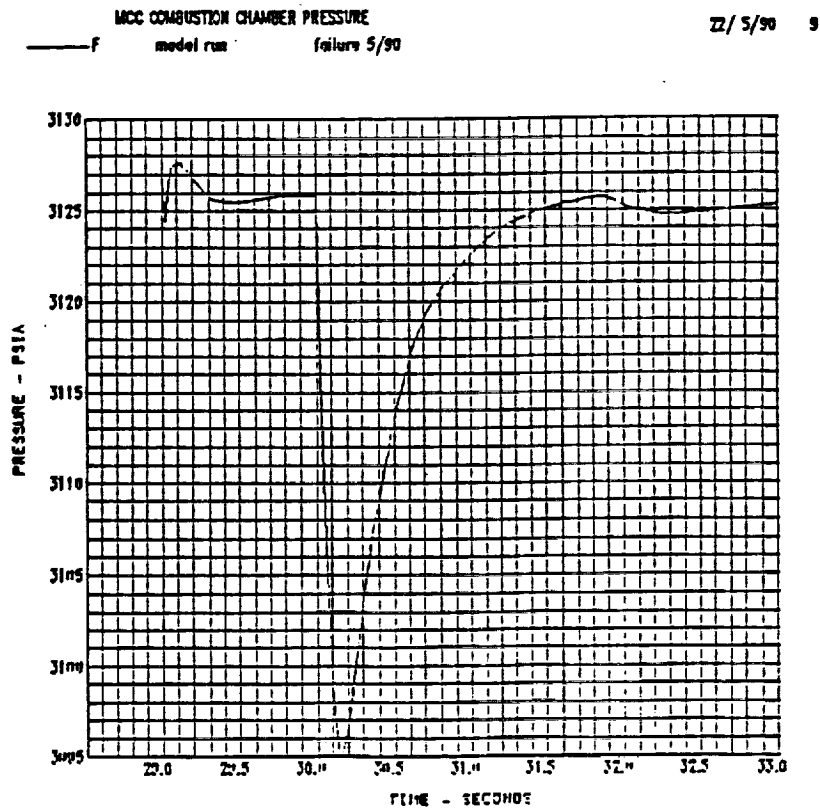


Figure 12N - Hypothetical Leakage Effect



Figures Showing the Effects of a 5 lb/sec Lox Leak Downstream of the Preburner Pump

ORIGINAL PAGE IS
OF POOR QUALITY

Figure 120 - Hypothetical Leakage Effect

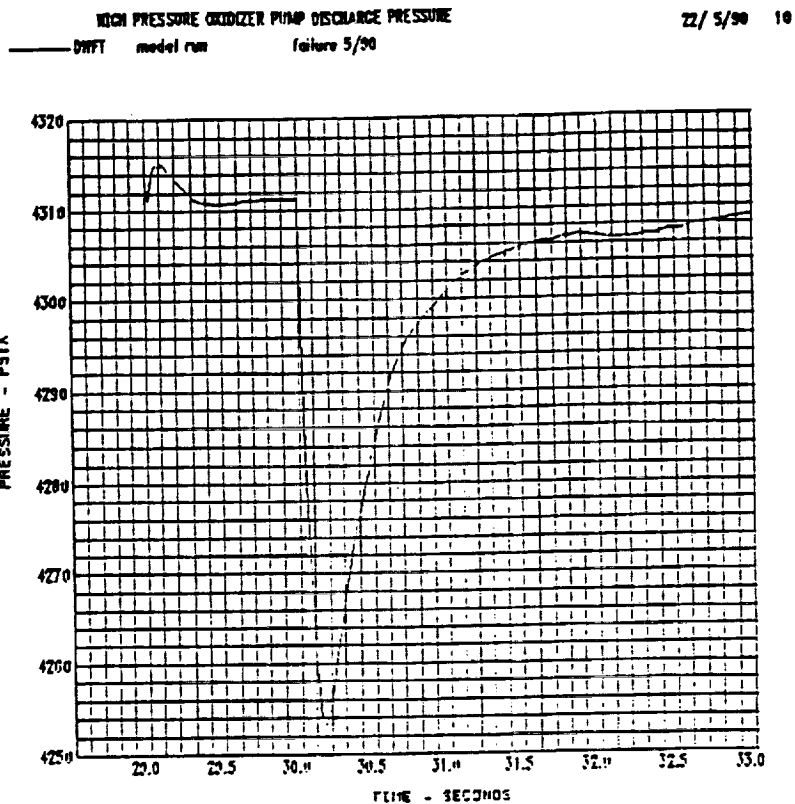
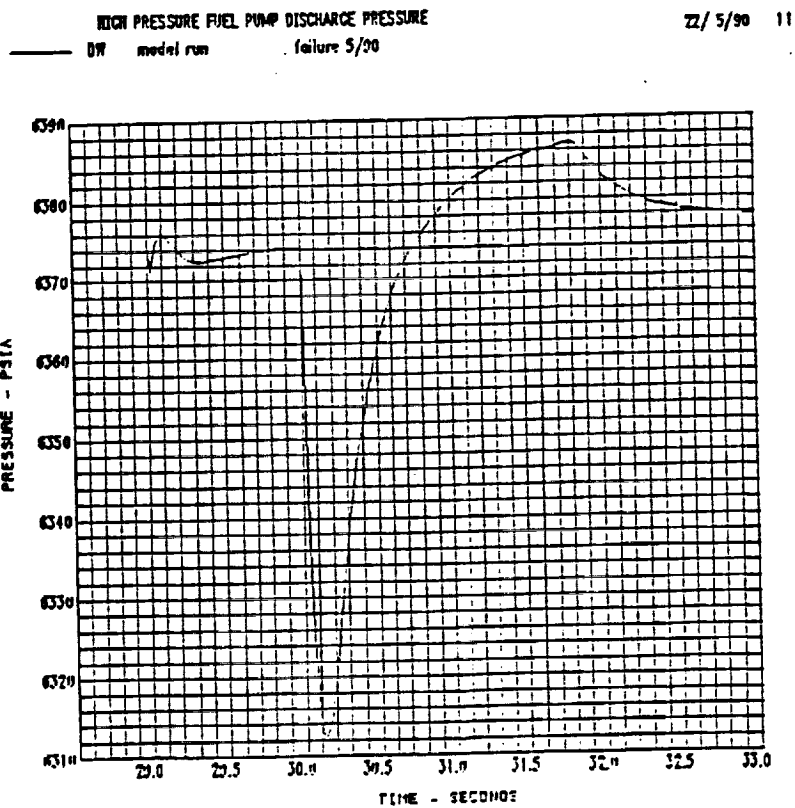


Figure 12P - Hypothetical Leakage Effect



Figures Showing the Effects of a 5 lb/sec Lox Leak Downstream of the Preburner Pump

ORIGINAL PAGE IS OF POOR QUALITY

Figure 12Q - Hypothetical Leakage Effect

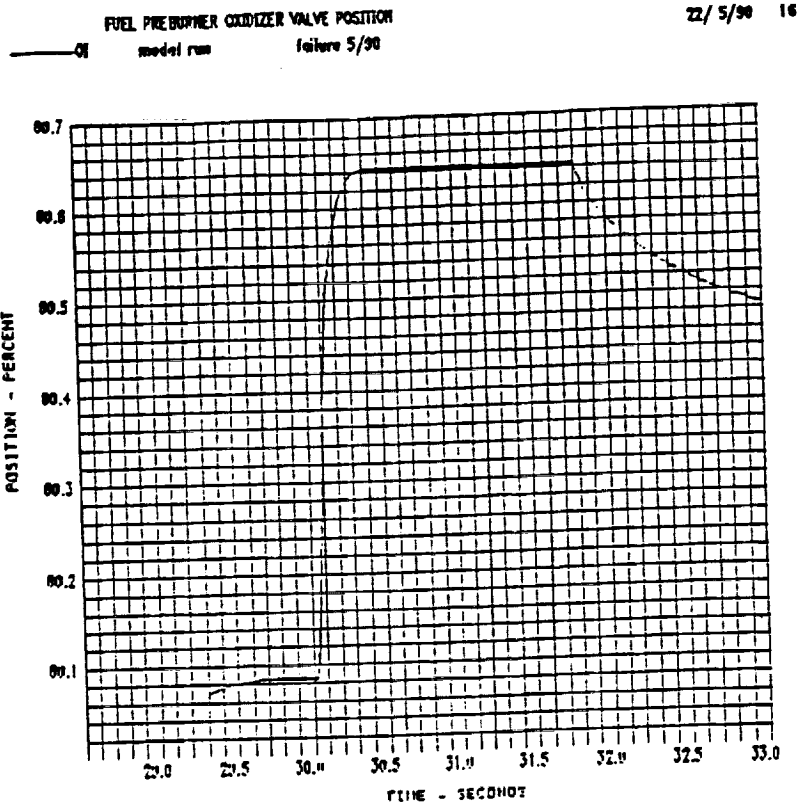
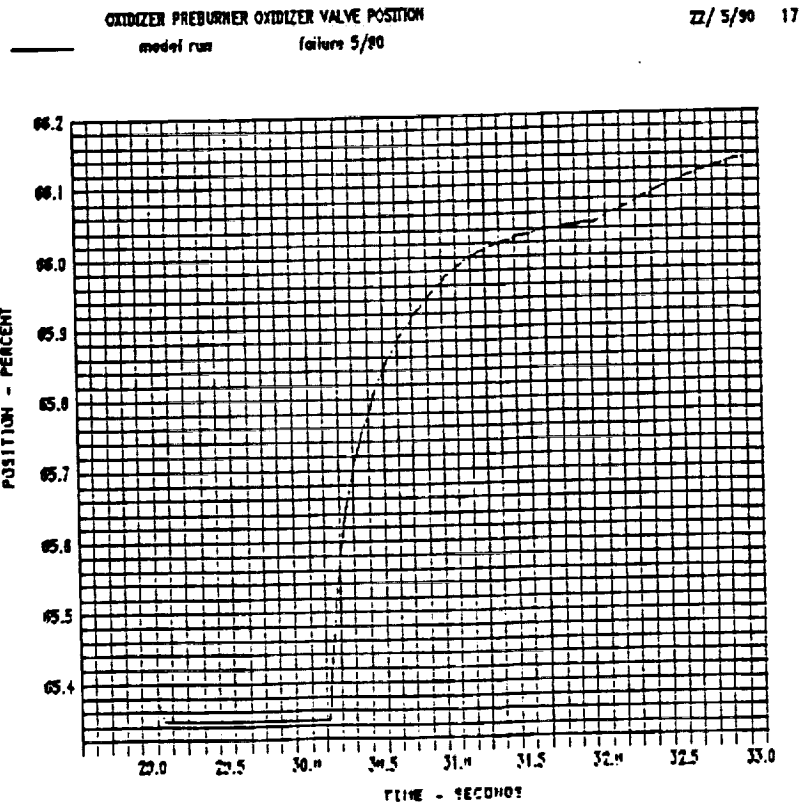


Figure 12R - Hypothetical Leakage Effect



Figures Showing the Effects of a 5 lb/sec Lox Leak Downstream of the Preburner Pump

ORIGINAL PAGE IS OF POOR QUALITY

Figure 12S - Hypothetical Leakage Effect

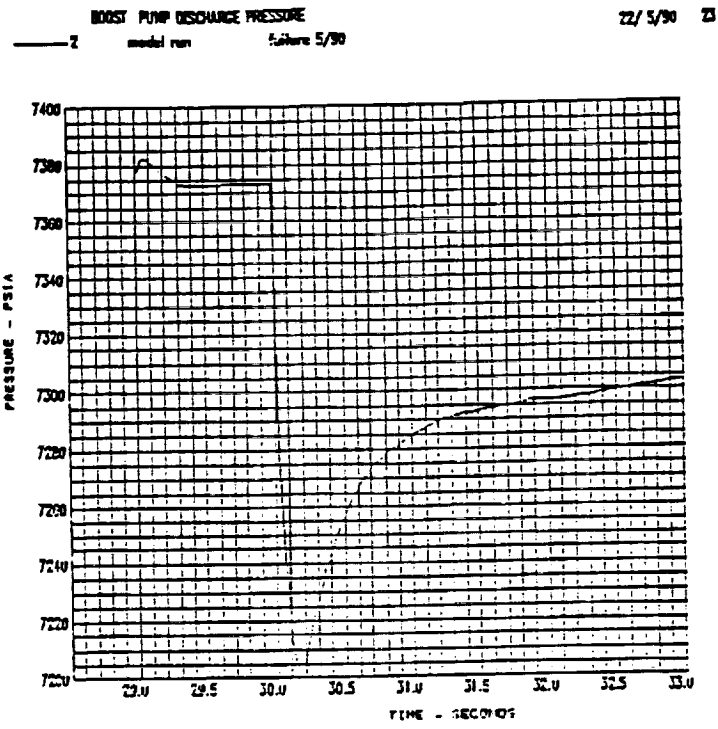
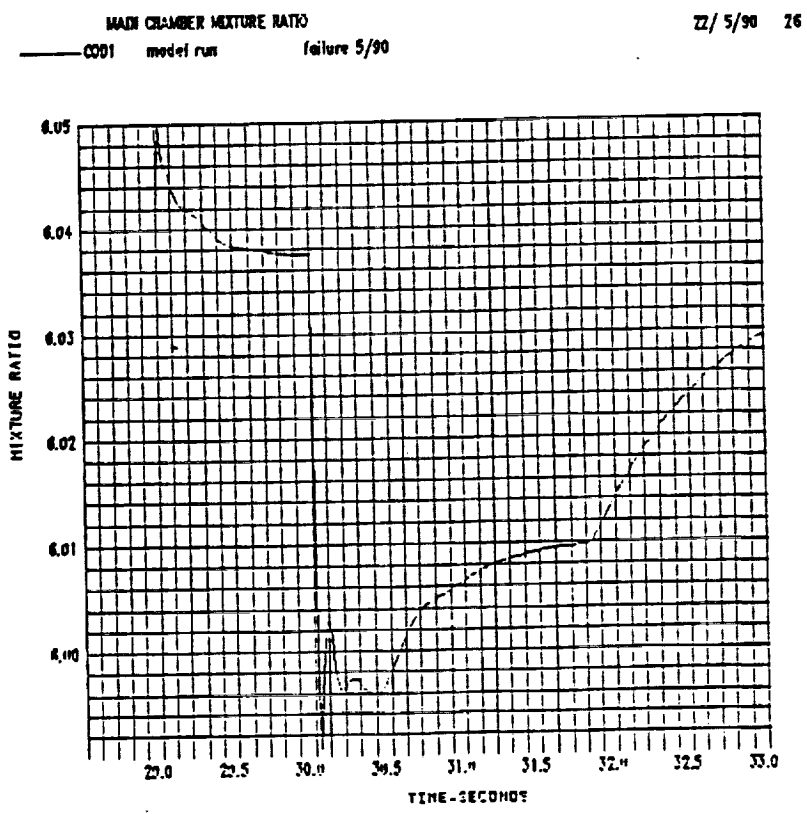


Figure 12T - Hypothetical Leakage Effect



Figures Showing the Effects of a 5 lb/sec Lox Leak Downstream of the Preburner Pump

ORIGINAL PAGE IS OF POOR QUALITY

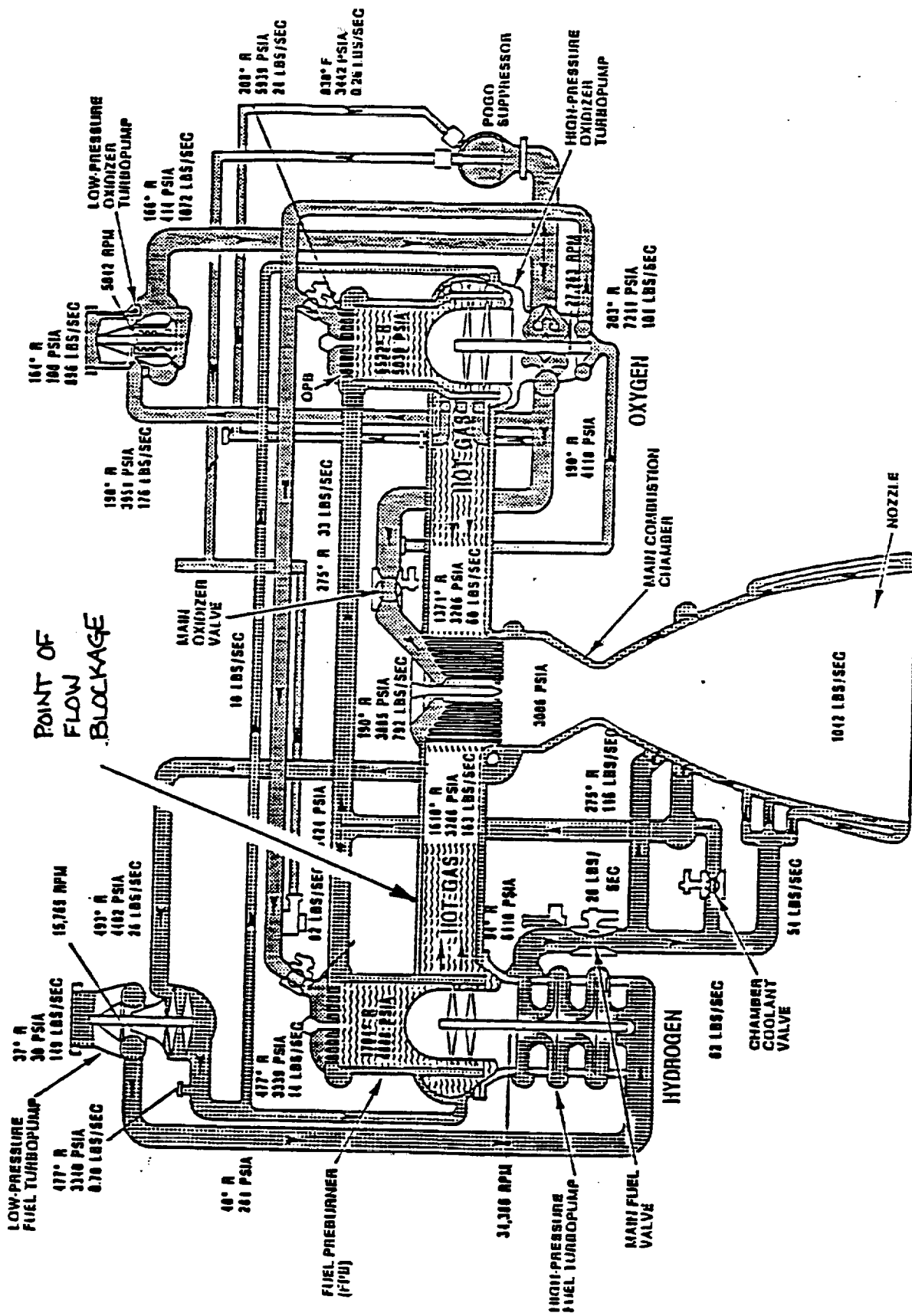


Figure 13A SSME Flow Schematic 100% RPL

Figure 13B - Hypothetical Blockage Effect

FUEL PREBURNER TEMPERATURE
28/ 6/90 5
OWLO model run for hplp dis blockage 6/90

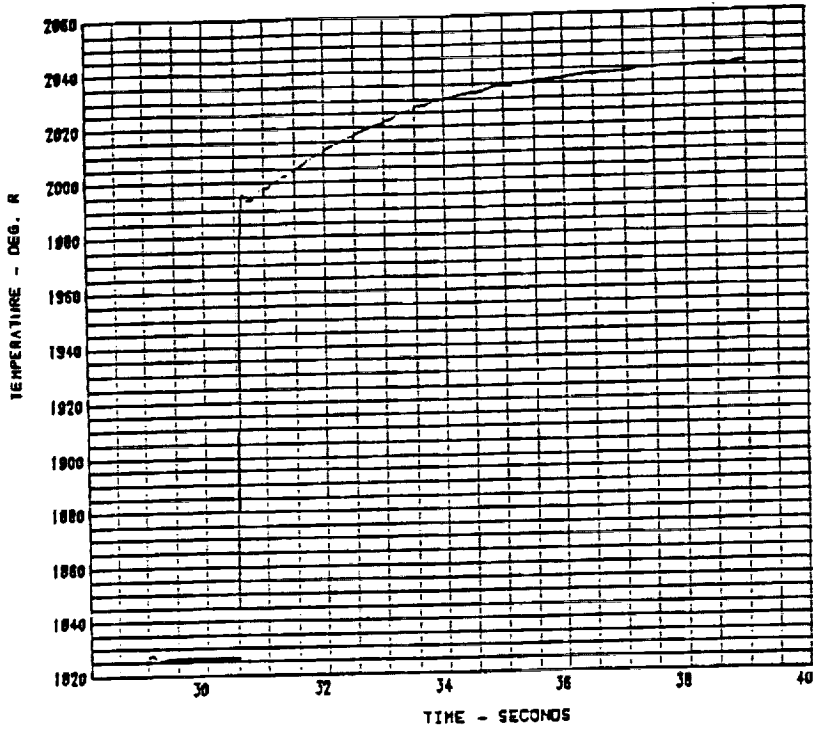
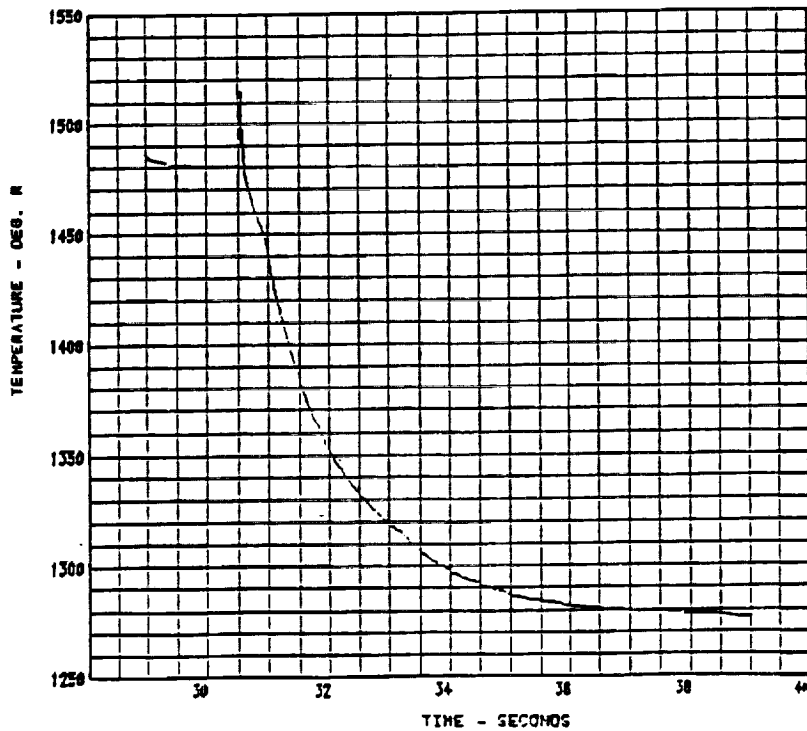


Figure 13C - Hypothetical Blockage Effect

TEMPERATURE OXIDIZER PREBURNER
28/ 6/90 6
model run for hplp dis blockage 6/90



ORIGINAL PAGE IS
OF POOR QUALITY

Figure 13D - Hypothetical Blockage Effect

FUEL PREBURNER PRESSURE

26/ 6/90

— DWFP model run for hp1fp dis blockage 6/90

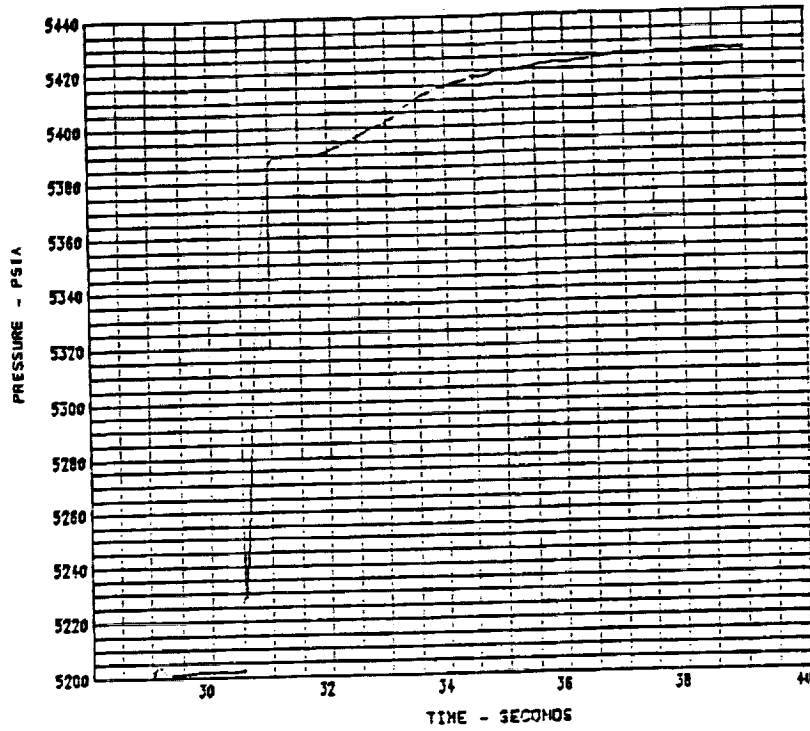
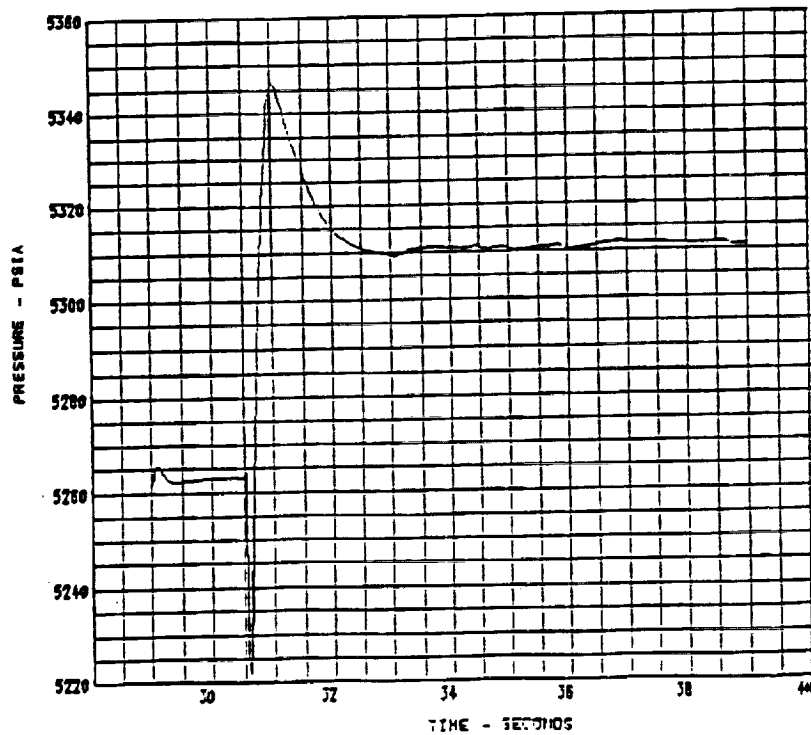


Figure 13E - Hypothetical Blockage Effect

PRESSURE OXIDIZER PREBURNER

26/ 6/90

— DWCP model run for hp1fp dis blockage 6/90



ORIGINAL PAGE IS
OF POOR QUALITY

Figure 413F - Hypothetical Blockage Effect

MCC COMBUSTION CHAMBER PRESSURE

28/ 8/90

— F model run for hplp dia blockage 8/90

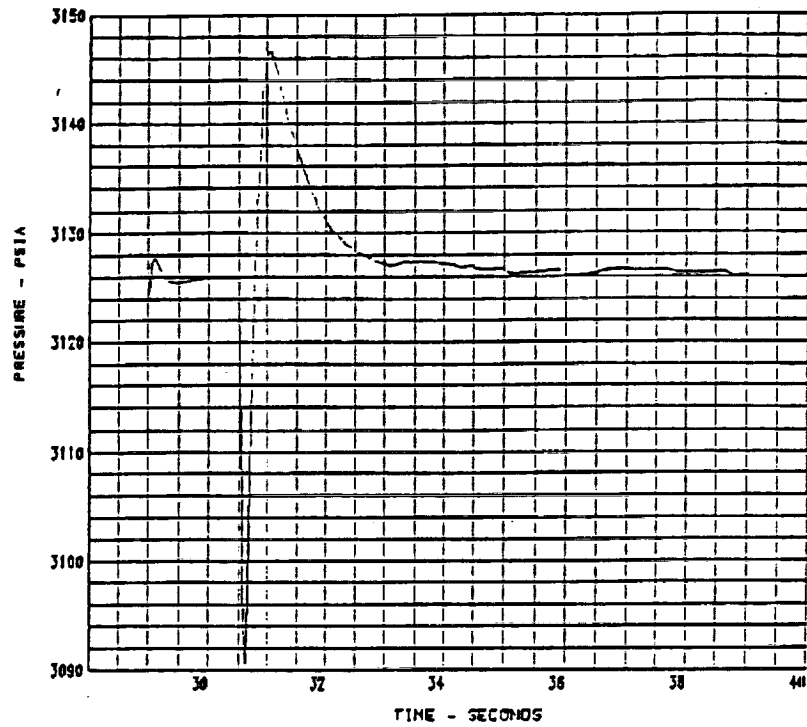
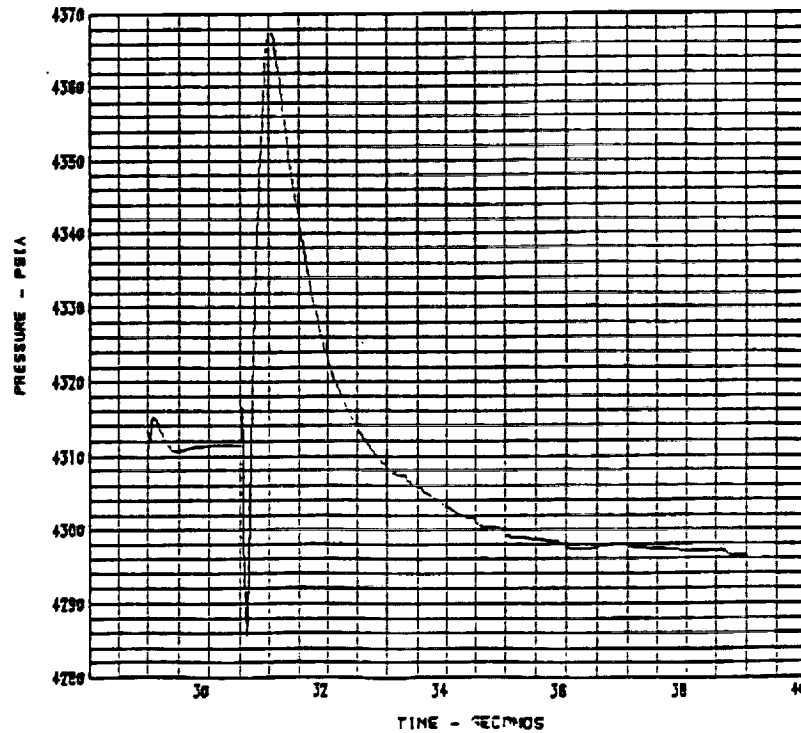


Figure 413C - Hypothetical Blockage Effect

HIGH PRESSURE OXIDIZER PUMP DISCHARGE PRESSURE

28/ 8/90

— DWFT model run for hplp dia blockage 8/90



ORIGINAL PAGE IS
OF POOR QUALITY

Figure 13H - Hypothetical Blockage Effect

HIGH PRESSURE FUEL PUMP DISCHARGE PRESSURE

20/ 6/90

model run for hptp die blockage 6/90

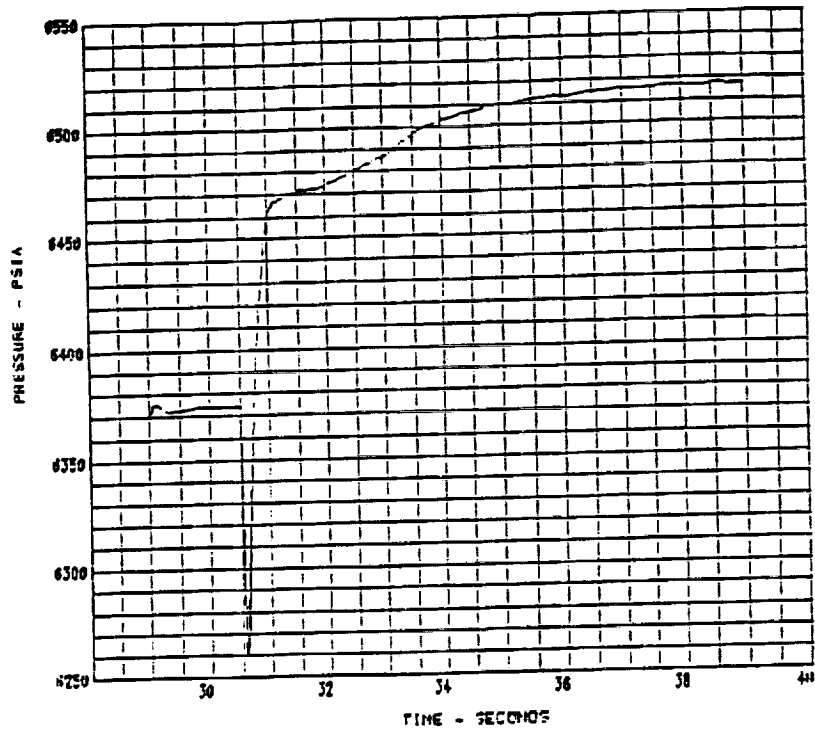
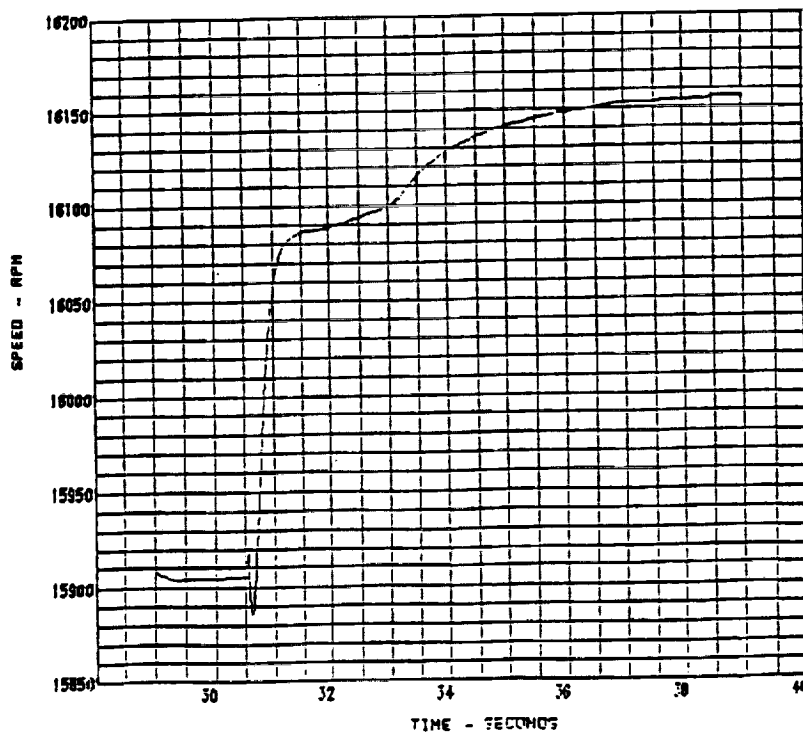


Figure 4.13I - Hypothetical Blockage Effect

LOW PRESSURE FUEL PUMP SPEED

20/ 6/90

model run for hptp die blockage 6/90



ORIGINAL PAGE IS
OF POOR QUALITY

Figure 13J - Hypothetical Blockage Effect

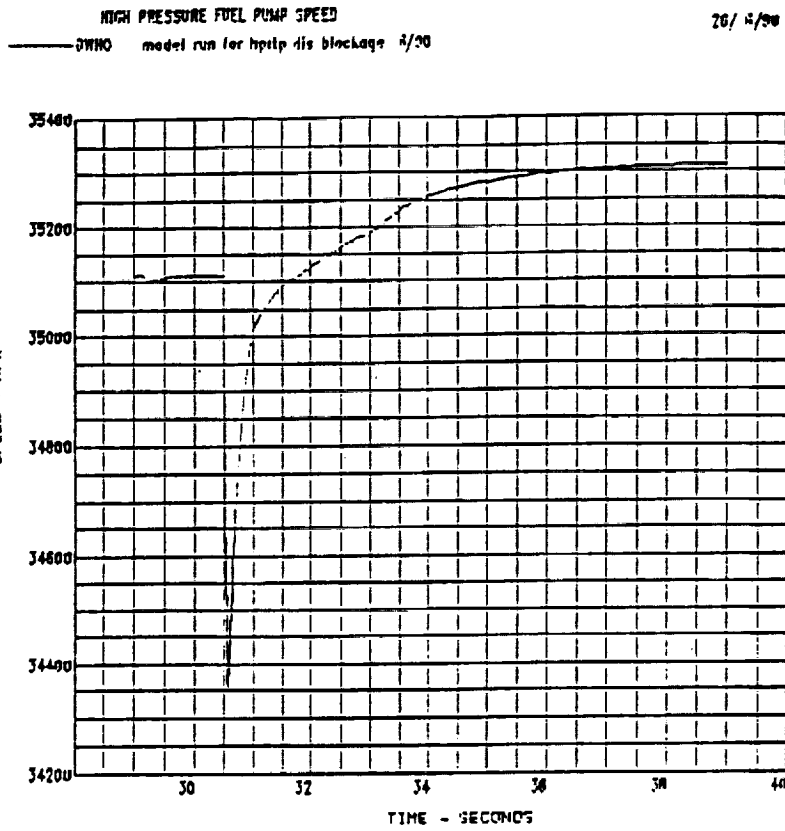
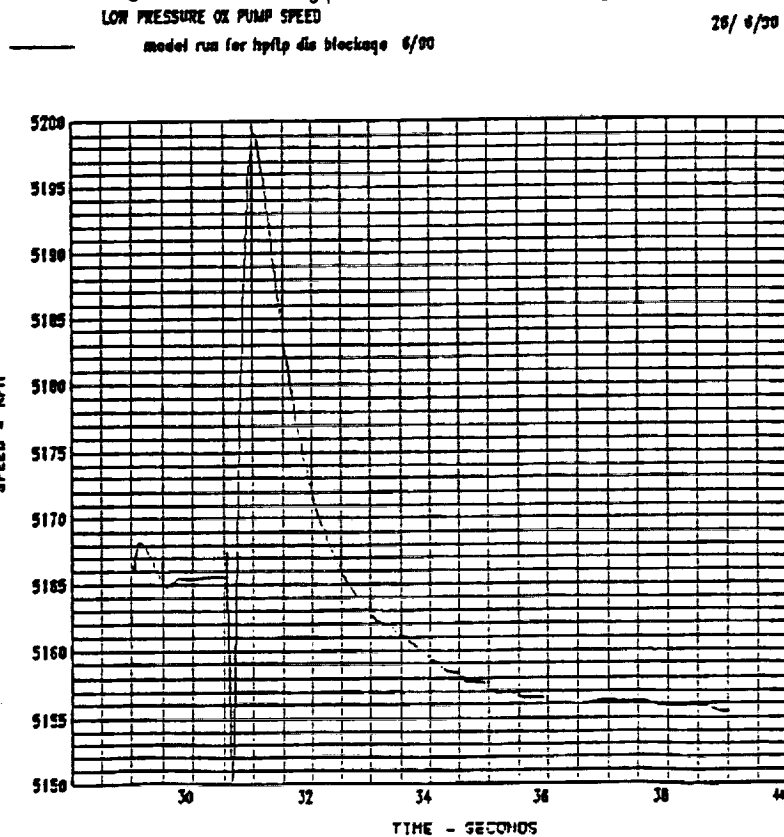


Figure 13K - Hypothetical Blockage Effect



ORIGINAL PAGE IS
OF POOR QUALITY

Figure 13L - Hypothetical Blockage Effect

HIGH PRESSURE OX PUMP SPEED

28/8/90

OW model run for hprlp dia blockage 8/90

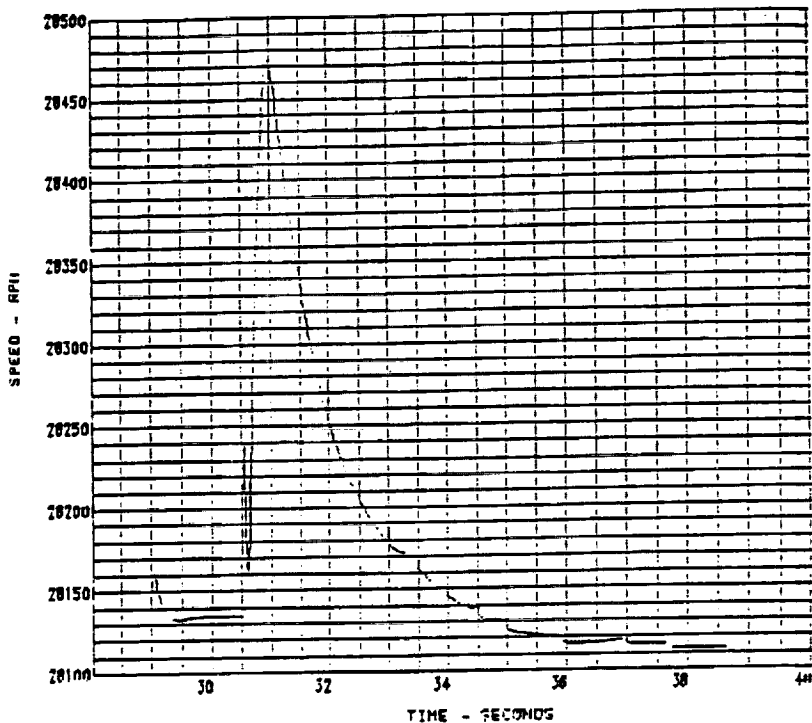
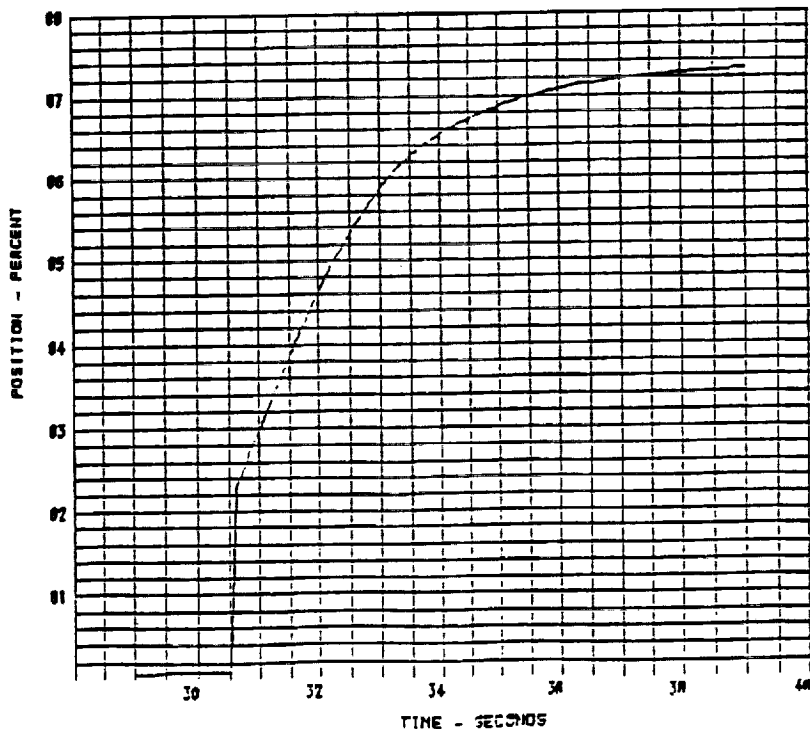


Figure 13M - Hypothetical Blockage Effect

FUEL PREBURNER OXIDIZER VALVE POSITION

28/8/90

OX model run for hprlp dia blockage 8/90



ORIGINAL PAGE IS
OF POOR QUALITY

Figure 13N - Hypothetical Blockage Effect

OXIDIZER PREBURNER OXIDIZER VALVE POSITION

28/4/90

model run for hplp dis blockage 6/90

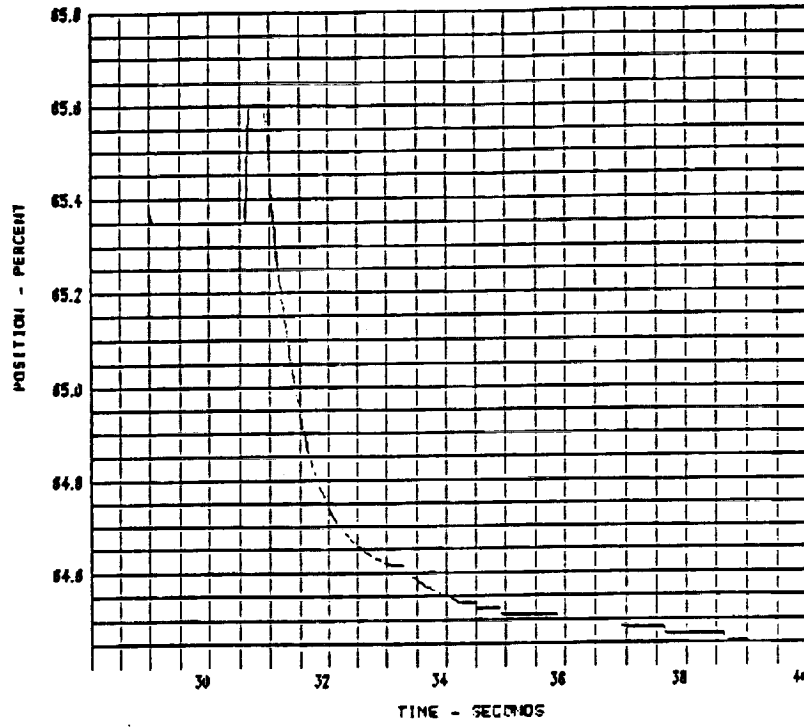
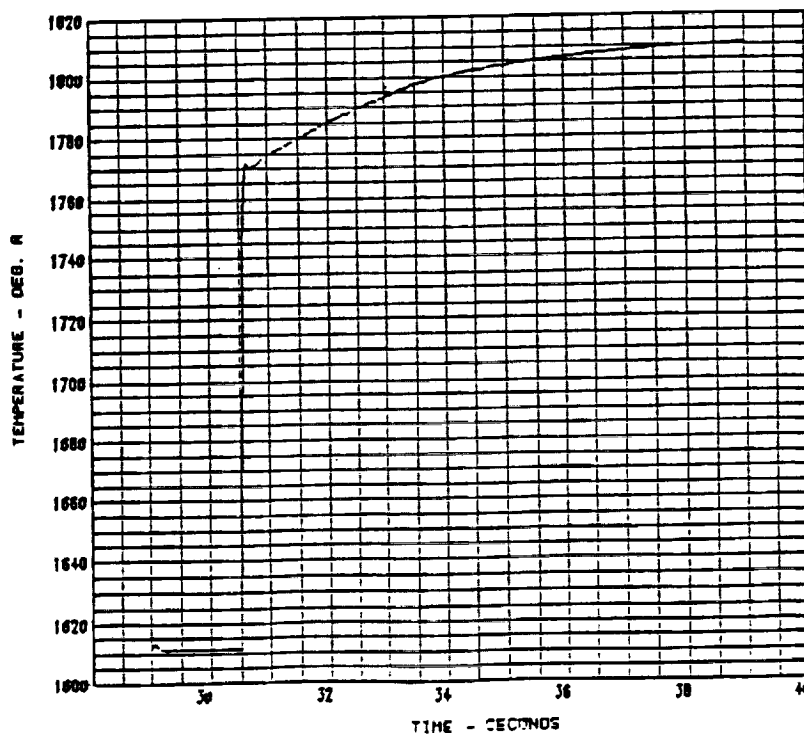


Figure 130 - Hypothetical Blockage Effect

HIGH PRESSURE FUEL TURBINE DISCHARGE TEMPERATURE

28/4/90

DR model run for hplp dis blockage 6/90



ORIGINAL PAGE IS
OF POOR QUALITY

Figure 13P - Hypothetical Blockage Effect

HIGH PRESSURE OXIDIZER TURRET DISCHARGE TEMPERATURE

28/ 6/90

PR model run for hpfp dia blockage 6/90

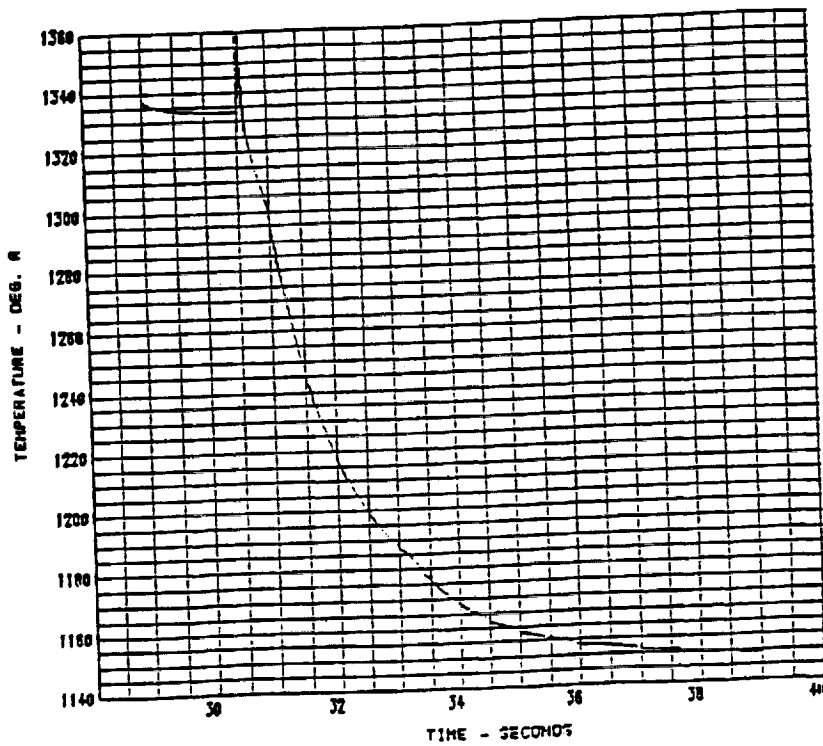
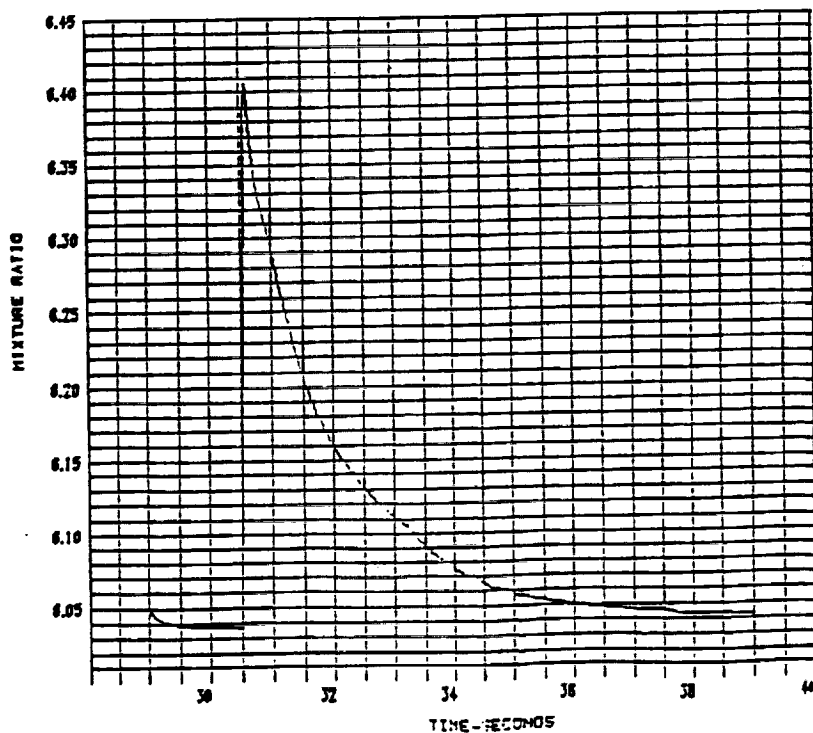


Figure 13Q - Hypothetical Blockage Effect

MAIN CHAMBER MIXTURE RATIO

28/ 6/90

CC01 model run for hpfp dia blockage 6/90



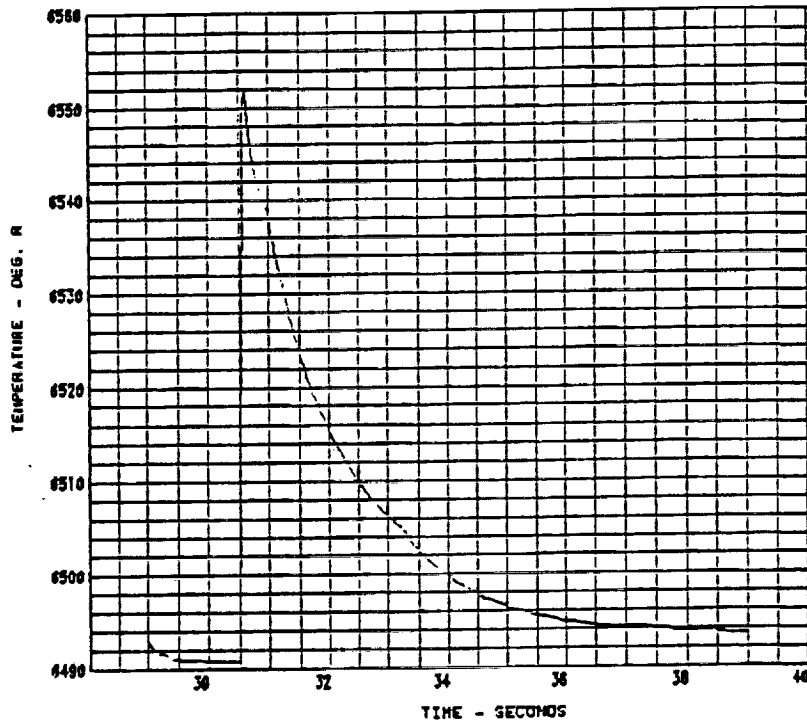
ORIGINAL PAGE IS OF POOR QUALITY

Figure 13R - Hypothetical Blockage Effect

MAIN CHAMBER TEMPERATURE

28/ 8/90

— ROP model run for hp/tp dia blockage 6/90



ORIGINAL PAGE IS
OF POOR QUALITY

TABLE 6.5.1

ID	PARAMETER DESCRIPTION	TRANSIENT MODEL VARIABLE	SAFD VARIABLE
1	HPFT Radial Accel		PARAM(1)
2	HPFP Balance Cavity Pres.		PARAM(2)
3	HPOT Dis. Pres.	POT2D	PARAM(3)
4	HPOTP Intermediate Seal Purge Pres.		PARAM(4)
5	HPOTP Secondary Seal Drain Pres.		PARAM(5)
6	HPOTP bBoost Pump Dis.Pres.	POD3	PARAM(6)
7	HPOTP Boost Pump Radial		PARAM(7)
8	HPOTP Boost Pump Bearing Coolant Dis. Temp.		PARAM(8)
9	MCC PC	PC1E	PARAM(9)
10	MCC Liner Cavity Pres.		PARAM(10)
11	HPFP Speed (RPM)	ENF2	PARAM(11)
12	HPFT DS T1 A	TFT2D	PARAM(12)
13	HPFT DS T1 B	TFT2D	PARAM(13)
14	HPOT DS T1	TOT2D	PARAM(14)
15	HPOT DS T2	TOT2D	PARAM(15)
16	LPFTP Shaft Speed (RPM)	ENF1	PARAM(16)
17	LPOTP Pump Dis. Pres.,	POD1	PARAM(17)
18	HPFT DIS.PRES.	PFT2D	PARAM(18)
19	HPFTP Coolant Liner Pres.	PTD	PARAM(19)
20	HEX Int. Temp		PARAM(20)
21	HEX Vent Delta Pres.		PARAM(21)
22	OPOV Actuator Position	XOPOV	PARAM(22)
23	FPOV Actuator Position	XFPOV	PARAM(23)
24	Fuel Flowmeter	DW(2)	PARAM(24)

HPOTP DIS PRES

27/ 6/90

——	SENS03	SSME/SAFD	Closed-Loop	Sim., Noz. Rupture Failure (5 lb ox leak)
----	AV2N03	SSME/SAFD	Closed-Loop	Sim., Noz. Rupture Failure (5 lb ox leak)
----	LP1N03	SSME/SAFD	Closed-Loop	Sim., Noz. Rupture Failure (5 lb ox leak)
----	LW1N03	SSME/SAFD	Closed-Loop	Sim., Noz. Rupture Failure (5 lb ox leak)

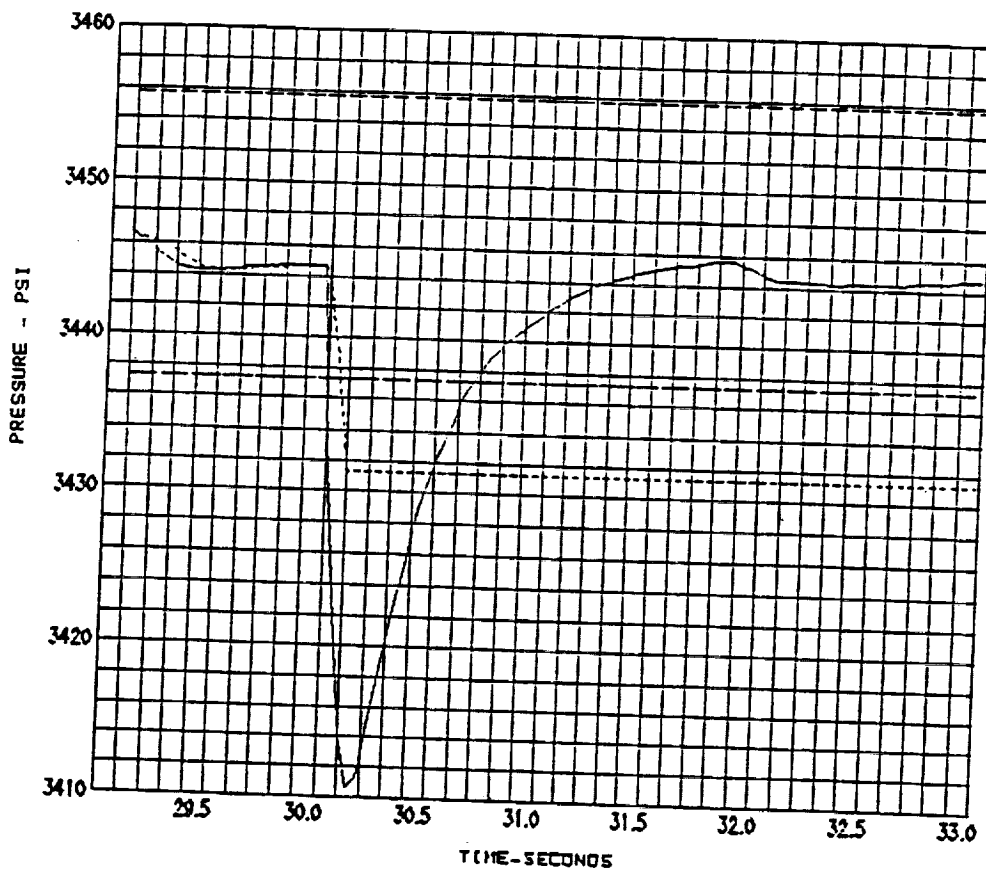


Figure 14A - Closed-Loop Simulation of Leakage: Approach 1

ORIGINAL PAGE IS OF POOR QUALITY

HPOTP BOOST PUMP DIS PRES

27/ 6/90

- SENS06 SSME/SAFD Closed-Loop Sim., Noz. Rupture Failure (5 lb ox leak)
- AV2N06 SSME/SAFD Closed-Loop Sim., Noz. Rupture Failure (5 lb ox leak)
- UP1N06 SSME/SAFD Closed-Loop Sim., Noz. Rupture Failure (5 lb ox leak)
- LWIN06 SSME/SAFD Closed-Loop Sim., Noz. Rupture Failure (5 lb ox leak)

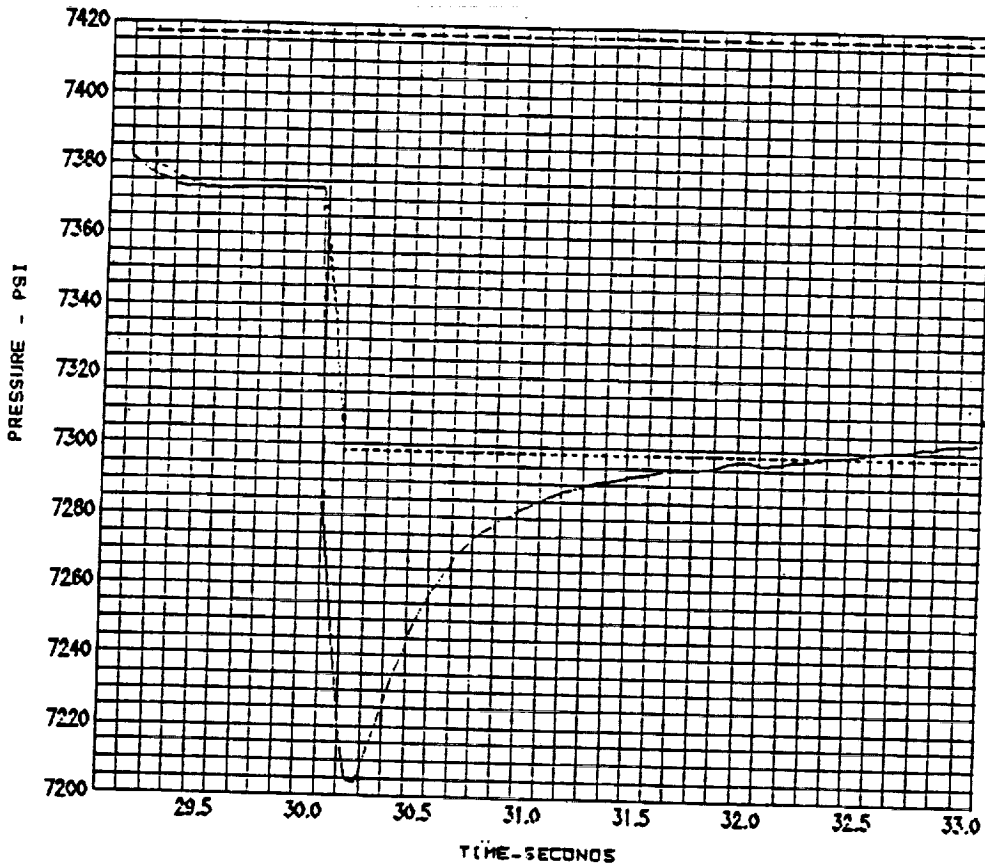


Figure 14B - Closed-Loop Simulation of Leakage: Approach 1

ORIGINAL PAGE IS OF POOR QUALITY

MAIN COMBUSTION CHAMBER (MCC) PC

27/ 6/90

- SENS09 SSME/SAFD Closed-Loop Sim., Noz. Rupture Failure (5 lb ox leak)
- AV2N09 SSME/SAFD Closed-Loop Sim., Noz. Rupture Failure (5 lb ox leak)
- LP1N09 SSME/SAFD Closed-Loop Sim., Noz. Rupture Failure (5 lb ox leak)
- LW1N09 SSME/SAFD Closed-Loop Sim., Noz. Rupture Failure (5 lb ox leak)

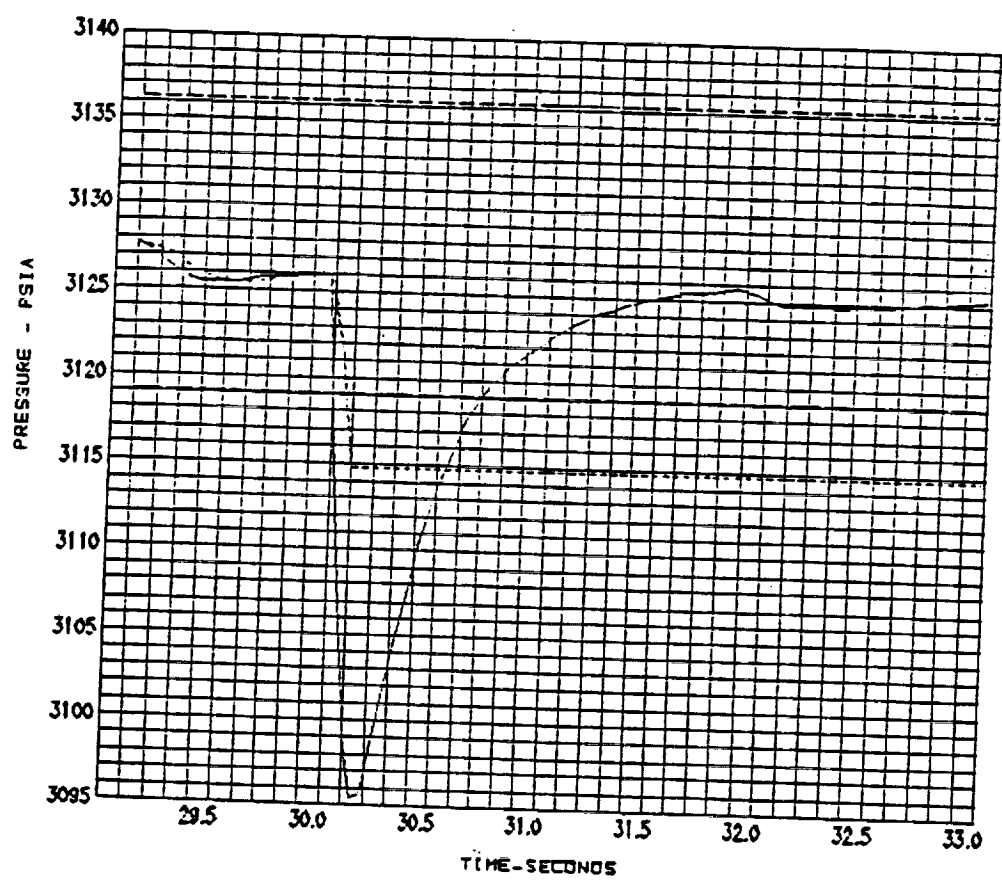


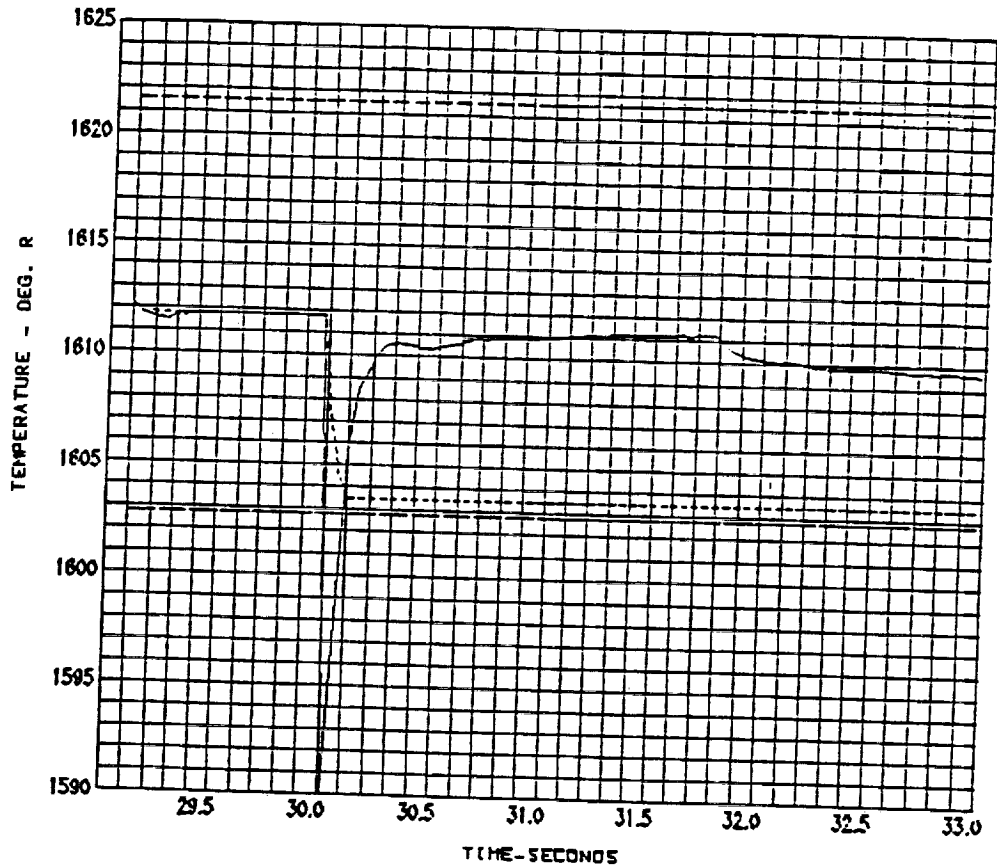
Figure 14C - Closed-Loop Simulation of Leakage: Approach 1

REPLACEMENT PAGE IS OF POOR QUALITY

HIGH PRESSURE FUEL TURBINE (HPFT) DS TEMP2

27/ 6/90

- SENS13 SSME/SAFD Closed-Loop Sim., Noz. Rupture Failure (5 lb ox leak)
- AV2N13 SSME/SAFD Closed-Loop Sim., Noz. Rupture Failure (5 lb ox leak)
- UP1N13 SSME/SAFD Closed-Loop Sim., Noz. Rupture Failure (5 lb ox leak)
- SSME/SAFD Closed-Loop Sim., Noz. Rupture Failure (5 lb ox leak)



TIME-SECONDS
 Figure 14D - Closed-Loop Simulation
 of Leakage: Approach 1

HIGH PRESSURE OX TURBINE DS TEMP2

27/ 6/90

- SENS15 SSME/SAFD Closed-Loop Sim., Noz. Rupture Failure (5 lb ox leak)
- AV2N15 SSME/SAFD Closed-Loop Sim., Noz. Rupture Failure (5 lb ox leak)
- LP1N15 SSME/SAFD Closed-Loop Sim., Noz. Rupture Failure (5 lb ox leak)
- SSME/SAFD Closed-Loop Sim., Noz. Rupture Failure (5 lb ox leak)

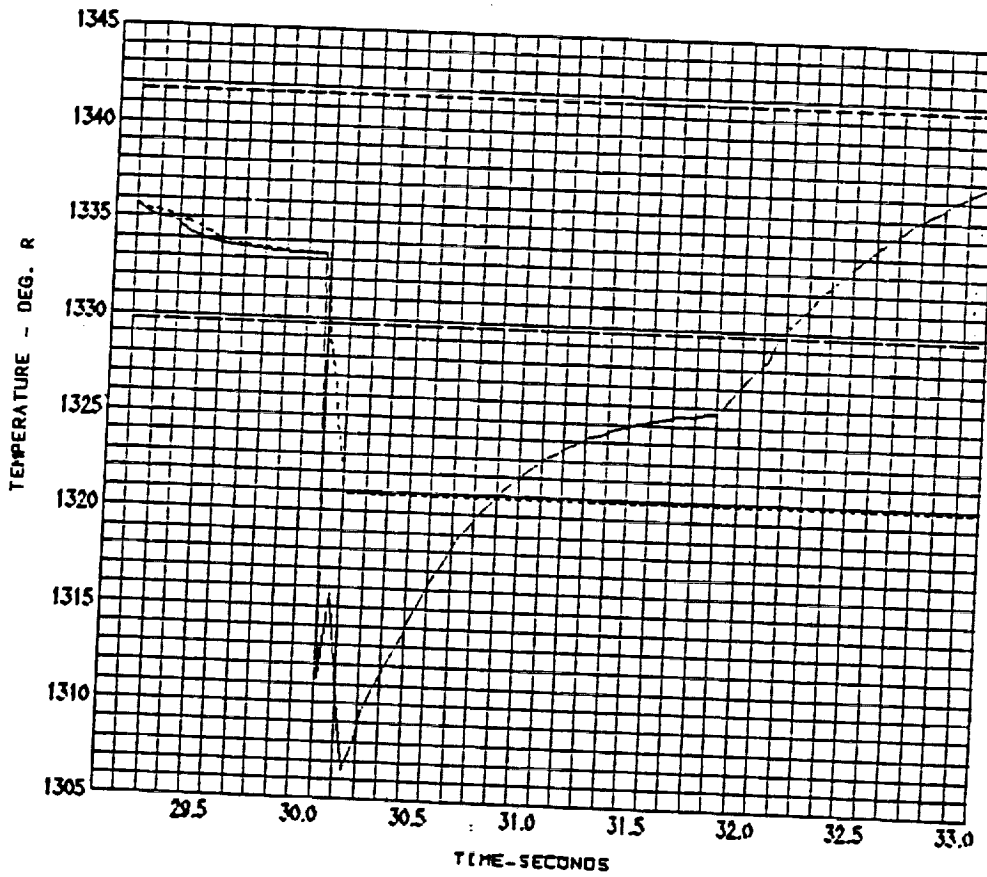


Figure 14E - Closed-Loop Simulation of Leakage: Approach 1

ORIGINAL PAGE IS OF POOR QUALITY

LPOP DIS PRES

27/ 6/90

- SENS17 SSME/SAFD Closed-Loop Sim., Noz. Rupture Failure (5 lb ox leak)
- - - - AV2H17 SSME/SAFD Closed-Loop Sim., Noz. Rupture Failure (5 lb ox leak)
- · — · — UP1N17 SSME/SAFD Closed-Loop Sim., Noz. Rupture Failure (5 lb ox leak)
- SSME/SAFD Closed-Loop Sim., Noz. Rupture Failure (5 lb ox leak)

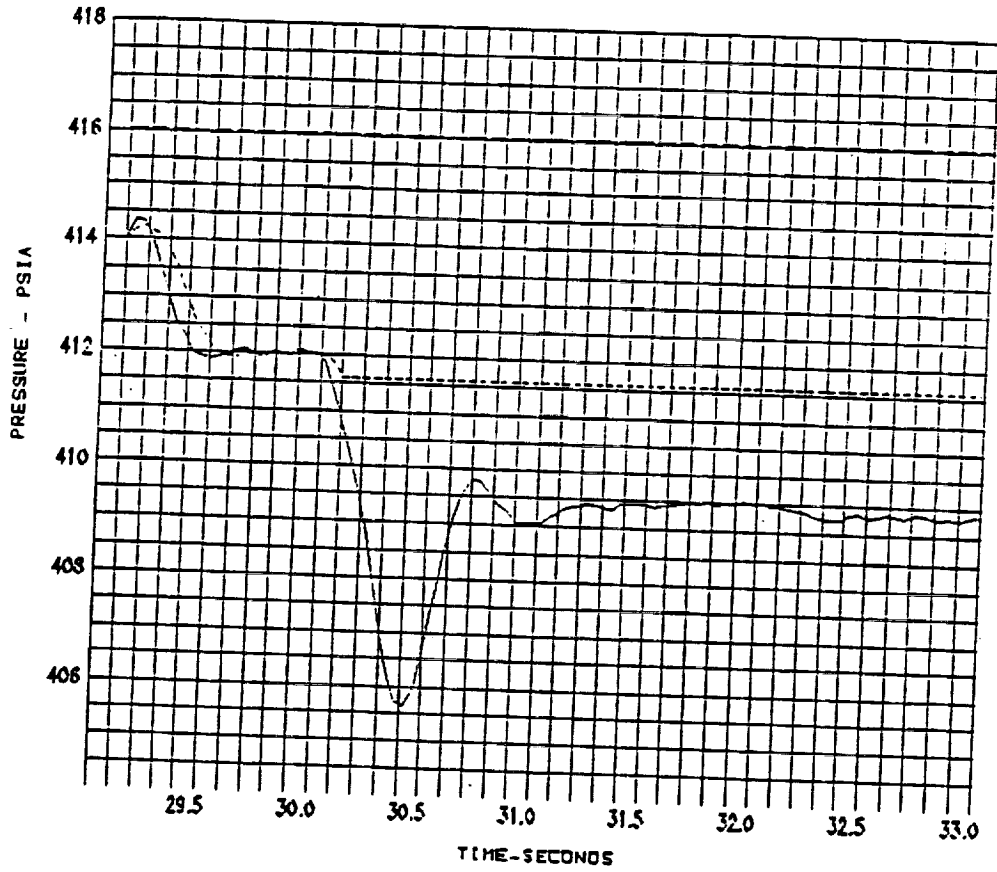


Figure 14F - Closed-Loop Simulation of Leakage: Approach 1

ORIGINAL PAGE IS OF POOR QUALITY

HPFTP DIS PRES

27/ 6/90 1

- SENS18 SSME/SAFD Closed-Loop Sim., Noz. Rupture Failure (5 lb ox leak)
- - - - AV2N18 SSME/SAFD Closed-Loop Sim., Noz. Rupture Failure (5 lb ox leak)
- CP1N18 SSME/SAFD Closed-Loop Sim., Noz. Rupture Failure (5 lb ox leak)
- SSME/SAFD Closed-Loop Sim., Noz. Rupture Failure (5 lb ox leak)

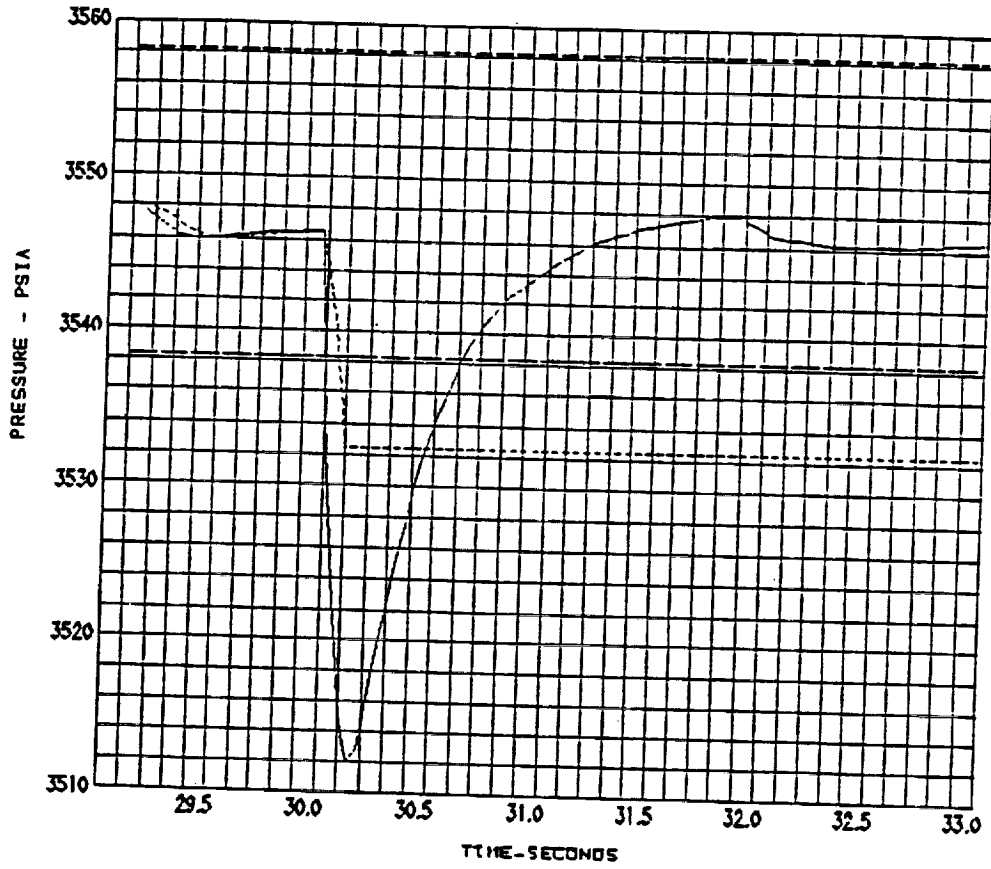


Figure 14G - Closed-Loop Simulation of Leakage: Approach 1

HPFTP COOL LNR PRES

27/ 6/90 12

- SENS19 SSME/SAFD Closed-Loop Sim., Noz. Rupture Failure (5 lb oz leak)
- AV2N19 SSME/SAFD Closed-Loop Sim., Noz. Rupture Failure (5 lb oz leak)
- UP1N19 SSME/SAFD Closed-Loop Sim., Noz. Rupture Failure (5 lb oz leak)
- SSME/SAFD Closed-Loop Sim., Noz. Rupture Failure (5 lb oz leak)

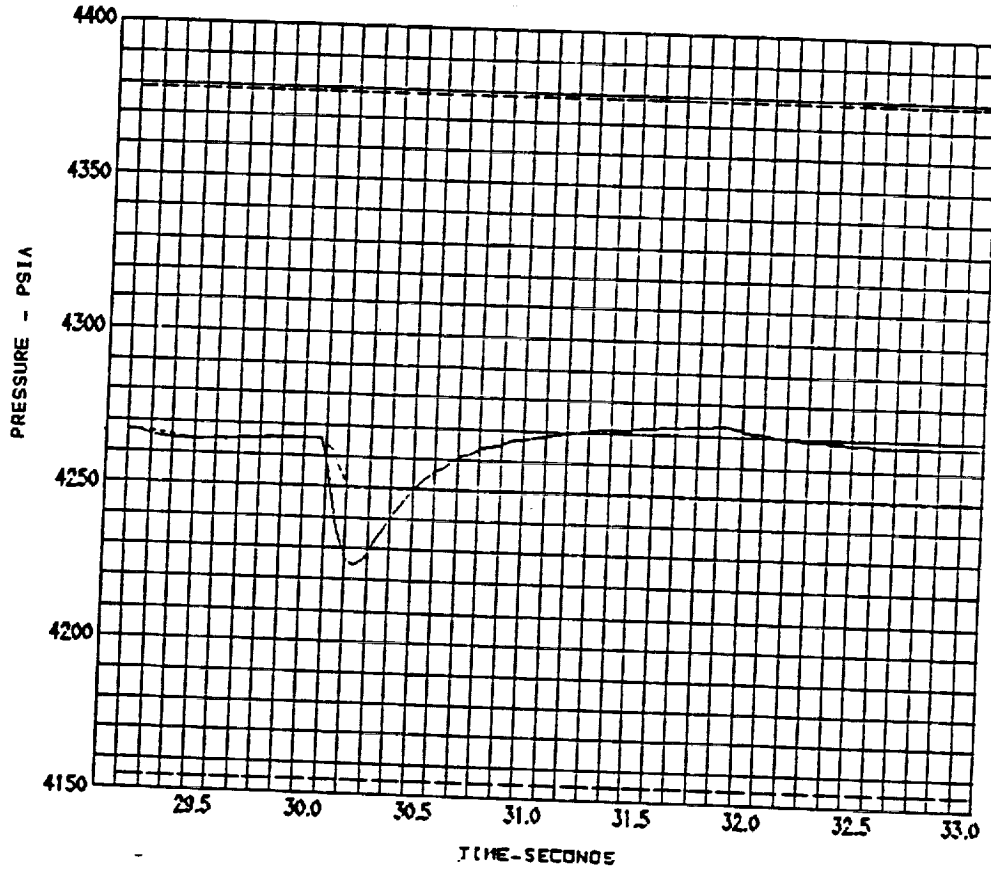


Figure 14H - Closed-Loop Simulation of Leakage: Approach 1

FPOV ACT POSITION

27/ 6/90

- SENS23 SSME/SAFD Closed-Loop Sim., Noz. Rupture Failure (5 lb ox leak)
- AV2N23 SSME/SAFD Closed-Loop Sim., Noz. Rupture Failure (5 lb ox leak)
- LP1N23 SSME/SAFD Closed-Loop Sim., Noz. Rupture Failure (5 lb ox leak)
- SSME/SAFD Closed-Loop Sim., Noz. Rupture Failure (5 lb ox leak)

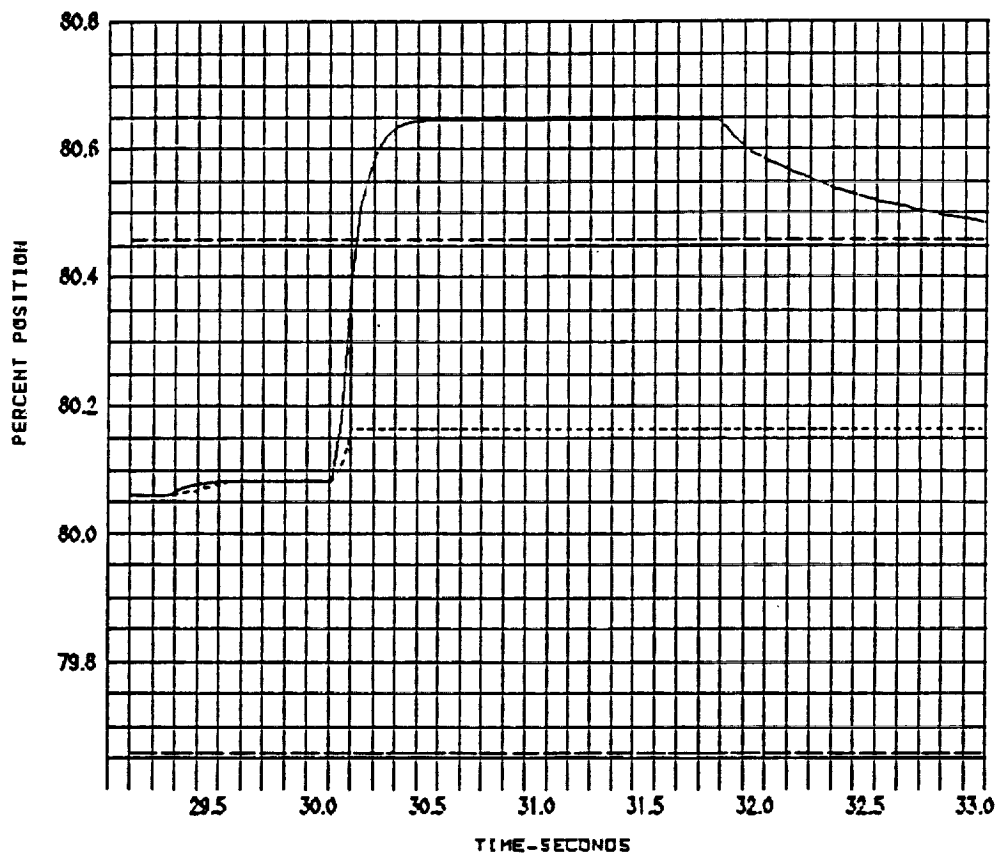


Figure 14I - Closed-Loop Simulation of Leakage: Approach 1

ORIGINAL PAGE IS OF POOR QUALITY

MAIN COMBUSTION CHAMBER (MCC) PC

5/7/90 3

- SENS01 SSME/SAFD Closed-Loop Sim., HPFT Dis Flow Blockage Failure
- AV2101 SSME/SAFD Closed-Loop Sim., HPFT Dis Flow Blockage Failure
- UP2101 SSME/SAFD Closed-Loop Sim., HPFT Dis Flow Blockage Failure
- LW2101 SSME/SAFD Closed-Loop Sim., HPFT Dis Flow Blockage Failure

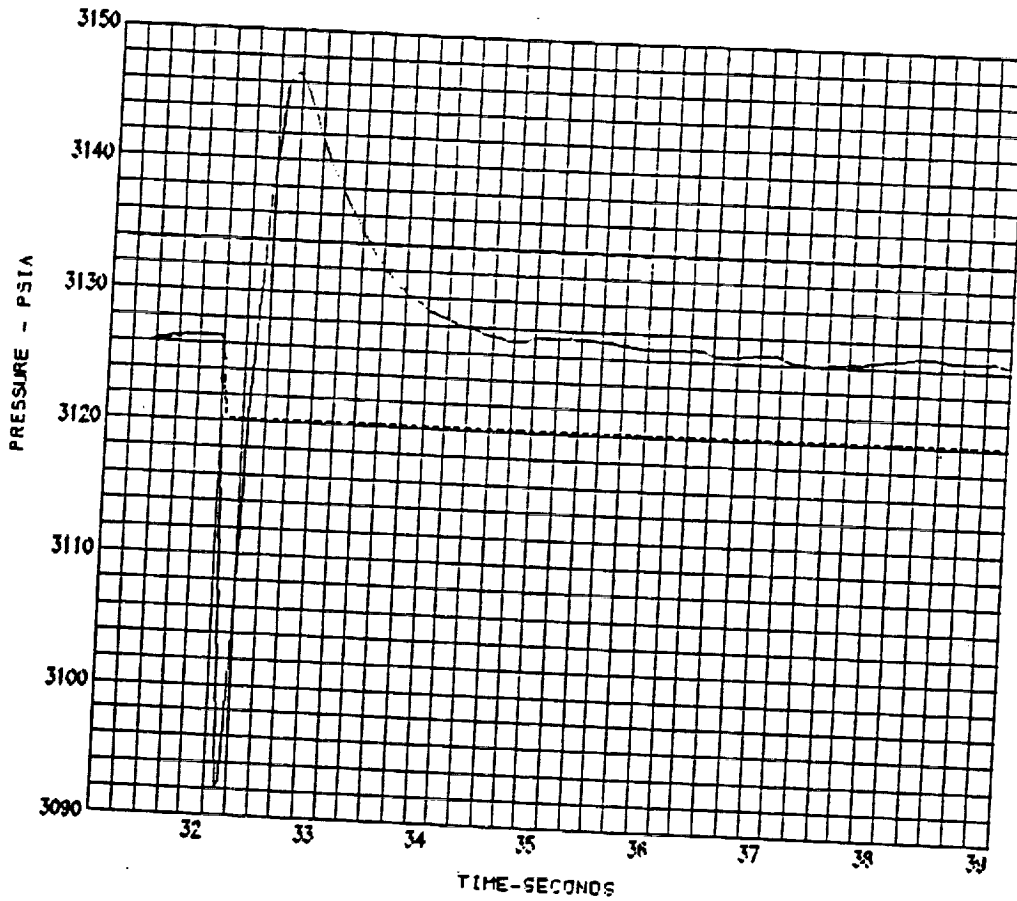


Figure 15A - Closed-Loop Simulation of blockage Approach 2

ORIGINAL PAGE IS OF POOR QUALITY

HPFTP DIS PRES

5/7/90 11

- SENS18 SSME/SAFD Closed-Loop Sim., HPFT Dis Flow Blockage Failure
- AV2N13 SSME/SAFD Closed-Loop Sim., HPFT Dis Flow Blockage Failure
- UP2N13 SSME/SAFD Closed-Loop Sim., HPFT Dis Flow Blockage Failure
- UNZM3⁹ SSME/SAFD Closed-Loop Sim., HPFT Dis Flow Blockage Failure

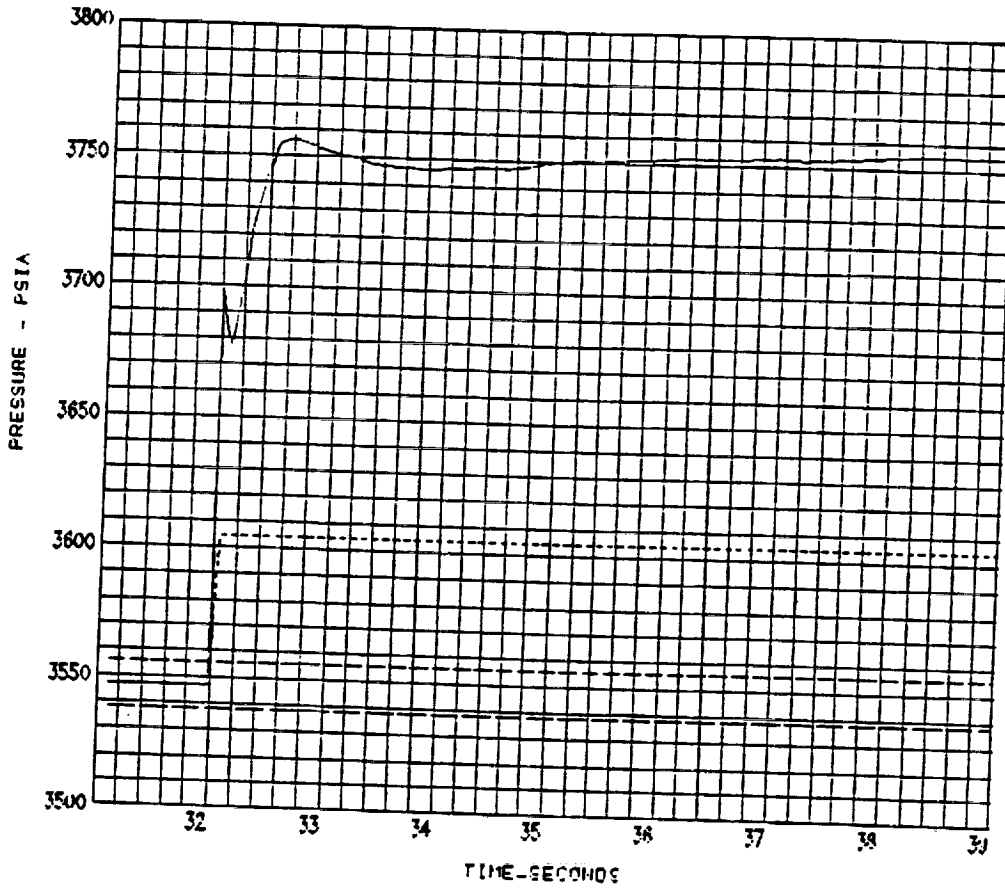


Figure 158 - Closed-Loop Simulation of blockage Approach 2

ORIGINAL PAGE IS OF POOR QUALITY

HPFTP COOL LNR PRES

5/7/90

- SENS19 SSME/SAFD Closed-Loop Sim., HPFT Dis Flow Blockage Failure
- AV2N19 SSME/SAFD Closed-Loop Sim., HPFT Dis Flow Blockage Failure
- UP2N19 SSME/SAFD Closed-Loop Sim., HPFT Dis Flow Blockage Failure
- LV2N19 SSME/SAFD Closed-Loop Sim., HPFT Dis Flow Blockage Failure

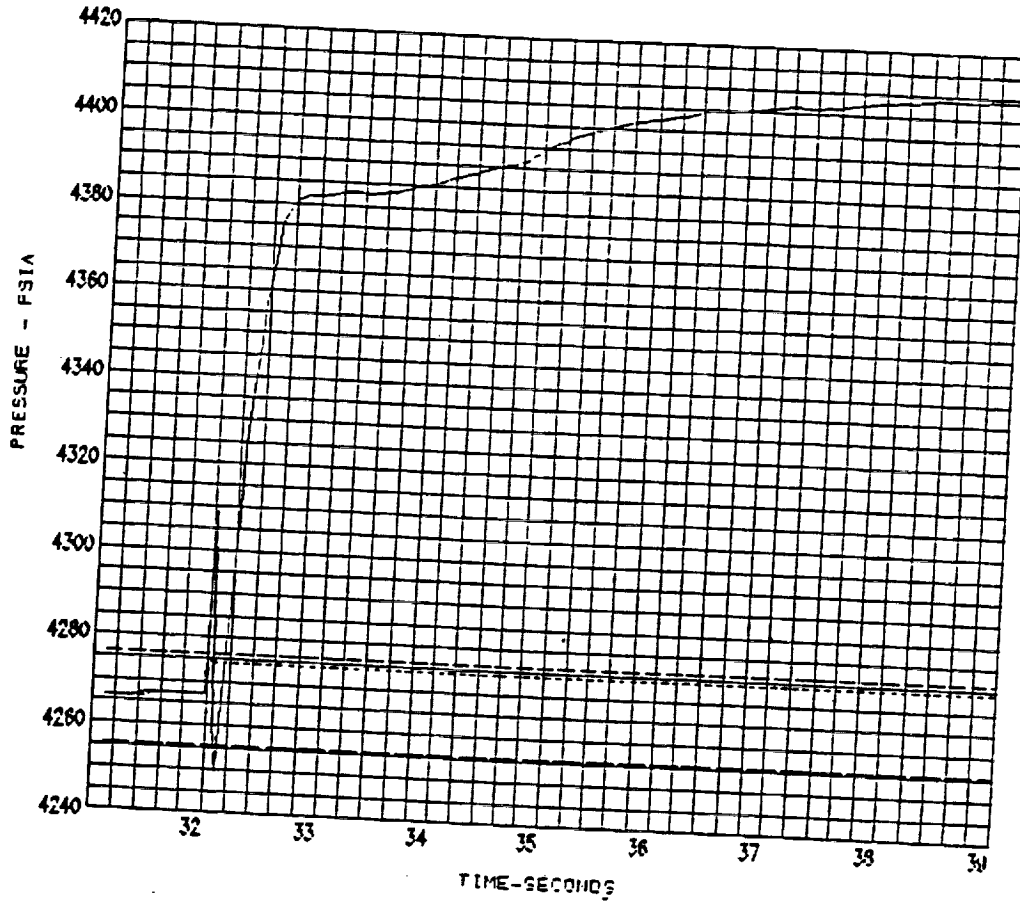


Figure 15C - Closed-Loop Simulation of blockage Approach 2

HIGH PRESSURE FUEL TURBINE (HPFT) DS TEMP1

5/7/90 5

———	SENS12	SSME/SAFD Closed-Loop Sim., HPFT Dis Flow Blockage Failure
----	AV2N12	SSME/SAFD Closed-Loop Sim., HPFT Dis Flow Blockage Failure
----	UP2N12	SSME/SAFD Closed-Loop Sim., HPFT Dis Flow Blockage Failure
----	LN2A20	SSME/SAFD Closed-Loop Sim., HPFT Dis Flow Blockage Failure

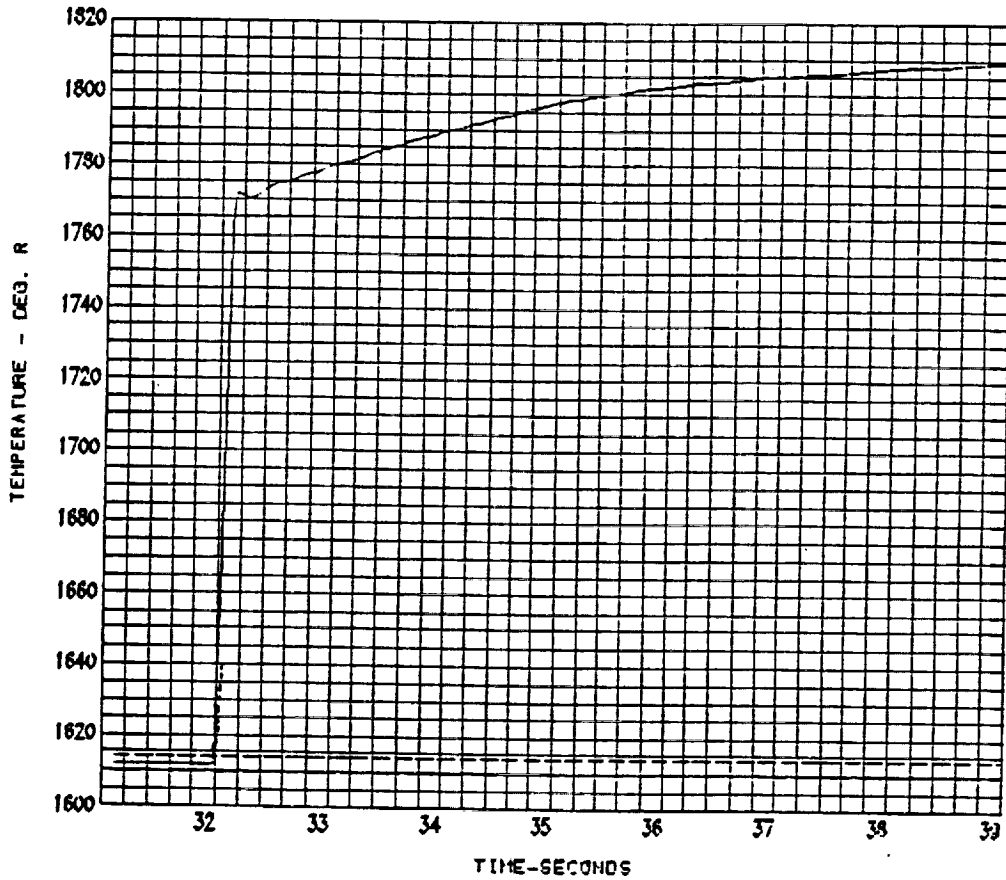


Figure 15D - Closed-Loop Simulation of blockage Approach 2

HIGH PRESSURE OX TURBINE DS TEMPI

5/7/80

- SENS14 SSME/SAFD Closed-Loop Sim., HPFT Dis Flow Blockage Failure
- AV2114 SSME/SAFD Closed-Loop Sim., HPFT Dis Flow Blockage Failure
- UP2114 SSME/SAFD Closed-Loop Sim., HPFT Dis Flow Blockage Failure
- *LW2114* SSME/SAFD Closed-Loop Sim., HPFT Dis Flow Blockage Failure

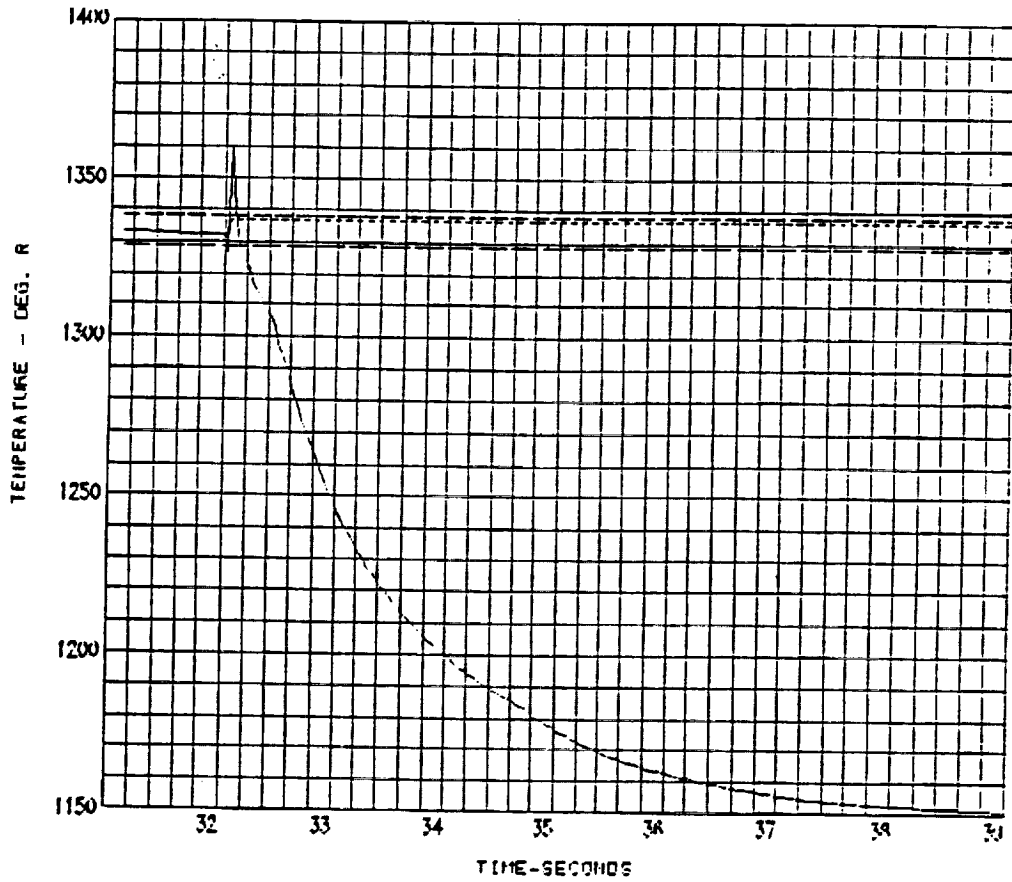


Figure 15E - Closed-Loop Simulation of blockage Approach 2

HIGH PRESSURE FUEL PUMP (HPFP) SPEED

5/7/90

- SENS11 SSME/SAFD Closed-Loop Sim., HPFT Dis Flow Blockage Failure
- AV2N11 SSME/SAFD Closed-Loop Sim., HPFT Dis Flow Blockage Failure
- UP2N11 SSME/SAFD Closed-Loop Sim., HPFT Dis Flow Blockage Failure
- LW2N11 SSME/SAFD Closed-Loop Sim., HPFT Dis Flow Blockage Failure

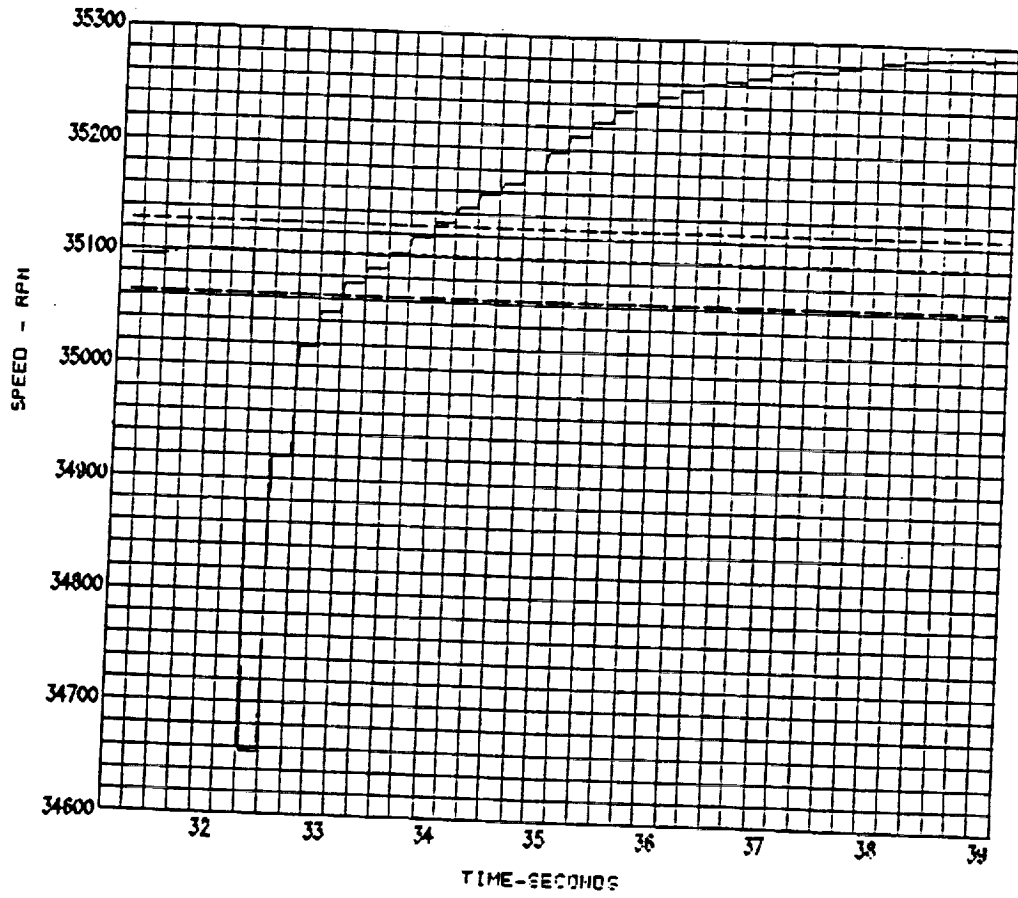


Figure 15F - Closed-Loop Simulation of blockage Approach 2

ORIGINAL PAGE IS OF POOR QUALITY

LPFTP SHAFT SPEED

5/7/90 3

- SENS16 SSME/SAFD Closed-Loop Sim., HPFT Dis Flow Blockage Failure
- - - - AV2N16 SSME/SAFD Closed-Loop Sim., HPFT Dis Flow Blockage Failure
- · — · — UP2N16 SSME/SAFD Closed-Loop Sim., HPFT Dis Flow Blockage Failure
- WZ2N16* SSME/SAFD Closed-Loop Sim., HPFT Dis Flow Blockage Failure

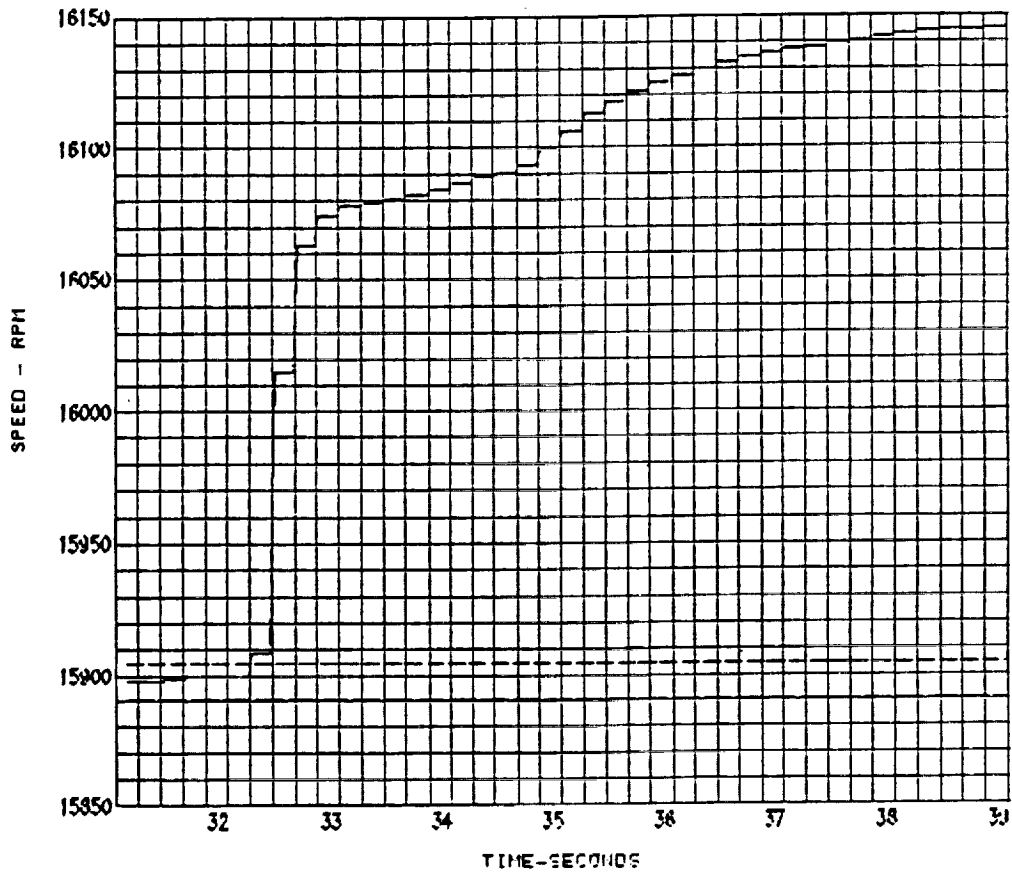


Figure 15G - Closed-Loop Simulation of blockage: Approach 2

ORIGINAL PAGE IS OF POOR QUALITY

FUEL FLOWMETER

5/7/90 1.

- SENS24 SSME/SAFD Closed-Loop Sim., HPFT Dis Flow Blockage Failure
- - - - AV2N24 SSME/SAFD Closed-Loop Sim., HPFT Dis Flow Blockage Failure
- - - - LP2N24 SSME/SAFD Closed-Loop Sim., HPFT Dis Flow Blockage Failure
- LN2N24 SSME/SAFD Closed-Loop Sim., HPFT Dis Flow Blockage Failure

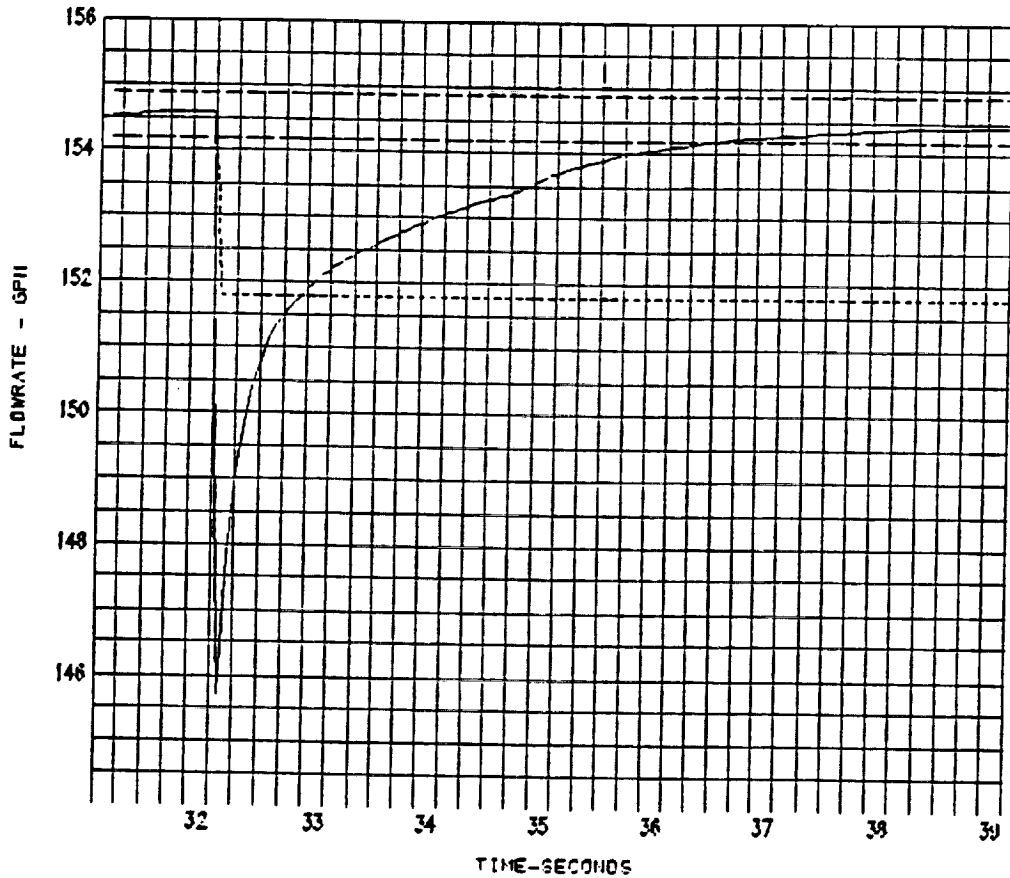


Figure 15H - Closed-Loop Simulation of blockage Approach 2

FPOV ACT POSITION

———— SENS23	SSME/SAFD Closed-Loop Sim., HPFT Dis Flow Blockage Failure
----- AV2N23	SSME/SAFD Closed-Loop Sim., HPFT Dis Flow Blockage Failure
----- UP2N23	SSME/SAFD Closed-Loop Sim., HPFT Dis Flow Blockage Failure
----- ZN2N23	SSME/SAFD Closed-Loop Sim., HPFT Dis Flow Blockage Failure

5/7/90 4

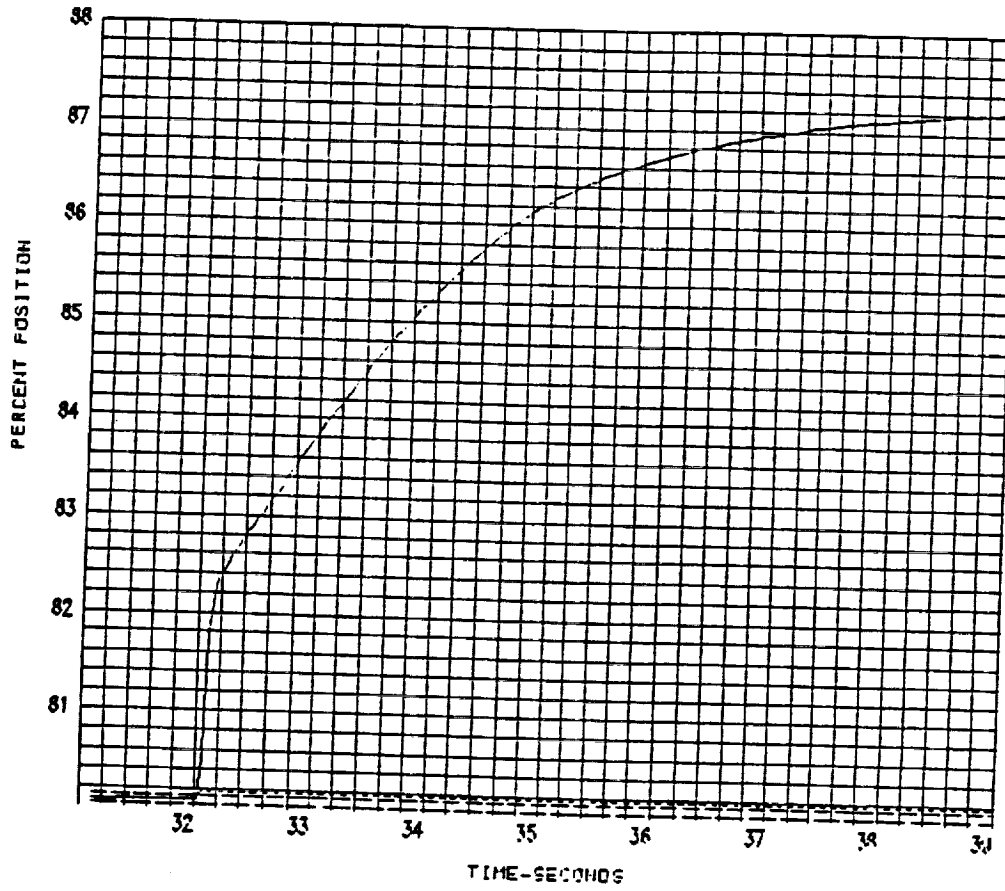
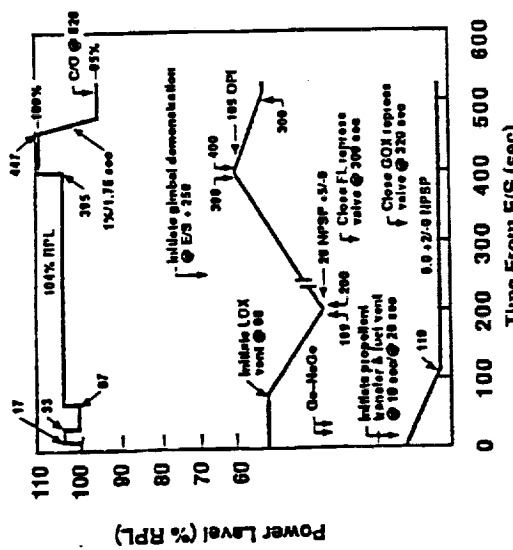


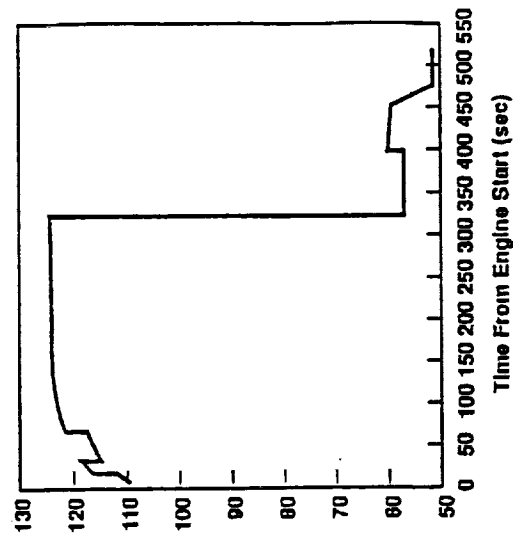
Figure 151 - Closed-Loop Simulation of blockage Approach 2

ORIGINAL PAGE IS OF POOR QUALITY

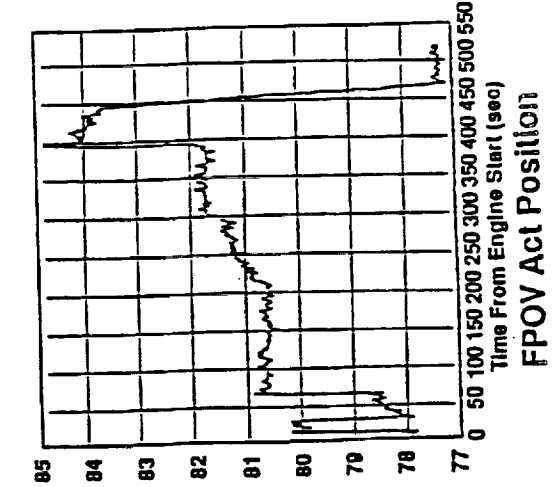
Effects of GOX & Fuel Repressurization Valve Closures



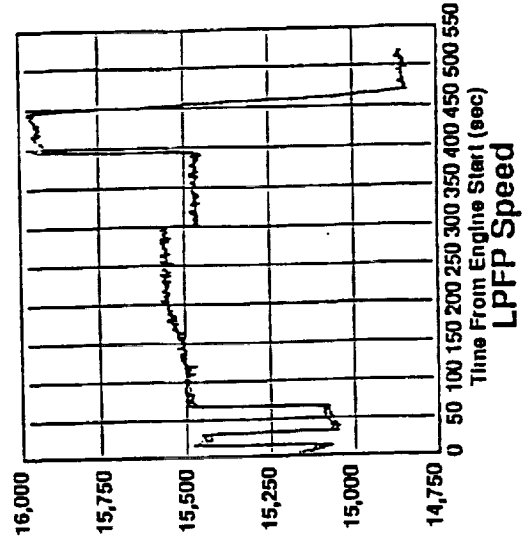
Engine 2019 - Test 901-551 Thrust Profile



HEX Venturi Delta Pressure



FPOV Act Position

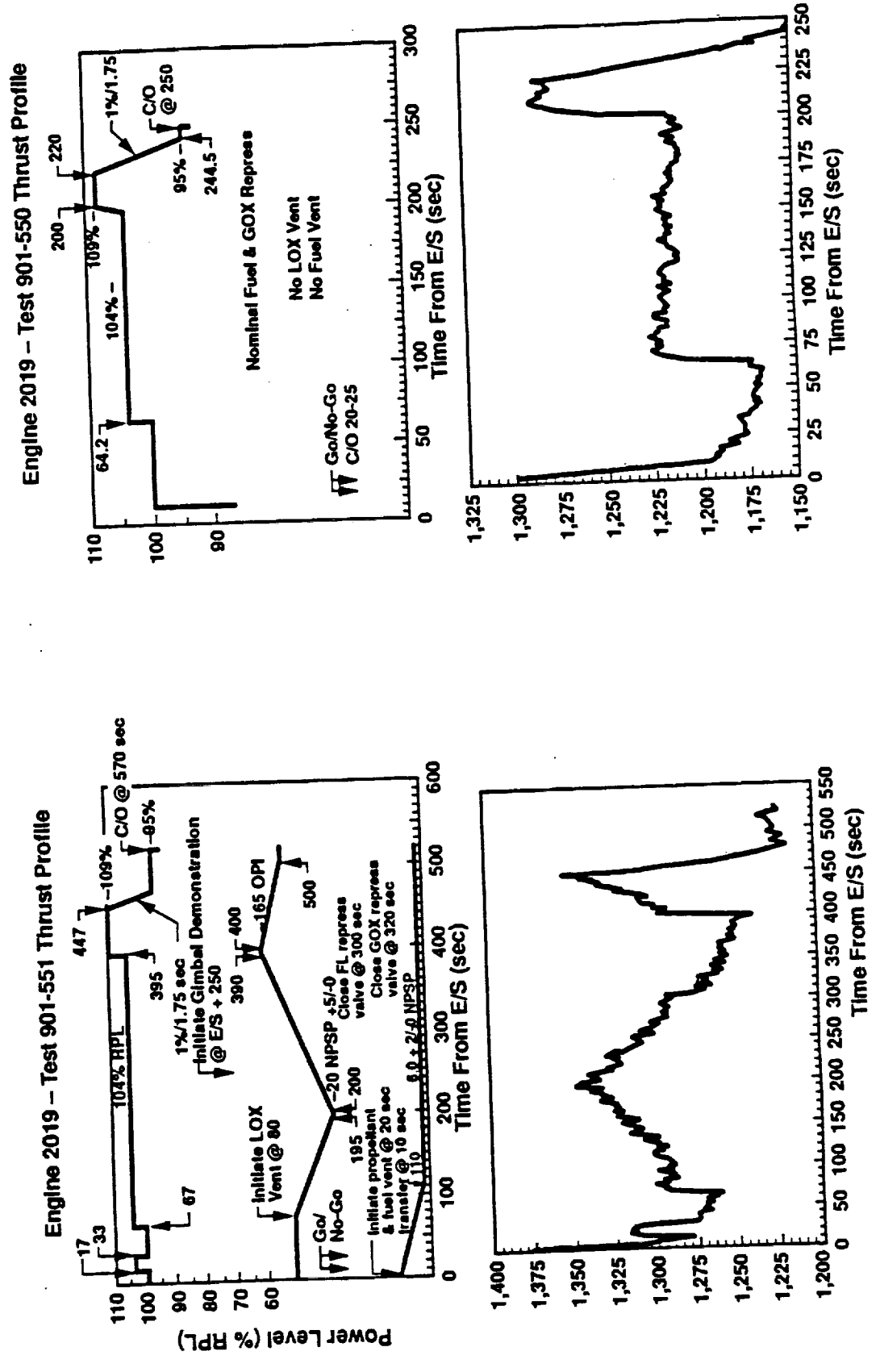


LPFP Speed

ORIGINAL PAGE IS OF POOR QUALITY

Effects of Venting/Repressurization

FIGURE 17



ORIGINAL PAGE IS OF POOR QUALITY

FIGURE 18A

Nonlinear Behavior HPOT Turbine Discharge Temperature Channel A

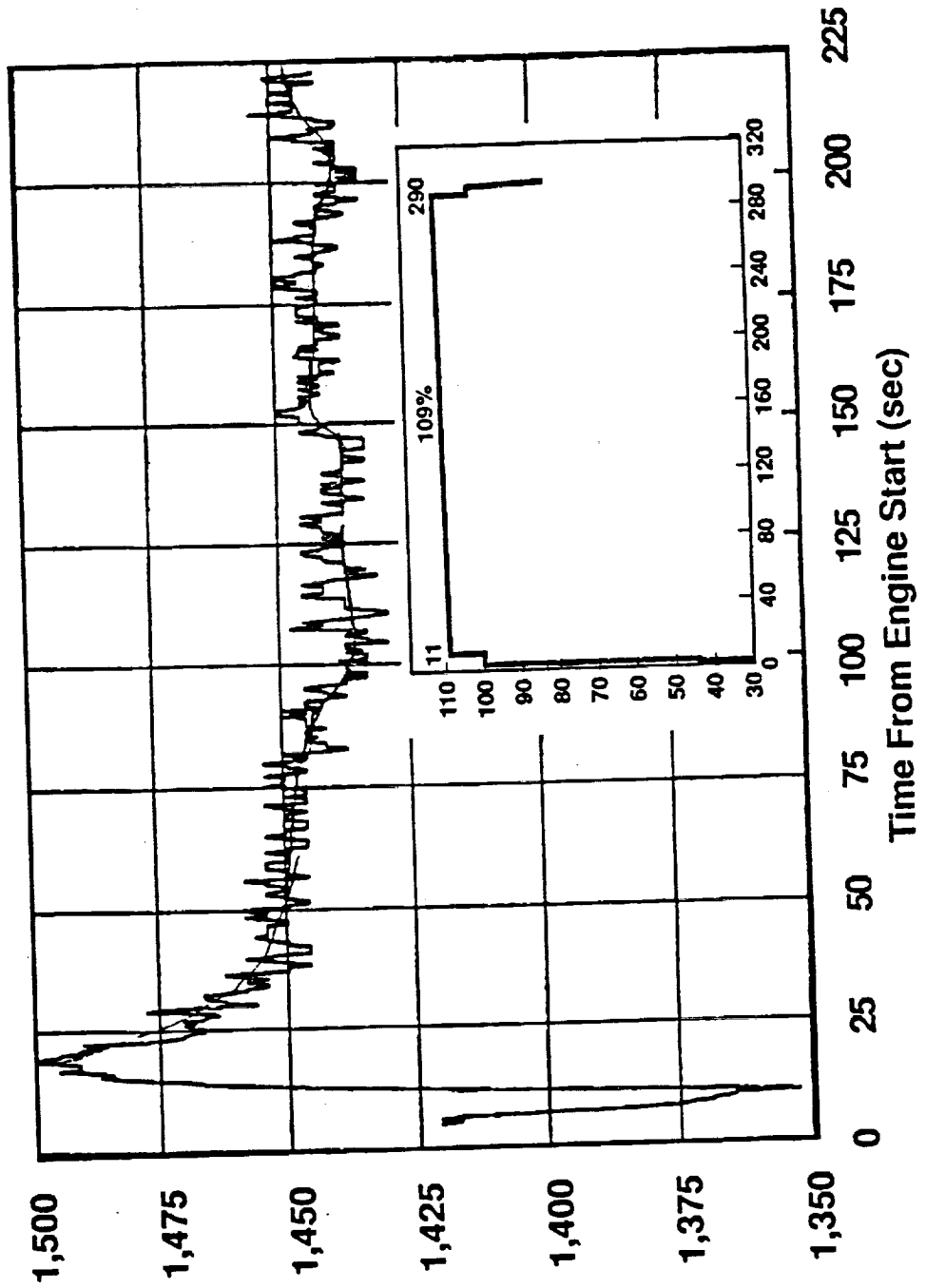


Figure 188

Nonlinear Behavior HPOT Turbine Discharge Temperature Channel B

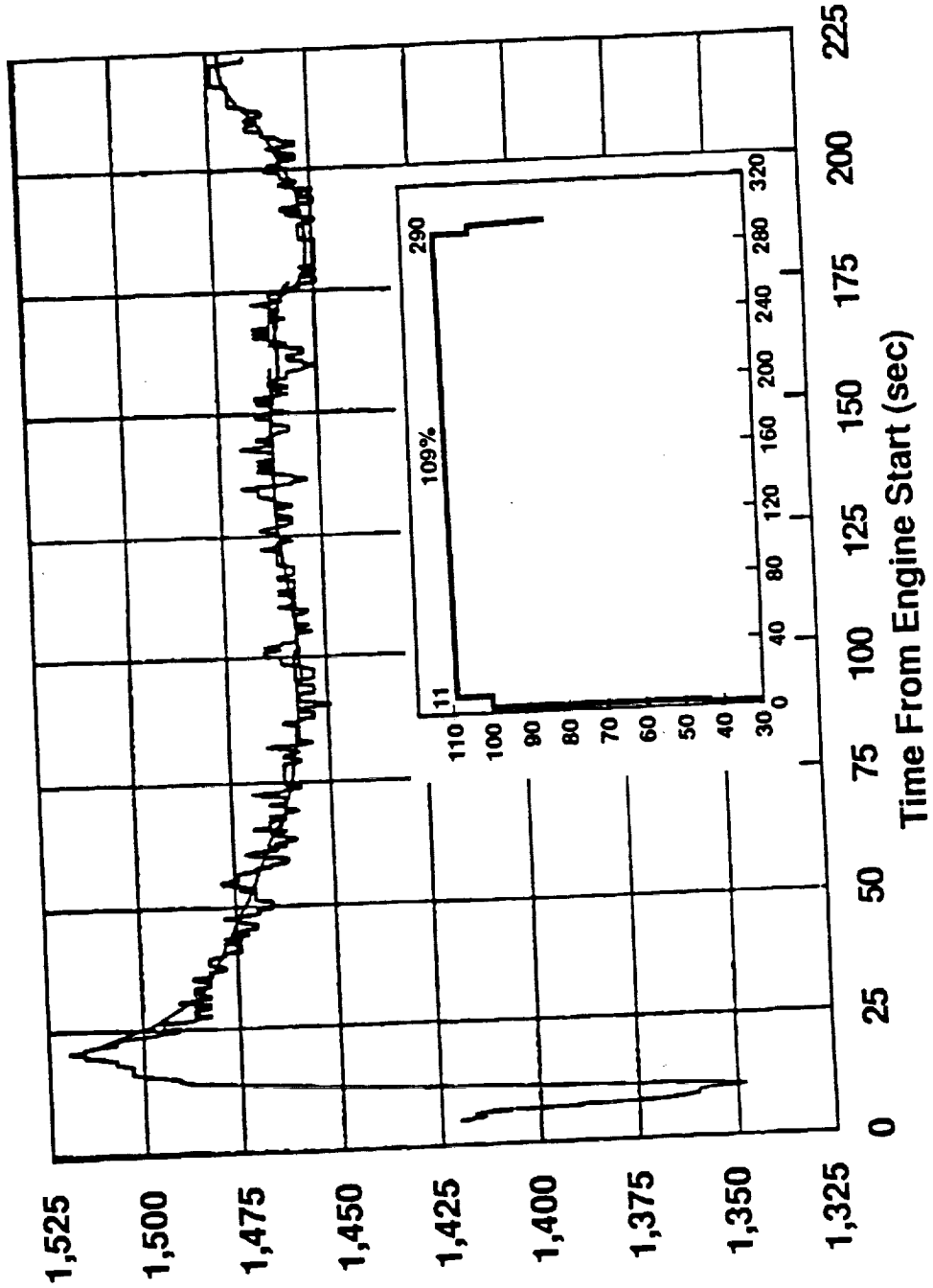


FIGURE 18C

Nonlinear Behavior MCC Liner Cavity Pressure

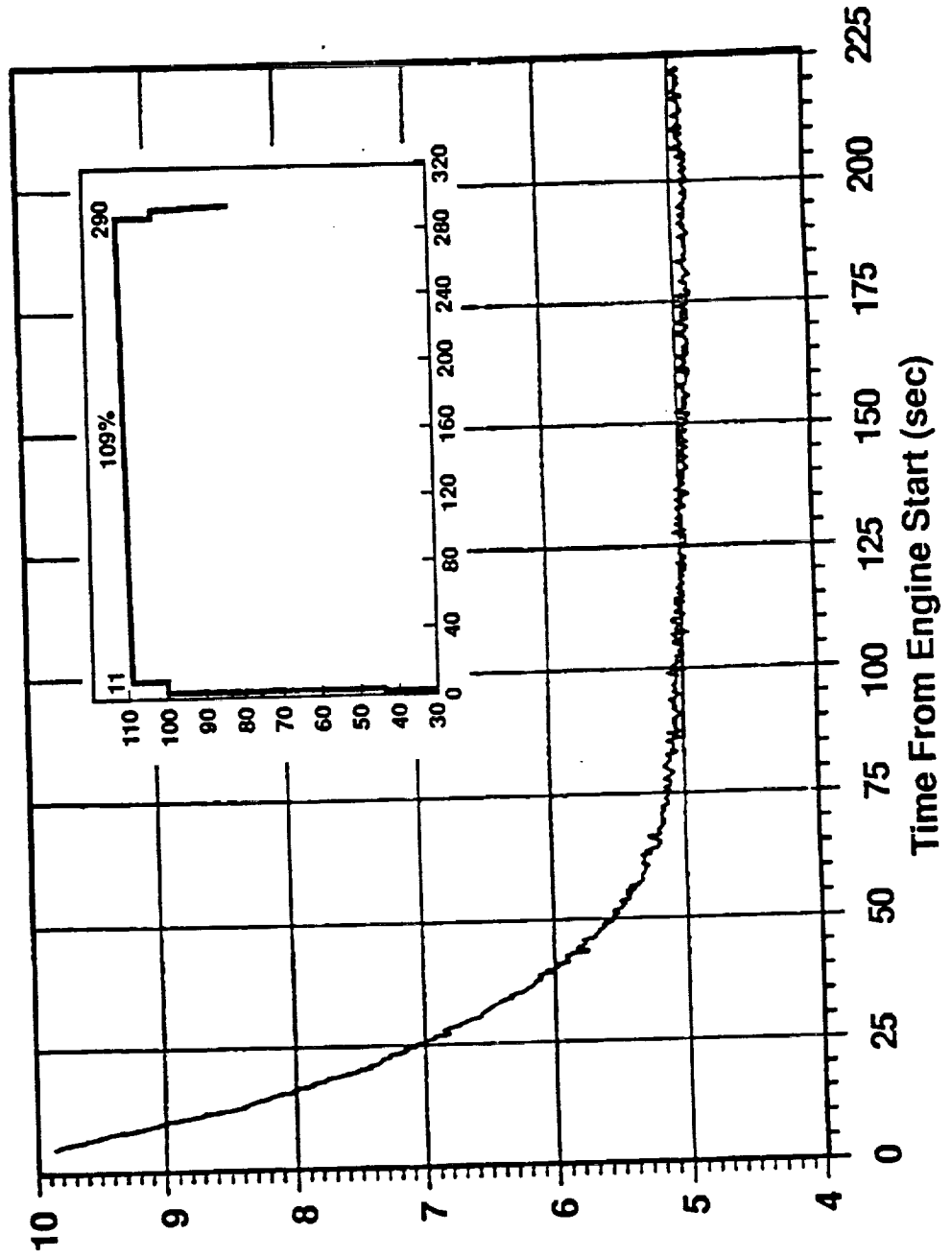


FIGURE 18D

Nonlinear Behavior HPOT Seal Cavity Pressure

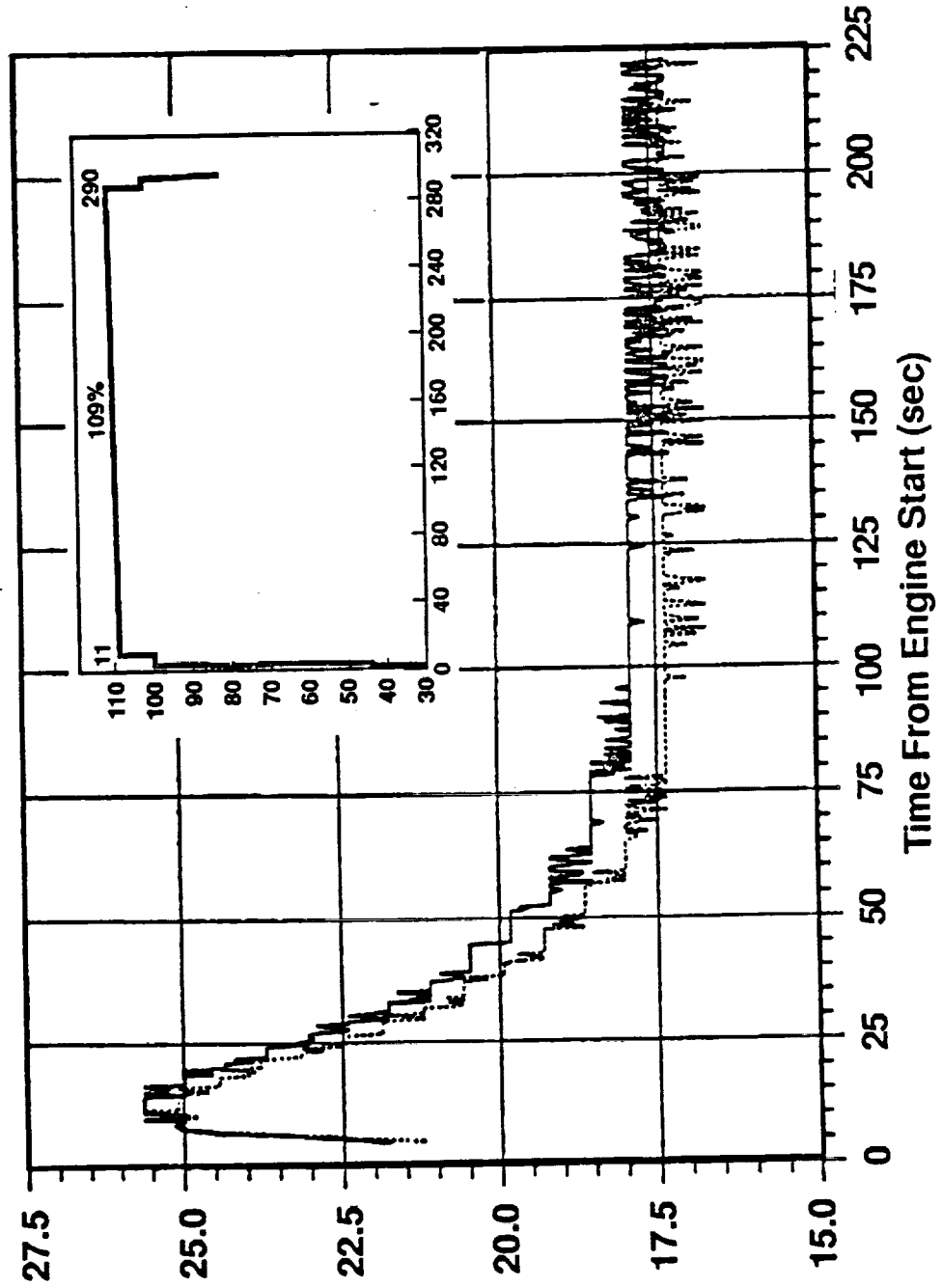


Figure 18E

Nonlinear Behavior HPOP IMSL Purge Pressure

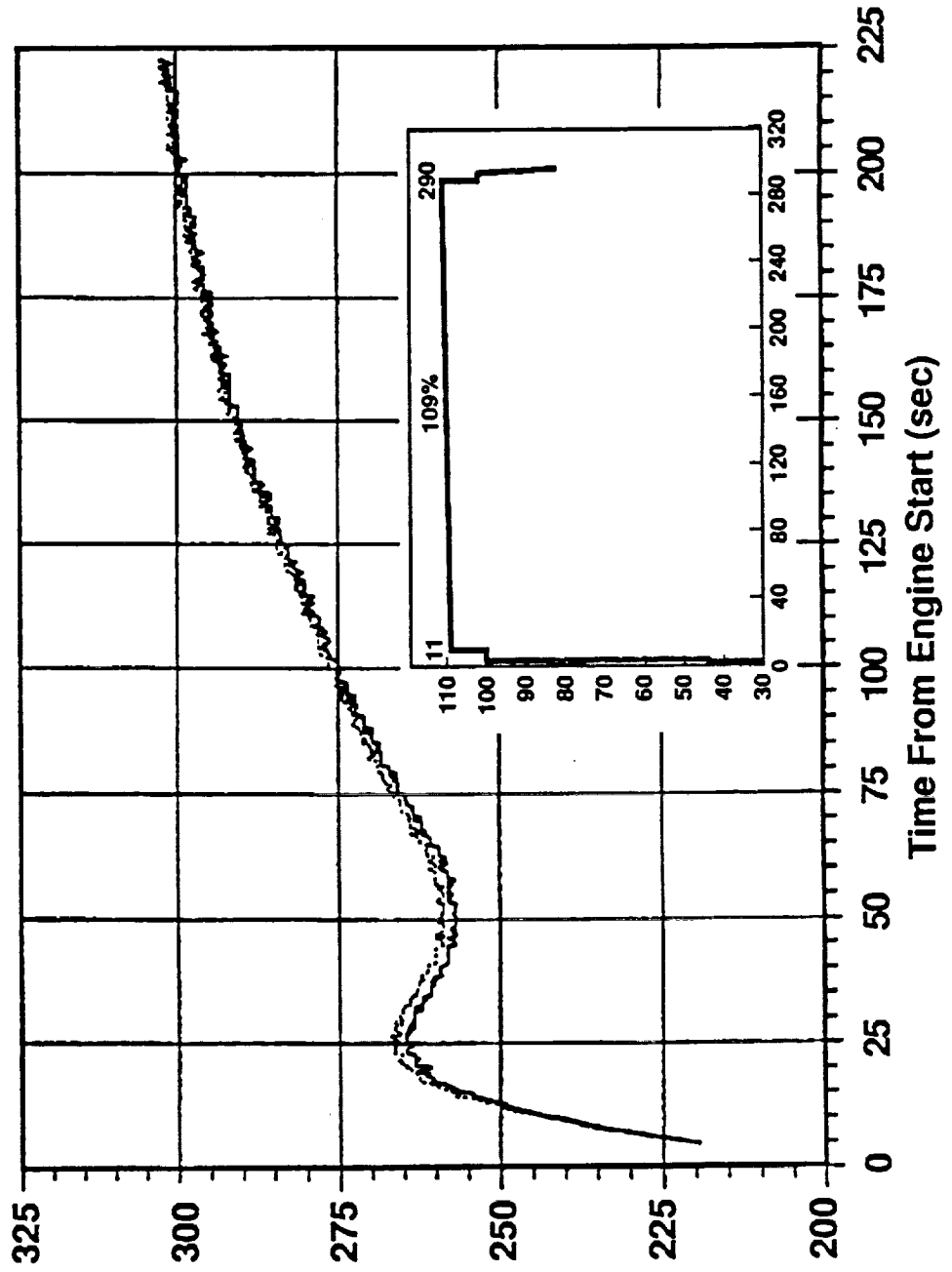
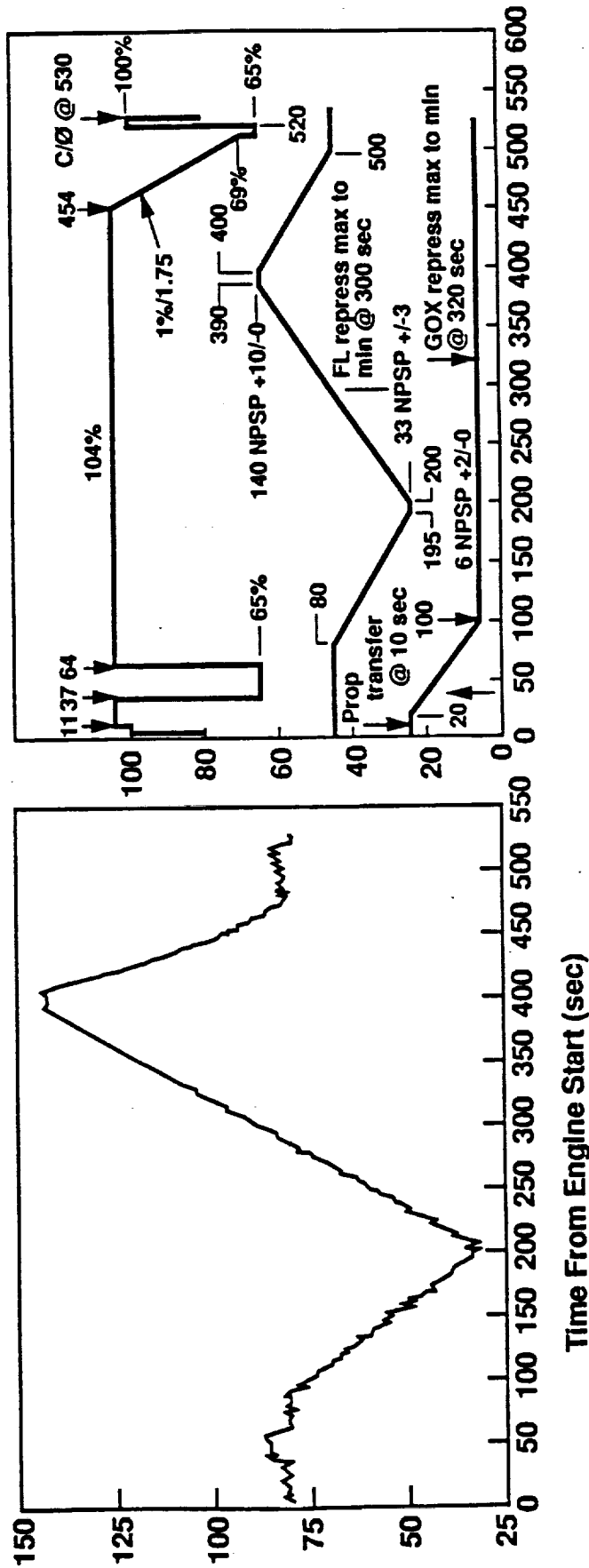


FIGURE 19

LOX Venting/Repressurization Profile Planned vs Achieved



Thrust Profile
Engine 0213 - Test 904-076

2332 Eng LOX Inlet NPSP

FIGURE 20

Advanced Fault Detection

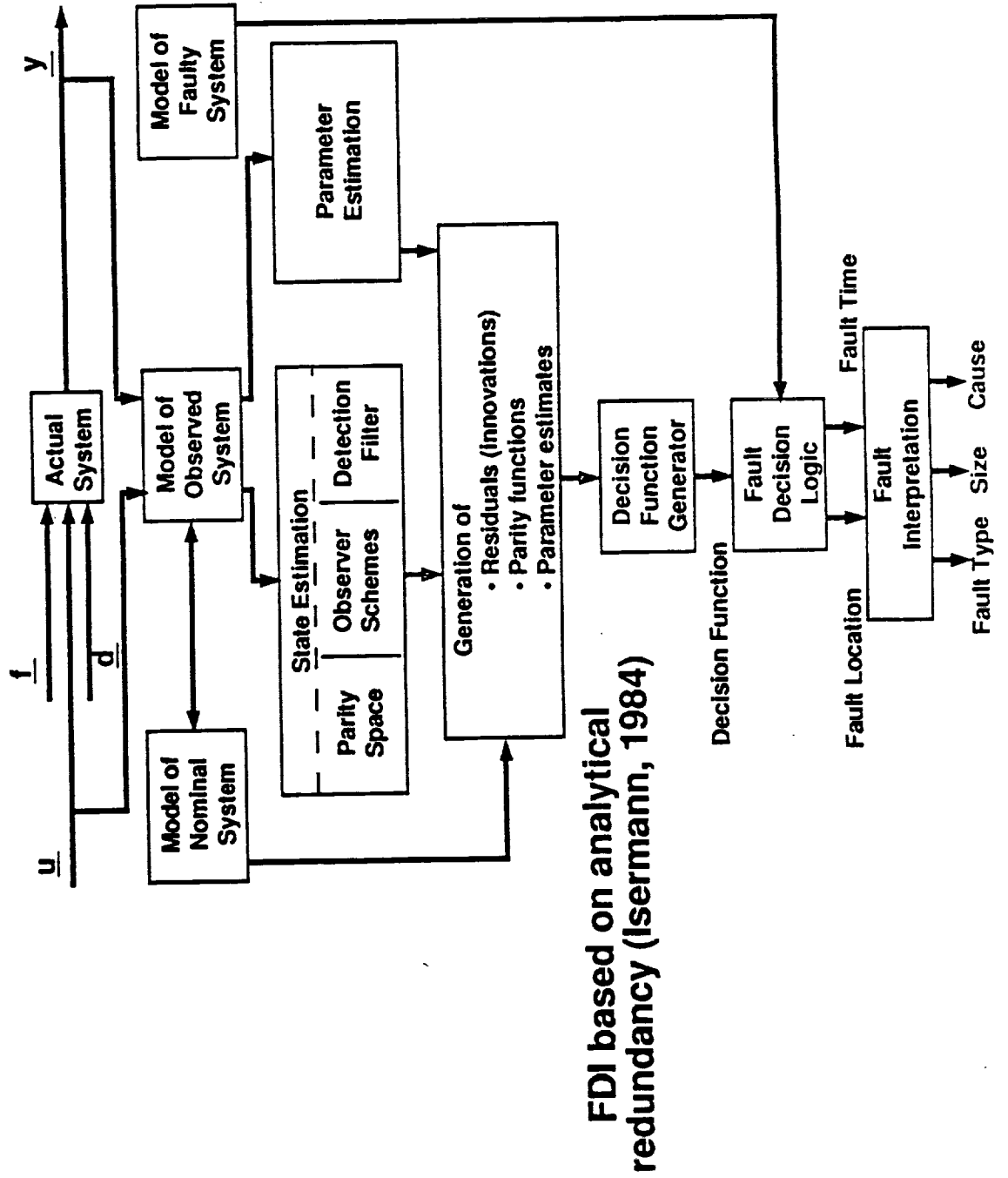


FIGURE 21

SSME Flight 51F HPFT Discharge Temperature Sensor Failure Engine Was Shut Down

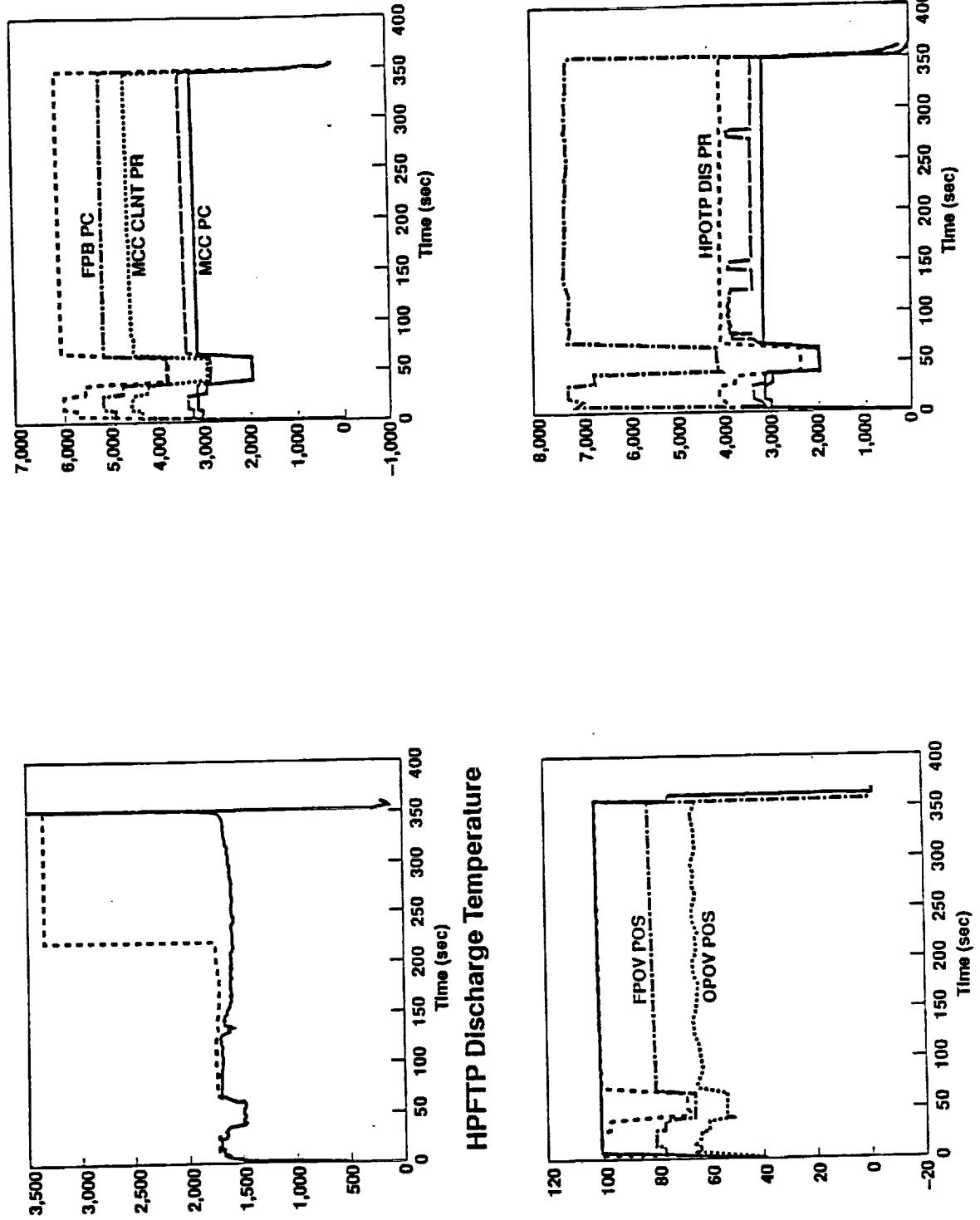


FIGURE 22

Sensor Failure Detection & Identification Simulated Data

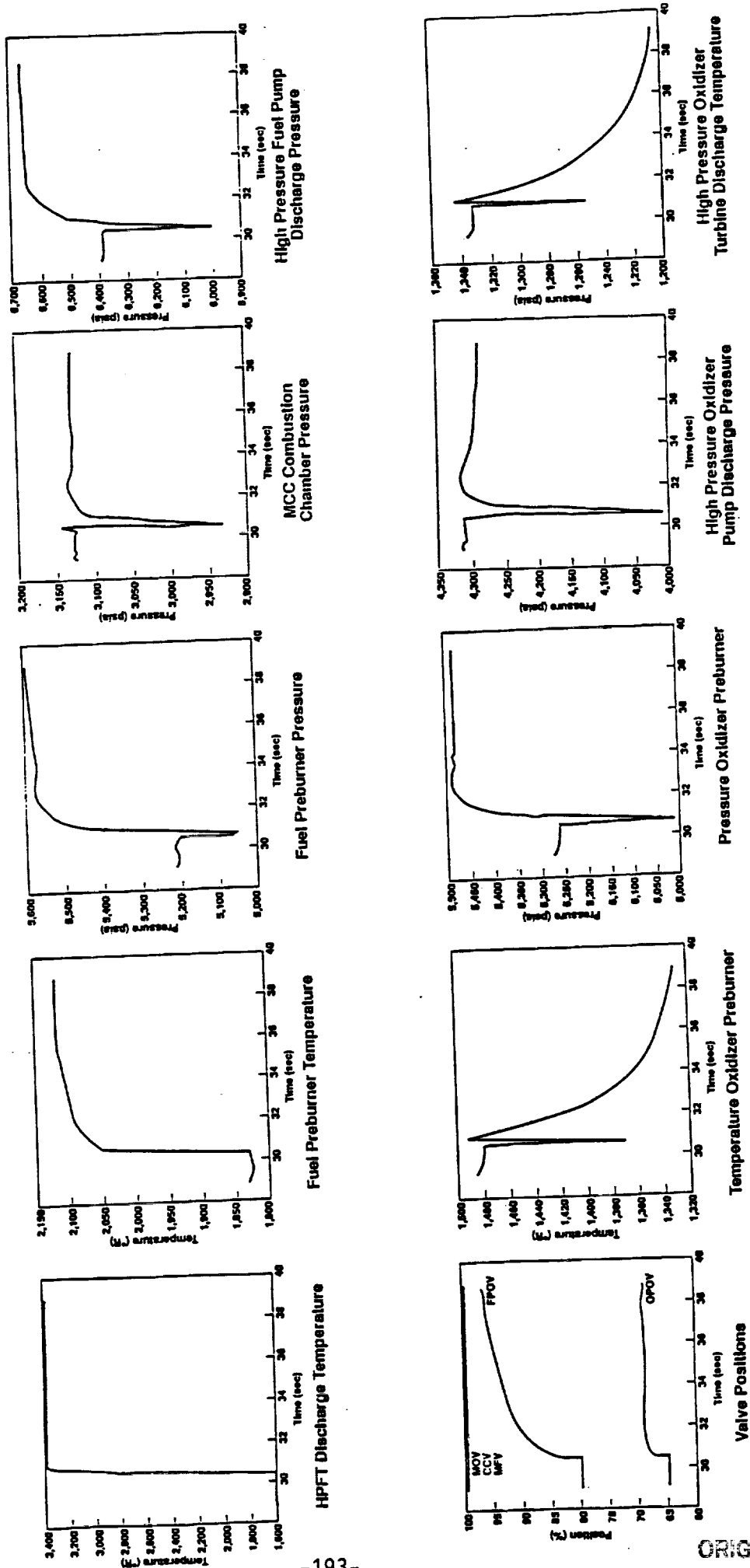
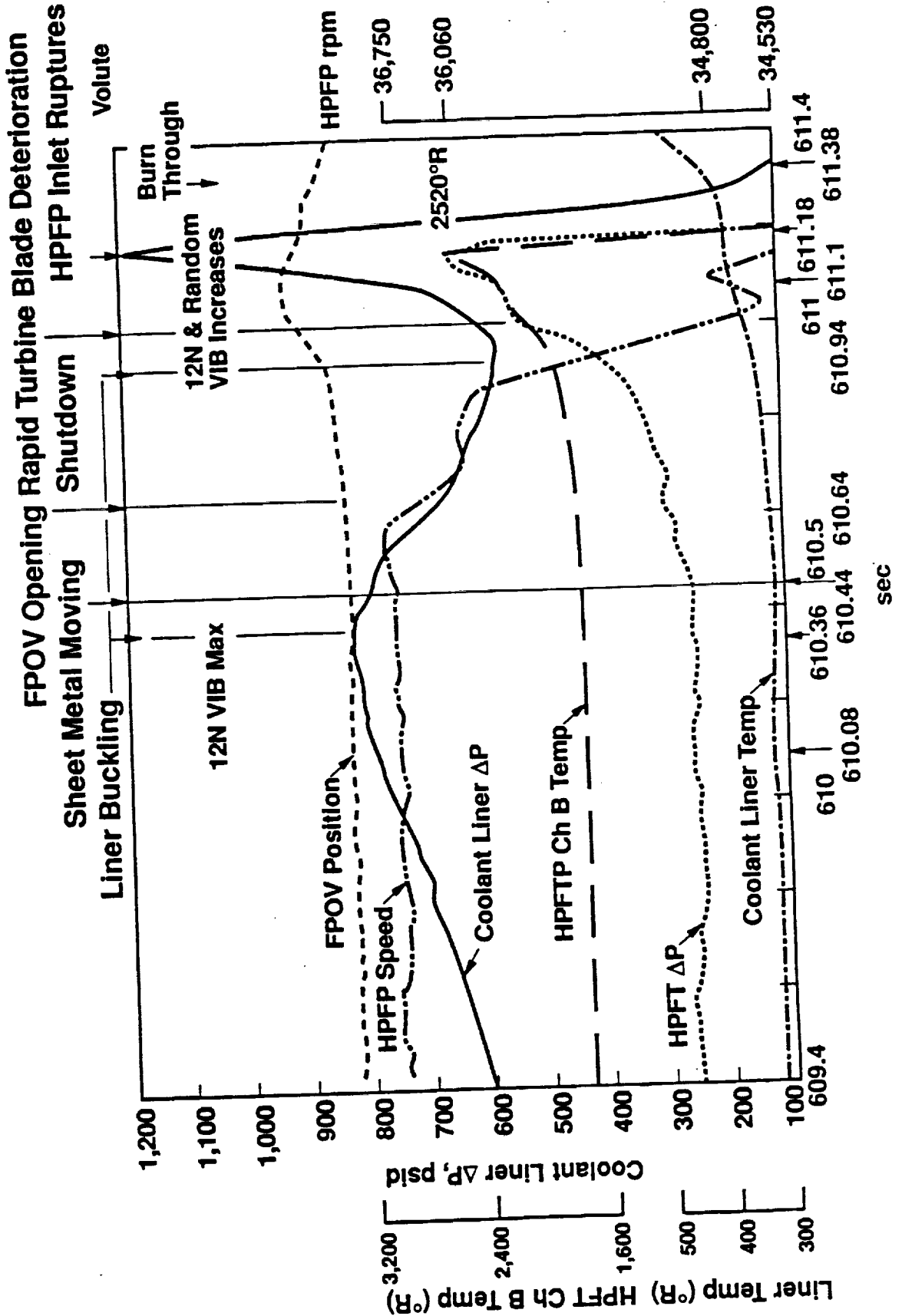


FIGURE 23

Test 901-436 Simultaneous Changes in Various Parameters



END DATE - Dec 18, 1990